AMERICAN INSTITUTE OF STEEL CONSTRUCTION
AISC
FOUNDED 1921

MBMA
METAL BUILDING MANUFACTURERS ASSOCIATION®

25
Steel Design Guide

Frame Design Using Web-Tapered Members

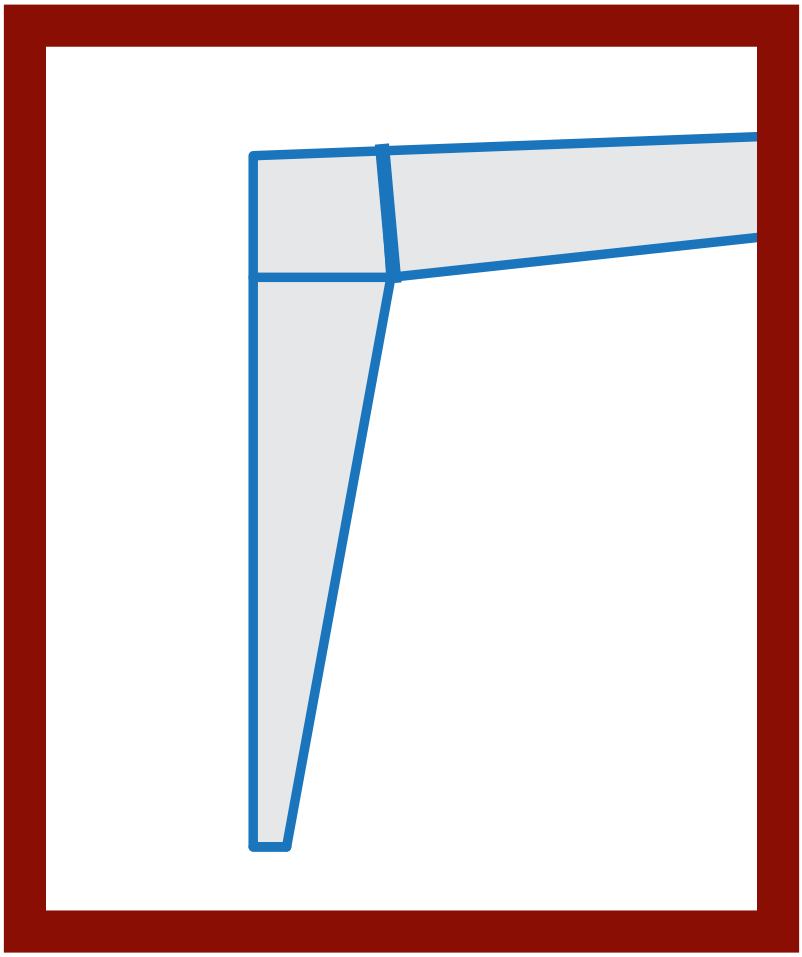

Steel Design Guide

25

Frame Design Using Web-Tapered Members

RICHARD C. KAEHLER
Computerized Structural Design, S.C.
Milwaukee, Wisconsin

DONALD W. WHITE
Georgia Institute of Technology
Atlanta, Georgia

YOON DUK KIM
Georgia Institute of Technology
Atlanta, Georgia

AMERICAN INSTITUTE OF STEEL CONSTRUCTION

AISC © 2011

by

American Institute of Steel Construction

All rights reserved. This book or any part thereof must not be reproduced in any form without the written permission of the publisher.

The information presented in this publication has been prepared in accordance with recognized engineering principles and is for general information only. While it is believed to be accurate, this information should not be used or relied upon for any specific application without competent professional examination and verification of its accuracy, suitability and applicability by a licensed professional engineer, designer or architect. The publication of the material contained herein is not intended as a representation or warranty on the part of the American Institute of Steel Construction, or of any other person named herein, that this information is suitable for any general or particular use or of freedom from infringement of any patent or patents. Anyone making use of this information assumes all liability arising from such use.

Caution must be exercised when relying upon other specifications and codes developed by other bodies and incorporated by reference herein since such material may be modified or amended from time to time subsequent to the printing of this edition. The Institute bears no responsibility for such material other than to refer to it and incorporate it by reference at the time of the initial publication of this edition.

Printed in the United States of America

Authors

Richard C. Kaehler, P.E. is a vice president at Computerized Structural Design, S.C. in Milwaukee, WI. He is a member of the AISC Committee on Specifications and its task committees on Stability and Member Design, and chairs its Editorial task committee.

Donald W. White, Ph.D is a Professor at the Georgia Institute of Technology School of Civil and Environmental Engineering. He is a member of the AISC Committee on Specifications and its task committees on Member Design and Stability.

Yoon Duk Kim, Ph.D is a postdoctoral fellow at the Georgia Institute of Technology School of Civil and Environmental Engineering.

Acknowledgments

The authors express their gratitude to the Metal Building Manufacturers Association (MBMA) and the American Iron and Steel Institute (AISI), who provided the funding for both the preparation of this document and the research required to complete it. The authors also appreciate the guidance of the MBMA Steering Committee:

Al Harrold	Butler Manufacturing
Allam Mahmoud	United Structures of America
Dean Jorgenson	Metal Building Software
Dennis Watson	BC Steel Buildings
Duane Becker	Chief Buildings
Jeff Walsh	American Buildings
Norman Edwards	Questware
Scott Russell	Nucor Building Systems
Steve Thomas	Varco Pruden Buildings

Dr. Efe Guney of Intel Corporation and Mr. Cagri Ozgur of Georgia Tech provided assistance with several investigations of design calculation procedures.

The authors also appreciate the efforts of the AISC reviewers and staff members who contributed many excellent suggestions.

Preface

This design guide is based on the 2005 AISC *Specification for Structural Steel Buildings.* It provides guidance in the application of the provisions of the *Specification* to the design of web-tapered members and frames composed of web-tapered members. The recommendations of this document apply equally to the 2010 AISC *Specification for Structural Steel Buildings,* although some section and equation numbers have changed in the 2010 *Specification.*

Table of Contents

Chapter 1
Introduction

This document provides suggested methods for the design of web-tapered I-shaped beams and columns, as well as frames that incorporate web-tapered I-shaped beams and/or columns. Both the requirements for analysis and rules for proportioning of web-tapered framing members are addressed. The emphasis is on members and frames with proportions and bracing details commonly used in metal building systems. However, this information is equally applicable to similar tapered members used in conventional steel construction.

The methods contained herein are primarily interpretations of, and extensions to, the provisions of the 2005 *AISC Specification for Structural Steel Buildings* (AISC, 2005), hereafter referred to as the AISC *Specification*. The recommendations of this document apply equally to the 2010 *AISC Specification for Structural Steel Buildings*, although some section and equation numbers have changed in the 2010 AISC *Specification*. These recommendations are not intended to apply to structures designed using earlier editions of the AISC *Specification*.

The 2005 AISC *Specification* is a significant departure from past AISC *Specifications*, particularly the ASD Specifications, with which almost all metal buildings have been designed in the United States. Engineers and other users familiar with the previous ASD editions will find significant changes in the presentation of the AISC *Specification*, the member design provisions, and the requirements for analysis. The AISC *Specification* contains no provisions specific to tapered members.

The methods presented in this document comply with the 2005 AISC *Specification* and provide additional information needed to apply the *Specification* to tapered members. In some instances, procedures are provided for situations not addressed by the AISC *Specification*. These are noted where they occur.

The publication of the recommendations in this document is not intended to preclude the use of other methods that comply with the AISC *Specification*.

1.1 BASIS FOR RECOMMENDATIONS

The following sources were used extensively in the preparation of this document, are referenced extensively herein, and should be used in conjunction with this publication for a fuller understanding of its recommendations:

1. ANSI/AISC 360-05, *Specification for Structural Steel Buildings* (AISC, 2005) and its commentary
2. "A Prototype Application of the AISC (2005) Stability Analysis and Design Provisions to Metal Building Structural Systems" (White and Kim, 2006)

The References and Annotated Bibliography sections of this document provide references to other publications relevant to the design of tapered members and frames composed of tapered members. Additional requirements for seismic design and detailing can be found in the ANSI/AISC 341-05, *Seismic Provisions for Structural Steel Buildings* (AISC, 2005a).

A significant research program was conducted as part of the development of this Design Guide. This research was conducted by White, Kim and others at the Georgia Institute of Technology. The focus of this work was the verification and adaptation of the AISC *Specification* provisions for tapered members and frames composed of tapered members. The researched topics included studies on the following:

1. Beam lateral-torsional buckling (LTB)
2. Column in-plane and out-of-plane flexural buckling
3. Column torsional and flexural-torsional buckling
4. Influence of local buckling on member resistances
5. Combined influence of local buckling and member yielding on overall structure stiffness and strength
6. Synthesis of approaches for calculation of second-order forces and moments in general framing systems
7. Benchmarking of second-order elastic analysis software
8. Consideration of rotational restraint at nominally simply supported column bases
9. Consideration of general end restraint effects on the LTB resistance of web-tapered members

The reader is referred to Kim and White (2006a, 2006b, 2007a, 2007b); Kim (2010); Ozgur et al. (2007); and Guney and White (2007) for a detailed presentation of research results for these topics.

1.2 LIMITATIONS

Except where otherwise noted in the text, these recommendations apply to members satisfying the following limits:

1. Specified minimum yield strength, $F_y \leq 55$ ksi.
2. Homogeneous members only (hybrid members are not

considered); i.e., $F_{yf} = F_{yw}$, where F_{yf} and F_{yw} are the flange and web minimum specified yield strengths.

3. Web taper is linear or piecewise linear.
4. Web taper angle is between 0° and 15°.
5. Thickness of each flange is greater than or equal to the web thickness.
6. Flange slenderness ratio is such that

$$\frac{b_f}{2t_f} \le 18$$

where

b_f = flange width, in.

t_f = flange thickness, in.

7. Flange width is such that

$$b_f \ge \frac{h}{7}$$

throughout each unbraced length, L_b. Exception: if $L_b \le 1.1\, r_t \sqrt{E/F_y}$

$$b_f \ge \frac{h}{9}$$

throughout the unbraced length. In the foregoing equations,

h = web height, in.

r_t = radius of gyration of the flange in flexural compression plus one third of the web area in compression due to the application of major axis bending moment alone, calculated using the largest section depth within the length under consideration, in.

8. Web slenderness (without transverse stiffeners or with stiffeners at $a/h > 1.5$) is such that

$$\frac{h}{t_w} \le \frac{0.40E}{F_y} \le 260$$

where

E = modulus of elasticity, ksi

t_w = web thickness, in.

9. Web slenderness (with transverse stiffeners at $a/h \le 1.5$) is such that

$$\frac{h}{t_w} \le 12\sqrt{\frac{E}{F_y}}$$

It is expected that these recommendations can be extended to homogeneous members with larger yield strengths. However, the background research for these recommendations was focused on $F_y = 55$ ksi, because the use of larger yield strengths is not common in current practice.

In addition, it is expected that the recommendations can be extended to hybrid members. The background research for the recommendations in this Design Guide was focused on homogeneous members and the AISC *Specification* does not address hybrid members. Comprehensive provisions for flexural design of hybrid members are provided in the American Association of State Highway and Transportation Officials (AASHTO) *LRFD Bridge Design Specifications* (AASHTO, 2004, 2007).

Furthermore, it is expected that the recommendations can be applied to members with parabolic or other tapered web geometries. However, calculation of the elastic buckling resistances of these types of members is beyond the scope of this document. The general approach provided in this document also accommodates members with steps in the cross-section geometry at field splices or transitions in cross-section plate dimensions. However, the primary focus of this document is on members with linear or piecewise linear web taper.

1.3 BENEFITS OF WEB-TAPERED MEMBERS

Web-tapered members have been utilized extensively in buildings and bridges for more than 50 years.

Design Optimization—Web-tapered members can be shaped to provide maximum strength and stiffness with minimum weight. Web depths are made larger in areas with high moments, and thicker webs are used in areas of high shear. Areas with less required moment and shear strength can be made shallower and with thinner webs, respectively, saving significant amounts of material when compared with rolled shapes.

Fabrication Flexibility—Fabricators equipped to produce web-tapered members can create a wide range of optimized members from a minimal stock of different plates and coil. This can result in time and cost savings compared with the alternative of ordering or stocking an array of rolled shapes. In many cases, the savings in material can offset the increased labor involved in fabricating web-tapered members.

1.4 FABRICATION OF WEB-TAPERED MEMBERS

Web-tapered I-shaped members are fabricated by welding the inside and outside flange plates to a tapered web plate. In the metal building industry, this welding is generally performed by automated welding machines. One typical process is as follows:

1. Flanges and webs are cut to size or selected from plate, coil, or bar stock, and spliced as required to length.
2. Flanges and webs are punched as required for attachments (bracing, purlin and girt bolts, etc.).

3. Flanges are tack-welded to the web, with the web in a horizontal position.
4. With the web in the horizontal position, both flanges are simultaneously welded to the webs from the top side only, using an automated process that proceeds along the length of the member from one end to the other. Exception: welding on both sides of the web at member ends may be required for intermediate moment frames (IMF) and special moment frames (SMF) used in seismic applications.
5. End plates and stiffeners, if required, are manually welded to complete the member.

Although the thicknesses of the two flanges at any given cross section generally need not be the same, the constraints of most automated welding equipment require that the flanges be of the same width along the full length of a fabricated member. Consequently, web-tapered members in metal building construction usually have the same flange widths on the inside and outside of the members. Other welding systems, such as vertical pull-through welders and horizontal welders with blocking, permit the automated welding of cross sections with different flange widths but are not as common. The production of members with unequal flange widths therefore is usually avoided. I-shaped members with unequal flange sizes (thickness and/or width) are categorized as singly symmetric in the AISC *Specification*.

The automated equipment used by metal building manufacturers to join the flanges with the web is typically capable of welding from one side only. These flange-to-web welds must be capable of transferring the local shear flow (VQ/I) as well as any localized concentrated loads between the webs and flanges, where V is the required shear strength, Q is the static moment of area of the flange taken about the neutral axis, and I is the moment of inertia of the full cross section. In most cases, the calculated strength requirements can be met easily with one-sided welds. In special cases, such as for IMF and SMF seismic applications, additional strength is provided where required by reinforcing the automated weld with additional manual welding on one or both sides of the web-to-flange junction.

The one-sided automated welds used in tapered member production in the metal building industry have a long history of satisfactory performance. Two-sided welds are not required unless the calculated required weld strength exceeds the strength of a one-sided weld. Research by Chen et al. (2001) shows that one-sided welds are acceptable to transfer shear loads.

1.5 GENERAL NOTES ON DOCUMENT

(1) Unless otherwise noted, references to a section or chapter are references to the sections and chapters of this Design Guide.

(2) Extensive references to prior research and development efforts are provided in the Annotated Bibliography (Chapter 7). The Annotated Bibliography is organized chronologically under several topic areas. References cited within the other chapters of this Design Guide may be found in the Annotated Bibliography but are also included in the main reference list for the convenience of the reader.

Chapter 2
Web-Tapered Member Behavior and Design Approaches

The behavior of web-tapered members is not qualitatively different from that of prismatic members. Tapered members are subject to the same limit states as prismatic members, but adjustments in the calculation of the strengths are required for some limit states due to the continuously varying geometry.

Strength limit states involving "local" member behavior do not differ from those of prismatic members. These include the limit states of:

1. Tension yielding
2. Compression yielding
3. Tension rupture
4. Shear yielding
5. Shear rupture
6. Local buckling
7. Shear buckling of unstiffened web panels

Local member strengths for these limit states can be calculated by directly applying the provisions of the AISC *Specification* using the section properties at the point of interest on the member.

The calculation of strengths involving the overall member behavior requires adjustments to the procedures given in the AISC *Specification*. These include the limit states of:

1. In-plane buckling (strong-axis flexural column buckling)
2. Out-of-plane buckling (weak-axis flexural, torsional or flexural-torsional column buckling, as well as lateral-torsional beam buckling)
3. Strength under combined axial load and bending, where in-plane or out-of plane buckling is a controlling limit state
4. Shear buckling strength or shear tension-field strength of stiffened web panels

Strength calculations in the AISC *Specification* for these limit states are based on the assumption of constant section properties over the member unsupported lengths. When designing web-tapered members, adjustments to the procedures are needed to account for the varying section properties along the unsupported lengths. These adjustments are detailed in Chapters 4 and 5 of this Design Guide.

2.1 PREVIOUS RESEARCH

Research on stability of members of varying cross sections can be traced back to the work of Euler (Ostwald, 1910), who derived the differential equation of the deflection curve and discussed columns of various shapes, including a truncated cone or pyramid. Lagrange (1770–1773) discussed the stability of bars bounded by a surface of revolution of the second degree. Timoshenko (1936) summarized various analytical and energy method solutions for the elastic buckling of nonprismatic columns, and cited related work as early as Bairstow and Stedman (1914) and Dinnik (1914, 1916, 1929, 1932). He also discussed a powerful procedure called the method of successive approximations, which makes it possible to estimate buckling loads along with upper and lower bounds for any variation of the geometry and/or axial loading along a member length. Timoshenko demonstrated a graphical application of the method of successive approximations to a simply supported column with a stepped cross section subjected to a constant axial load.

Bleich (1952) provided analytical solutions for the elastic buckling of simply supported columns with linear and parabolically varying depths between their "chords." Furthermore, he provided an overview of the method of successive approximations in his Sections 27 and 28 (Bleich, 1952, pp. 81–91), including a proof of its convergence. In addition, Bleich provided detailed discussions of numerical solution procedures utilized with the method of successive approximations for column flexural buckling and thin-walled open section beam lateral-torsional buckling problems. These developments were based largely on the research by Newmark (1943) as well as by Salvadori (1951).

Timoshenko and Gere (1961) retained the solutions presented in Timoshenko's earlier work (Timoshenko, 1936) and added a numerical solution for Timoshenko's original stepped column demonstration of the method of successive approximations (see Timoshenko, 1936, pp. 116–125). Timoshenko and Gere attributed the specific numerical implementation details they presented to Newmark (1943), and referenced Newmark for more extensive discussions and additional applications. More recent discussions of the method of successive approximations are provided by Chen and Lui (1987) in their Section 6.7, and by Bazant and Cedolin (1991) in their Section 5.8. Timoshenko and Gere (1961) also discussed the calculation of inelastic strengths of bars with variable cross section using column curves based on the tangent modulus, E_t, at the cross section with the maximum compressive stress.

In 1966, the Column Research Council (CRC) and the Welding Research Council (WRC) initiated the first concerted effort to address the complete strength behavior of metal building frames composed of tapered I-shaped members. Prior experimental studies by Butler and Anderson (1963) and Butler (1966) had addressed the elastic stability behavior of I-shaped beams tapered in both the flanges and webs, and tested as cantilevered beam-columns. Starting in 1966, researchers at the State University of New York at Buffalo worked on numerous aspects of the problem. This research concluded with the development of the provisions in AISC (1978), as well as a synthesis of these provisions, plus additional design procedures and recommendations by Lee et al. (1981).

The first set of experimental tests aimed at understanding the inelastic stability behavior of tapered I-shaped beam-columns was conducted under the technical guidance of the CRC-WRC joint task committee, and was documented by Prawel et al. (1974). These tests and other analytical studies provided the basis for an overall design approach summarized by Lee et al. (1972). These developments targeted members with linearly tapered web depths. A key characteristic of the resulting design calculations was the use of member length modification factors. The modification factors mapped the physical linearly tapered member to an equivalent prismatic member composed of the cross section at its shallower end. The modified length for the equivalent prismatic member was selected such that this hypothetical member would buckle elastically at the same applied load as the physical linearly tapered member. Length modification factors were developed by curve fitting to representative results from members with five different cross sections. For in-plane flexural buckling under constant axial load, the modification factor was denoted by the symbol, g. For out-of-plane lateral-torsional buckling (LTB) under approximately constant compression flange stress, two length modification factors were developed that paralleled the idealizations used in the AISC *Specification* two-equation approach. One modification factor, h_s, was based on considering only the St. Venant torsional stiffness, while the other, h_w, was based on considering only the warping torsion stiffness.

The equivalent column length, gL, only addressed the in-plane flexural buckling of columns with simply supported end conditions. Therefore, a second length modification factor was applied to this length to account for the rotational restraint provided at the column ends by adjacent members. Idealized rectangular frame models similar to those employed in the development of the AISC alignment charts were used to derive design charts for the corresponding effective length factors, K_γ. Both of the ideal rectangular frame alignment chart cases—sidesway inhibited and sidesway uninhibited—were addressed. The total equivalent prismatic column length was therefore taken as the product of g and K_γ with the resulting physical tapered member length, $K_\gamma gL$. Actually, the g parameter was absorbed into the charts provided for determination of K_γ, but the two factors are shown separately here to emphasize the concepts.

Once the equivalent prismatic column length, $K_\gamma gL$, was determined, the AISC ASD equations were used to determine the column elastic or inelastic design strengths (LRFD). It is important to note that all the preceding steps were simply a means of estimating the maximum axial stress along the length of the column at incipient elastic buckling. This was followed by the mapping of this elastic buckling stress to the elastic or inelastic design stress. This last step used the same mapping of the theoretical to the design buckling resistance employed for prismatic members.

The preceding calculations only addressed the in-plane flexural buckling column resistance of linearly tapered web I-shaped members. The out-of-plane flexural buckling resistance was addressed in exactly the same way as for prismatic members, because the weak-axis moment of inertia, I_y, is nearly constant along the length for members with prismatic flanges.

The calculation of the LTB strength involved the combination of the square root of the sum of the squares of the two elastic LTB contributions (one corresponding to the St. Venant torsional resistance and one corresponding to the warping torsional resistance) to determine an estimate of the theoretical total elastic LTB stress under uniform bending and simply supported end conditions. This stress was then multiplied by an additional parameter, labeled B in AISC (1978), which increased the calculated elastic buckling stress accounting for an estimate of end restraint from adjacent unbraced segments and/or the effects of a flexural stress gradient along the tapered member length. The B parameter equations were developed by Lee et al. (1972), Morrell and Lee (1974), and Lee and Morrell (1975). The base elastic LTB stress modified by B was taken as the estimated maximum flexural stress at incipient elastic LTB of the tapered member. Similar to the column strength determination, this elastic stress was used with the AISC ASD prismatic member mapping from the theoretical elastic buckling resistance to the design LTB resistance (LRFD).

Lee et al. (1972) recommended interaction equations for checking of linearly tapered web I-shaped members for combined axial and flexural loadings that paralleled the AISC ASD beam-column strength interaction equations for prismatic I-shaped members. The only change in the interaction equations implemented in AISC (1978) was a simplification in the C_m parameter, referred to as C'_m in the AISC tapered member provisions. Lee et al. (1972) developed a relatively general C_m equation to approximate the second-order elastic amplification of the maximum major-axis bending stress in linearly tapered members at load levels corresponding to the nominal first-yield condition. The general equation accounts

for the influence of linear web taper and a linear variation of the bending moment between the member ends. The AISC (1978) C'_m equations are identical to the general C_m equation but correspond to the specific cases of single-curvature bending with equal maximum flexural stress at both ends of the member and single-curvature bending with zero moment (or flexural stress) at the smaller end.

The preceding procedures formed the primary basis for the AISC design provisions in Appendix D of the ASD *Specification for Design, Fabrication and Erection of Structural Steel for Buildings* (AISC, 1978), Appendix F, Section F4 of the *Load and Resistance Factor Design Specification for Structural Steel Buildings* (AISC, 1986), Appendix F, Section F7 of the *Specification for Structural Steel Buildings—Allowable Stress and Plastic Design* (AISC, 1989), and Appendix F, Section F3 of the *Load and Resistance Factor Design Specification for Structural Steel Buildings* (AISC, 1993, 1999).

These approaches did not account for torsional or flexural-torsional buckling limit states in tapered columns and beam-columns. The flexural-torsional buckling limit state can be of particular importance for tapered members with unequal flange areas. Lee and Hsu (1981) addressed this design requirement by providing an alternative beam-column strength interaction equation that estimated the flexural-torsional buckling resistance of tapered members subjected to combined bending and axial compression, and charts that provided a coefficient required in the alternative beam-column strength interaction equation. These charts were included in Lee et al. (1981) but were never formally adopted within any of the AISC *Specification* provisions.

Furthermore, these approaches did not address the in-plane stability design of I-shaped members consisting of two or more linearly tapered segments. These types of members are used commonly for roof girders or rafters in metal building frames. Lee et al. (1979) developed another extensive set of design charts that permitted the calculation of (1) the equivalent pinned-end prismatic column length for doubly symmetric, doubly tapered I-shaped members (analogous to the length gL), and (2) the *effective* equivalent prismatic column length accounting for the influence of end rotational end restraints for these members (analogous to the length $K_\gamma gL$). The second of these calculations was based again on idealized rectangular frame models similar to those associated with the AISC alignment charts. The authors provided charts and procedures for calculation of the equivalent rotational stiffness provided by adjacent tapered members again using the concept of the equivalent length of an alternative prismatic member composed of the shallowest cross-section along the tapered member length. These charts were included in Lee et al. (1981) but were never formally adopted within any of the AISC *Specification* provisions.

The provisions within the AISC *Specifications* from AISC (1978) through AISC (1999) were limited only to I-shaped members with equal-size flanges and linearly varying web depths. This, combined with the unpopularity of design charts without underlying equations for calculation of the corresponding parameters, led to limited use of these provisions. Instead, metal building manufacturers have tended to develop their own specific mappings of the AISC prismatic member equations for design of the wide range of general nonprismatic member geometries encountered in practice, often based upon research to validate their design approaches. As a result, the AISC Committee on Specifications decided to remove the explicit consideration of nonprismatic I-shaped members entirely from the AISC *Specification* in favor of subsequent development of separate updated guidelines for these member types. It was anticipated that the subsequent developments could take significant advantage of the many advances that have been implemented for member and frame stability design in the time since the seminal work by Lee et al. (1981).

Since the culmination of the work by Lee et al. (1981), numerous other studies have been conducted to investigate various attributes of the behavior of nonprismatic I-shaped members and frames composed of these member types. Salter et al. (1980); Shiomi et al. (1983); and Shiomi and Kurata (1984) have reported on additional experimental tests of isolated doubly symmetric beam-columns with linearly tapered webs. However, these tests focused only on members with compact webs and flanges.

Practical web-tapered members produced by American manufacturers often have noncompact or slender webs and flanges. Forest and Murray (1982) tested eight full-scale clear-span gable frames with proportions representative of American design practices under the sponsorship of Star Building Systems. They provided an early assessment of the Star Building Systems design rules in place at that time, as well as the procedures recommended by Lee et al. (1981). Forest and Murray concluded, "No consistent set of design rules adequately predicted the frame strengths for all the loading combinations." However, the Star Building Systems design rules were judged to be safe.

Jenner et al. (1985a, 1985b) tested four clear-span frames. These tests demonstrated the importance of providing sufficient panel zone thickness to maintain the stiffness of the knee joint area. Davis (1996) conducted comparisons of AISC load and resistance factor design (LRFD) (AISC, 1993) calculation procedures to the results from two other full-scale, clear-span gable frame tests conducted at Virginia Tech. Local buckling of the rafter flanges governed the design resistances as well as the experimental failure modes. The predictions of the experimental resistances were consistently conservative by a small margin.

Watwood (1985) discussed the calculation of the appropriate effective length of the rafters in an example gable frame, accounting for the rafter axial compression and its effect on the sidesway stability of the overall structure. Watwood also investigated the sensitivity of his example frame design to foundation boundary conditions and unbalanced gravity loads. He suggested an approach for design of the rafters that in essence equates the buckling load of these members to their axial force at incipient sidesway buckling of the full structure. This typically results in an effective length factor for the rafters significantly larger than one. Numerous other researchers have considered the influence of axial compression in the rafters of gable clear-span frames in the calculation of the overall sidesway buckling loads and in the design of the gable frame columns, [e.g., Lu (1965), Davies (1990), Silvestre and Camotim (2002), and White and Kim (2006)].

These results highlight an anomaly of the effective length method (ELM) for structural stability design. Members that have small axial stress at incipient buckling of the frame generally have large effective length factors (K). In some cases, these K factors are justified, while in other cases they are not. If the member is indeed participating in the governing buckling mode, a large K value is justified. If the member is largely undergoing rigid-body motion in the governing buckling mode, or if it has a relatively light axial load and is predominantly serving to restrain the buckling of other members, a large K value is sometimes not justified. The distinction between these two situations requires engineering judgment (White and Kim, 2006). In any case, the ELM procedures recommended by Lee et al. (1981) rely on the first-order elastic stiffness of the adjacent members in determining the K_γ values. Unfortunately, if the adjacent members are also subjected to significant axial compression, their effective stiffnesses can be reduced substantially. In these cases, the Lee et al. (1981) K_γ procedures in essence rely on one member to restrain the buckling of its neighbor, then turn around and rely on the neighbor to restrain the buckling of the member. Watwood (1985) shows a clear example illustrating the fallacy of this approach.

Cary and Murray (1997) developed a significant improvement upon the traditional calculation of alignment chart frame effective length factors for sway frames. Their approach built upon Lui's (1992) development of a story-stiffness-based method for prismatic member frameworks. A common useful attribute of story-stiffness-based methods is that they use the results of a first-order elastic drift analysis (usually conducted for service design lateral loadings) to quantify the overall story buckling resistance. In addition, one of the most significant attributes of these methods is the fact that they account for the influence of leaning (gravity-only) columns on the frame sidesway buckling resistance. Conversely, the traditional AISC alignment chart and the Lee et al. (1981) effective length factor methods do not account for such influences. This attribute can be a very important factor in the proper stability design of wide modular frames having multiple bays and a large number of leaning columns. Cary and Murray (1997) did not address the potential significant degradation in the story buckling resistance due to axial compression in the beams or rafters of metal building structures. This axial compression is often negligible for modular building frames, but it can be quite significant in some clear-span gable frames, such as the frame considered by Watwood (1985). Also, these investigators did not account for the influence of different height columns. This characteristic generally needs to be addressed in modular building frames as well as in monoslope roof clear-span frames. White and Kim (2006) explain how the story-stiffness equations from the Commentary on the AISC *Specification* (AISC, 2005a) can be extended to account both for the influence of axial compression in the roof girders as well as variable column heights. EuroCode3 (CEN, 2005) provides guidance on when these approximations are appropriate for gable frames, although the origins and basis for the EuroCode3 guidelines are unknown.

White and Kim (2006) explain that all of the preceding sidesway buckling analysis developments focus on the wrong parts of the stability design problem, because the behavior of metal building frames is almost always a moment amplification (load-deflection) problem rather than a sidesway buckling (bifurcation) problem. The behavior of metal building frames is typically dominated by the moment terms. Therefore, calculation of the appropriate amplified moment from a load-deflection analysis of the structure is key, not the determination of a buckling load that is typically many times larger than the ultimate strength of the structure. The Direct Analysis Method in the AISC *Specification* allows the engineer to focus more appropriately on the most important part of the metal building frame design problem, i.e., the calculation of the amplified internal moments (or bending stresses) under relatively small axial loads (or axial stresses), and the corresponding proportioning of the structural system to resist these actions.

Metal building frame members are usually proportioned such that they encounter some yielding prior to reaching their maximum resistance. Subsequent to Lee et al. (1981), a number of other research studies have focused on evaluation of inelastic beam and beam-column resistances and frame design. Jimenez (1998, 2005, 2006) and Jimenez and Galambos (2001) conducted numerous inelastic stability studies of linearly tapered I-shaped members accounting for a nominal initial out-of-straightness, the nominal Lehigh (Galambos and Ketter, 1959) residual stress pattern commonly used in the literature for rolled wide-flange members, and assuming compact cross-section behavior (i.e., no consideration of web or flange plate slenderness effects). Jimenez showed that the AISC (1999) provisions predicted

the column inelastic buckling resistance with some minor conservatism for these types of members. Also, he observed that the inelastic LTB curve for these types of members, predicted from inelastic buckling analyses, exhibited more of a pinched or concave up shape [rather than the linear transition curve assumed for the inelastic LTB range in AISC (1999)]. In addition, he observed that very short unbraced lengths were necessary for the compact I-shaped members considered in his study to reach their plastic moment capacity. Nevertheless, it is important to note that this type of behavior has been observed as well in some inelastic buckling studies of prismatic I-shaped members. White and Jung (2008) and White and Kim (2008) show that the linear transition curve for inelastic LTB in AISC (2005) is a reasonable fit to the mean resistances from experimental test data for all types of prismatic I-shaped members and justify the AISC (2005) resistance factor $\phi_b = 0.90$.

Other researchers have suggested simpler and more intuitive ways of determining the elastic buckling resistance of I-shaped members than the equivalent prismatic member (with a modified length) approach. Polyzois and Raftoyiannis (1998) reexamined the B factor equations from AISC (1978, 1986, 1989, 1993 and 1999) and suggested changes that covered a wider range of geometry and loading cases. They questioned the use of the single modification factor, B, to account for both the stress gradient effects and the influence of LTB end restraint from adjacent segments, and they developed separate modification factors for each of these contributions to the elastic LTB resistance. In other developments, Yura and Helwig (1996) suggested a method of determining the elastic LTB resistance of linearly tapered I-shaped members based on (1) the use of the AISC (2005) C_b equations but written in terms of the compression flange stresses rather than the member moments, and (2) the use of the tapered member cross section at the middle of the segment unbraced length. Kim and White (2007a) have validated the Yura and Helwig (1996) approach and have generalized this approach to other elastic member buckling calculations.

Numerous researchers have worked on refined calculations of elastic LTB resistances for tapered I-shaped members in recent years. Andrade et al. (2005) and Boissonnade and Maquoi (2005) show that the use of prismatic beam elements for the analysis of tapered beams (i.e., subdivision of the member into a number of small prismatic element lengths) can lead to significant errors when the behavior involves torsion. Kim and White (2007a) use a three-dimensional beam finite element formulation similar to the formulations by Andrade et al. (2005) and Boissonnade and Maquoi (2005) for their elastic buckling studies. More recently, Andrade et al. (2007) provide further validations of their one-dimensional beam model for capturing elastic LTB of web-tapered cantilevers and simply-supported beams.

Kim (2010) demonstrates that the procedures presented in this design guide for calculating the LTB resistances may be applied equivalently to both tapered and prismatic I-section members. That is, given the calculation of an elastic buckling resistance and the moment gradient parameter, C_b, the physical flexural strength is effectively the same at the most highly stressed section regardless of whether the member is tapered or prismatic. Kim (2010) also addresses the fact that virtual test simulation studies by refined full-nonlinear finite element analysis typically lead to smaller nominal strength estimates than obtained by analysis of experimental test data. These differences appear to be largely due to the geometric imperfections and internal residual stresses being smaller on average in the physical tests compared to common deterministic values assumed in viritual simulation studies. The nominal flexural strengths calculated using the AISC *Specification* and this Design Guide essentially give the mean of the resistances from experimental tests (White and Jung, 2008; White and Kim, 2008; Kim, 2010)

Davies and Brown (1996), King (2001a, 2001b), and Silvestre and Camotim (2002) have presented substantial information about the overall design of gable frame systems, including clear-span frames and multiple-span gable frames with moment continuity throughout and lightweight interior columns. Much of their discussions are oriented toward European practices and design standards, including plastic analysis and design of single-story gable frames using compact rolled I-shaped members with haunches at the frame knees. However, these studies also provide useful insights that are of value to American practices, which typically involve welded I-shapes with thinner web and flange plates.

There are numerous other prior efforts that deserve mention, but due to the abbreviated scope of this section are not referenced herein. See Chapter 7 for an extensive annotated bibliography on the stability design of frames composed of tapered and general nonprismatic I-shaped members.

2.2 RELATIONSHIP TO PRIOR AISC PROVISIONS FOR WEB-TAPERED MEMBERS

The member resistance provisions provided in this Design Guide differ somewhat from the Appendix F provisions of AISC (1989). Nevertheless, the fundamental concepts are largely the same. The primary differences between the current provisions and those in AISC (1989) are as follows:

1. The prior AISC (1989) provisions required the flanges to be of equal and constant area. The recommended provisions apply generally to cases such as singly symmetric members and unbraced segments having cross-section transitions.
2. The prior AISC (1989) provisions required the depth to vary linearly between the ends of the unbraced lengths. The recommended provisions apply to all

cases within the scope of this document, including unbraced lengths having cross-section transitions and/or multiple tapered segments.

3. The recommended resistance provisions define a mapping of the beam and column resistances from a theoretical elastic buckling value to an elastic or inelastic resistance using the AISC (2005) beam and column resistance equations as a base. The Appendix F provisions of AISC (1989) define a similar mapping to the design resistances, but use the AISC (1989) beam and column equations. The AISC (2005) design resistance equations provide improved simplicity and accuracy for the base prismatic member cases compared to the AISC (1989) equations (White and Chang, 2007).

4. The prior AISC (1989) column resistance equations for tapered members were based on the calculation of an equivalent elastic effective length factor, $K_\gamma g$. The effective length, $K_\gamma gL$, was the length at which an equivalent prismatic member composed of the smallest cross section would buckle elastically at the same constant axial load as in the actual tapered column of length L. As noted in Section 2.1, the separate g parameter, which gives the equivalent length for simply supported end conditions, was actually absorbed into charts for determination of the rotational end restraint effects. Therefore, AISC (1989) shows just one factor, labeled as K_γ [i.e., K_γ in AISC (1989) is the same as $K_\gamma g$ in this discussion]. The length $K_\gamma gL$ was used in the AISC (1989) equations to accomplish the preceding mapping from the theoretical elastic buckling stress to the column buckling resistance, expressed in terms of the allowable axial stress. The AISC (1989) column buckling resistance corresponded specifically to the axial stress state at the smallest cross section.

   The recommended provisions focus directly on the calculation of the controlling elastic buckling load (or stress) ratio,

$$\gamma_e = \frac{P_e}{P_r} = \frac{F_e}{f_r} \qquad (2.2\text{-}1)$$

   where

   F_e = corresponding axial stress at the most highly stressed cross section (the smallest cross section if the axial force is constant along the member length), ksi

   P_e = smallest member axial force at flexural buckling about the major- or minor-axis of bending, torsional buckling, or flexural-torsional buckling, kips

   P_r = member required axial load resistance, kips

   $f_r = P_r/A_g$ at the most highly stressed cross section, ksi

   A_g = gross area of member, in.^{2}

   The calculation of γ_e, which is the same for all cross sections along the member length (because it is an overall member buckling load ratio), is more easily generalized to address all potential column buckling limit states for all types of member geometries than the equivalent length procedures of AISC (1989). Also, it accommodates all three of the overall stability analysis-and-design approaches in AISC (2005), i.e., the Direct Analysis Method, the Effective Length Method and the First-Order Analysis Method. Simplified procedures are provided in this design guide for calculation of γ_e. Furthermore, the ratio $\gamma_e = P_e/P_r = F_e/f_r$ can be obtained directly from general buckling analysis methods. Nevertheless, both the prior calculation of $K_\gamma gL$ and the current calculation of γ_e focus on the same fundamental question: what is the elastic buckling load (or stress) for the unsupported length under consideration?

5. The prior AISC (1989) flexural resistance equations also focused on a modification of the tapered member length, L. The basic concept was to replace the tapered beam by an "equivalent" prismatic beam with a different length, and with a cross section identical to the one at the smaller end of the tapered beam. The equivalency condition was that both the actual tapered member and the equivalent prismatic member buckle elastically at the same flexural stress if the compression flange is subjected to uniform flexural compression. This led to two different length modifiers, labeled h_s and h_w, which were used with the ASD two-equation lateral-torsional buckling (LTB) resistance equations depending on whether the LTB resistance was dominated by the St. Venant torsion stiffness or the warping torsion stiffness. Rather than taking the elastic buckling stress as the larger of these two estimates, $F_{s\gamma}$ and $F_{w\gamma}$, as in the AISC (1989) prismatic member provisions, AISC (1989) Appendix F used the more refined estimate of $(F_{s\gamma}^2 + F_{w\gamma}^2)^{0.5}$ to determine the base elastic LTB stress. A separate modifier, labeled B, was applied to this elastic buckling estimate to account for moment gradient effects and lateral restraint offered by adjacent unbraced segments. Finally, for $B(F_{s\gamma}^2 + F_{w\gamma}^2)^{0.5} > F_y/3$, the AISC (1989) flexural resistance equations mapped the above elastic buckling stress estimate, $B(F_{s\gamma}^2 + F_{w\gamma}^2)^{0.5}$, to an inelastic LTB design resistance using the prismatic member equations [for $B(F_{s\gamma}^2 + F_{w\gamma}^2)^{0.5} \le F_y/3$, the design LTB resistance was taken the same as the theoretical elastic LTB resistance]. The maximum flexural stress within

the unbraced segment was then compared against this design LTB resistance.

In contrast, the recommended LTB resistance provisions focus on the calculation of (1) the buckling load ratio $(\gamma_{e.LTB})_{C_b=1} = (M_{e.LTB})_{C_b=1}/M_r$ and the moment gradient modifier, C_b, or more generally the buckling load ratio, $\gamma_{e.LTB} = M_{e.LTB}/M_r$, including the moment gradient effects for the unbraced length under consideration, where $M_{e.LTB}$ is the elastic lateral-torsional buckling strength and M_r is the required flexural strength (ASD or LRFD), and (2) the calculated flexural stress state, f_r/F_y, at key locations along the length. Simplified procedures are provided for the calculation of C_b and $(\gamma_{e.LTB})_{C_b=1}$ for linearly tapered members. The parameters C_b, $(\gamma_{e.LTB})_{C_b=1}$ and f_r/F_y are then used with a form of the base AISC (2005) flexural resistance equations to accomplish a general mapping from the theoretical elastic LTB resistance to the elastic or inelastic design LTB resistance.

6. Both the prior AISC (1989) provisions as well as the recommended provisions address compression flange local buckling (FLB) on a cross section by cross section basis using the base prismatic member equations. The AISC (2005) FLB equations, on which the recommended provisions are based, give a simpler and more accurate characterization of the FLB resistance of I-shaped members (White and Chang, 2007) than the prior AISC (1989) provisions.
7. The AISC (1989) provisions restrict both the tension and the compression flange to the same allowable LTB stress. The recommended provisions specify a more rational tension flange yielding (TFY) limit for singly symmetric I-shaped members with a smaller tension flange and a larger depth of the web in flexural tension.
8. The AISC (1989) Appendix F provisions applied the base ASD prismatic beam-column strength interaction equations to assess the resistance of members subjected to combined flexure and axial force. A modified factor, labeled C'_m, was defined for two specific cases: (1) single curvature bending and approximately equal computed bending stresses at the ends; and (2) computed bending stress at the smaller end equal to zero. The recommended provisions utilize the base AISC (2005) prismatic beam-column strength interaction equations. These equations are applied to define the strength interaction for all types of beam-column geometries and all combinations of column and beam resistance limit states.
9. The prior AISC (1989) Appendix F provisions required extensive use of charts for the calculation of the in-plane column buckling resistances (i.e., for the determination of $K_\gamma g$). The current provisions do not require the use of any charts.

The prior AISC LRFD provisions (AISC, 1999) for web-tapered members were patterned largely after AISC ASD provisions (AISC, 1989). The flexural resistance provisions were essentially identical to the latter. The column resistance provisions utilized the same $K_\gamma g$ as in the AISC ASD provisions (AISC, 1989) but applied these parameters with the AISC LRFD column curve [which is retained as the AISC (2005) column curve]. Furthermore, the beam-column resistance was checked using the AISC LRFD (AISC, 1999) bilinear interaction curve, but with the C'_m from the AISC ASD provisions (AISC, 1989). The AISC LRFD (AISC, 1999) bilinear equations are retained as the base beam-column strength curve in AISC (2005).

The recommended provisions represent a natural progression in terms of simplification, improvement in accuracy, and improvement in breadth of applicability from the AISC ASD (AISC, 1989) and the AISC LRFD (AISC, 1999) provisions.

Chapter 3
Design Basis

The primary basis for the following design recommendations is the AISC *Specification*. In cases where supplemental recommendations are given to account for the unique nature of web-tapered members, these procedures conform to the intent of the AISC *Specification*. Users are cautioned against selecting individual provisions and incorporating them into their current design methods based on earlier AISC *Specifications*.

Structures may be designed using the AISC *Specification* using either allowable strength design (ASD) or load and resistance factor design (LRFD). The *Specification* voices no preference, so the choice can be made by the designer on the basis of personal preference. Designs produced by ASD and LRFD may differ slightly, but both are acceptable according to the AISC *Specification* and the building codes that reference the AISC *Specification*.

The LRFD procedure is intended to provide a mathematically predictable level of reliability, i.e., a known probability that the strength of the structure will exceed the demands imposed upon it over its lifetime. The safety factors used in ASD have been derived from LRFD to provide a similar level of safety and reliability.

3.1 KEY TERMINOLOGY

The five following terms are used throughout the AISC *Specification* and this document:

1. *Required strength* is the member (or component) force or moment that must be resisted. This usually comes from a structural analysis. The required strength for any given load combination is calculated using the appropriate ASD or LRFD load combinations. In this document, required strength is represented by the following symbols:

   R_r = Generalized required strength, which applies to both ASD and LRFD. R_r is a generic term that can refer to forces or moments. The specific required forces and moments are designated by:

   P_r = required axial strength using LRFD or ASD load combinations, kips

   V_r = required shear strength using LRFD or ASD load combinations, kips

   M_r = required flexural strength using LRFD or ASD load combinations, kip-in.

   R_a = ASD required strength calculated using ASD load combinations. R_a is a generic term that can refer to forces or moments. The specific required ASD forces and moments are designated by:

   P_a = required axial strength using ASD load combinations, kips

   V_a = required shear strength using ASD load combinations, kips

   M_a = required flexural strength using ASD load combinations, kip-in.

   R_u = LRFD required strength calculated using LRFD load combinations. R_u is a generic term that can refer to forces or moments. The specific required LRFD forces and moments are designated by:

   P_u = required axial strength using LRFD load combinations, kips

   V_u = required shear strength using LRFD load combinations, kips

   M_u = required flexural strength using LRFD load combinations, kip-in.

2. *Nominal strength* is the calculated strength without reduction by safety factors (ASD) or resistance factors (LRFD). Nominal strength is represented by the following symbols:

   R_n = Generalized nominal strength. Specific nominal axial forces, shear forces and moments are designated by:

   P_n = nominal axial strength, kips

   V_n = nominal shear strength, kips

   M_n = nominal flexural strength, kip-in.

3. *Available strength* is the generalized term for calculated strength including reductions by safety factors (ASD) or resistance factors (LRFD). Available strength refers inclusively to both allowable strength and design strength.

   P_c = available axial strength (allowable strength in ASD or design strength in LRFD), kips

M_c = available flexural strength (allowable strength in ASD or design strength in LRFD), kip-in.

4. *Allowable strength* is the nominal strength divided by the safety factor (ASD),

$$\text{Allowable strength} = \frac{R_n}{\Omega}$$

5. *Design strength* is the nominal strength multiplied by the resistance factor (LRFD),

$$\text{Design strength} = \phi R_n$$

3.2 LIMIT STATES DESIGN

Although the AISC *Specification* permits design by either the ASD or LRFD methods, all designs produced using the provisions of the AISC *Specification* are limit states based. In both ASD and LRFD, required strengths are compared against available strengths calculated for each of the limit states by which the member can be governed.

The roots of the AISC *Specification* are primarily the provisions from the 1999 LRFD *Specification*, enhanced with numerous changes based on more recent research and aspects of ASD that were preferable or better for practice. Safety factors have been provided for use in ASD. The safety factors are calibrated to give essentially identical results to LRFD for each limit state when the ratio of live load to dead load is 3.0.

When the live load to dead load ratio is higher than 3.0, ASD will tend to produce a somewhat lighter design. When the live load to dead load ratio is less than 3.0, LRFD will tend to produce a lighter design. The differences between designs produced using the two methods are rather small, even when the ratio of live-to-dead load becomes extreme. A similar result occurs for other load combinations. For structures with large second-order effects, the ASD second-order analysis requirements (i.e., the second-order effects must be considered at an ultimate strength load level taken as 1.6 times the load combinations in ASD) tend to reduce or eliminate the apparent economic advantage ASD has for structures with high live load to dead load ratios.

Although the 1.6 factor used to increase ASD loads to ultimate levels is usually more conservative than the load factors used for LRFD, this value is lower than that used in previous editions of the ASD *Specifications*. In the 1989 and earlier editions, second-order amplification was handled by the term [see AISC (1989) Equation H1-1],

$$\frac{C_m}{1-\frac{f_a}{F_e'}}$$

where

F_e' = Euler stress for a prismatic member divided by a safety factor, ksi

f_a = computed axial stress, ksi

The safety factor of 23/12 = 1.92 in the term F_e' effectively resulted in second-order amplification occurring at 1.92 times the ASD load levels.

Other than the load combinations, the safety and resistance factors, and a few details of second-order analysis, there are no significant differences between the ASD and LRFD design procedures in the AISC *Specification*.

3.2.1 LRFD Design Basis

The design basis for LRFD is formally expressed as:

$$R_u \le \phi R_n \quad \text{(3.2-1, } \textit{Spec.} \text{ Eq. B3-1)}$$

where

R_u = required strength computed using LRFD load combinations, kips

R_n = nominal strength of the applicable limit state, kips

ϕ = LRFD resistance factor corresponding to the limit state

Stated simply, the required strength, R_u, must be less than or equal to the design strength, ϕR_n.

3.2.2 ASD Design Basis

There is an important difference between ASD as defined in the AISC *Specification* and ASD as has been customarily practiced in the United States. In prior ASD *Specifications*, ASD was an acronym for *allowable stress design*. In past editions, the *Specification* provided maximum allowable stresses that were compared with calculated working load stresses in the member. In the AISC *Specification*, ASD is an acronym for *allowable strength design*. The *Specification* now provides maximum allowable forces and moments that are compared with required forces and moments in the member. This is the same format that has been used in the *Specification for Cold-Formed Structural Steel Members* (AISI, 1996, 2001, 2007) since 1996.

The design basis for ASD is formally expressed as:

$$R_a \le \frac{R_n}{\Omega} \quad \text{(3.2-2, Spec. Eq. B3-2)}$$

where

R_a = required strength computed using ASD load combinations, kips

R_n = nominal strength of the applicable limit state, kips

Ω = ASD safety factor corresponding to the limit state

Stated simply, the required strength, R_a, must be less than or equal to the allowable strength, R_n/Ω.

3.2.3 Allowable Stress Design

Although the AISC *Specification* provides ASD strengths in terms of forces and moments, it is possible to convert these strengths to a stress-based format for the convenience of users accustomed to working with stresses. Stress-based design holds several advantages over load-based design. These include the ability of the engineer to more readily assess the reasonableness of the allowable strengths, in most cases, and the potential for greater compatibility with the existing ASD software base. This technique has been presented in an article by Fisher (2005) and in literature distributed by AISC on the AISC website at www.aisc.org and at seminars. Although this procedure is not explicitly endorsed in the AISC *Specification*, it produces mathematically identical results to load-based ASD designs produced in accordance with the *Specification* when properly used.

Required strengths are converted to required stresses by dividing the required strength by the appropriate section property [gross area (A), section modulus (S), area of web, etc.] in the usual way. *Allowable strengths* are converted to allowable stresses by dividing the allowable strength by the same section property used to calculate the corresponding required stress. Thus, the design basis becomes:

$$\text{Required stress} \le \text{Allowable stress} \qquad (3.2\text{-}3)$$

$$\text{For axial compression force, } \frac{P_a}{A} \le \frac{P_n}{A\Omega_c} \qquad (3.2\text{-}4)$$

$$\text{For flexure, } \frac{M_a}{S} \le \frac{M_n}{S\Omega_b} \qquad (3.2\text{-}5)$$

Allowable flexural stresses computed in this manner can exceed $0.66F_y$ in cases where the nominal flexural strength approaches the plastic moment. This is particularly the case for highly singly symmetric sections, which can have a shape factor, M_p/M_y, significantly larger than 1.1, where M_p is the plastic bending moment and M_y is the yield moment.

The design calculations are mathematically equivalent to those produced by the allowable strength design procedure if the details of these conversions are handled consistently. This stress-based procedure should not be used to produce predicted strengths in excess of those calculated using forces and moments.

Chapter 4
Stability Design Requirements

The most significant and possibly the most challenging changes in the AISC *Specification* are in the area of stability design, that is, the analysis of framing systems and the application of rules for proportioning of the frame components accounting for stability effects. With a few exceptions, designers using the 1989 AISC *Specification for Structural Steel Buildings—Allowable Stress and Plastic Design* (AISC, 1989) have conducted linearly elastic structural analysis without any explicit consideration of second-order effects, geometric imperfections, residual stresses, or other nonideal conditions. Changes in the AISC *Specification* make explicit consideration of some, or all, of these factors mandatory in the analysis phase.

4.1 KEY TERMINOLOGY

The following key terms are used in the AISC *Specification* and this document.

P-Δ *effect*. Additional force or moment (couple) due to axial force acting through the relative transverse displacement of the member (or member segment) ends (see Figure 4-1).

P-δ *effect*. Additional bending moment due to axial force acting through the transverse displacement of the cross-section centroid relative to a chord between the member (or member segment) ends (see Figure 4-2). In singly symmetric web-tapered I-shaped members, and in members with steps in the cross-section geometry along their length, this transverse displacement includes both the deflections relative to the chord between the member or element ends, due to applied loads, as well as the offset of the (nonstraight) cross-section centroidal axis from the chord. When members are subdivided into shorter-length elements in a second-order matrix analysis, the *P*-δ effects at the member level are captured partly by *P*-Δ effects at the individual member or segment level (see Figure 4-3).

Second-order analysis. Structural analysis in which the equilibrium conditions are formulated on the deformed structure. Second-order effects (both *P*-δ and *P*-Δ, unless specified otherwise) are included. First-order elastic analysis with appropriate usage of amplification factors is a second-order analysis. Other methods of second-order elastic analysis include matrix formulations based on the deformed geometry and *P*-Δ analysis procedures applied with a sufficient number of elements per member. See Chapter 6, Section 6.2, for a brief summary and assessment of different methods of second-order analysis. See Chapter 6, Section 6.2.1, for a discussion of the required number of elements per member for various types of second-order matrix analysis.

Second-order effect. Effect of loads acting on the deformed configuration of a structure; includes *P*-δ effect and *P*-Δ effect.

4.2 ASCE 7 AND IBC SEISMIC STABILITY REQUIREMENTS

Requirements for consideration of second-order effects under some conditions were introduced into the seismic provisions of the American Society of Civil Engineers' standard, ASCE 7, beginning in 1998 (ASCE, 1998) and the International Building Code (IBC) beginning in 2000 (IBC,

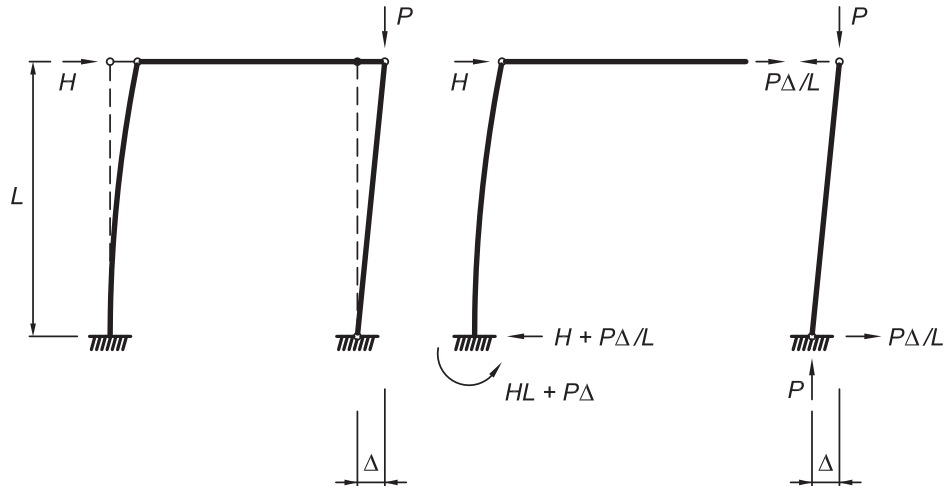

Fig. 4-1. Illustration of P-Δ *effect.*

2000). These provisions established limits on the maximum P-Δ effects and imposed second-order analysis requirements in some cases. The current provisions, summarized from ASCE/SEI 7-05 (ASCE, 2005), are as follows:

Section 12.8.7 requires the calculation of a *seismic stability coefficient*, θ, for each seismic load combination:

$$\theta = \frac{P_x \Delta}{V_x h_{sx} C_d} \qquad \text{(4.2-1, ASCE/SEI 7 12.8-16)}$$

where

P_x = gravity load in the combination (with a maximum load factor of 1.0), kips

$\frac{\Delta}{V_x C_d}$ = elastic sidesway flexibility of the structure under a lateral load, V_x, calculated using the nominal elastic (unreduced) structural stiffness, in./kip

h_{sx} = story height at the level being considered, in.

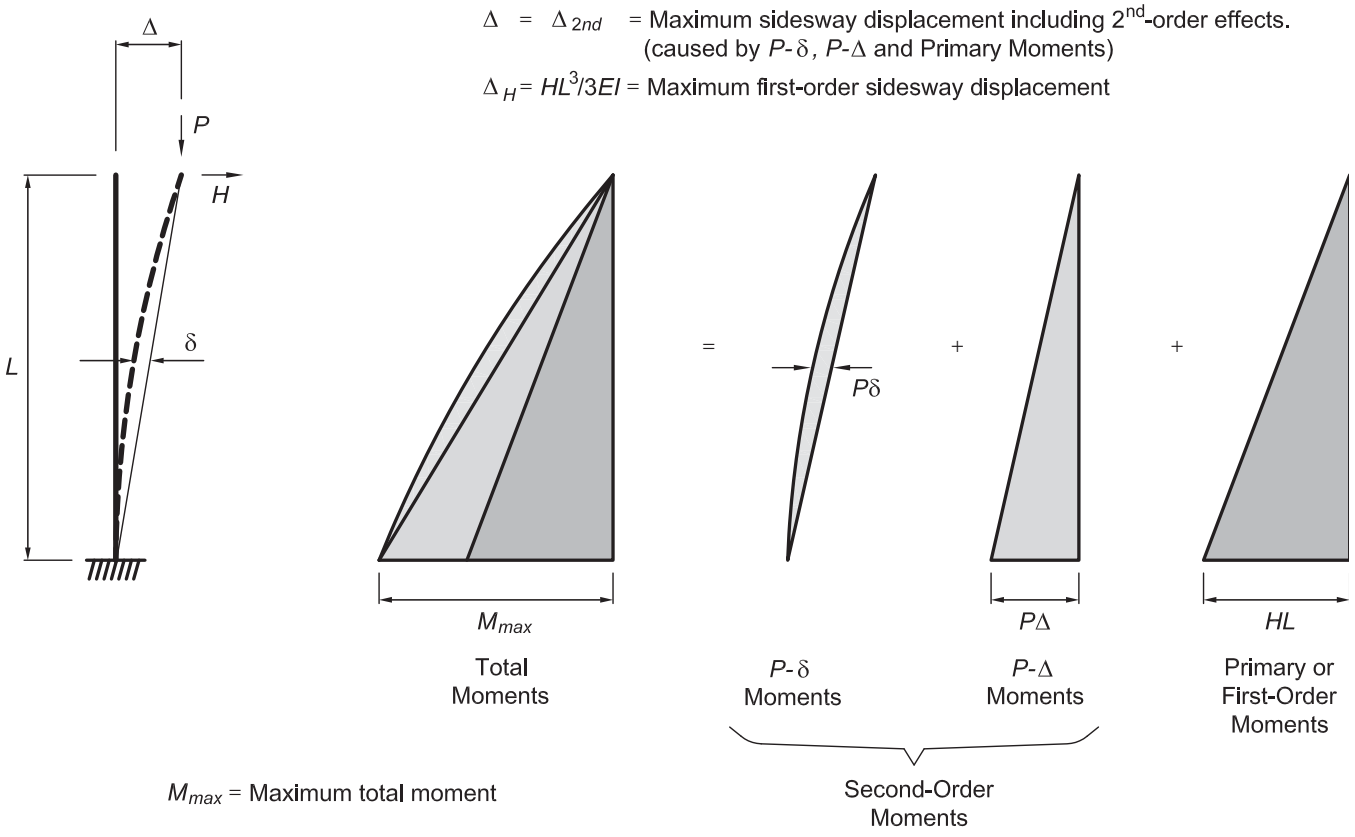

Fig. 4-2. Illustration of combined P-δ *and* P-Δ *effects on sidesway moments and displacements.*

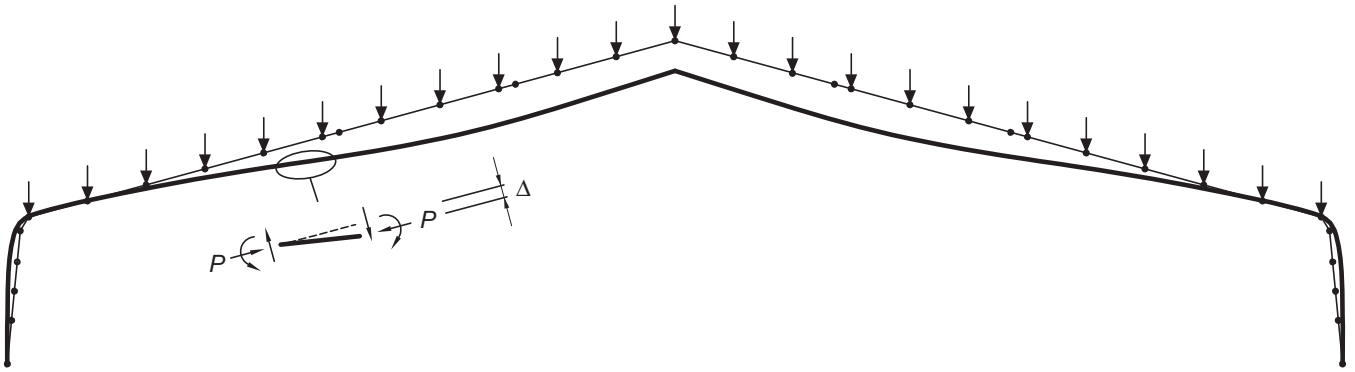

Fig. 4-3. Capture of member P-δ *effects by subdivision into shorter-length elements.*

Here, θ is an estimate of the ratio of the gravity load to the elastic sidesway buckling strength of the frame and is an indicator of the magnitude of the expected P-Δ effects. Structures with θ less than or equal to 0.10 have small P-Δ effects and are exempt from any ASCE 7 second-order analysis requirement. Structures with θ between 0.10 and an upper limit that can range as high as 0.25 are permitted, but must be designed using an analysis that includes P-Δ effects. Structures with θ above the upper limit of 0.25, corresponding to a P-Δ amplification of the sidesway deflections and moments of $1/(1 - 0.25) = 1.33$, are not permitted.

These provisions have been interpreted to apply only to seismic load combinations. Bachman et al. (2004) indicate that the calculation of θ need never include the roof live load or snow load except in the case of flat roof snow loads of greater than 30 psf, where 20% of the snow load is to be included unless otherwise required by the authority having jurisdiction. This usually limits P_x to a fairly small percentage of the full gravity design load. As a result, for single-story metal building frames, θ seldom exceeds the upper limit. Wide modular frames can have θ exceeding 0.10, but θ can usually be brought down to 0.10 or less by increasing the frame lateral stiffness slightly.

These provisions require consideration of significant P-Δ effects under seismic loading but do not provide any assurance of adequate second-order response under other load combinations that have much higher gravity loading. These conditions are addressed in Section 4.3.

4.3 AISC STABILITY REQUIREMENTS

Section C1 of the AISC *Specification* requires that "Stability shall be provided for the structure as a whole and for each of its elements." Stability for the individual members of the structure is provided by compliance with the design provisions of Chapters E, F, G, H and I along with the member bracing requirements of Appendix 6. Overall stability of the structure is provided by selecting an appropriate analysis approach combined with a corresponding set of member (or component) design constraints.

Any method of design that considers the following effects is permitted by the AISC *Specification*.

1. Second-order effects
   - P-Δ effects
   - P-δ effects
2. Geometric imperfections
   - System out-of-plumbness
   - Member out-of-straightness
3. Member stiffness reductions due to residual stress
4. Member flexural, shear and axial deformations
5. Connection flexibility

The second-order effects required for the design calculations are those from the geometric nonlinearity of the elastic structure. In essence, this means that equilibrium must be considered in the deflected elastic configuration of the structure rather than in the initial geometry, as is the case for first-order elastic analysis. A wide variety of approaches for handling elastic geometric nonlinearity are available in commercial and in-house software, some of which are discussed in Chapter 6. Various approximate hand methods are also available and are satisfactory in certain cases.

Overall geometric imperfections in a frame can be handled in the preceding elastic analysis in two ways. The most intuitively obvious approach is to incorporate the maximum expected or permitted out-of-plumbness of the structure in the initial modeling of the geometry of the structure. An alternative approach is to include notional loads, which are lateral loads calibrated to produce the same sidesway as the expected out-of-plumbness. Member out-of-straightness has traditionally been handled in the column strength curves but can alternatively be handled by explicit modeling of out-of-straightness between member ends, if preferred. For members and frames subjected predominantly to in-plane bending, the geometric imperfections represented by explicit modeling or notional loads are those in the plane of the member and/or frame.

The effect of member stiffness reduction due to residual stress has traditionally been incorporated in the column strength equations in conjunction with the use of member effective lengths, rather than being considered directly in the analysis. This approach is still permitted in the Effective Length Method. However, it is now possible to consider this effect directly in the analysis. This is the approach taken in the direct analysis method and the first-order analysis method procedures outlined later, which do not require calculation of effective length factors.

The calculation of axial and flexural deformations is a basic component of the direct stiffness approach used in most modern elastic frame analysis software. Shear deformations are not often included in the analysis because their influence on the results is usually small, and therefore, the extra required calculations are not justified. For cases in which shear deformations are significant, they are an option to include in most general analysis programs and can be incorporated into in-house software.

Connection flexibility is routinely handled in elastic analysis software for cases in which the connections are fully restrained (FR) moment connections or simple shear connections by specifying ideally rigid or ideally pinned connections, respectively. For prismatic members, the AISC *Specification* Commentary (AISC, 2005) suggests that a connection with a rotational secant spring stiffness of at least $20EI/L$ at full-service loads can be considered rigid and one with a stiffness below $2EI/L$ can be considered pinned with

respect to stiffness. However, connection strength must also be considered when evaluating whether connections may be considered as ideally rigid or ideally pinned.

Bjorhovde, Colson and Brozzetti (1990) propose a connection classification system that may be interpreted as follows: Connections may be considered rigid when they have a secant rotational stiffness greater than $0.5EI/d$ at $0.7M_p$ of the connecting member, where d is the member depth. Connections with a secant rotational stiffness less than $0.1EI/d$ at $0.2M_p$ of the connecting member should be considered as pinned. Although the Bjorhovde et al. (1990) system was originally developed with prismatic members in mind, it may be applied as an approximate classification approach in frames composed of web-tapered members, using d as the depth of the member at the connection. Connections with stiffnesses between these limits are classified as partially restrained (PR). Inclusion of PR connection stiffness and strength in the analysis is required by Section B3.6b of the AISC *Specification*. Including PR spring stiffnesses in off-the-shelf or in-house software is technically straightforward, but is complicated by shakedown behavior in PR connections and the fact that connections cannot be designed until after the members are selected. A number of commercial software programs currently allow the engineer to also address connection strength by defining the connection's full moment-rotation response. Section B3.6 of the *Specification* also requires that the ductility of simple and PR connections be checked.

4.4 STABILITY DESIGN METHODS

The AISC *Specification* provides three stability design methods that account for items 1 through 3 in Section 4.3. In the following discussions these methods are referred to as:

1. The Effective Length Method (ELM), referred to as "design by second-order analysis" in Section C2.2a of the AISC *Specification*.
2. The Direct Analysis Method (DM) in Appendix 7 of the AISC *Specification*.
3. The First-Order Analysis Method (FOM), referred to as "design by first-order analysis" in Section C2.2b of the AISC *Specification*.

Each of the methods holds certain advantages. The AISC *Specification* also permits the use of any other design method that accounts for all of the elements listed in Section 4.3; however, selecting from the three methods included in the AISC *Specification* is the most practical approach for most engineers.

The primary advantage of the ELM is that experienced steel engineers will already be familiar with many of its elements. The DM holds the advantages that (1) it may be used for all structures and load combinations, (2) it provides the most accurate assessment of internal forces and moments, and (3) columns may be designed without calculation of K factors. The virtues of the FOM are that (1) it permits design without a second-order analysis (an assumed second-order amplification is implicit in this method), and (2) it permits the design of columns without the calculation of K factors.

Theoretical details of the differences between the methods are covered in the AISC *Specification* Commentary and numerous research papers (Maleck and White, 2003; Deierlein, 2003, 2004; Kuchenbecker et al., 2004; Surovek-Maleck and White, 2004a, 2004b; Nair, 2005; Martinez-Garcia and Ziemian, 2006; White et al., 2007a; and White et al., 2007b) and are not discussed in this document. From an implementation viewpoint, the differences between the methods are in the areas of:

1. Limits on structural characteristics that establish the applicability of the methods
2. The type of structural analysis to be employed (first-order or second-order)
3. The method of accounting for nominal out-of-straightness and out-of-plumbness (use of notional loads or explicit modeling of imperfections in the analysis, or implicit inclusion in column strength equations via effective lengths)
4. The method for considering stiffness reduction from residual stress effects (directly in the analysis or implicitly in column strength equations via effective lengths)
5. Corresponding design constraints

The three methods differ (in analysis details, notional loads, and stiffness reductions, for example) and result in somewhat different required strengths for use in design. In general, for structures with significant second-order effects, the DM and the FOM will generate larger and more realistic sidesway moments than those determined using the ELM. On the other hand, the calculated in-plane column available strengths are larger and more easily determined using the DM and FOM. This is because these methods increase the member required flexural strengths, M_r, rather than reduce the member required axial strengths, P_c, to account for sidesway instability effects. Conversely, the ELM accounts for sidesway stability effects by reducing P_c via the use of $K > 1$ in moment frames, where K is the effective length factor, or by explicit use of buckling analyses to determine the theoretical column buckling loads.

The following sections provide an overview of the major implementation differences between the three methods.

4.4.1 Limits of Applicability

The DM is permitted for all structures and all load combinations. The usage of the other two methods is restricted to load combinations in which $\Delta_{2nd}/\Delta_{1st} \leq 1.5$, where Δ_{2nd} is the second-order drift and Δ_{1st} is the first-order drift for the strength combination being considered (the ASD load combinations multiplied by 1.6 or the LRFD load combinations). The limit of $\Delta_{2nd}/\Delta_{1st} \leq 1.5$ is applicable to an analysis conducted using unreduced stiffness, *EA* and *EI*. If reduced member stiffness is used for the analysis, as discussed in Section 4.4.4, this limit is $\Delta_{2nd}/\Delta_{1st} \leq 1.71$. Clear span frames often meet this restriction for all load combinations, but wide modular frames will often exceed this limit under the maximum gravity load combinations. As a result, the DM is the only method suitable for some load combinations of many metal building frames unless the designer is willing to limit $\Delta_{2nd}/\Delta_{1st}$ to no more than 1.5 for every load combination.

4.4.2 Type of Analysis

Both the ELM and the DM require that a second-order analysis be performed. As the name implies, the FOM does not require a second-order analysis. It provides a second-order amplification indirectly through the use of larger notional loads. The detailed requirements for the second-order analysis calculations required by the ELM and DM differ somewhat and are covered later in the sections that describe each method in detail.

4.4.3 Out-of-Plumbness

Each of the three methods requires the application of notional loads, or explicit modeling of the out-of-plumbness on which the notional loads are based, for at least some load combinations in the structural analysis. Notional loads are artificial lateral loads applied to the structure to account for geometric imperfections and other nonideal conditions that can induce or increase the sway of a structure.

Notional Loads

In all the methods of the AISC *Specification*, the equations for calculating notional loads are based on an assumed uniform out-of-plumbness of $L/500$. However, Appendix 7, Section 7.3(2), of the *Specification* states that this can be adjusted by the ratio of the expected out-of-plumbness to $L/500$ to account for a lesser assumed out-of-plumbness. Prior to the 2007 edition, Section 6.8 of Common Industry Standards in the *Metal Building Systems* (MBMA, 2002) specified an out-of-plumbness erection tolerance of $L/300$. Structures to be built to this standard should have their notional loads or nominal out-of-plumbness increased by the factor of $(L/300)/(L/500) = 1.67$ relative to the specified AISC value to account for this more liberal tolerance. The latest edition of the *Metal Building Systems Manual* (MBMA, 2007) has eliminated this exception; therefore, structures to be built to the 2007 MBMA standard should be designed using the notional loads specified in the AISC *Specification*.

Notional loads are calculated for each load combination as a percentage of the vertical load acting at each level for that load combination. Although the text of the AISC *Specification* defines notional loads as a percentage of the *gravity* load, the notional loads are more properly defined as a percentage of the *vertical* load, regardless of the source. This is apparent based on the direct correspondence between notional loads and the alternative explicit modeling of out-of-plumbness.

The physical out-of-plumb imperfections in the structure may be in either sidesway direction. However, the direction of application of the notional loads for each load combination is selected to increase the overall destabilizing effect for that combination. For gravity-only load combinations that cause a net (i.e., weighted average) sidesway either due to nonsymmetry of loads or geometry, the notional loads should be applied in the direction that increases the net sidesway. For structures with multiple stories or levels, and in which the sidesway deformations are in different directions in different stories or levels, it is necessary to include a pair of load combinations, separately considering the notional loads associated with a uniform out-of-plumbness in each direction. For load combinations involving lateral loads, the notional loads should be applied only in the direction that adds to the effect of the lateral loads. One need not apply notional loads in a direction opposite from the total lateral loads to minimize the reduction in internal forces in certain components due to the lateral load. For gravity load combinations with no sidesway, it is necessary to include a pair of load combinations, separately considering notional loads in each direction, unless symmetry of the frame is enforced by other means.

Separate notional loads should be applied at the top of each of the columns in proportion to the vertical load transferred to each column. In columns with axial forces applied at an intermediate location along the length, a proportional notional load should be placed at that location on the column. For any instances in which questions arise about the calculation and application of notional loads, the question may be answered by determining the lateral forces that are equivalent to the effect of the intended uniform nominal out-of-plumbness.

For ASD designs, notional loads calculated based on ASD load combination factors must be increased by a factor of 1.6 in all three methods. The 1.6 factor overestimates the second-order effects somewhat in ASD designs relative to LRFD, particularly where second-order effects are significant.

Explicit Modeling of Out-of-Plumbness

The AISC *Specification* permits explicit modeling of out-of-plumbness in the structural analysis in lieu of the use of notional loads for the DM. This avoids the need to determine how to apply notional loads in buildings with sloping roofs or floors, where the building geometry is nonrectangular or nonregular, or in structures where axial loads are applied at intermediate positions along the length of a member. This approach is easy to automate in computer-based design, and it allows the designer to better understand the true nature of internal forces set up in the structure from out-of-plumbness effects. However, unless automated methods of specifying out-of-plumbness are available in analysis software, it is often easier to apply notional loads along with the other applied loads on the structure rather than to modify the structure geometry.

The modeled out-of-plumbness should be consistent with the erection tolerances specified for the structure. Therefore, if the erection tolerances are smaller than $L/500$, a reduced uniform out-of-plumbness equal to the specified erection tolerance may be employed. Also, where a larger erection tolerance is permitted, this larger tolerance should be used as the modeled uniform out-of-plumbness in the structural analysis.

The physical out-of-plumb imperfections in the structure may be in either sidesway direction. However, the direction of the modeled uniform out-of-plumbness for each load combination is selected to increase the overall destabilizing effect for that combination. For gravity-only load combinations that induce a net sidesway, the modeled out-of-plumbness should be in the direction of the net sidesway. For structures with multiple stories or levels and in which the sidesway deformations are in different directions in different stories or levels, two different uniform out-of-plumb geometries are required to capture the potential overall destabilizing effects in both directions. For load combinations involving lateral loads, the out-of-plumbness should be in the direction of the lateral loads. For a gravity load combination with no sidesway, it is necessary to consider a uniform out-of-plumbness in both directions unless any symmetry of the design is enforced by other means.

Only two different out-of-plumb geometries are typically required to cover the overall destabilizing effects for all load combinations. In contrast, the corresponding notional loads discussed in the previous section are, in general, different for each load combination (although the notional loads may be taken conservatively as the maximum values from all the load combinations).

For the ELM in all cases, and the DM in some cases, the notional loads are specified as minimum lateral loads in the gravity-only load combinations. That is, they are not used in combination with other lateral loads. Consequently, out-of-plumbness need not be included in the model for these load combinations. Modeling out-of-plumbness for all load combinations is permitted but will result in conservative results for lateral load combinations in which notional loads are not required. In cases where the notional loads are specified as additive rather than minimum, the model must include out-of-plumbness (or out-of-plumbness effects via notional loads) regardless of the magnitude of the lateral loads.

4.4.4 Stiffness Reduction

Only the DM requires explicit consideration of member stiffness reduction due to the combined effects of residual stresses and distributed yielding with member axial forces and moments in the structural analysis. This is handled by reducing the flexural stiffness in moment frames and the axial stiffness in braced frames to 80% of their nominal elastic values in the second-order structural analysis. Where the axial compression load in a flexural member contributing to lateral stability exceeds 50% of the yield load, the flexural stiffness is further reduced. This is discussed in detail later. The other two methods consider member stiffness reductions only implicitly, either via the calculation of the column strengths using effective lengths or by the calculation of a larger notional lateral load.

4.4.5 Design Constraints

The DM and the FOM permit the design of columns for in-plane buckling using a length equal to the actual unsupported length ($K = 1$), or a smaller length in some cases. For moment frames, the ELM requires the calculation and use of elastic buckling load values (or the corresponding K factors) determined using a sidesway buckling analysis of the structure unless $\Delta_{2nd}/\Delta_{1st} \leq 1.1$. If $\Delta_{2nd}/\Delta_{1st} \leq 1.1$, the in-plane flexural buckling load may be calculated based on the actual member length and idealized pinned-pinned end conditions (i.e., $K = 1$).

4.5 COMMON ANALYSIS PARAMETERS

Several parameters are used throughout the text of the stability requirements in the AISC *Specification* to establish limits of applicability of various provisions and in other calculations. These are defined as follows:

4.5.1 αP_r

αP_r is the required axial compressive strength, P_r, multiplied by the factor α where $\alpha = 1.6$ for ASD and $\alpha = 1.0$ for LRFD.

For LRFD, αP_r is simply the required axial compressive strength determined using the LRFD load combination factors for the load combination under consideration. For ASD, αP_r is the required axial compression strength determined

using ASD load combination factors multiplied by 1.6, to give an approximation of the required strength under ultimate conditions.

αP_r is used in the determination of whether the FOM may be used. It is also used in the DM to determine whether P-δ effects can be neglected in the calculation of the sidesway displacements, and to calculate the required stiffness reduction. αP_r is also used in approximate second-order analysis techniques such as the B_1-B_2 method.

4.5.2 P_{eL} or $\gamma_{eL}P_r$

P_{eL} is the nominal in-plane elastic flexural buckling strength of a member subjected to axial compression force and having assumed ideally pinned-pinned end conditions. This parameter is used extensively in the provisions for both the ELM and the DM as well as in the member design provisions. Consideration of the actual member rotational and sidesway restraint end conditions is handled subsequently within the AISC design procedures, via the calculation of other buckling loads or the corresponding effective length factors in the ELM, and via the modeling of the structure for the structural analysis.

In many cases it is more convenient to work with the equivalent parameter $\gamma_{eL}P_r$, which is the required strength, P_r, multiplied by the elastic buckling load ratio, $\gamma_{eL} = P_{eL}/P_r$. That is,

$$P_{eL} = \gamma_{eL}P_r \qquad (4.5\text{-}1)$$

where

P_{eL} = Euler buckling load, evaluated in the plane of bending, kips. This is the internal axial force at elastic buckling of the member, assuming simply supported end conditions.
P_r = required axial strength for the column, kips
γ_{eL} = a scalar ratio

Regardless of the complexity of the loadings (e.g., stepped loading or distributed axial loading) or the member geometry (e.g., tapered and/or stepped geometry), there is only one γ_{eL} corresponding to the member elastic flexural bucking strength. However, for stepped or distributed axial loading, P_r and P_{eL} vary along the member length.

The elastic flexural buckling strength can also be expressed as:

$$F_{eL} = \gamma_{eL}F_r \qquad (4.5\text{-}2)$$

where

F_{eL} = axial stress at elastic buckling of the member, assuming simply supported end conditions, ksi
Fr = required axial stress for the column, ksi

For a straight, geometrically perfect prismatic column with a constant axial loading,

$$P_{eL} = \frac{\pi^2 EI}{L^2} \qquad (4.5\text{-}3)$$

For a tapered I-shaped member, there is no exact closed-form solution for P_{eL}. However, several approaches to a solution are available:

1. P_{eL} can be determined by an elastic eigenvalue buckling analysis. Many advanced finite element and/or frame analysis programs can be used to calculate elastic buckling multipliers, γ_{eL}, corresponding to a given required axial strength using numerical eigenvalue solution techniques. P_{eL} is then determined as the required axial compression strength, used in the analysis, multiplied by γ_{eL}. The quality of such solutions depends on the accuracy of tapered member modeling, element choice, and meshing. The engineer should run the benchmark problems provided in Appendix C to establish the appropriateness of the computer program and modeling techniques prior to use in design. Although this approach has the advantage of handling essentially any imaginable geometry and loading, it may not be practical in a production environment unless the finite element modeling is automated and integrated into analysis-design software.

2. P_{eL} can be determined by the method of successive approximations (Timoshenko and Gere, 1961). This technique uses an iterative beam analysis to find the axial load, $\gamma_{eL}P_r$, at which the beam deflections resulting from applied P-δ moments are a uniform multiple of the deflections assumed to calculate the P-δ moments. This is an iterative process in which (1) a load, P_r, and a deflected buckling mode shape are assumed; (2) the P-δ moments from the assumed deflections times the assumed axial load are calculated; (3) the calculated P-δ moments are applied in a beam analysis of the member to compute a new deflected shape; and (4) the new deflected shape is substituted as a new approximation for the buckled geometry. The process is continued iteratively until the calculated deflections everywhere along the beam are a uniform multiple, γ_{eL}, of the assumed deflections. P_{eL} is then determined as the assumed axial load, P_r, multiplied by γ_{eL}.

   The method of successive approximations requires relatively few calculations compared with eigenvalue solution techniques, is easily programmed, and is adaptable to handle various tapers and steps in the member loading and geometry. The method is illustrated in Timoshenko and Gere (1961) with an example in a format easily adapted to a spreadsheet or procedural computer program. See Appendix C of this Guide for benchmark examples of web-tapered members.

3. P_{eL} can be approximated with good accuracy for a single linearly tapered member with simply supported conditions and supporting a constant internal axial force, and having no plate or taper changes, as:

$$P_{eL} = \frac{\pi^2 EI'}{L^2} \quad (4.5\text{-}4)$$

where

I' = moment of inertia calculated using the depth at $0.5L$ $(I_{small}/I_{large})^{0.0732}$ from the small end, in.^{4}

This empirically derived expression gives results accurate to within several percentage points for the range of members addressed in this document. The preceding approximation should not be used for any buckling solution in which anything other than simply supported end conditions are assumed. That is, the preceding expression for I' is valid solely for idealized simply supported end conditions.

4. For linearly tapered members subjected to nonuniform axial compression, γ_{eL} can be calculated conservatively as $P_{eL}/(P_r)_{max}$, where P_{eL} is calculated using Equation 4.5-4 and $(P_r)_{max}$ is the largest internal axial compression along the member length.

4.5.3 $\Delta_{2nd}/\Delta_{1st}$

$\Delta_{2nd}/\Delta_{1st}$ is the ratio of story drifts calculated from a second-order and first-order analysis, respectively. This ratio is used to establish the applicability of the approved design methods, to establish the applicability of the $K = 1$ provisions of the ELM [2005 AISC *Specification* Section C2.2a(4)], to determine whether notional loads are additive to lateral loads in the DM, and also in the B_1-B_2 method.

Unless otherwise noted, this ratio is calculated from analyses using unreduced member stiffnesses. For information on calculating $\Delta_{2nd}/\Delta_{1st}$ for gable frames, see Section 6.3.3.

$\Delta_{2nd}/\Delta_{1st}$ is calculated separately for each load combination. This parameter gives an indication of the significance of the second-order effects in a load combination. No maximum limit on $\Delta_{2nd}/\Delta_{1st}$ is established by the AISC *Specification* (AISC, 2005). Values below 1.1 are considered insignificant. Values above 1.5 are considered large second-order effects. As such, the design must be conducted using the DM when this threshold is exceeded. Values between 1.1 and 1.5 are considered moderate second-order effects. The design may be conducted either by the DM or by the ELM in these cases.

The reader is cautioned against using the ratio M_{2nd}/M_{1st} as a substitute for $\Delta_{2nd}/\Delta_{1st}$. The moments usually include significant first-order gravity components that will obscure the magnitude of the second-order effects.

4.6 DETAILED REQUIREMENTS OF THE STABILITY DESIGN METHODS

The following sections summarize the detailed requirements for each of the three stability design methods discussed earlier. Additional information on first-order and second-order frame analysis is given in Chapter 6.

4.6.1 The Effective Length Method (ELM)

1. The ELM is only permitted for load combinations where $\Delta_{2nd}/\Delta_{1st} \le 1.5$.
2. A second-order analysis, considering both P-Δ and P-δ effects as detailed below, is required:
   (a) The P-Δ effects on the nodal displacements must be considered. The P-δ effects on the nodal displacements may be neglected in the calculation of required strengths because the ELM beam-column unity checks are insensitive to these effects.
   (b) The P-δ effects on the internal element moments (between the nodes) may be neglected in individual elements in load combinations when $\alpha P_r \le 0.02 P_{e\ell}$ for that element,

   where

   $P_{e\ell}$ = flexural column buckling load based on the cross-section geometry and the element length between the nodal locations with idealized simply supported nodal end conditions, kips

   Otherwise, they must be considered.
   (c) Internal P-δ moments may be included by performing a second-order analysis to determine the nodal displacements, forces and moments, and then calculating the second-order internal moments in each element as follows (Guney and White, 2007):
      (i) Calculate δ_{1st}, the first-order displacement perpendicular to the element chord caused by the second-order nodal forces and any applied loads within the element length, at any locations of interest.
      (ii) Calculate the second-order displacement at each of the preceding locations as

$$\delta_{2nd} = \frac{\delta_{1st}}{1 - \alpha P_r / P_{e\ell}} \quad (4.6\text{-}1)$$

where $P_{e\ell}$ may be estimated for linearly tapered segments using P_{eL} from Equation 4.5-4, but applied to the element length, ℓ.

(iii) Calculate the required internal second-order moment at each of the above locations as

$$M_r = M_{1st} + \alpha P_r \delta_{2nd} \qquad (4.6\text{-}2)$$

where

M_{1st} = first-order moment at a given position along the element length, caused by the second-order nodal forces and any applied loads within the element length, kip-in.

This procedure provides good accuracy for general cases involving prismatic or nonprismatic member geometry for values of $\alpha P_r/P_{e\ell} \le 0.7$. This limit is satisfied in all cases when (1) a P-Δ only analysis or a second-order analysis using an element geometric stiffness based on element cubic transverse displacements is used, and (2) the number of elements per member is greater than or equal to that specified by the guidelines discussed subsequently in Section 6.2. Alternatively, the nonsway amplifier

$$B_1 = \frac{C_m}{1 - \alpha P_r / P_{e\ell}} \ge 1.0 \qquad (4.6\text{-}3a)$$

may be applied to all the moments M_{1st} throughout the length of a given element, except those at the ends. Equation 4.6-3a is useful for elements in linearly tapered members that do not have any applied transverse loads. In this case, the equivalent uniform moment factor, C_m, may be expressed approximately as

$$C_m = 0.6 + 0.4\left(f_1/f_2\right) \qquad (4.6\text{-}3b)$$

where

f_2 = the absolute value of the largest compressive flexural stress at either element end node, ksi

f_1 = $2f_{mid} - f_2$, ksi (4.6-3c)

f_{mid} = flexural stress due to M_{1st} at the mid-length of the element in the flange containing the stress f_2, taken as positive for compression and negative for tension, ksi

Equation 4.6-3b accounts for the fact that a linear variation in M_{1st} produces a nonlinear variation in the corresponding flexural stress along the length of a tapered member. The value f_1 is the flange stress obtained by extending a line through f_2 and f_{mid} to the opposite element end node.

In many cases, Equation 4.6-3a gives $B_1 = 1.0$, indicating that the second-order amplification of the internal moments may be neglected. Equations 4.6-1 and 4.6-2 generally provide better accuracy for both prismatic and nonprismatic members compared to the amplified moments determined using Equation 4.6-3a. This is particularly true for elements with transverse applied loads, where the AISC *Specification* gives a conservative value of $C_m = 1.0$ and Table C-C2.1 in the AISC *Specification* Commentary gives refined equations for C_m that are applicable only for prismatic members with ideally pinned or ideally fixed end conditions. The use of $C_m = 1.0$ is recommended for general cases with transverse applied loads.

(d) P-δ effects must be included in the calculation of elastic column buckling strengths, P_{eL}, when using either an eigenvalue or the successive approximation approach. See Appendix B1.2 for guidance on subdividing the members into a sufficient number of smaller-length elements for matrix eigenvalue analyses.

(e) The accuracy of any second-order analysis program used should be tested using appropriate benchmark problems such as those provided in Appendix C. Particular care should be taken to establish whether P-δ effects are correctly included in the analysis. Sections 6.2.1 and 6.2.2 provide guidelines for subdivision of members to ensure sufficient accuracy with respect to these effects.

The *amplified first-order elastic analysis approach* (e.g., the B_1-B_2 approach) is an acceptable second-order analysis method. If this approach is employed, Equation C2-6b in the AISC *Specification* (or the more refined Commentary Equation C-C2-6 not including the limit $1.7HL/\Delta_H$) is recommended for the definition of ΣP_{e2} in Equation C2-3.

Implementation of the B_1-B_2 may involve more work compared to other alternative approaches [e.g., a general P-Δ analysis as discussed earlier, or the alternate amplifier-based method discussed by White et al. (2007a, 2007b)]. The amplifier-based methods are particularly difficult to implement and lose accuracy for gable frames, where the sidesway column displacements are generally not the same, and for frames with unequal height columns, where the methods must be modified to account for the different column heights (White and Kim, 2006).

The reader should note that the term *amplified first-order elastic analysis* is typically used to refer to the specific B_1-B_2 method of calculating the second-order forces and moments. It is important to distinguish this term from the terms used for the different design methods, i.e., the ELM, the DM and the FOM. The B_1-B_2 second-order analysis method is one of many methods of second-order analysis that may be used for the calculation of the forces and moments in either of the design methods that require a second-order analysis (the ELM and the DM).

3. Given the satisfaction of the preceding requirements for the second-order elastic analysis calculations, the ELM structural analysis model must include the following attributes:

   (a) The analysis is conducted with nominal elastic stiffnesses, i.e., no member stiffness reductions.

   (b) Minimum lateral loads of 0.002 times the vertical load, Y_i, applied at each level are required for all gravity-only load combinations. For gable frames and for frames with stories having unequal height columns, it is recommended that individual notional lateral loads equal to $0.002y_i$ should be applied at the top of each column, where y_i is the vertical load transferred to the column at its top. Also, for columns with intermediate vertical loads along their length, a notional lateral load of $0.002y_i$ should be applied at the location of the intermediate vertical loads, where y_i is the intermediate vertical load applied to the column. This is necessary to capture the geometric imperfection effects on different height columns, as well as to capture the behavior in cases where the lateral displacements are generally different at the different column locations.

   In lieu of applying the notional lateral loads, one can impose an out-of-plumbness of $0.002H$ on the structure for analysis of the gravity-only load combinations, where H is the vertical height above the base, or in general, the node(s) having the minimum vertical coordinate. This may be implemented by shifting all the nodes of the analysis model horizontally by $0.002H$ relative to the node(s) at the base of the structure. For cases in which questions arise about the appropriate application of the notional lateral loads, one should always return to the model where the uniform out-of-plumbness is represented explicitly in the structural model. The appropriate notional loads are the ones that are equivalent to the effect of this out-of-plumbness.

   For both notional loads and explicit modeling of out-of-plumbness, the factor 0.002 is based on an assumed erection tolerance of $L/500$. For adjustments to this factor to account for structures built to different tolerances, see Section 4.4.3.

   (c) For ASD, the analysis is conducted using loads of 1.6 times those from ASD load combinations. The resulting member forces and moments are divided by 1.6 for the member design calculations. The 1.6 multiplier also applies to any notional loads added to satisfy item 3(b).

4. The in-plane flexural buckling strength of columns and beam-columns, P_{ni}, is determined as follows:

   (a) For members in load combinations where $\Delta_{2nd}/\Delta_{1st} \leq 1.1$, calculate P_{ni} based on the actual unbraced length with $K = 1.0$, i.e., assuming idealized pinned-pinned end conditions on the actual unbraced length.

   (b) For other cases, P_{ni} must be calculated using an effective length factor, K, or the corresponding column buckling stress, F_e, determined from a sidesway buckling analysis of the structure. Because member taper violates one of the inherent assumptions of the traditional alignment charts, more advanced methods of determining K or F_e are normally required. See Appendix B for further information on the calculation of elastic buckling strengths of tapered columns and frames.

4.6.2 The Direct Analysis Method (DM)

1. The DM is permitted for all structures and load combinations.

2. A second-order analysis with characteristics similar to those discussed in item 2 of Section 4.6.1 is required. However, there are a few important differences. The following discussion repeats much of the discussion in item 2 of Section 4.6.1 with an emphasis on the specific requirements in the context of the DM.

   (a) Generally, both the P-Δ and P-δ effects on the nodal displacements must be considered in the DM. The AISC *Specification* Appendix 7, Section 7.3(1), indicates that if $\alpha P_r < 0.15P_{eL}$ for all members whose flexural stiffnesses are considered to contribute to the lateral stability of the structure, the P-δ effect on the lateral displacements may be neglected in the analysis. Although not defined in the AISC *Specification*, "members whose flexural stiffnesses are considered to contribute to the lateral stability" in this context is intended to apply to both beams and columns in unbraced frames. For

nonrectangular structures such as gable frames, the term "lateral displacements" may be interpreted as the general nodal displacements in the frame analysis model.

With the exception of sway columns without significant transverse member loads, where both ends have substantial rotational restraints, this Guide recommends that when $\alpha P_r > 0.05\ \overline{P}_{eL}$, where $\overline{P}_{eL}$ is the elastic buckling load based on the overall member length determined as discussed in Section 4.5.2 but using the reduced elastic stiffness of the DM analysis model discussed later, the member should be subdivided with intermediate nodes along its length when a P-Δ only analysis is employed. This ensures better accuracy of the element nodal displacements and moments along the member length than will be achieved using the previous AISC *Specification* rule when αP_r exceeds $0.05\ \overline{P}_{eL}$. The sidesway moments in fixed-base columns, and columns with top and bottom rotational restraint from adjacent framing, may be analyzed sufficiently with a P-Δ only analysis and a single element per member when $\alpha P_r \le 0.12\ \overline{P}_{eL}$. Second-order analysis procedures that include both P-Δ and P-δ effects in the formulation require fewer elements. Detailed guidelines for the necessary number of elements are provided subsequently in Sections 6.2.1 and 6.2.2 of this Guide. These guidelines and the above recommendations are based on Guney and White (2007). In many cases a sufficient subdivision will occur naturally with tapered members due to the frequency of plate and/or geometry changes. However, extra nodes may be required for prismatic members and long tapered members without changes of plates or taper.

(b) The P-δ effects on the internal element moments (between the nodes) may be neglected in individual elements in load combinations when $\alpha P_r \le 0.02\ \overline{P}_{e\ell}$ for that element (Guney and White, 2007),

where

$\overline{P}_{e\ell}$ = flexural buckling load based on the cross-section geometry and the element length between the nodal locations with idealized simply supported nodal end conditions, determined using the reduced elastic stiffnesses of the DM analysis model discussed later, kips

(c) Internal P-δ moments may be included by performing a second-order analysis to determine the nodal displacements, forces and moments, then calculating the second-order internal moments in each element using the forces, moments, and displacements calculated with the reduced stiffness from the DM analysis as follows:

(i) Calculate δ_{1st}, the first-order displacement perpendicular to the element chord caused by the second-order nodal forces and any applied loads within the element length, at any locations of interest.

(ii) Calculate the second-order displacement at each of the preceding locations as

$$\delta_{2nd} = \frac{\delta_{1st}}{1 - \alpha P_r / \overline{P}_{e\ell}} \tag{4.6-4}$$

where $\overline{P}_{e\ell}$ may be estimated for linearly-tapered segments using $\overline{P}_{eL}$ from Equation 4.5-4, but applied to the element length, ℓ, and using the reduced elastic stiffness of the DM analysis model.

(iii) Calculate the required internal second-order moment at each of the above locations as

$$M_r = M_{1st} + \alpha P_r \delta_{2nd} \tag{4.6-5}$$

where

M_{1st} = the first-order moment at a given position along the element length, caused by the second-order nodal forces and any applied loads within the element length, kip-in.

This procedure provides good accuracy for general cases involving prismatic or nonprismatic member geometry for values of $\alpha P_r / \overline{P}_{e\ell} \le 0.7$ (Guney and White, 2007). This limit is satisfied in all cases when a sufficient number of elements is employed in a P-Δ-only analysis or a second-order analysis using an element geometric stiffness based on element cubic transverse displacements using the guidelines discussed subsequently in Section 6.2. Alternatively, the AISC (2005) nonsway amplifier

$$B_1 = \frac{C_m}{1 - \alpha P_r / \overline{P}_{e\ell}} \ge 1.0 \tag{4.6-6a, from \textit{Spec.} Eq. C2-2}$$

may be applied to all the moments, M_{1st}, throughout the length of a given element, except those at the ends. Equation 4.6-6a is useful for elements in linearly tapered members that do not have any transverse applied loads. In this case, the equivalent uniform moment factor, C_m, may be expressed approximately as

$$C_m = 0.6 + 0.4\left(f_1/f_2\right) \qquad (4.6\text{-}6b)$$

where

f_2 = the absolute value of the largest compressive flexural stress at either element end node, ksi

f_1 = $2f_{mid} - f_2$, ksi (4.6-6c)

f_{mid} = flexural stress due to M_{1st} at the mid-length of the element in the flange containing the stress f_2, taken as positive for compression and negative for tension, ksi

Equation 4.6-6b accounts for the fact that a linear variation in M_{1st} produces a nonlinear variation in the corresponding flexural stress along the length of a tapered member. The value f_1 is the flange stress obtained by extending a line through f_2 and f_{mid} to the opposite element end node.

In many cases, Equation 4.6-6a gives B_1 = 1.0, indicating that the second-order amplification of the internal moments may be neglected. Equation 4.6-4 in conjunction with Equation 4.6-5 generally provides better accuracy for both prismatic and nonprismatic members compared to the application of Equation 4.6-6a. This is particularly true for elements with transverse applied loads, where the AISC *Specification* gives a conservative value of C_m = 1.0 and Table C-C2.1 in the AISC Commentary gives refined equations for C_m that are applicable only for prismatic members with ideally pinned or ideally fixed end conditions. The use of C_m = 1.0 is recommended for general cases with transverse applied loads.

(d) The accuracy of any second-order analysis program used should be tested using appropriate benchmark problems such as those provided in Appendix C. If the benchmark tests are satisfied, the software may be assumed to provide adequate results without subdividing the members into multiple elements as recommended in item 2(a).

3. Given the satisfaction of the preceding requirements for the second-order elastic analysis calculations, the DM analysis model must include the following attributes:

(a) The analysis must be conducted with elastic stiffness reductions for all members whose flexural stiffness is considered to contribute to the lateral stability of the structure. Although not defined in the AISC *Specification*, "members whose flexural stiffness is considered to contribute to the lateral stability" in this context is intended to apply only to columns in unbraced frames. This is accomplished by reducing the value of *EI* and/or *EA* in the formulation of the member stiffnesses.

For members whose flexural stiffnesses contribute to the lateral stability:

If $\alpha P_r/P_y \le 0.5$, use $0.8EI$ in the flexural stiffness terms of the second-order analysis.

If $\alpha P_r/P_y > 0.5$, use $0.8\tau_b EI$ in the flexural stiffness terms of the second-order analysis,

where

$$\tau_b = 4\frac{\alpha P_r}{P_y}\left(1 - \frac{\alpha P_r}{P_y}\right) \qquad (4.6\text{-}7)$$

P_y = smallest value of $A_g F_y$ of the member, kips

This reduction need only be applied to the portion of a member where $\alpha P_r/P_y > 0.5$. Alternatively, notional loads of $0.001Y_i$, in addition to those required by item 3(b) (following), may be used along with a stiffness of $0.8EI$ in lieu of reducing the stiffness to $0.8\tau_b EI$.

For members whose axial stiffnesses contribute to the lateral stability (primarily members of braced frames), use $0.8EA$ in the axial stiffness terms of the second-order analysis.

In lieu of modifying the cross-section properties, *A* and *I,* by 0.8, it is acceptable (and recommended) to reduce the modulus of elasticity, *E*, by the factor 0.8 for all members in the second-order elastic analysis. This avoids small problems that can occur in some cases, such as unintended additional drift of a frame due to differential column axial shortening between gravity columns and lateral-load resisting columns when beams or rafters from the lateral-load resisting system are framed into the gravity columns. This approach also gives results that more closely match those from the more advanced methods to which the DM was calibrated. Note that the value of *E* is not reduced when applying other *Specification* provisions, such as slenderness limit checks (2005 AISC *Specification* Table B4.1) or column strength equations.

(b) Minimum lateral loads of 0.002 times the vertical load, Y_i, applied at each level are required for gravity-only load combinations when $\Delta_{2nd}/\Delta_{1st} \le 1.5$ ($\Delta_{2nd}/\Delta_{1st} \le 1.71$ based on the reduced stiffness). Alternatively, explicit out-of-plumbness may be

modeled in lieu of notional loads.

For load combinations where $\Delta_{2nd}/\Delta_{1st} > 1.5$ ($\Delta_{2nd}/\Delta_{1st} > 1.71$ based on the reduced stiffness), the notional lateral loads must be added to any lateral loads already present in the combination.

For gable frames and for frames with stories having unequal height columns, it is recommended that individual notional lateral loads equal to $0.002y_i$ be applied at the top of each column, where y_i is the vertical load transferred to the column at its top. Also, for columns with intermediate vertical loads along their length, a notional lateral load of $0.002y_i$ should be applied at the location of the intermediate vertical loads, where y_i is the intermediate vertical load applied to the column.

These notional load and out-of-plumbness magnitudes are based on a specified maximum out-of-plumbness of $L/500$. For structures where a different out-of-plumbness is specified, the notional loads should be scaled linearly. Further discussions of this implementation of the notional lateral loads are provided in item 3(b) of Section 4.6.1 and in Section 4.4.3.

(c) For ASD, the analysis is conducted using loads of 1.6 times those from ASD load combinations. The resulting member forces and moments are divided by 1.6 for member design calculations. The 1.6 multiplier also applies to any notional loads added to satisfy item 3(b).

4. The in-plane flexural buckling strength of columns and beam-columns, P_{ni}, is calculated based on the actual unbraced length with $K = 1.0$ except as noted for the three cases discussed here, where simplifying extensions to the AISC *Specification* are provided. The reduced member stiffnesses in item 3(a) should not be used in the member strength calculations. The member resistances are always calculated using nominal (unreduced) stiffnesses.

   (a) For members with $\alpha P_r \le 0.10P_{eL}$ at all locations along their length, or stated more simply, for $\alpha/\gamma_{eL} \le 0.10$, P_{ni} may be taken as the equivalent cross-section axial yield strength accounting for local buckling effects, QP_y. This simplification is permissible because the in-plane stability effects are very minor at the member level for columns or beam-columns that satisfy the preceding limit. Many members in a typical single-story metal building frame will satisfy this limit. Note that P_{eL} and γ_{eL} in these expressions do not contain an overbar, i.e., these limits are checked using the nominal elastic stiffness.

   (b) If P-δ effects are included in the analysis model and an appropriate member out-of-straightness between nodes is also included in the model, P_{ni} may be taken as QP_y, even when $\alpha/\gamma_{eL} > 0.10$. This is permissible because the reduced stiffness and out-of-straightness in the analysis account sufficiently for the in-plane stability effects at the member level. The appropriate member out-of-straightness is an imperfection of $0.001L$ in the direction that the member deforms relative to a chord between its support points or points of connection to other members. A chorded representation of the out-of-straightness with a maximum amplitude at the middle of the unsupported length is considered sufficient.

   (c) For gable rafters, when the midspan work point (cross-section centroid) is offset above the rafter chord by $L_{chord}/50$ or more, where L_{chord} is the span length along the rafter chord between the cross-section centroids at the tops of the columns, P_{ni} may be taken as QP_y. This is permissible because the offset of the midspan work point for these types of members nullifies the importance of any out-of-straightness relative to the chord between the ends of the on-slope length of the rafters. For rafters framing between equal height columns, this requirement is satisfied in all cases when the pitch of the rafter centroidal axis is at least ½ in 12 throughout the span length.

4.6.3 The First-Order Method (FOM)

1. The FOM is only permitted for load combinations where $\Delta_{2nd}/\Delta_{1st} \le 1.5$. Because the objective of using the FOM is likely to be the avoidance of a second-order analysis, it is suggested that the ratio $\Delta_{2nd}/\Delta_{1st}$ be determined using the AISC *Specification* Equation C2-3 for B_2 with ΣP_{e2} taken from Equation C2-6b.

   In addition, for all members whose flexural stiffness contributes to the lateral stability, αP_r must be less than or equal to $0.5P_y$, where P_y is the lowest axial yield strength of the member.

2. A first-order analysis is performed as follows:

   (a) The analysis is conducted without member stiffness reductions.

   (b) Notional loads must be applied in addition to any lateral loads in each load combination. These are calculated as:

$$N_i = 2.1\left(\Delta/L\right)Y_i \ge 0.0042Y_i \qquad \text{(4.6-8, } \textit{Spec.} \text{ Eq. C2-8)}$$

where

Δ/L = highest ratio of first-order story drift under the strength load combination, Δ, to the story height, L, for all stories of the structure calculated using first-order deflection results
Contrary to the user note in AISC *Specification* Section C2.2b, for the FOM it is not necessary to multiply the gravity loads in the ASD load combinations by 1.6 prior to the analysis and then subsequently divide the results by 1.6, because the analysis is linear. Therefore, for design by ASD, Δ in Equation 4.6-8 should be based on 1.0 times the ASD load combinations. It is emphasized that this is the maximum first-order drift of all the stories under the strength load combination being considered.

Y_i = vertical load introduced at each level for each load combination, kips. For ASD, multiply the vertical loads by 1.6.

For gable frames or frames with stories with unequal height columns, Equation 4.6-8 should be used to determine a notional lateral load, N_i, applied at the top of each column; Y_i is defined as the vertical load transferred to each column at its top; and Δ/L is the maximum ratio of the individual column Δ values to the individual column heights, L, throughout the structure. For columns with intermediate vertical loads along their length, the equation should be used to determine a notional lateral load, N_i, applied at the location of the intermediate vertical loads, where Y_i is the intermediate vertical load applied to the column.

(c) The first-order analysis is carried out using the normal LRFD or ASD combinations. For ASD, do not use the 1.6 factor on the loads or results other than as required in the calculation of the notional loads in item 2(b).

(d) All moments from the first-order analysis must be multiplied by B_1. For web-tapered members, the amplification factor in Equation 4.6-1 is recommended for the calculation of B_1.

3. The in-plane flexural buckling strength of columns and beam-columns, P_{ni}, is determined based on the actual unbraced length between stories and idealized pinned-pinned end conditions ($K = 1.0$).

Chapter 5
Member Design

The following sections present specific member design provisions from the AISC *Specification* adapted to tapered members. For tapered members, some calculations, limit states and strength ratios are better expressed in terms of stresses rather than forces or moments; therefore, stress expressions are sometimes used in the following presentations, even where force-based design is ultimately used.

Because most members used in metal building frames are beam-columns, the results for the individual force or moment checks are presented in terms of strength ratios for further use in the combined strength equations.

In all of the following examples, it is assumed that the required strengths, P_r and M_r, include all second-order effects that must be determined from the structural analysis (see Section 4.6).

In the examples, in places where LRFD and ASD calculations should result in identical intermediate results but do not, due to rounding, the ASD value is arbitrarily used for further calculations. These places are indentified in the text.

5.1 KEY TERMINOLOGY

The following term is used extensively in this section:

γ_e = the ratio of the member elastic buckling force or moment to the required strength. This term is convenient for expressing the elastic buckling strength of the various buckling limit states. Its meaning is discussed in detail in Section 5.3.

5.2 AXIAL TENSION

Axial tension in tapered members is handled using the provisions of Chapter D of the AISC *Specification* with no modifications. Like prismatic members, tapered tension members are subject to the limit states of tensile yielding and tensile rupture. The available strength is the lower of the available strengths calculated from these two limit states.

For tapered members, the available strength varies along the length of the member due to the taper, so the selection of cross sections to evaluate depends both on the change in loading and the geometry along the length of the member. For a pure tension member under a constant tension load, such as a hanger, the available strength is determined at the locations of minimum gross or effective area, as applicable. For members in combined tension and flexure or members with tension that varies along the length, additional tensile strength checks will normally be necessary at other possible critical locations.

5.2.1 Tensile Yielding

Nominal strength for the tensile yielding limit state is calculated as the yield stress multiplied by the gross area:

$$P_n = F_y A_g \quad \text{(5.2-1, } \textit{Spec.} \text{ Eq. D2-1)}$$

$$\phi_t = 0.90\,(\text{LRFD}) \qquad \Omega_t = 1.67\,(\text{ASD})$$

or expressed as strength or stress ratios for use in interaction equations:

$$\frac{P_r}{P_c} = \frac{f_r}{F_c} = \frac{\Omega_t P_a}{P_n} = \frac{\Omega_t f_a}{F_y} \quad \text{(ASD)} \qquad (5.2\text{-}2)$$

$$\frac{P_r}{P_c} = \frac{f_r}{F_c} = \frac{P_u}{\phi_t P_n} = \frac{f_u}{\phi_t F_y} \quad \text{(LRFD)} \qquad (5.2\text{-}3)$$

5.2.2 Tensile Rupture

Nominal strength for the tensile rupture limit state is calculated as the tensile stress multiplied by the effective net area:

$$P_n = F_u A_e \quad \text{(5.2-4, } \textit{Spec.} \text{ Eq. D2-2)}$$

$$\phi_t = 0.75\,(\text{LRFD}) \qquad \Omega_t = 2.00\,(\text{ASD})$$

or expressed as strength or stress ratios for use in interaction equations:

$$\frac{P_r}{P_c} = \frac{f_r}{F_c} = \frac{\Omega_t P_a}{P_n} = \frac{\Omega_t f_a}{F_u} \quad \text{(ASD)} \qquad (5.2\text{-}5)$$

$$\frac{P_r}{P_c} = \frac{f_r}{F_c} = \frac{P_u}{\phi_t P_n} = \frac{f_u}{\phi_t F_u} \quad \text{(LRFD)} \qquad (5.2\text{-}6)$$

For the common case in metal building construction where isolated bolt holes in columns and beams are present for attachment of connected items, such as purlins and flange braces, but are not used as the means of connection between frame members, the effective net area, A_e, is taken as the gross area less the area of each bolt hole in the cross section calculated using a hole width 1/16 in. wider than the nominal hole diameter. In other cases, where the member tension force is transferred by bolts or welds on some, but not all, elements of the cross section, A_e must be calculated using AISC *Specification* Equation D3-1 with the appropriate shear lag factor, U, from *Specification* Table D3.1.

Example 5.1—Tapered Tension Member with Bolt Holes

Given:

Determine the available tensile strength of the member shown in Figure 5-1. Assume two 11/16-in.-diameter holes in each flange, 12 in. from the small end, provided for the attachment of connected items.

Material Properties

$F_y = 55$ ksi
$F_u = 70$ ksi

Geometric Properties

Top flange = PL ¼ × 6
Bottom flange = PL ¼ × 6
Web thickness = 0.125 in.

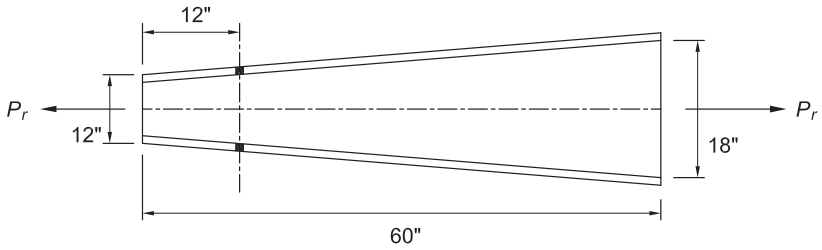

Fig. 5-1. Tapered tension member with bolt holes.

Solution:

Check tensile yielding limit state

The small end controls by inspection. Using AISC *Specification* Section D2, determine the available tensile yielding strength.

$A_g = (2)(6.00 \text{ in.})(0.250 \text{ in.}) + (12.0 \text{ in.})(0.125 \text{ in.})$
$= 4.50 \text{ in.}^2$

$P_n = F_y A_g$ (*Spec.* Eq. D2-1)
$= 55 \text{ ksi } (4.50 \text{ in.}^2)$
$= 248 \text{ kips}$

LRFD	ASD
$P_c = \phi_t P_n$ $= 0.90(248 \text{ kips})$ $= 223 \text{ kips}$	$P_c = \dfrac{P_n}{\Omega_t}$ $= \dfrac{248 \text{ kips}}{1.67}$ $= 149 \text{ kips}$

Check tensile rupture limit state

The cross section at the bolt holes controls by inspection. The bolt holes are provided for the attachment of connected items; therefore, using AISC *Specification* Table D3.1, assume $U = 1.0$. Using *Specification* Sections D2 and D3, determine the available tensile rupture strength:

At the cross section location with the bolt holes,

$h = 12.0 \text{ in} + (12.0 \text{ in./}60.0 \text{ in.})(18.0 \text{ in.} - 12.0 \text{ in.})$
$= 13.2 \text{ in.}$

$A_e = A_n U$ (*Spec.* Eq. D3-1)
$= \left[(2)(6.00 \text{ in.})(0.250 \text{ in.}) + (13.2 \text{ in.})(0.125 \text{ in.}) - (4)(11/16 \text{ in.} + 1/16 \text{ in.})(0.250 \text{ in.})\right] 1.0$
$= 3.90 \text{ in.}^2$

$P_n = F_u A_e$ (*Spec.* Eq. D2-2)
$= 70 \text{ ksi}(3.90 \text{ in.}^2)$
$= 273 \text{ kips}$

LRFD	ASD
$P_c = \phi_t P_n$ $= 0.75(273\,\text{kips})$ $= 205\,\text{kips}$	$P_c = \frac{P_n}{\Omega_t}$ $= \frac{273\,\text{kips}}{2.00}$ $= 137\,\text{kips}$

Tensile rupture at the bolt holes controls the design strength.

LRFD	ASD
$P_c = 205\,\text{kips}$	$P_c = 137\,\text{kips}$

5.3 AXIAL COMPRESSION

Tapered columns are subject to the same limit states as prismatic columns, but they are more likely to be governed by limit states that do not control the design of hot-rolled wide flange members. Tapered members used in metal buildings frequently have slender flanges and/or webs with respect to column axial compression. For this reason, the following column design provisions are based on AISC *Specification* Section E7, which incorporates the effects of slender elements. When all elements are nonslender, these provisions are an extension of Sections E3 and E4, which address members with nonslender elements.

The procedure for calculating the column strength of a slender-element prismatic I-shaped member in the AISC *Specification* is as follows:

1. For each unbraced length, calculate the elastic buckling stress, F_e, for each applicable buckling limit state, the calculation of which varies according to limit state. For prismatic I-shaped members, the AISC *Specification* provides equations for the calculation of the elastic buckling stress, F_e, for the limit states of:

   (a) Flexural buckling of all doubly or singly symmetric members, checked independently about each axis,

   $$F_e = \frac{\pi^2 E}{\left(\frac{KL}{r}\right)^2} \qquad \text{(5.3-1, } \textit{Spec.} \text{ Eq. E3-4)}$$

   (b) Torsional buckling of doubly symmetric members,

   $$F_e = \left[\frac{\pi^2 E C_w}{(K_z L)^2} + GJ\right]\frac{1}{I_x + I_y}$$

   (5.3-2, *Spec.* Eq. E4-4)

   (c) Flexural-torsional buckling of singly symmetric sections,

   $$F_e = \left(\frac{F_{ey} + F_{ez}}{2H}\right)\left[1 - \sqrt{1 - \frac{4F_{ey}F_{ez}H}{\left(F_{ey} + F_{ez}\right)^2}}\right]$$

   (5.3-3, *Spec.* Eq. E4-5)

2. Use the smallest of these elastic stresses in the AISC *Specification* Equations E7-2 or E7-3, as applicable, with $Q = 1$ to calculate a nominal buckling stress, F_{cr}.

   When $F_e \geq 0.44QF_y$

   $$F_{cr} = \left(0.658^{\frac{QF_y}{F_e}}\right)QF_y \qquad \text{(5.3-4, } \textit{Spec.} \text{ Eq. E7-2)}$$

   When $F_e < 0.44QF_y$

   $$F_{cr} = 0.877\,F_e \qquad \text{(5.3-5, } \textit{Spec.} \text{ Eq. E7-3)}$$

3. Check the slenderness of the web and both flanges to determine an overall slenderness reduction factor, Q. For the web slenderness check, use $f = F_{cr}$ as calculated in Step 2 to calculate Q_a (see AISC *Specification* Section E7.2). For the slenderness checks of the flanges, calculate Q_s for each flange (see AISC *Specification* Section E7.1) that will be in net compression when the axial force is combined with any bending moment present in the load combination under consideration. If both flanges are in compression under the combined loading, use the smaller of the two Q_s terms calculated; otherwise, use Q_s for the flange in compression. Calculate $Q = Q_s Q_a$.

4. If $Q = 1$, the nominal buckling stress, F_{cr}, is as calculated in Step 2. Otherwise, if $Q < 1.0$, recalculate F_{cr} using the governing F_e with Q as calculated in Step 3.

5. The nominal buckling stress, F_{cr}, is multiplied by the gross column area to obtain the nominal strength, P_n.

$$P_n = F_{cr}A_g \qquad \text{(5.3-6, } \textit{Spec.} \text{ Eq. E7-1)}$$

$$\phi_c = 0.90\,(\text{LRFD}) \qquad \Omega_c = 1.67\,(\text{ASD})$$

or expressed as strength or stress ratios for use in AISC *Specification* Equations H1-1 or H2-1:

$$\frac{P_r}{P_c} = \frac{f_r}{F_c} = \frac{\Omega_c P_a}{P_n} = \frac{\Omega_c f_a}{F_{cr}} \text{ (ASD)} \qquad (5.3\text{-}7)$$

$$\frac{P_r}{P_c} = \frac{f_r}{F_c} = \frac{P_u}{\phi_c P_n} = \frac{f_u}{\phi_c F_{cr}} \text{ (LRFD)} \qquad (5.3\text{-}8)$$

For tapered columns the basic steps are the same; however, the foregoing procedure must be modified somewhat to account for variation of the required stress under load, f_r, and the elastic buckling stress, F_e, that occurs over the length of the member in a tapered column.

The following procedures make extensive use of the term γ_e. For any column under compression loading, there is a buckling multiplier, γ_e, by which the required strength (loading) is multiplied to obtain the elastic buckling strength of the column ($F_e = \gamma_e f_r$). γ_e is also algebraically equivalent to the factor by which the required stress, f_r, at every point in the column is multiplied to arrive at the stress at that point when elastic buckling is reached; that is, $\gamma_e f_r$ is the elastic buckling stress, F_e, at each point in the column. γ_e can be computed using a number of methods outlined in Appendix A, including finite element eigenvalue buckling solutions, the method of successive approximations or, for simple cases, an approximate closed-form equation.

The use of the term γ_e provides several advantages. First, it makes it possible to describe the elastic buckling strength of members ranging from a prismatic member with a uniform axial load to a geometrically complex nonprismatic member subject to a nonuniform axial loading. In addition, both the finite element and successive approximation methods provide their buckling strength results directly as γ_e, a multiplier of the applied load used in the analysis.

Because $F_e = \gamma_e f_r$, AISC *Specification* Equations E7-2 and E7-3 can be rewritten in an algebraically equivalent form as

When $\dfrac{QF_y}{\gamma_e f_r} \le 2.25$

$$F_{cr} = \left(0.658^{\frac{QF_y}{\gamma_e f_r}}\right) QF_y \qquad (5.3\text{-}9)$$

When $\dfrac{QF_y}{\gamma_e f_r} > 2.25$

$$F_{cr} = 0.877\gamma_e f_r$$

The method for calculating the strength of a tapered column follows the five basic steps outlined earlier, with some modification. In the subsequent discussion, it is assumed for convenience that the columns are oriented with the plane of the web in the plane of the frame. Buckling in the plane of the member web is designated by the subscript x. With tapered I-shaped members, the slenderness of the web varies along the length of the member. Also, the slenderness of the web and flanges can vary along the length due to changes in the cross-section plates at specific locations. For prismatic I-shaped members subjected to uniform axial compression, one can determine the smallest γ_e value from each of the potential buckling modes and each of the applicable unbraced lengths. Given this minimum γ_e, or the corresponding F_e, the column strength may be determined by substituting this single value into Equations 5.3-9 or 5.3-10. However, because both γ_e and the cross-section element slenderness values affect the column resistance, one cannot determine the governing unbraced length and buckling limit state simply by finding the smallest γ_e value when the cross-section slenderness values are not constant along the member length. For nonprismatic members, it is necessary in general to compute and compare the nominal strengths for each buckling limit state in each applicable unbraced length.

In the following discussion, it is assumed that each member is oriented with its strong (or x-) axis in the plane of the frame and its weak (or y-) axis perpendicular to the frame. In cases where members are rotated 90°, x and y subscripts continue to refer to the in-plane and out-of-plane axes, respectively.

Find the governing limit state and unbraced length by determining the highest ratio of required strength to available strength, P_r/P_c, for the column, considering both the in-plane and out-of-plane behavior and the applicable buckling limit states. Columns with equal flanges should be checked for flexural buckling about both axes. Columns with equal flanges also should be checked for torsional buckling whenever the torsional buckling unbraced length, K_zL, is larger than the minor-axis flexural buckling unbraced length, K_yL_b (K_zL and K_yL_b are defined in subsequent sections). Columns with unequal flanges are classified as singly symmetric sections. They should be checked for flexural-torsional buckling involving bending about the cross-section axis of symmetry and for flexural buckling about the other cross-section principal axis. Columns with different out-of-plane flange brace spacing on each flange should also be checked for constrained-axis torsional buckling.

In the usual case where out-of-plane bracing is provided by girts and purlins and diagonal flange braces connected to them, there is a single in-plane unbraced length for the member, the length between the member supports or the connection(s) to other members in the plane of bending. However, there is usually a series of out-of-plane unbraced lengths to consider. Find the highest ratio of required

strength to available strength, P_r/P_c, from the one in-plane unbraced length, $(P_r/P_c)_i$, and the one or more out-of-plane unbraced lengths, $(P_r/P_c)_o$.

For each applicable column buckling limit state and each of the corresponding unbraced lengths, perform the following procedure:

5.3.1 Calculate Elastic Buckling Strength

For all elastic buckling modes given herein, with the exception of in-plane flexural buckling, it is assumed that the required axial strength, P_r, within the unbraced length is essentially constant. For constant P_r, γ_e is calculated as P_e/P_r. For in-plane buckling in cases in which the internal axial force varies along the member length, the method of successive approximations and eigenvalue analysis are useful tools for determining the multiple of the internal forces, P_r, or internal stresses, f_r, at which the theoretical member elastic flexural buckling occurs. For the unbraced lengths associated with other buckling modes, the variation in P_r along the unbraced length is usually minor. In these cases, P_r should be taken as the largest axial force within the applicable unbraced length. Acceptable accuracy is not ensured using an average or weighted average value for P_r.

In-Plane Flexural Buckling

For in-plane flexural buckling, calculate the elastic buckling ratio, γ_{ex}, or P_{ex} using the appropriate end conditions (see Equation 2.2-1). For members designed using the DM or the FOM, assume pinned end conditions. For members designed using the ELM with $\Delta_{2nd}/\Delta_{1st} > 1.1$, the actual sidesway restraint must be included in a buckling analysis either explicitly or implicitly through the use of a K factor. Note that γ_{ex} is a function of the magnitude and distribution of the axial load and is therefore potentially different for each load combination. This step is not necessary if using the DM and an explicit member out-of-straightness is included using an analysis model that accounts for both P-Δ and P-δ effects (the possibility of elastic buckling in the plane of the member is captured within the analysis model in this case). It also is not necessary if using the DM and $\alpha/\gamma_{eL} \leq 0.10$ (the influence of in-plane stability considerations on P_n is negligible in this case). Several techniques for calculating γ_{ex} and P_{ex} are given in Appendix A.

Out-of-Plane Flexural Buckling

Doubly symmetric I-shaped members must be checked for out-of-plane flexural buckling. Calculate the elastic buckling strength using the following equation, which is algebraically equivalent to AISC *Specification* Equation E3-4:

$$P_{ey} = \frac{\pi^2 EI_y}{\left(K_y L_b\right)^2} \tag{5.3-11}$$

Use the section properties at the midpoint of the unbraced length. K_y is normally taken as 1.0 with the exception of members designed by the ELM and where sidesway is unrestrained in the direction normal to the cross-section y-axis. K_y may be taken less than 1.0 if an analysis shows that a smaller value may be used. However, in this case, if an adjacent unbraced length is assumed to provide restraint such that $K_y < 1.0$, the adjacent unbraced length must be checked using the corresponding $K_y > 1.0$ for the load combination under consideration. Calculate γ_{ey} as P_{ey}/P_r.

For sections with a change in the flange plates at no more than 20% of the distance from the smaller end of the unbraced length, and if the change in the lateral moment of inertia of the flanges is less than a factor of 2, the change in the flange plates may be neglected. Use the I_y of the cross section within the longer portion of the unbraced length. For other cases, such as unbraced lengths with more than one change of flange plates, flange changes further from the ends of the unbraced length or significantly stepped axial loads, P_{ey} should be determined using analytical methods similar to those used for determining in-plane flexural buckling strength. The method of successive approximations is very useful for these cases.

For doubly or singly symmetric members with different brace spacing on the two flanges, check the shorter unbraced lengths using these provisions, and check the longer unbraced lengths between the locations where both flanges are braced using the constrained-axis torsional buckling provisions below.

Torsional Buckling

Doubly symmetric I-shaped members with flange braces on both flanges at the same locations along the length of the column are potentially subject to torsional buckling. However, the member nominal resistance based on torsional buckling is never more than a few percent smaller than that due to out-of-plane flexural buckling for all practical member geometries (and out-of-plane flexural buckling usually governs). That is, for $K_zL \leq K_yL_b$, torsional buckling of doubly symmetric I-shaped members does not need to be considered (White and Kim, 2006). For cases where $K_zL > K_yL_b$, calculate the elastic torsional buckling strength from the following equation, which is algebraically equivalent to AISC *Specification* Equation E4-4:

$$P_{ez} = \left[\frac{\pi^2 EC_w}{\left(K_z L\right)^2} + GJ\right]\frac{1}{r_x^2 + r_y^2} \tag{5.3-12}$$

using the section properties at the midpoint of the torsional unbraced length. The length, K_zL, is usually taken as the distance between locations where the member is restrained against twisting. For the case of a cantilevered column fully restrained against twisting and warping at one end and with

the other end free, $K_zL = 2L$, where L is the length between the fixed and free ends. Calculate γ_{ez} as P_{ez}/P_r.

Although J is frequently taken as $\sum \frac{bt^3}{3}$, a more accurate expression for I-shaped members of normal proportions is recommended instead:

$$J = \frac{ht_w^3}{3} + \frac{b_{ft}t_{ft}^3}{3}\left(1 - 0.63\frac{t_{ft}}{b_{ft}}\right) + \frac{b_{fc}t_{fc}^3}{3}\left(1 - 0.63\frac{t_{fc}}{b_{fc}}\right) \quad (5.3\text{-}13)$$

where

b_{fc} = compression flange width, in.
b_{ft} = tension flange width, in.
h = web height, in.
t_{fc} = compression flange thickness, in.
t_{ft} = tension flange thickness, in.
t_w = web thickness, in.

Flexural-Torsional Buckling

Singly symmetric members with significantly different flanges having flange braces on both flanges at the same locations along the length of the column are subject to flexural-torsional buckling. This limit state need not be checked unless the flange widths are different, or in cases where the flange widths are the same, if the ratio of the thicker to thinner flange thickness exceeds 1.5 (White and Kim, 2006). Calculate the elastic flexural-torsional strength from the following equation, which is algebraically equivalent to AISC *Specification* Equation E4-2, using the section properties at the midpoint of the unbraced length:

$$P_{eFT} = \left(\frac{P_{ey} + P_{ez}}{2H}\right)\left[1 - \sqrt{1 - \frac{4P_{ey}P_{ez}H}{\left(P_{ey} + P_{ez}\right)^2}}\right] \quad (5.3\text{-}14)$$

where

A_g = gross section area, in.^{2}
$H = 1 - \frac{x_o^2 + y_o^2}{\bar{r}_o^2}$
P_{ey} = elastic flexural column buckling strength, kips
P_{ez} = elastic torsional buckling strength, kips
x_o, y_o = coordinates of shear center with respect to the centroid, in.
$\bar{r}_o$ = polar radius of gyration about the shear center, in.

Calculate γ_{eFT} as P_{eFT}/P_r.

Constrained-Axis Torsional Buckling

If the inside flange brace spacing is larger than the outside girt or purlin spacing, calculate the elastic constrained-axis torsional buckling strength as (Timoshenko and Gere, 1961):

$$P_{eCAT} = \left[\frac{\pi^2 E\left(C_w + I_y a_s^2\right)}{\left(K_z L_{b\,inside}\right)^2} + GJ\right]\frac{1}{r_x^2 + r_y^2 + a_c^2} \quad (5.3\text{-}15)$$

where

$$C_w = \frac{h_o^2 I_{y1}}{\frac{I_{y1}}{I_{y2}} + 1} \quad (5.3\text{-}16)$$

h_o = distance between flange centroids, in.

$$I_{y1} = \frac{t_{f1}b_{f1}^3}{12} \text{ (outside flange)} \quad (5.3\text{-}17)$$

$$I_{y2} = \frac{t_{f2}b_{f2}^3}{12} \text{ (inside flange)} \quad (5.3\text{-}18)$$

a_c = distance from centroid of girt or purlin to centroid of column, in., as shown in Figure 5-2
a_s = distance from centroid of girt or purlin to shear center of column, in., as shown in Figure 5-2

$$y_o = \frac{t_{f1}}{2} + \frac{h_o I_{y2}}{I_y} - \bar{y} \quad (5.3\text{-}19)$$

For usual cases, $K_zL_{b\,inside}$ is the distance between braced points on the inside flange.

Use the section properties at the midpoint of the inside unbraced length, $L_{b\,inside} > L_{b\,outside}$. Calculate γ_{eCAT} as P_{eCAT}/P_r.

5.3.2 Calculate Nominal Buckling Stress Without Slender Element Effects, F_{n1}

The critical nominal buckling stress without slender element effects, F_{n1}, is calculated at the location within the unbraced length with the highest ratio of required strength to yield strength, f_{rmax}/F_y. F_{n1} is used to establish the stresses used in calculating the slenderness reduction factor for the web, Q_a, throughout the unbraced length.

Locate the highest ratio of f_r/F_y in the unbraced length. This will be at the small end of the unbraced length under consideration or at a location where flange or web plates change. Using this maximum value of f_{rmax}/F_y and γ_e for the buckling limit state being checked, calculate F_{n1} from

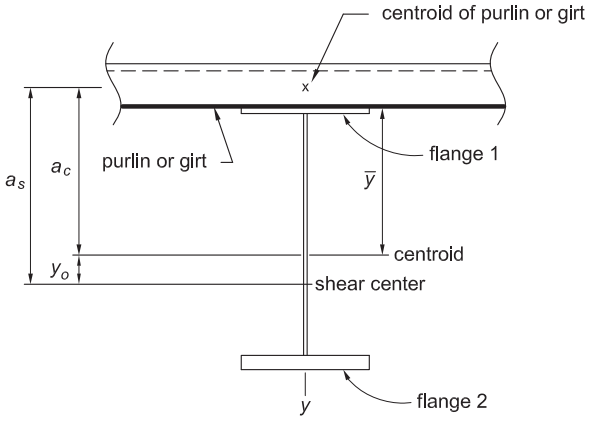

Fig. 5-2. Constrained-axis torsional buckling parameters.

Equations 5.3-20 or 5.3-21 as appropriate:

For $\dfrac{F_y}{\gamma_e f_{rmax}} \le 2.25$,

$$F_{n1} = \left(0.658^{\frac{F_y}{\gamma_e f_{rmax}}} \right) F_y \qquad (5.3\text{-}20a)$$

For $\dfrac{F_y}{\gamma_e f_{rmax}} > 2.25$,

$$F_{n1} = 0.877 \gamma_e f_{rmax} \qquad (5.3\text{-}21a)$$

Alternatively, these equations may be expressed as:

For $\dfrac{F_y}{F_e} \le 2.25$,

$$F_{n1} = \left(0.658^{\frac{F_y}{F_e}} \right) F_y \qquad (5.3\text{-}20b)$$

For $\dfrac{F_y}{F_e} > 2.25$,

$$F_{n1} = 0.877 F_e \qquad (5.3\text{-}21b)$$

As an alternative form:

For $\dfrac{P_y}{P_e} \le 2.25$,

$$F_{n1} = \left(0.658^{\frac{P_y}{P_e}} \right) F_y \qquad (5.3\text{-}20c)$$

For $\dfrac{P_y}{P_e} > 2.25$,

$$F_{n1} = 0.877 \frac{P_e}{A_g} \qquad (5.3\text{-}21c)$$

Calculate the nominal buckling strength multiplier, γ_{n1}, as:

$$\gamma_{n1} = F_{n1} / f_{rmax} \qquad (5.3\text{-}22)$$

using the required stress, f_{rmax}, at the location where F_{n1} was computed.

5.3.3 Calculate Slenderness Reduction Factor, *Q*, and Locate Critical Section

By checking various locations along the unbraced length, determine the maximum value of f_r/QF_y, where Q is calculated according to the AISC *Specification* Section E7 with the following modifications. For calculation of the web slenderness, Q_a, use $f = \gamma_{n1} f_r$ at each location along the column to be checked. In computing Q_s, use the smaller of the values of Q_s computed for both flanges. For a particular load combination, if there is no net compression stress in one of the flanges due to a larger offsetting flexural tension, that flange need not be considered in the Q_s calculations for that load combination.

For members with nonslender flanges over the entire unbraced length, the critical location will always be at the small end of the unbraced length under consideration or at a plate transition unless there is a step in the load between locations of plate changes. In many cases, this will be the same location at which F_{n1} and γ_{n1} were computed.

For unbraced lengths with slender flanges, the shallow end may be the critical location; however, there is also a local minimum for the effective area at the location where $h/t_w = 131$. This is the slenderness limit at which there is no further decrease in the flange reduction factor, Q_s, as the web depth increases [see AISC *Specification* Section E7.1(b)]. If $h/t_w = 131$ anywhere along the unbraced length, those locations also should be checked. If $h/t_w < 131$ at all locations along the unbraced length, the deep end also should be checked. These rules may be further simplified by checking both ends, the location with the deepest web if not at an end, and any locations where $h/t_w = 131$.

If the axial load varies significantly along the length of the member, checks at more locations may be necessary to identify the critical location.

5.3.4 Calculate Nominal Buckling Stress with Consideration of Slender Elements, F_{cr}

Calculate the nominal buckling stress, F_{cr}, at the critical location determined in Section 5.3.3, using γ_e for the buckling limit state under consideration with Q and f_r at the critical location (i.e., the location with the maximum f_r/QF_y).

For $\dfrac{QF_y}{\gamma_e f_r} \le 2.25$,

$$F_{cr} = \left(0.658^{\frac{QF_y}{\gamma_e f_r}} \right) QF_y \qquad (5.3\text{-}23a)$$

For $Q = 1.0$ or $\dfrac{QF_y}{\gamma_e f_r} > 2.25$,

$$F_{cr} = F_{n1} \qquad (5.3\text{-}24a)$$

or

For $\dfrac{QF_y}{F_e} \le 2.25$,

$$F_{cr} = \left(0.658^{\frac{QF_y}{F_e}} \right) QF_y \qquad (5.3\text{-}23b)$$

For $Q = 1.0$ or $\dfrac{QF_y}{F_e} > 2.25$,

$$F_{cr} = F_{n1} \qquad (5.3\text{-}24b)$$

If $Q = 1$ or if $\dfrac{QF_y}{\gamma_e f_r} > 2.25$, there is no influence of local buckling of the plate elements on the column resistance. In this case, the critical location will be the same as the location at which F_{n1} was calculated and $F_{cr} = F_{n1}$.

5.3.5 Strength Ratio

Calculate the strength or stress ratio for the buckling limit state under consideration using the required strength, f_r, and the nominal buckling stress, F_{cr}, at the critical location determined in Section 5.3.3:

$$\frac{P_r}{P_c} = \frac{f_r}{F_c} = \frac{\Omega_c f_a}{F_{cr}} \quad \text{(ASD)} \qquad (5.3\text{-}25)$$

$$\frac{P_r}{P_c} = \frac{f_r}{F_c} = \frac{f_u}{\phi_c F_{cr}} \quad \text{(LRFD)} \qquad (5.3\text{-}26)$$

5.3.6 Other Considerations

The strength of a purely axially loaded column is the smallest of the in-plane strength for the column and the strength of each possible out-of-plane buckling limit state for each unbraced length. In the case of beam-columns, it is generally necessary to evaluate the combination of axial force and flexure separately for each unbraced length. In this case, for each unbraced length, the axial strength is the lower of the in-plane strength for the whole column and the governing out-of-plane strength determined for that unbraced length.

As a simplification, it is always conservative to calculate Q_a using $F_{n1} = F_y$, rather than calculating a more precise F_{n1} in Section 5.3.2. Also, it is always conservative to skip Section 5.3.2 altogether and simply to use $f = F_y$ at all the member cross sections in determining Q in Section 5.3.3.

In some cases, the preceding process can be simplified even further for the in-plane strength calculation. When using the DM, if the in-plane elastic buckling strength is sufficiently large or the second-order analysis is sufficiently refined, the in-plane strength may be computed as follows:

(1) Use f based either on $F_{n1} = F_y$, or more simply $f = F_y$ at all the member cross sections in Section 5.3.3 to determine the cross section Q values.

(2) Calculate P_r/P_{ni} as the largest value of f_r/QF_y along the member length.

This procedure may be used when any of the following conditions are met:

(1) When $\alpha/\gamma_{eL} \le 0.10$

(2) When an analysis is performed that includes both P-Δ and P-δ effects along with the inclusion of an explicit member out-of-straightness in the analysis (in addition to the structure out-of-plumbness)

(3) In the case of gable frame rafters, when the midspan work point is offset above the rafter chord by $L_{chord}/50$ or more, where L_{chord} is the span length along the rafter chord between the cross-section centroids at the tops of the columns

These conditions were discussed previously in items 4a through 4c of Section 4.6.2.

Example 5.2—Tapered Column with Simple Bracing

Given:

Evaluate the compressive strength of the member shown in Figure 5-3. The required concentric axial strength, including all second-order effects, is constant over the height of the column, neglecting the accumulating self-weight. Assume $K_x = K_y = K_z = 1.0$.

Material Properties

$F_y = 55$ ksi
$F_u = 70$ ksi

Geometric Properties

Left flange = PL ¼ × 6
Right flange = PL ¼ × 6
Web thickness = 0.125 in.
Left and right flange bracing at 90.0 in. above the bottom

By inspection, the member is subject to:

A. In-plane flexural buckling (one strength for the entire column)

B. Out-of-plane flexural buckling—lower unbraced length

C. Out-of-Plane flexural buckling—upper unbraced length

Torsional buckling need not be checked because the cross section is doubly symmetric and the torsional buckling length does not exceed the largest out-of-plane buckling length. Flexural-torsional buckling is not applicable since the cross section is doubly symmetric. Constrained axis torsional buckling need not be checked, because the brace spacing is identical on both flanges.

Solution:

Table 5-1. Section Properties		
Top	h	24.0 in.
	h/t_w	192
	A_g	6.00 in.^{2}
	I_x	585 in.^{4}
At girt	h	19.5 in
	h/t_w	156
	A_g	5.44 in.^{2}
At h/t_w = 131	h	16.4 in.
	h/t_w	131
	A_g	5.05 in.^{2}
Bottom	h	12.0 in.
	h/t_w	96.0
	A_g	4.50 in.^{2}
	I_x	131 in.^{4}

A. In-Plane Flexural Buckling Strength

Determine P_{ex}

Because the member has a single taper with no plate changes, use Equation 4.5-4.
At the bottom end, web height = 12.0 in., $I_{x,small}$ = 131 in.^{4}
At the top end, web height = 24.0 in., $I_{x,large}$ = 585 in.^{4}
From Section 4.5.2, calculate I'_x at a distance x from the small end, where

$$x = 0.5L\left(\frac{I_{x,small}}{I_{x,large}}\right)^{0.0732}$$

$$= 0.5(144\text{ in.})\left(\frac{131\text{ in.}^4}{585\text{ in.}^4}\right)^{0.0732}$$

$$= 64.5\text{ in. from small end}$$

Web height = 12.0 in. + (64.5 in./144 in.)(24.0 in. −12.0 in.)

= 17.4 in.

I'_x = 289 in.^{4} (calculations not shown)

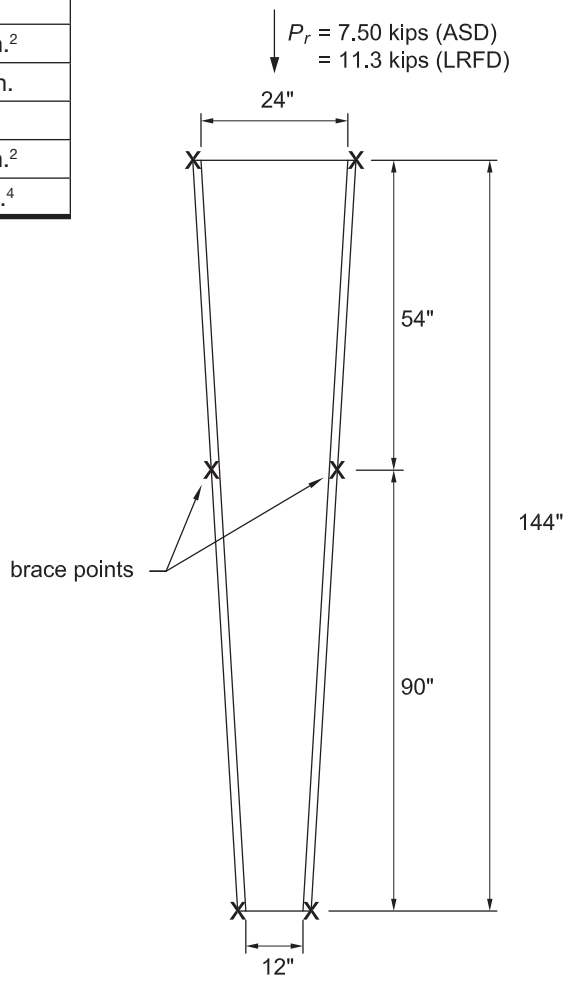

Fig. 5-3. Column.

$$P_{ex} = \frac{\pi^2 EI'_x}{L^2}$$
$$= \frac{\pi^2 (29{,}000\,\text{ksi})\left(289\,\text{in.}^4\right)}{\left(144\,\text{in.}\right)^2}$$
$$= 3{,}990\ \text{kips} \qquad (4.5\text{-}4)$$

Compare with the method of successive approximations solution (see Appendix C, Section C.3.1):

$$P_{ex} = 3{,}980\ \text{kips}$$
$$\approx 3{,}990\ \text{kips}$$

Calculate F_{n1}, the nominal buckling stress, without consideration of slender elements
By inspection, under a constant axial force, the location with the largest ratio of f_r/F_y is the bottom end of the column.
From Table 5-1, $A_g = 4.50$ in.^{2}, and

$$F_e = \frac{P_{ex}}{A_g}$$
$$= \frac{3{,}990\,\text{kips}}{4.50\,\text{in.}^2}$$
$$= 887\,\text{ksi}$$
$$\frac{F_y}{F_e} = \frac{55\,\text{ksi}}{887\,\text{ksi}}$$
$$= 0.0620 < 2.25;\ \text{therefore, use Equation 5.3-20b}$$
$$F_{n1} = \left(0.658^{\frac{F_y}{F_e}}\right)F_y \qquad (5.3\text{-}20b)$$
$$= \left(0.658^{0.0620}\right)55\,\text{ksi}$$
$$= 53.6\,\text{ksi}$$

Calculate the nominal buckling strength multiplier, γ_{n1}, using the required stress, $f_{r\,max}$, at the location where F_{n1} was computed:

LRFD	ASD
$f_{r\,max} = P_r/A_g$ $= 11.3$ kips/4.50 in.^{2} $= 2.51$ ksi	$f_{r\,max} = P_r/A_g$ $= 7.50$ kips/4.50 in.^{2} $= 1.67$ ksi
$\gamma_{n1} = F_{n1}/f_{r\,max}$ $= 53.6$ ksi/2.51 ksi $= 21.4$	$\gamma_{n1} = F_{n1}/f_{r\,max}$ $= 53.6$ ksi/1.67 ksi $= 32.1$

Locate critical section and calculate slenderness reduction factor, Q
Calculate $\frac{f_r}{QF_y}$ at the bottom end of the column.
First, determine the slenderness reduction factor by checking the flange slenderness using AISC *Specification* Table B4.1. The flange width-thickness ratio is,

$$\lambda = \frac{b}{t}$$
$$= \frac{b_f}{2t_f}$$
$$= \frac{6.00\,\text{in.}}{2(0.25\,\text{in.})}$$
$$= 12.0$$

From Table 5-1, at the bottom end of the column, $h/t_w = 96.0$.

From AISC *Specification* Table B4.1, for uniform compression in flanges of built-up I-shaped sections,

$$\lambda_r = 0.64\sqrt{k_c E/F_y}$$

where

$k_c = \frac{4}{\sqrt{h/t_w}}$ (AISC *Specification* Table B4.1 footnote a)

$h/t_w = 96.0$ (at the bottom end of the column)

$$k_c = \frac{4}{\sqrt{h/t_w}}$$
$$= \frac{4}{\sqrt{96.0}}$$
$$= 0.408 \quad \text{where } 0.35 < k_c < 0.76 \quad \textbf{o.k.}$$

Therefore,

$$\lambda_r = 0.64\sqrt{k_c E/F_y}$$
$$= 0.64\sqrt{0.408(29{,}000\,\text{ksi})/55\,\text{ksi}}$$
$$= 9.39 < 12.0; \text{ therefore, flanges are slender}$$

Determine the slenderness reduction factor, Q, using AISC *Specification* Section E7.1. For slender-element sections,

$$Q = Q_s Q_a$$

Determine which equation for Q_s applies in AISC *Specification* Section E7.1(b). The equation used for Q_s is dependent on the flange slenderness, λ, compared to the following value:

$$1.17\sqrt{k_c E/F_y} = 1.17\sqrt{0.408(29{,}000\text{ ksi})/55\text{ ksi}}$$
$$= 17.2$$

$9.39 < 12.0 < 17.2$; therefore, use AISC *Specification* Equation E7-8.

$$Q_s = 1.415 - 0.65\left(\frac{b}{t}\right)\sqrt{\frac{F_y}{Ek_c}} \qquad \text{(}\textit{Spec.}\text{ Eq. E7-8)}$$
$$= 1.415 - 0.65(12.0)\sqrt{\frac{55\,\text{ksi}}{29{,}000\,\text{ksi}(0.408)}}$$
$$= 0.883$$

Check web slenderness using AISC *Specification* Table B4.1, for uniform compression in webs of doubly symmetric I-shaped sections:

$$\lambda = \frac{h}{t_w}$$
$$= \frac{12.0\,\text{in.}}{0.125\,\text{in.}}$$
$$= 96.0$$

$$\lambda_r = 1.49\sqrt{\frac{E}{F_y}}$$
$$= 1.49\sqrt{\frac{29{,}000\,\text{ksi}}{55\,\text{ksi}}}$$
$$= 34.2 < 96.0;\ \text{therefore, the web is slender}$$

Calculate Q_a using AISC *Specification* Section E7.2:

$$Q_a = \frac{A_{eff}}{A} \qquad \text{(Spec. Eq. E7-16)}$$

where

$$A = A_g$$
$$= 4.50\ \text{in. from Table 5-1}$$
$$A_{eff} = 2A_f + b_e t_w$$
$$b_e = 1.92t\sqrt{\frac{E}{f}}\left[1 - \frac{0.34}{(b/t)}\sqrt{\frac{E}{f}}\right] \le b \qquad \text{(Spec. Eq. E7-17)}$$

With $f_r = f_{rmax}$ at the bottom of the column, the stress, f, at which the effective width is calculated is determined as follows:

LRFD	ASD
$f = \gamma_{n1} f_{rmax}$	$f = \gamma_{n1} f_{rmax}$
$= 21.4(2.51\,\text{ksi})$	$= 32.1(1.67\,\text{ksi})$
$= 53.7\,\text{ksi}$	$= 53.6\,\text{ksi}$

Note that the difference in f between LRFD and ASD is due to rounding. Use ASD value: $f = 53.6$ ksi.

From AISC *Specification* Section E7,

$$b_e = 1.92t\sqrt{\frac{E}{f}}\left[1 - \frac{0.34}{(b/t)}\sqrt{\frac{E}{f}}\right] \le b \qquad \text{(Spec. Eq. E7-17)}$$
$$= 1.92(0.125\,\text{in.})\sqrt{\frac{29{,}000\ \text{ksi}}{53.6\ \text{ksi}}}\left[1 - \frac{0.34}{96.0}\sqrt{\frac{29{,}000\ \text{ksi}}{53.6\ \text{ksi}}}\right]$$
$$= 5.12\ \text{in.} < 12.0\ \text{in.}$$

$$A_{eff} = 2A_f + b_e t_w$$
$$= 2(6\ \text{in.})(¼\ \text{in.}) + 5.12(0.125\ \text{in.})$$
$$= 3.64\ \text{in.}^2$$

Therefore,

$$Q_a = \frac{A_{eff}}{A}$$
$$= \frac{3.64 \text{ in.}^2}{4.50 \text{ in.}^2} \qquad \text{(Spec. Eq. E7-16)}$$
$$= 0.809$$
$$Q = Q_s Q_a$$
$$= 0.883(0.809)$$
$$= 0.714$$

Determine the maximum value of f_r/QF_y to locate the critical section. At the bottom of the column,

LRFD	ASD
$\frac{f_{rmax}}{QF_y} = \frac{2.51\,\text{ksi}}{0.714(55\,\text{ksi})}$	$\frac{f_{rmax}}{QF_y} = \frac{1.67\,\text{ksi}}{0.714(55\,\text{ksi})}$
$= 0.0639$	$= 0.0425$

Calculate $\frac{f_r}{QF_y}$ at the top end of the column (note that this is not likely to control).

From Table 5-1, $A_g = 6.00$ in.^{2} at the top end of the column.

Check flange slenderness

From AISC *Specification* Table B4.1 footnote a,

$\lambda = 12.0$ from earlier

$$k_c = \frac{4}{\sqrt{\frac{h}{t_w}}}$$
$$= \frac{4}{\sqrt{\frac{24.0\,\text{in.}}{0.125\,\text{in.}}}}$$
$$= 0.289 < 0.35, \text{ therefore, use } k_c = 0.35$$

From AISC *Specification* Table B4.1, for uniform compression in flanges of built-up I-shaped sections,

$$\lambda_r = 0.64\sqrt{\frac{k_c E}{F_y}}$$
$$= 0.64\sqrt{\frac{0.35(29{,}000\,\text{ksi})}{55\,\text{ksi}}}$$
$$= 8.69 < 12.0; \text{ therefore, the flanges are slender}$$

Determine the slenderness reduction factor, Q, using AISC *Specification* Section E7.1. For slender-element sections,

$$Q = Q_s Q_a$$

Determine which equation for Q_s applies in AISC *Specification* Section E7.1(b):

$$1.17\sqrt{\frac{k_c E}{F_y}} = 1.17\sqrt{\frac{0.35(29{,}000\,\text{ksi})}{55\,\text{ksi}}}$$

$$= 15.9 > 12.0;\ \text{therefore, use AISC } \textit{Specification} \text{ Equation E7-8}$$

$$Q_s = 1.415 - 0.65\left(\frac{b}{t}\right)\sqrt{\frac{F_y}{Ek_c}} \qquad (\textit{Spec.}\ \text{Eq. E7-8})$$

$$= 1.415 - 0.65(12.0)\sqrt{\frac{55\,\text{ksi}}{29{,}000\,\text{ksi}(0.35)}}$$

$$= 0.841$$

Check web slenderness,

$$\lambda = \frac{h}{t_w}$$

$$= \frac{24.0\,\text{in.}}{0.125\,\text{in.}}$$

$$= 192$$

From earlier calculation, $\lambda_r = 34.2$,

$$\lambda_r = 34.2 < 192.0;\ \text{therefore, the web is slender}$$

Calculate the reduction factor, Q_a, using AISC *Specification* Section E7.2.

$$Q_a = \frac{A_{eff}}{A} \qquad (\textit{Spec.}\ \text{Eq. E7-16})$$

where

$$A = A_g$$

$$= 6.00\ \text{in.}^2\ \text{(from Table 5-1)}$$

$$A_{eff} = 2A_f + b_e t_w$$

$$b_e = 1.92t\sqrt{\frac{E}{f}}\left[1 - \frac{0.34}{(b/t)}\sqrt{\frac{E}{f}}\right] \le b \qquad (\textit{Spec.}\ \text{Eq. E7-17})$$

$$= 1.92(0.125\,\text{in.})\sqrt{\frac{29{,}000\ \text{ksi}}{40.1\,\text{ksi}}}\left[1 - \frac{0.34}{192}\sqrt{\frac{29{,}000\ \text{ksi}}{40.1\,\text{ksi}}}\right]$$

$$= 6.15\,\text{in.} \le 24.0\,\text{in.}$$

The stress, f, at the top of the column is determined as follows:

LRFD	ASD
$f_r = P_r/A_g$ $= 11.3\ \text{kips}/6.00\ \text{in.}^2$ $= 1.88\ \text{ksi}$	$f_r = P_r/A_g$ $= 7.50\ \text{kips}/6.00\ \text{in.}^2$ $= 1.25\ \text{ksi}$
$f = \gamma_{n1} f_r$ $= 21.4(1.88\,\text{ksi})$ $= 40.2\ \text{ksi}$	$f = \gamma_{n1} f_r$ $= 32.1(1.25\,\text{ksi})$ $= 40.1\ \text{ksi}$

Note that the difference in f between LRFD and ASD is due to rounding. Use ASD value: $f = 40.1$ ksi.

Therefore,

$$A_{eff} = 2A_f + b_e t_w$$
$$= 2\left(¼\text{in.}\right)\left(6\,\text{in.}\right) + 6.15\,\text{in.}\left(0.125\,\text{in.}\right)$$
$$= 3.77\,\text{in.}^2$$

The reduction factor for slender stiffened elements is:

$$Q_a = \frac{A_{eff}}{A}, \text{ where } A = A_g \qquad \text{(Spec. Eq. E7-16)}$$
$$= \frac{3.77\,\text{in.}^2}{6.00\,\text{in.}^2}$$
$$= 0.628$$

From AISC *Specification* Section E7, the reduction factor is:

$$Q = Q_s Q_a$$
$$= 0.841\left(0.628\right)$$
$$= 0.528$$

The value of f_r/QF_y at the top of the column is,

LRFD	ASD
$\frac{f_r}{QF_y} = \frac{1.88\,\text{ksi}}{0.528\left(55\,\text{ksi}\right)}$ $= 0.0647$	$\frac{f_r}{QF_y} = \frac{1.25\,\text{ksi}}{0.528\left(55\,\text{ksi}\right)}$ $= 0.0430$

Calculate $\frac{f_r}{QF_y}$ at $h/t_w = 131$ (location where k_c reaches lower limit of 0.35)

From Table 5-1, $A_g = 5.05$ in.^{2} at $h/t_w = 131$.

Check flange slenderness using AISC *Specification* Table B4.1 as follows:

$\lambda = 12.0$ from earlier

From AISC *Specification* Table B4.1 footnote a,

$$k_c = \frac{4}{\sqrt{\frac{h}{t_w}}}$$
$$= \frac{4}{\sqrt{131}}$$
$$= 0.349 < 0.35; \text{ therefore, use } k_c = 0.35$$

As determined earlier, the flange is slender and AISC *Specification* Section E7 applies. Determine the reduction factor,

$$Q = Q_s Q_a$$

Because all terms are identical to those at the top of the column for the determination of Q_s,

$$Q_s = 0.841$$

Check web slenderness for uniform compression in webs of doubly symmetric I-shaped sections.

$$\lambda = \frac{h}{t_w}$$
$$= 131$$

Based on earlier calculations using AISC *Specification* Table B4.1,

$\lambda_r = 34.2 < 131$; therefore, the web is slender.

Calculate the reduction factor, Q_a, using AISC *Specification* Section E7.2.

$$Q_a = \frac{A_{eff}}{A} \qquad \text{(Spec. Eq. E7-16)}$$

where

$$A = A_g$$
$$= 5.05 \text{ in.}^2 \text{ from Table 5-1}$$
$$A_{eff} = 2A_f + b_e t_w$$
$$b_e = 1.92t\sqrt{\frac{E}{f}}\left[1 - \frac{0.34}{(b/t)}\sqrt{\frac{E}{f}}\right] \le b \qquad \text{(Spec. Eq. E7-17)}$$
$$= 1.92(0.125\text{ in.})\sqrt{\frac{29{,}000 \text{ ksi}}{47.8 \text{ ksi}}}\left[1 - \frac{0.34}{131}\sqrt{\frac{29{,}000 \text{ ksi}}{47.8 \text{ ksi}}}\right]$$
$$= 5.53 \text{ in.} \le 16.4 \text{ in.}$$

The stress, f, at the location where $h/t_w = 131$ is determined as follows:

LRFD	ASD
$f_r = \frac{P_r}{A_g}$	$f_r = \frac{P_r}{A_g}$
$= \frac{11.3 \text{ kips}}{5.05 \text{ in.}^2}$	$= \frac{7.50 \text{ kips}}{5.05 \text{ in.}^2}$
$= 2.24$ ksi	$= 1.49$ ksi
$f = \gamma_{n1} f_r$	$f = \gamma_{n1} f_r$
$= 21.4(2.24 \text{ ksi})$	$= 32.1(1.49 \text{ ksi})$
$= 47.9$ ksi	$= 47.8$ ksi

Note that the difference in f between LRFD and ASD is due to rounding. Use ASD value: $f = 47.8$ ksi.

$$A_{eff} = 2A_f + b_e t_w$$
$$= 2(¼ \text{ in.})(6 \text{ in.}) + 5.53 \text{ in.}(0.125 \text{ in.})$$
$$= 3.69 \text{ in.}^2$$

$$Q_a = \frac{A_{eff}}{A}, \text{ where } A = A_g \qquad \text{(Spec. Eq. E7-16)}$$
$$= \frac{3.69 \text{ in.}^2}{5.05 \text{ in.}^2}$$
$$= 0.731$$

Therefore,

$$Q = Q_s Q_a$$
$$= 0.841(0.731)$$
$$= 0.615$$

The value of f_r/QF_y at the location where $h/t_w = 131$ is,

LRFD	ASD
$\frac{f_r}{QF_y} = \frac{2.24\,\text{ksi}}{0.615(55\,\text{ksi})}$ $= 0.0662$	$\frac{f_r}{QF_y} = \frac{1.49\,\text{ksi}}{0.615(55\,\text{ksi})}$ $= 0.0441$

The location where $h/t_w = 131$ is the critical location for in-plane flexural strength, because $\frac{f_r}{QF_y}$ is the largest at that point.

Calculate the nominal buckling strength at the critical location with the highest ratio of f_r/QF_y

As determined, the critical location occurs where $h/t_w = 131$ and $Q = 0.615$. Using AISC *Specification* Section E7 and Section 5.3 of this Design Guide, determine the nominal axial compressive strength as follows:

$$F = P_{ex}/A_g$$
$$= 3.990 \text{ kips}/5.05 \text{ in.}^2$$
$$= 790 \text{ ksi}$$

$$\frac{QF_y}{F_e} = \frac{0.615(55\,\text{ksi})}{790\,\text{ksi}} = 0.0428 < 2.25, \text{ therefore,}$$

$$F_{cr} = \left(0.658^{\frac{QF_y}{F_e}}\right)QF_y \qquad \text{(5.3-23b)}$$
$$= \left(0.658^{0.0428}\right)0.615(55\,\text{ksi})$$
$$= 33.2\,\text{ksi}$$

$$P_n = F_{cr}A_g \qquad \text{(5.3-6, } \textit{Spec.} \text{ Eq. E7-1)}$$
$$= 33.2\,\text{ksi}\left(5.05\,\text{in.}^2\right)$$
$$= 168\,\text{kips}$$

Calculate the in-plane strength ratio at the location of the highest ratio of f_r/QF_y

LRFD	ASD
$\frac{P_r}{P_c} = \frac{P_r}{\phi_c P_n}$ $= \frac{11.3\,\text{kips}}{0.90(168\,\text{kips})}$ $= 0.0747$	$\frac{P_r}{P_c} = \frac{\Omega_c P_r}{P_n}$ $= \frac{1.67(7.50\,\text{kips})}{168\,\text{kips}}$ $= 0.0746$

B. *Out-of-Plane Flexural Buckling Strength—Lower Unbraced Length*

Determine P_{ey}

Calculate the out-of-plane elastic buckling strength, P_{ey}, using properties at the middle of the 90-in. lower unbraced length.

At bottom end of the 90-in. lower unbraced length, web height = 12.0 in.
At top end of the 90-in. lower unbraced length, web height = 19.5 in.
At mid-length of the 90-in. lower unbraced length, web height = 15.8 in.

The moment of inertia about the weak axis, I_y, is,

$$I_y = \frac{2(0.250\,\text{in.})(6.00\,\text{in.})^3}{12} + \frac{15.8\,\text{in.}(0.125\,\text{in.})^3}{12}$$
$$= 9.00\ \text{in.}^4$$

The nominal elastic buckling strength, P_{ey}, at the middle of the 90-in. lower unbraced length is,

$$P_{ey} = \frac{\pi^2 E I_y}{(KL_b)^2} \qquad \text{(from 5.3-11)}$$
$$= \frac{\pi^2 29{,}000(9.00\,\text{in.}^4)}{[1.0(90.0\,\text{in.})]^2}$$
$$= 318\ \text{kips}$$

Calculate F_{n1}, the nominal buckling stress without consideration of slender elements.
By inspection, under a constant axial force, the location with the largest ratio of f_r/F_y is the bottom end.

From Table 5-1, $A_g = 4.50$ in.^{2} at the bottom end and therefore,

$$F_e = \frac{P_{ey}}{A_g}$$
$$= \frac{318\ \text{kips}}{4.50\ \text{in.}^2}$$
$$= 70.7\ \text{ksi}$$

$$\frac{F_y}{F_e} = \frac{55\,\text{ksi}}{70.7\,\text{ksi}}$$
$$= 0.778 < 2.25;\ \text{therefore, use Equation 5.3-20b}$$

$$F_{n1} = \left(0.658^{\frac{F_y}{F_e}}\right) F_y \qquad \text{(5.3-20b)}$$
$$= \left(0.658^{0.778}\right) 55\,\text{ksi}$$
$$= 39.7\,\text{ksi}$$

Calculate the nominal buckling strength multiplier, γ_{n1}, using the required stress, f_{rmax}, at the location where F_{n1} was computed:

LRFD	ASD
$f_{rmax} = \frac{P_r}{A_g}$	$f_{rmax} = \frac{P_r}{A_g}$
$= \frac{11.3\ \text{kips}}{4.50\ \text{in.}^2}$	$= \frac{7.50\ \text{kips}}{4.50\ \text{in.}^2}$
$= 2.51\ \text{ksi}$	$= 1.67\ \text{ksi}$
$\gamma_{n1} = \frac{F_{n1}}{f_{rmax}}$	$\gamma_{n1} = \frac{F_{n1}}{f_{rmax}}$
$= \frac{39.7\,\text{ksi}}{2.51\,\text{ksi}}$	$= \frac{39.7\,\text{ksi}}{1.67\,\text{ksi}}$
$= 15.8$	$= 23.8$

Locate critical section and calculate slenderness reduction factor, Q

Calculate $\frac{f_r}{QF_y}$ at bottom end of the column.

The reduction factor, Q, is determined from AISC *Specification* Section E7 as follows,

$$Q = Q_s Q_a$$

From the in-plane check at the bottom end of the column, $Q_s = 0.883$.

From in-plane calculations above, the web is slender.

With $f_r = f_{rmax}$, the stress, f, at which the effective width is calculated at the bottom end of the column is determined as follows:

LRFD	ASD
$f = \gamma_{n1} f_{rmax}$ $= 15.8(2.51\,\text{ksi})$ $= 39.7\,\text{ksi}$	$f = \gamma_{n1} f_{rmax}$ $= 23.8(1.67\,\text{ksi})$ $= 39.7\,\text{ksi}$

The reduction factor, Q, is determined in accordance with AISC *Specification* Section E7:

$$Q = Q_s Q_a$$

where

$$b_e = 1.92t\sqrt{\frac{E}{f}}\left[1 - \frac{0.34}{(b/t)}\sqrt{\frac{E}{f}}\right] \le b \qquad \text{(}Spec.\text{ Eq. E7-17)}$$

$$= 1.92(0.125\text{ in.})\sqrt{\frac{29{,}000\text{ ksi}}{39.7\text{ ksi}}}\left[1 - \frac{0.34}{96.0}\sqrt{\frac{29{,}000\text{ ksi}}{39.7\text{ ksi}}}\right]$$

$$= 5.87\text{ in.} < 12.0\text{ in.}$$

A_{eff} = summation of the effective areas of the cross section based on the reduced effective width, b_e

$$= 2(0.25\text{ in.})(6.00\text{ in.}) + 5.87\text{ in.}(0.125\text{ in.})$$

$$= 3.73\,\text{in.}^2$$

$$Q_a = \frac{A_{eff}}{A_g} \qquad \text{(}Spec.\text{ Eq. E7-16)}$$

$$= \frac{3.73\,\text{in.}^2}{4.50\,\text{in.}^2}$$

$$= 0.829$$

Therefore,

$$Q = Q_s Q_a$$

$$= 0.883(0.829)$$

$$= 0.732$$

At the bottom end,

LRFD	ASD
$\frac{f_r}{QF_y} = \frac{2.51\,\text{ksi}}{0.732(55\,\text{ksi})}$ $= 0.0623$	$\frac{f_r}{QF_y} = \frac{1.67\,\text{ksi}}{0.732(55\,\text{ksi})}$ $= 0.0415$

Calculate $\frac{f_r}{QF_y}$ at top end of lower unbraced length.

From Table 5-1, $A_g = 5.44$ in.^{2} at the top end of the lower unbraced length.

Check flange slenderness.

$$\lambda = \frac{b}{t}$$
$$= 12.0 \text{ from previous calculation}$$

$$k_c = \frac{4}{\sqrt{\frac{h}{t_w}}}$$
$$= \frac{4}{\sqrt{\frac{19.5\,\text{in.}}{0.125\,\text{in.}}}}$$
$$= 0.32 < 0.35, \text{ therefore use } k_c = 0.35$$

Because k_c is at the minimum, $Q_s = 0.841$ from the in-plane check above

Check web slenderness.

From Table 5-1,

$$\lambda = \frac{h}{t_w}$$
$$= 156$$

$\lambda_r = 34.2 < 156$; therefore, the web is slender

LRFD	ASD
$f_r = \frac{P_r}{A_g}$ $= \frac{11.3\,\text{kips}}{5.44\,\text{kips}}$ $= 2.08$ ksi	$f_r = \frac{P_r}{A_g}$ $= \frac{7.50\,\text{kips}}{5.44\,\text{kips}}$ $= 1.38$ ksi
$f = \gamma_{n1} f_r$ $= 15.8(2.08\,\text{ksi})$ $= 32.9$ ksi	$f = \gamma_{n1} f_r$ $= 23.8(1.38\,\text{ksi})$ $= 32.8$ ksi

Note that the difference in f between LRFD and ASD is due to rounding. Use ASD value: $f = 32.8$ ksi.

$$b_e = 1.92t\sqrt{\frac{E}{f}}\left[1 - \frac{0.34}{(b/t)}\sqrt{\frac{E}{f}}\right] \le b \qquad \text{(}\textit{Spec.}\text{ Eq. E7-17)}$$
$$= 1.92(0.125\text{ in.})\sqrt{\frac{29{,}000\text{ ksi}}{32.8\text{ ksi}}}\left[1 - \frac{0.34}{156}\sqrt{\frac{29{,}000\text{ ksi}}{32.8\text{ ksi}}}\right]$$
$$= 6.67\,\text{in.} < 19.5\text{ in.}$$

From AISC *Specification* Section E7.2,

$$A_{eff} = 2(0.25\text{ in.})(6.00\text{ in.}) + 6.67\text{ in.}(0.125\text{ in.})$$
$$= 3.83\text{ in.}^2$$

$$Q_a = \frac{A_{eff}}{A_g} \qquad \text{(Spec. Eq. E7-16)}$$
$$= \frac{3.83\,\text{in.}^2}{5.44\,\text{in.}^2}$$
$$= 0.704$$

From AISC *Specification* Section E7,

$$Q = Q_s Q_a$$
$$= 0.841(0.704)$$
$$= 0.592$$

LRFD	ASD
$\frac{f_r}{QF_y} = \frac{2.08\,\text{ksi}}{0.592(55\,\text{ksi})}$ $= 0.0639$	$\frac{f_r}{QF_y} = \frac{1.38\,\text{ksi}}{0.592(55\,\text{ksi})}$ $= 0.0424$

Calculate $\frac{f_r}{QF_y}$ at $h/t_w = 131$ (location where k_c reaches lower limit of 0.35).

From Table 5-1, $h = 16.4$ in. and $A_g = 5.05$ in.^{2}

Check flange slenderness.

$Q_s = 0.841$ (from previous calculation)

Check web slenderness.

$$\lambda = \frac{h}{t_w}$$
$$= 131$$

$\lambda_r = 34.2 < 131$; therefore, the web is slender

LRFD	ASD
$f_r = 2.24\,\text{ksi}$ (from previous calculation) $f = \gamma_{n1} f_r$ $= 15.8(2.24\,\text{ksi})$ $= 35.4\,\text{ksi}$	$f_r = 1.49\,\text{ksi}$ (from previous calculation) $f = \gamma_{n1} f_r$ $= 23.8(1.49\,\text{ksi})$ $= 35.5\,\text{ksi}$

Note that the difference in f between LRFD and ASD is due to rounding. Use ASD value: $f = 35.5$ ksi.

$$b_e = 1.92t\sqrt{\frac{E}{f}}\left[1 - \frac{0.34}{(b/t)}\sqrt{\frac{E}{f}}\right] \le b \qquad \text{(Spec. Eq. E7-17)}$$
$$= 1.92(0.125\,\text{in.})\sqrt{\frac{29{,}000\ \text{ksi}}{35.5\,\text{ksi}}}\left[1 - \frac{0.34}{131}\sqrt{\frac{29{,}000\ \text{ksi}}{35.5\,\text{ksi}}}\right]$$
$$= 6.35\ \text{in.} < 16.4\ \text{in.}$$

From AISC *Specification* Section E7.2,

$$A_{eff} = 2\left(0.25\text{ in.}\right)\left(6.00\text{ in.}\right) + 6.35\text{ in.}\left(0.125\text{ in.}\right)$$
$$= 3.79\text{ in.}^2$$

$$Q_a = \frac{A_{eff}}{A_g} \qquad \text{(}Spec.\text{ Eq. E7-16)}$$
$$= \frac{3.79\text{ in.}^2}{5.05\text{ in.}^2}$$
$$= 0.751$$

From AISC *Specification* Section E7,

$$Q = Q_s Q_a$$
$$= 0.841\left(0.751\right)$$
$$= 0.632$$

LRFD	ASD
$\frac{f_r}{QF_y} = \frac{2.24\,\text{ksi}}{0.632\left(55\,\text{ksi}\right)}$ $= 0.0644$	$\frac{f_r}{QF_y} = \frac{1.49\,\text{ksi}}{0.632\left(55\,\text{ksi}\right)}$ $= 0.0429$

The location where $h/t_w = 131$ is the critical location, because $\frac{f_r}{QF_y}$ is the largest at that point.

Calculate the nominal buckling strength at the critical location

$Q = 0.632$ from the location where $h/t_w = 131$

$$F_e = \frac{P_{ey}}{A_g}$$
$$= \frac{318\,\text{kips}}{5.05\,\text{in.}^2}$$
$$= 63.0\,\text{ksi}$$

$$\frac{QF_y}{F_e} = \frac{0.632\left(55\,\text{ksi}\right)}{63.0\,\text{ksi}}$$
$$= 0.552 < 2.25;\ \text{therefore,}\ \text{use Equation 5.3-23b}$$

$$F_{cr} = \left(0.658^{\frac{QF_y}{F_e}}\right)QF_y \qquad \text{(5.3-23b)}$$
$$= \left(0.658^{0.552}\right)0.632\left(55\,\text{ksi}\right)$$
$$= 27.6\,\text{ksi}$$

$$P_n = F_{cr}A_g \qquad \text{(5.3-6, }Spec.\text{ Eq. E7-1)}$$
$$= 27.6\,\text{ksi}\left(5.05\,\text{in.}^2\right)$$
$$= 139\,\text{kips}$$

Calculate the out-of-plane strength ratio for the lower unbraced length

LRFD	ASD
$\frac{P_r}{P_c} = \frac{P_r}{\phi_c P_n}$ $= \frac{11.3\,\text{kips}}{0.90(139\,\text{kips})}$ $= 0.0903$	$\frac{P_r}{P_c} = \frac{\Omega_c P_r}{P_n}$ $= \frac{1.67(7.50\,\text{kips})}{139\,\text{kips}}$ $= 0.0901$

C. Out-of-Plane Flexural Buckling Strength—Upper Unbraced Length

Calculate the out-of-plane elastic buckling strength, P_{ey}, using properties at the middle of the 54-in. upper unbraced length.

At bottom end, web height = 19.5 in.
At top end, web height = 24.0 in.
At mid-length, web height = 21.8 in.

$$I_y = \frac{2(0.250\,\text{in.})(6.00\,\text{in.})^3}{12} + \frac{21.8\,\text{in.}(0.125\,\text{in.})^3}{12}$$
$$= 9.00\,\text{in.}^4$$

$$P_{ey} = \frac{\pi^2 E I_y}{(KL_b)^2}$$
$$= \frac{\pi^2 29{,}000(9.00\,\text{in.}^4)}{[1.0(54.0\,\text{in.})]^2}$$
$$= 883\ \text{kips}$$

Calculate F_{n1}, the nominal buckling stress without consideration of slender elements

By inspection, under a constant axial force, the location with largest ratio of f_r/F_y is the bottom end of the upper unbraced length.

From Table 5-1, $A_g = 5.44\ \text{in.}^2$ at the bottom end of the upper unbraced length.

$$F_e = \frac{P_{ey}}{A_g}$$
$$= \frac{883\ \text{kips}}{5.44\ \text{in.}^2}$$
$$= 162\ \text{ksi}$$

$$\frac{F_y}{F_e} = \frac{55\ \text{ksi}}{162\ \text{ksi}}$$
$$= 0.340 < 2.25;\ \text{therefore,}\ \text{use Equation 5.3-20b}$$

$$F_{n1} = \left(0.658^{\frac{F_y}{F_e}}\right) F_y \qquad (5.3\text{-}20b)$$

$$= \left(0.658^{0.340}\right) 55\,\text{ksi}$$
$$= 47.7\,\text{ksi}$$

Determine γ_{n1} at the bottom end of the upper unbraced length.

LRFD	ASD
$f_{rmax} = 2.08$ ksi (from previous calculation) $\gamma_{n1} = \dfrac{F_{n1}}{f_{rmax}}$ $= \dfrac{47.7\,\text{ksi}}{2.08\,\text{ksi}}$ $= 22.9$	$f_{rmax} = 1.38$ ksi (from previous calculation) $\gamma_{n1} = \dfrac{F_{n1}}{f_{rmax}}$ $= \dfrac{47.7\,\text{ksi}}{1.38\,\text{ksi}}$ $= 34.6$

Locate critical section and calculate slenderness reduction factor, Q

Calculate $\dfrac{f_r}{QF_y}$ at the bottom end of the upper unbraced length.

Check flange slenderness.

From calculations for the top of the lower unbraced length,

$Q_s = 0.841$

Check web slenderness.

From in-plane calculations above, the web is slender.

$f_r = f_{rmax}$

LRFD	ASD
$f = \gamma_{n1} f_r$ $= 22.9(2.08\text{ ksi})$ $= 47.6$ ksi	$f = \gamma_{n1} f_r$ $= 34.6(1.38\text{ ksi})$ $= 47.7$ ksi

Note that the difference in f between LRFD and ASD is due to rounding. Use ASD value: $f = 47.7$ ksi.

$$b_e = 1.92t\sqrt{\frac{E}{f}}\left[1-\frac{0.34}{(b/t)}\sqrt{\frac{E}{f}}\right] \le b \qquad \text{(}\textit{Spec.}\text{ Eq. E7-17)}$$

$$= 1.92(0.125\,\text{in.})\sqrt{\frac{29{,}000\text{ ksi}}{47.7\,\text{ksi}}}\left[1-\frac{0.34}{156}\sqrt{\frac{29{,}000\text{ ksi}}{47.7\,\text{ksi}}}\right]$$

$$= 5.60\,\text{in.} < 19.5\,\text{in.}$$

From AISC *Specification* Section E7.2,

$$A_{eff} = 2(0.25\text{ in.})(6.00\text{ in.}) + 5.60\,\text{in.}(0.125\,\text{in.})$$

$$= 3.70\text{ in.}^2$$

$$Q_a = \frac{A_{eff}}{A_g} \qquad \text{(}\textit{Spec.}\text{ Eq. E7-16)}$$

$$= \frac{3.70\,\text{in.}^2}{5.44\,\text{in.}^2}$$

$$= 0.680$$

From AISC *Specification* Section E7,

$$Q = Q_s Q_a$$

$$= 0.841(0.680)$$

$$= 0.572$$

LRFD	ASD
$\frac{f_r}{QF_y} = \frac{2.08\,\text{ksi}}{0.572(55\,\text{ksi})}$ $= 0.0661$	$\frac{f_r}{QF_y} = \frac{1.38\,\text{ksi}}{0.572(55\,\text{ksi})}$ $= 0.0439$

Calculate $\frac{f_r}{QF_y}$ at the top end of the upper unbraced length.

$A_g = 6.00 \text{ in.}^2$

From calculations at the bottom end of the upper unbraced length, k_c is limited to a minimum of 0.35 and $Q_s = 0.841$. Check web slenderness.

$$\lambda = \frac{h}{t_w}$$
$$= \frac{24.0\,\text{in.}}{0.125\,\text{in.}}$$
$$= 192$$

$\lambda_r = 34.2 < 192$; therefore, the web is slender and the reduction factor, Q, is determined from AISC *Specification* Section E7 as follows:

$$Q = Q_s Q_a$$

where

$$Q_a = \frac{A_{eff}}{A_g}$$

$A_g = 6.00 \text{ in.}^2$

$A_{eff} = 2A_f + b_e t_w$

$$b_e = 1.92t\sqrt{\frac{E}{f}}\left[1 - \frac{0.34}{(b/t)}\sqrt{\frac{E}{f}}\right] \le b \qquad \text{(}\textit{Spec.}\text{ Eq. E7-17)}$$

where the stress, f, is:

LRFD	ASD
$f_r = 1.88$ ksi (as determined previously)	$f_r = 1.25$ ksi (as determined previously)
$f = \gamma_{n1} f_r$ $= 22.9(1.88\,\text{ksi})$ $= 43.1\,\text{ksi}$	$f = \gamma_{n1} f_r$ $= 34.6(1.25\,\text{ksi})$ $= 43.3\,\text{ksi}$

Note that the difference in f between LRFD and ASD is due to rounding. Use ASD value: $f = 43.3$ ksi.

$$b_e = 1.92t\sqrt{\frac{E}{f}}\left[1 - \frac{0.34}{(b/t)}\sqrt{\frac{E}{f}}\right] \le b \qquad \text{(}\textit{Spec.}\text{ Eq. E7-17)}$$
$$= 1.92(0.125\,\text{in.})\sqrt{\frac{29{,}000\text{ ksi}}{43.3\,\text{ksi}}}\left[1 - \frac{0.34}{192}\sqrt{\frac{29{,}000\text{ ksi}}{43.3\,\text{ksi}}}\right]$$
$$= 5.93\,\text{in.} < 24.0\,\text{in.}$$

From AISC *Specification* Section E7.2,

$$A_{eff} = 2A_f + b_e t_w$$
$$= 2\left(¼\text{ in.}\right)\left(6.00\,\text{in.}\right) + 5.93\,\text{in.}\left(0.125\,\text{in.}\right)$$
$$= 3.74\,\text{in.}^2$$

$$Q_a = \frac{A_{eff}}{A_g}$$
$$= \frac{3.74\,\text{in.}^2}{6.00\,\text{in.}^2}$$
$$= 0.623$$

$$Q = Q_s Q_a \qquad \text{(}\textit{Spec.}\text{ Eq. E7-16)}$$
$$= 0.841\left(0.623\right)$$
$$= 0.524$$

Calculate f_r/QF_y:

LRFD	ASD
$\frac{f_r}{QF_y} = \frac{1.88\,\text{ksi}}{0.524\left(55\,\text{ksi}\right)}$ $= 0.0652$	$\frac{f_r}{QF_y} = \frac{1.25\,\text{ksi}}{0.524\left(55\,\text{ksi}\right)}$ $= 0.0434$

The bottom of upper unbraced length is the critical location, because $\frac{f_r}{QF_y}$ is the largest at that point.

Calculate the nominal buckling strength at the critical location

As determined for the bottom end of the upper unbraced length, $Q = 0.572$ and $F_e = 162$ ksi.

$$\frac{QF_y}{F_e} = \frac{0.572\left(55\,\text{ksi}\right)}{162\,\text{ksi}}$$
$$= 0.194 < 2.25\text{; therefore, use Equation 5.3-23b for the calculation of the nominal buckling strength}$$

$$F_{cr} = \left(0.658^{\frac{QF_y}{F_e}}\right)QF_y \qquad \text{(5.3-23b)}$$
$$= \left(0.658^{0.194}\right)0.572\left(55\,\text{ksi}\right)$$
$$= 29.0\,\text{ksi}$$

$$P_n = F_{cr}A_g \qquad \text{(5.3-6, }\textit{Spec.}\text{ Eq. E7-1)}$$
$$= 29.0\,\text{ksi}\left(5.44\,\text{in.}^2\right)$$
$$= 158\,\text{kips}$$

Calculate the out-of-plane strength ratio for the upper unbraced length

LRFD	ASD
$\frac{P_r}{P_c} = \frac{P_r}{\phi_c P_n}$ $= \frac{11.3\,\text{kips}}{0.90(158\,\text{kips})}$ $= 0.0795$	$\frac{P_r}{P_c} = \frac{\Omega_c P_r}{P_n}$ $= \frac{1.67(7.50\,\text{kips})}{158\,\text{kips}}$ $= 0.0793$

Column Strength

For the condition of pure axial compression, the column strength is the lowest strength calculated for the limit states of in-plane buckling of the whole column, out-of-plane buckling of the lower unbraced length, and out-of-plane buckling of the upper unbraced length. These are summarized below.

Summary of Axial Strengths	
In-Plane Flexural Buckling	
LRFD	ASD
$\frac{P_r}{P_c} = \frac{P_r}{\phi_c P_n}$ $= \frac{11.3\,\text{kips}}{0.90(168\,\text{kips})}$ $= 0.0747$	$\frac{P_r}{P_c} = \frac{\Omega_c P_r}{P_n}$ $= \frac{1.67(7.50\,\text{kips})}{168\,\text{kips}}$ $= 0.0746$
Out-of-Plane Flexural Buckling—Lower Unbraced Length	
LRFD	ASD
$\frac{P_r}{P_c} = \frac{11.3\,\text{kips}}{0.90(139\,\text{kips})}$ $= 0.0903$	$\frac{P_r}{P_c} = \frac{1.67(7.50\,\text{kips})}{139\,\text{kips}}$ $= 0.0901$
Out-of-Plane Flexural Buckling—Upper Unbraced Length	
LRFD	ASD
$\frac{P_r}{P_c} = \frac{11.3\,\text{kips}}{0.90(158\,\text{kips})}$ $= 0.0795$	$\frac{P_r}{P_c} = \frac{1.67(7.50\,\text{kips})}{158\,\text{kips}}$ $= 0.0793$

Out-of-plane flexural buckling of the lower unbraced length governs the strength of the column.

The available strengths are calculated as:

LRFD	ASD
$\phi_c P_n = 0.90(139\,\text{kips})$ $= 125\ \text{kips}$	$\frac{P_n}{\Omega_c} = \frac{139\ \text{kips}}{1.67}$ $= 83.2\,\text{kips}$

5.4 FLEXURE

Engineers accustomed to the 1989 AISC *Specification* (AISC, 1989) will find the AISC *Specification* flexural provisions to be substantially different. In addition to the overall change in format from stress to moment, the fundamental lateral-torsional buckling equations have been simplified as has the treatment of webs with slendernesses in the range between the compact and noncompact limits.

Tapered beams are subject to the same limit states as prismatic members, that is, the strength is the lowest of that determined for any of the following applicable limit states:

1. Compression flange yielding
2. Lateral-torsional buckling
3. Compression flange local buckling
4. Tension flange yielding
5. Tension flange rupture

Sections F2 to F5 of the AISC *Specification* have been organized for the maximum convenience of users of hot-rolled shapes. In each of these sections, the nominal strength equations for a given limit state (e.g., lateral-torsional buckling) are simplified from a more general form by removing terms not needed for the type of member addressed. In contrast, the following procedure combines slightly modified provisions of Sections F2, F3, F4 and F5 to produce a single procedure that is algebraically equivalent to the individual procedures for cases with uniform bending stresses across an unbraced length. Any combination of compact, noncompact, and slender flange and web elements can be handled. For nontapered members, the results of the procedure converge to those of the applicable section in Chapter F with the exception of the handling of C_b for members with nonuniform flexural stresses across the unbraced length and the definition of L_p for compact I-shaped members. The equations presented in this guide are more convenient when dealing routinely with a mix of flange and web slenderness.

The principal difference between the procedures for prismatic and tapered beams is in the calculation of lateral-torsional buckling strength. To properly account for the effect of taper on the stress gradient in the compression flange, C_b is calculated using flexural stresses rather than moments, per the method proposed by Yura and Helwig (1996). Based on the research by Kim and White (2007a), it is also recommended that C_b be calculated using the AASHTO (2004, 2007) equation, rather than the AISC *Specification* equation written in terms of flange flexural stresses. For most cases, the two equations give very similar results. In cases where they differ significantly, the AASHTO equation generally gives more accurate results for members with multiple brace points along their length (Kim and White, 2007a; White, 2010). The AISC (2005) C_b equation tends to be more conservative than the AASHTO (2004, 2007) equation. This is particularly the case for reverse-curvature bending of members with singly symmetric cross sections.

Because of the continuously changing cross-section geometry, it is generally necessary to check the applicable limit states at various locations along the length of the beam. In the absence of a more sophisticated strategy for finding the critical locations, it is suggested that checks be made at the middle and ends of the unbraced length, at any taper change or plate change, and at locations of maximum flexural stress for each of the applicable limit states.

5.4.1 Common Parameters

C_b, Lateral-Torsional Buckling Modification Factor

The lateral-torsional buckling modification factor, C_b, is calculated individually for each flange in an unbraced length using flexural stresses computed from that flange rather than moments (see Figure 5-4 for definitions of variables used in the determination of C_b). This term is used to modify the elastic lateral-torsional buckling stress equation to account for the favorable effect of moment gradient along an unbraced length. Several example calculations using the AASHTO (2004, 2007) procedure are illustrated in Figure 5-5.

Calculate C_b as:

For $\frac{f_{mid}}{f_2} \geq 1$, or $f_2 = 0$, or cantilevers,

$$C_b = 1.0$$

otherwise,

$$C_b = 1.75 - 1.05\frac{f_1}{f_2} + 0.3\left(\frac{f_1}{f_2}\right)^2 \leq 2.3 \qquad (5.4\text{-}1)$$

where

f_2 = the absolute value of the largest compressive flexural stress at either end of the unbraced

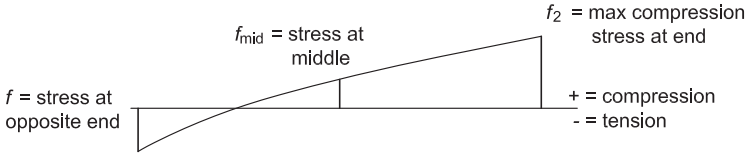

Fig. 5-4. Definition of C_b *stresses.*

length of the flange under consideration. If the stress is zero or is tensile at both ends of the flange, f_2 is taken as zero.

f_{mid} = flexural stress in the flange under consideration at the middle of the unbraced length, taken as positive for compression and negative for tension

f_0 = flexural stress in the flange under consideration at the opposite end of the unbraced length from f_2, taken as positive for compression and negative for tension

$$\text{For } |f_{mid}| < \left|\frac{f_0 + f_2}{2}\right|, \quad f_1 = f_0$$

$$\text{For } |f_{mid}| \geq \left|\frac{f_0 + f_2}{2}\right|, \quad f_1 = 2f_{mid} - f_2 \geq f_0 \qquad (5.4\text{-}2)$$

For doubly symmetric members under combined tension and flexure, Section H1.2 of the AISC *Specification* permits C_b to be multiplied by

$$\sqrt{1+\frac{P_u}{P_{ey}}} \text{ for LRFD or } \sqrt{1+\frac{1.5P_a}{P_{ey}}} \text{ for ASD}$$

where

P_a = required axial tensile strength using ASD load combinations, kips

$$P_{ey} = \frac{\pi^2 EI_y}{L_b^2}, \text{ ksi} \qquad (5.4\text{-}3)$$

P_u = required axial tensile strength using LRFD load combinations, kips

However, this increase in strength has not been demonstrated for the general case of tapered members and is thus not recommended for use in their design.

In the general approach presented next, which is applicable for all members within the scope of this document, C_b is used as a scale factor on the elastic buckling stress, $F_{e.LTB}$, rather than as a multiplier on the nominal moment, M_n, as in the AISC *Specification*. For elastic lateral-torsional buckling (LTB), this is equivalent to the AISC *Specification* approach of always scaling the nominal moment, M_n, directly. However, for inelastic LTB, it is equivalent to the approach in AISC (1989) Equation F1-6. The general approach is somewhat conservative relative to the AISC *Specification* for inelastic LTB of prismatic members with $C_b > 1.0$.

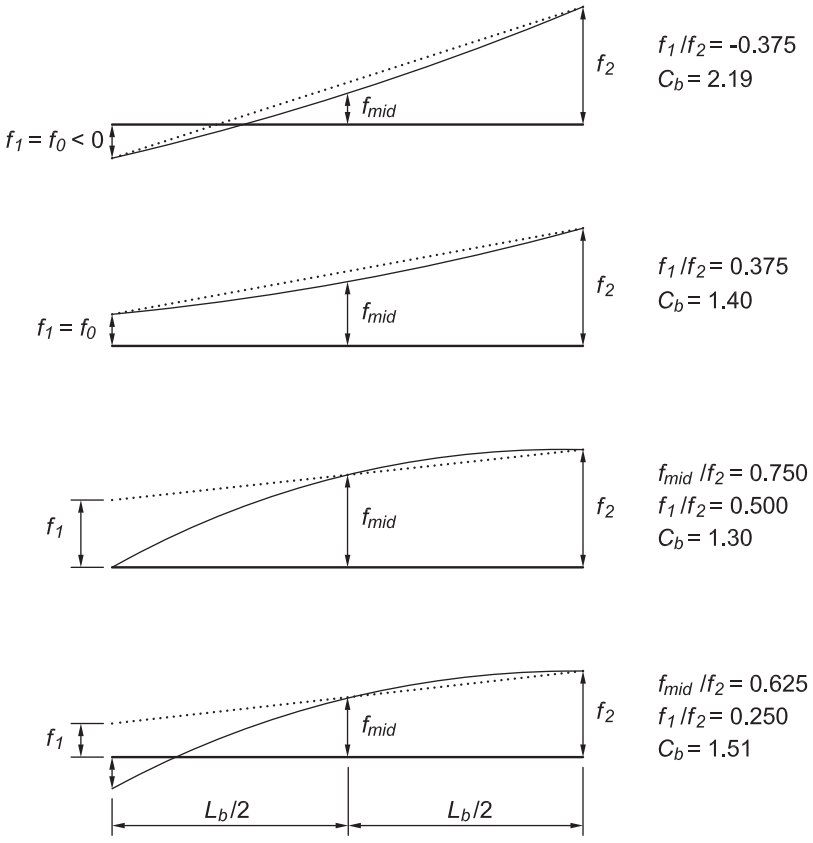

Fig. 5-5. Sample C_b *calculations, adapted from AASHTO (2007) Article C6.4.10.*

For linearly tapered members with no steps in the geometry of the flanges along the unbraced length, the AISC *Specification* approach of multiplying $M_{n(C_b=1)}$ by C_b can be applied. However, for general cases such as unbraced lengths with steps in the flange geometry and/or multiple web tapers, justification of the more liberal AISC *Specification* approach is difficult. This is because extensive yielding may occur within the span and the appropriateness of the *Specification* characterization of the inelastic LTB resistance in these types of members has not been studied extensively. At the limit where the compression flange flexural stress is close to uniform and $C_b \approx 1.0$, both of the preceding approaches give the same result.

R_{pc}, Web Plastification Factor—Compression

R_{pc} is the effective cross-section plastic shape factor, limited by compression, for cross sections with compact or noncompact webs. This term is used to adjust the flexural strength to account for the favorable effect of web plastification in cross sections with nonslender web elements. The value of R_{pc} ranges from 1.0 for sections with slender webs to M_p/M_{yc} for compact shapes. Using the section properties at the cross section under consideration, calculate R_{pc} as:

For $\frac{h_c}{t_w} \le \lambda_{pw}$,

$$R_{pc} = \frac{M_p}{M_{yc}} \qquad \text{(5.4-4, } \textit{Spec.} \text{ Eq. F4-9a)}$$

For $\lambda_{rw} > \frac{h_c}{t_w} > \lambda_{pw}$,

$$R_{pc} = \left[\frac{M_p}{M_{yc}} - \left(\frac{M_p}{M_{yc}} - 1\right)\left(\frac{\lambda - \lambda_{pw}}{\lambda_{rw} - \lambda_{pw}}\right)\right] \le \frac{M_p}{M_{yc}}$$

(5.4-5, *Spec.* Eq. F4-9b)

For $\frac{h_c}{t_w} \ge \lambda_{rw}$ or $\frac{I_{yc}}{I_y} \le 0.23$,

$$R_{pc} = 1.0 \le \frac{M_p}{M_{yc}}$$

where

$M_p = F_y Z_x \le 1.6 F_y S_{xc}$

$M_{yc} = F_y S_{xc}$

h_c = twice the distance from the cross-section centroid to the inside face of the compression flange, in.

h_p = twice the distance from the plastic neutral axis to the inside face of the compression flange, in.

$\lambda = h_c / t_w$

$\lambda_{pw} = 3.76\sqrt{E/F_y}$ for doubly symmetric sections (from *Spec.* Table B4.1)

$$\lambda_{pw} = \frac{\frac{h_c}{h_p}\sqrt{\frac{E}{F_y}}}{\left(0.54\frac{M_p}{M_{ymin}} - 0.09\right)^2} \le \lambda_{rw}$$ for singly symmetric sections

(from *Spec.* Table B4.1)

$\lambda_{rw} = 5.70\sqrt{E/F_y}$ (from *Spec.* Table B4.1)

In the denominator of the equation for the compact web slenderness limit, λ_{pw}, for singly symmetric sections from the AISC *Specification* Table B4.1, M_{ymin} has been substituted for M_y as shown in the AISC *Specification* to clarify the intent.

The recommendation to take R_{pc} as 1.0 when $I_{yc}/I_y \le 0.23$ is an extension of the AISC *Specification* based on White and Jung (2006), who show that a compression flange with a very small I_y leads to large web distortions and corresponding strength reductions, even for noncompact webs.

R_{pg}, Web Bend Buckling Factor

R_{pg} is the bending strength reduction factor for cross sections with slender webs. This term reduces the nominal flexural strength to account for the unfavorable effect of web bend buckling and the subsequent post-buckling behavior involving load shedding, to the flanges. This strength reduction is the result of local buckling of the web in the compression region.

The value of R_{pg} is 1.0 for sections with compact or noncompact webs and less than 1.0 for sections with slender webs. Using the section properties at the cross section under consideration, calculate R_{pg} as:

For $\frac{h_c}{t_w} \le \lambda_{rw}$,

$$R_{pg} = 1.0$$

For $\frac{h_c}{t_w} > \lambda_{rw}$,

$$R_{pg} = 1 - \frac{a_w}{1{,}200 + 300 a_w}\left(\frac{h_c}{t_w} - 5.7\sqrt{\frac{E}{F_y}}\right) \le 1.0$$

(5.4-6, *Spec.* Eq. F5-6)

where

$\lambda_{rw} = 5.70\sqrt{E/F_y}$ (*Spec.* Table B4.1)

$a_w = \frac{h_c t_w}{b_{fc} t_{fc}} \le 10.0$ (5.4-7, *Spec.* Eq. F4-11)

Although it involves additional calculations, Equation 5.4-6 can be modified to increase R_{pg} in cases where the web flexural stresses are limited by compression flange local

buckling, lateral-torsional buckling, or tension flange yielding. Substitute $M_{n(R_{pg}=1)}/S_{xc}$ for F_y in Equation 5.4-6, where $M_{n(R_{pg}=1)}$ is the nominal moment strength calculated with R_{pg} taken equal to 1.0. This refinement is incorporated within the AASHTO Specifications (2004, 2007) and the previous AISC ASD (AISC, 1989) and LRFD (AISC, 1999) Specifications, but was changed in the interest of simplicity for the nontapered section covered in the AISC *Specification*.

5.4.2 Compression Flange Yielding

Using the parameters defined in Section 5.4.1, the nominal flexural resistance based on compression flange yielding is calculated as:

$$\begin{aligned} M_n &= R_{pc} R_{pg} M_{yc} \\ &= R_{pc} R_{pg} F_y S_{xc} \end{aligned} \qquad (5.4\text{-}8)$$

For sections with compact webs, Equation 5.4-8 reduces to:

$$\begin{aligned} M_n &= M_p \\ &= F_y Z_x \end{aligned} \qquad (5.4\text{-}9, \textit{Spec.}\ \text{Eq. F2-1})$$

For doubly symmetric sections with noncompact or slender webs, Equation 5.4-8 reduces to AISC Equation F4-1 or F5-1, as appropriate. Because R_{pc} always has a value of 1.0 for sections with slender webs and R_{pg} always has a value of 1.0 for compact and noncompact webs, either R_{pc} or R_{pg} will be equal to 1.0 in all cases, except when the web is exactly at the limit between noncompact and slender, in which case both are equal to 1.0. The product $R_{pc}R_{pg}$ is usually greater than 1.0 for sections with noncompact webs, and it is always less than 1.0 for sections with slender webs.

Although identified as a separate limit state in the AISC *Specification*, the compression flange yielding limits are identical to the upper bounds given for lateral-torsional buckling. As a result, a separate check for this limit state is redundant if the lateral-torsional buckling upper limit is checked.

5.4.3 Lateral-Torsional Buckling (LTB)

The provisions for lateral-torsional buckling are modified versions of the AISC provisions to account for the influence of nonprismatic member geometry. The calculations describe three regions of behavior. Short unbraced lengths are governed by yielding and are not subject to lateral-torsional buckling. Long unbraced lengths are subject to elastic lateral-torsional buckling. Intermediate unbraced lengths are subject to inelastic buckling and have strengths linearly interpolated between the strengths at the transition points to the yielding and elastic LTB regions.

The LTB strength is checked as a single strength ratio for the entire unbraced length, in a manner similar to the handling of axial compression buckling. The procedure takes into account both the LTB behavior and the behavior represented by the web bend buckling and plastification factors, R_{pg} and R_{pc}.

The lateral-torsional buckling limit state must be checked for each flange having compression somewhere along its length. The smaller of the two strength ratios governs.

General Procedure

The following procedure for calculating the lateral-torsional buckling strength may be used for all members within the scope of this document:

1. Calculate the elastic lateral-torsional buckling stress, F_{eLTB}, of the unbraced length using AISC *Specification* Equation F4-5 with the section properties at the middle of the unbraced length and with C_b determined using Equations 5.4-1 and 5.4-2.

$$F_{eLTB} = \frac{C_b \pi^2 E}{\left(\frac{L_b}{r_t}\right)^2} \sqrt{1 + 0.078 \frac{J}{S_{xc} h_o} \left(\frac{L_b}{r_t}\right)^2} \qquad (5.4\text{-}10, \textit{Spec.}\ \text{Eq. F4-5})$$

where

h_o = distance between flange centroids

$$r_t = \frac{b_{fc}}{\sqrt{12\left(\frac{h_o}{d} + \frac{1}{6} a_w \frac{h^2}{h_o d}\right)}} \qquad (5.4\text{-}11, \textit{Spec.}\ \text{Eq. F4-10})$$

and a_w is as defined earlier for R_{pg}, except that the upper limit of 10 does not apply.

If the web is slender $\left(h_c/t_w\right) > 5.70\sqrt{E/F_y}$, or if $I_{yc}/I_y \le 0.23$,

take J as zero; otherwise,

$$J = \frac{h t_w^3}{3} + \frac{b_{ft} t_{ft}^3}{3}\left(1 - 0.63\frac{t_{ft}}{b_{ft}}\right) + \frac{b_{fc} t_{fc}^3}{3}\left(1 - 0\,63\frac{t_{fc}}{b_{fc}}\right) \qquad (5.4\text{-}12)$$

2. Determine the location of the maximum compressive flexural stress, f_r, within the unbraced length. This location will often be at or near one of the ends, but it can occur anywhere along the length. At this location, calculate the nominal buckling strength multiplier, γ_{eLTB}, as:

$$\gamma_{eLTB} = F_{eLTB}/f_r \qquad (5.4\text{-}13)$$

3. Calculate F_L. For most sections, F_L is $0.7F_y$.
For all members with slender webs and other members with $S_{xt}/S_{xc} \ge 0.7$,

$$F_L = 0.7F_y \qquad \text{(5.4-14, } \textit{Spec.} \text{ Eq. F4-6a)}$$

For members with compact and noncompact webs and $S_{xt}/S_{xc} < 0.7$,

$$F_L = \frac{F_y S_{xt}}{S_{xc}} \geq 0.5F_y \qquad \text{(5.4-15, } \textit{Spec.} \text{ Eq. F4-6b)}$$

4. At various locations along the unbraced length, determine which of the three lateral-torsional buckling regions applies, and calculate M_n, if applicable, using the buckling strength multiplier, γ_{eLTB}, and the compression flange flexural stress at that location, f_r.

   (a) If $\frac{\gamma_{eLTB} f_r}{F_y} \geq \frac{\pi^2}{1.1^2} = 8.2$ (the stress ratio corresponding to $L_b = L_p$ for prismatic members) (White and Kim, 2006), the lateral-torsional buckling limit state does not apply.

   (b) If $8.2 > \frac{\gamma_{eLTB} f_r}{F_y} > \frac{F_L}{F_y}$, calculate the inelastic nominal lateral-torsional buckling strength as:

$$M_n = R_{pg} R_{pc} M_{yc} \left[1 - \left(1 - \frac{F_L}{R_{pc} F_y} \right) \left(\frac{\pi \sqrt{\frac{F_y}{\gamma_{eLTB} f_r}} - 1.1}{\pi \sqrt{\frac{F_y}{F_L}} - 1.1} \right) \right]$$

$$\leq R_{pg} R_{pc} M_{yc} \qquad (5.4\text{-}16)$$

   This equation takes the place of AISC *Specification* Equations F4-2 and F5-3 and is written in terms of the stress ratio $\frac{\gamma_{eLTB} f_r}{F_y}$ (White and Kim, 2006).

   (c) If $\frac{\gamma_{eLTB} f_r}{F_y} \leq \frac{F_L}{F_y}$, calculate the elastic lateral-torsional buckling nominal strength as:

   For members with slender webs,

$$M_n = R_{pg} \gamma_{eLTB} f_r S_{xc} \qquad (5.4\text{-}17)$$

   For other members,

$$M_n = \gamma_{eLTB} f_r S_{xc} \qquad (5.4\text{-}18)$$

5. The largest ratio of M_r/M_n calculated along the unbraced length is the lateral-torsional buckling strength ratio for the entire unbraced length.

Procedure for Single Linear Tapered Members (Flange and Web Plates Remain Constant)

For tapered members with a single linear taper and no changes of flange or web plates within the unbraced length, the following more liberal procedure may be used:

1. Calculate $(F_{eLTB})_{C_b=1}$ as above, using $C_b = 1.0$.
2. Calculate $(\gamma_{eLTB})_{C_b=1}$ as above, substituting $(F_{eLTB})_{C_b=1}$ for F_{eLTB}.
3. Calculate F_L as above.
4. At various locations along the unbraced length, determine which of the three lateral-torsional buckling regions applies, and calculate M_n if applicable using the buckling strength multiplier, $(\gamma_{eLTB})_{C_b=1}$, and the compression flange flexural stress at that location, f_r.

   (a) If $\frac{(\gamma_{eLTB})_{C_b=1} f_r}{F_y} \geq \frac{\pi^2}{1.1^2} = 8.2$, the lateral-torsional buckling limit state does not apply.

   (b) If $8.2 > \frac{(\gamma_{eLTB})_{C_b=1} f_r}{F_y} > \frac{F_L}{F_y}$, calculate the inelastic lateral-torsional buckling nominal strength as:

$$M_n = C_b R_{pg} R_{pc} M_{yc} \times \left[1 - \left(1 - \frac{F_L}{R_{pc} F_y} \right) \left(\frac{\pi \sqrt{\frac{F_y}{(\gamma_{eLTB})_{C_b=1} f_r}} - 1.1}{\pi \sqrt{\frac{F_y}{F_L}} - 1.1} \right) \right]$$

$$\leq R_{pg} R_{pc} M_{yc} \qquad (5.4\text{-}19)$$

   This equation is an accurate approximation of the AISC *Specification* Equations F4-2 and F5-3 and is written in terms of the stress ratio $\frac{\gamma_{eLTB} f_r}{F_y}$ (White and Kim, 2006).

   (c) If $\frac{(\gamma_{eLTB})_{C_b=1} f_r}{F_y} \leq \frac{F_L}{F_y}$, calculate the elastic lateral-torsional buckling nominal strength as:

   For members with slender webs,

$$M_n = C_b R_{pg} (\gamma_{eLTB})_{C_b=1} f_r S_{xc} \leq R_{pg} M_{yc} \qquad (5.4\text{-}20)$$

   For other members,

$$M_n = C_b (\gamma_{eLTB})_{C_b=1} f_r S_{xc} \leq R_{pc} M_{yc} \qquad (5.4\text{-}21)$$

5.4.4 Compression Flange Local Buckling (FLB)

In the 1989 AISC *Specification* (AISC, 1989), strength reductions from local buckling were handled using Q factors similar to those used for axial compression. In the AISC *Specification*, a direct solution for the nominal strength is provided that does not involve the calculation of Q values.

The net effect is largely the same. The AISC *Specification* rectifies a few anomalies in the AISC (1989) equations (White and Chang, 2007).

As in the case of lateral-torsional buckling, compression flange local buckling (FLB) is defined over three regions. For compact (relatively thick) flanges, FLB is not a limit state. For slender flanges, the elastic FLB strength is calculated directly. For intermediate values of width-thickness ratios, an inelastic FLB strength is calculated by linear interpolation between the strengths at the transition points.

(a) For members with compact flanges, $\left(b_f/2t_f\right) \le 0.38\sqrt{E/F_y}$, the limit state of FLB does not apply.

(b) For members with noncompact flanges, $0.38\sqrt{E/F_y} < b_f/2t_f < 0.95\sqrt{k_cE/F_L}$, the nominal FLB strength is calculated from AISC *Specification* Equations F3-1, F4-12 and F5-8 as:

$$M_n = R_{pg} \times \left[R_{pc}M_{yc} - \left(R_{pc}M_{yc} - F_L S_{xc}\right) \left(\frac{\frac{b_f}{2t_f} - 0.38\sqrt{\frac{E}{F_y}}}{0.95\sqrt{\frac{k_cE}{F_L}} - 0.38\sqrt{\frac{E}{F_y}}} \right) \right] \quad (5.4\text{-}22)$$

(c) For members with slender flanges, $b_f/2t_f \ge 0.95\sqrt{k_cE/F_L}$, the nominal FLB strength is calculated from AISC *Specification* Equations F3-2, F4-13 and F5-9 as:

$$M_n = \frac{0.9R_{pg}Ek_cS_{xc}}{\left(\frac{b_f}{2t_f}\right)^2} \quad (5.4\text{-}23)$$

where

$$k_c = \frac{4}{\sqrt{\frac{h}{t_w}}}; \qquad 0.35 \le k_c \le 0.76 \quad (5.4\text{-}24)$$

5.4.5 Tension Flange Yielding (TFY)

Members with unequal flanges are subject to the limit state of tension flange yielding (TFY).

For members with $S_{xt} \ge S_{xc}$, the limit state of TFY does not apply.

For members with $S_{xt} < S_{xc}$, the nominal TFY strength is calculated as:

$$M_n = R_{pt}F_yS_{xt} \quad \text{(5.4-25, from } \textit{Spec.} \text{ Eq. F4-14)}$$

For $\frac{h_c}{t_w} \le \lambda_{pw}$,

$$R_{pt} = \frac{M_p}{M_{yt}} \quad \text{(5.4-26, } \textit{Spec.} \text{ Eq. F4-15a)}$$

For $\lambda_{pw} < \frac{h_c}{t_w} \le \lambda_{rw}$,

$$R_{pt} = \left[\frac{M_p}{M_{yt}} - \left(\frac{M_p}{M_{yt}} - 1 \right) \left(\frac{\lambda - \lambda_{pw}}{\lambda_{rw} - \lambda_{pw}} \right) \right] \le \frac{M_p}{M_{yt}} \quad \text{(5.4-27, } \textit{Spec.} \text{ Eq. F4-15b)}$$

For $\frac{h_c}{t_w} > \lambda_{rw}$ or $\frac{I_{yc}}{I_y} \le 0.23$,

$$R_{pt} = 1.0 \le \frac{M_p}{M_{yt}}$$

where

$M_p = F_yZ_x \le 1.6F_yS_{xt}$ (5.4-28)

$M_{yt} = F_yS_{xt}$ (5.4-29)

S_{xt} = the gross section modulus to the extreme fiber of the tension flange

and all other terms are as defined for R_{pc} previously.

The recommendation to take R_{pt} as 1.0 when $\frac{I_{yc}}{I_y} \le 0.23$ is an extension of the AISC *Specification* based on White and Jung (2006), who show that a compression flange with a very small I_y leads to large web distortions, even for noncompact webs.

5.4.6 Tension Flange Rupture

Members with holes in the tension flange are subject to the limit state of tension flange rupture. This provision is found in AISC *Specification* Section F13.1.

For members with $F_uA_{fn} \ge Y_tF_yA_{fg}$, the limit state of tension flange rupture does not apply.

For members with $F_uA_{fn} < Y_tF_yA_{fg}$, the nominal flexural strength of the cross section at the location of a hole or line of holes is calculated as:

$$M_n = \frac{F_uA_{fn}}{A_{fg}}S_{xt} \quad (5.4\text{-}30)$$

where

A_{fg} = gross area of tension flange, in.^{2}

A_{fn} = net area of tension flange
$= A_{fg} - t_f \sum \left(d_h + 1/16 \text{ in.} \right)$, in.^{2}
S_{xt} = section modulus to the extreme fiber of the tension flange, in.^{3}
Y_t = 1.0 for $F_y/F_u \le 0.8$
= 1.1 otherwise
d_h = diameter of hole, in.

Equation 5.4-30 is similar to AISC *Specification* Equation F13-1 with S_x equal to S_{xt}.

5.4.7 Strength Ratio

Calculate the strength ratio for the controlling limit state using the required strength, M_r, and the nominal flexural strength, M_n, determined earlier as:

$$\frac{M_r}{M_c} = \frac{\Omega_b M_a}{M_n} \text{ (ASD)} \qquad (5.4\text{-}31)$$

$$\frac{M_r}{M_c} = \frac{M_u}{\phi_b M_n} \text{ (LRFD)} \qquad (5.4\text{-}32)$$

$\phi_b = 0.90$ (LRFD) $\quad \Omega_b = 1.67$ (ASD)

Example 5.3—Doubly Symmetric Section Tapered Beam

Given:

Evaluate the flexural strength of the member from Example 5.2 with the required flexural strength shown in Figure 5-6. All required second-order effects are included in the moment diagram.

Material Properties
F_y = 55 ksi
F_u = 70 ksi

Geometric Properties
Left flange = PL 1/4 × 6
Right flange = PL 1/4 × 6
Web thickness = 0.125 in.
Two 11/16-in.-diameter bolt holes in both flanges at brace points

By inspection, the member is subject to the following limit states:

- Compression flange yielding
- Lateral-torsional buckling
- Compression flange local buckling
- Tension flange rupture at the bolt holes

The tension flange yielding limit state need not be checked because the cross section is doubly symmetric. The upper bound of the lateral-torsional buckling strength is equal to the compression flange yielding strength; thus, a separate check for compression flange yielding is not required unless the section is not subject to lateral-torsional buckling.

Solution:

Table 5-2. Section Properties and Strengths			
Locations	Property	Lower Unbraced Length	Upper Unbraced Length
Top (C-E)	h S_x M_y	19.5 in. 37.0 in.^{3} 2,040 kip-in.	24.0 in. 47.8 in.^{3} 2,630 kip-in.
Mid-Length (B-D)	h S_x M_y M_p	15.8 in 28.7 in.^{3} 1,580 kip-in. 1,750 kip-in.	21.8 in. 42.4 in.^{3} 2,330 kip-in. —
Bottom (A-C)	h S_x M_y	12.0 in. — —	19.5 in. 37.0 in.^{3} 2,040 kip-in.

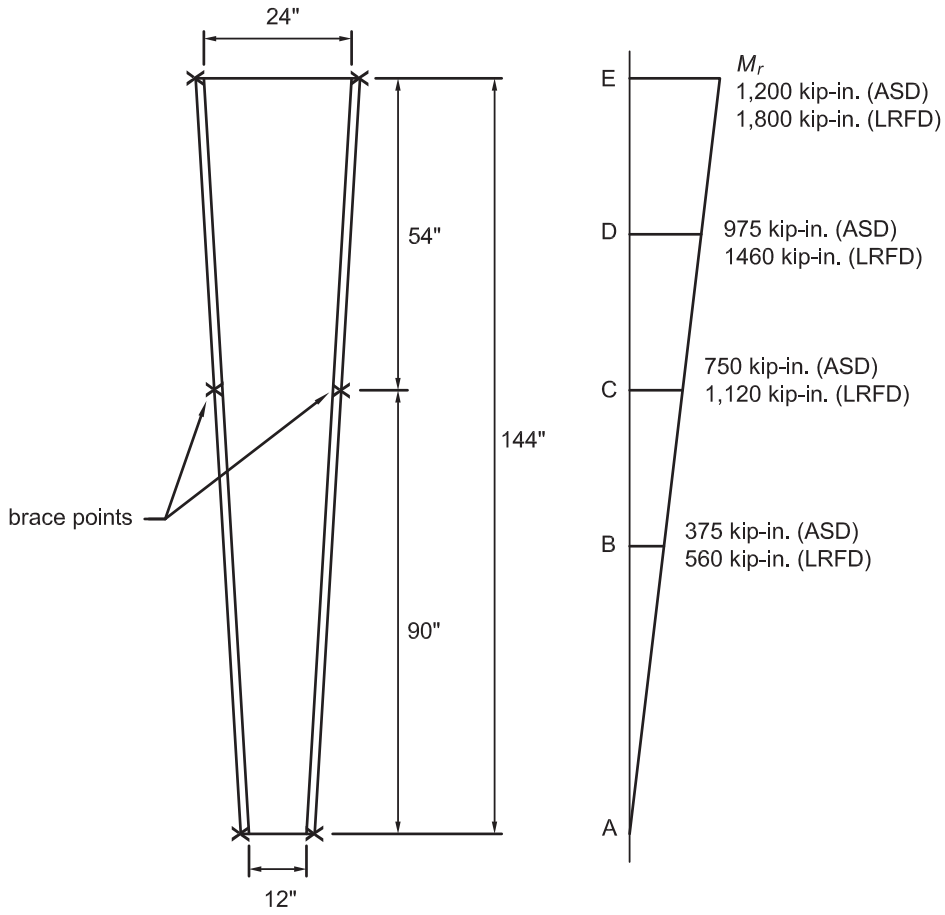

Fig. 5-6. Flexural member.

Web slenderness limits

From AISC *Specification* Table B4.1, for flexure in webs of doubly symmetric I-shaped sections,

$$\lambda_{pw} = 3.76\sqrt{\frac{E}{F_y}}$$

$$= 3.76\sqrt{\frac{29{,}000\,\text{ksi}}{55\,\text{ksi}}}$$

$$= 86.3 \text{ compact web limit}$$

$$\lambda_{rw} = 5.70\sqrt{\frac{E}{F_y}}$$

$$= 5.70\sqrt{\frac{29{,}000\,\text{ksi}}{55\,\text{ksi}}}$$

$$= 131 \text{ slender web limit}$$

Flange slenderness limits

From AISC *Specification* Table B4.1, for flexure in flanges of doubly symmetric I-shaped built-up sections,

$$\lambda_{pf} = 0.38\sqrt{\frac{E}{F_y}}$$

$$= 0.38\sqrt{\frac{29{,}000\,\text{ksi}}{55\,\text{ksi}}}$$

$$= 8.73 \text{ compact flange limit}$$

$$\lambda_{rf} = 0.95\sqrt{\frac{k_c E}{F_L}} \text{ slender flange limit (varies depending upon web height)}$$

Lower unbraced length, L_b = 90.0 in.

Check web slenderness at the middle and top of the 90-in. unbraced length. This check is not needed at the bottom because $M_r = 0$.

$$\left(\frac{h_c}{t_w}\right)_{mid\text{-}length} = \frac{15.8\,\text{in.}}{0.125\,\text{in.}}$$

$$= 126 < 131$$

$$\left(\frac{h_c}{t_w}\right)_{top} = \frac{19.5\,\text{in.}}{0.125\,\text{in.}}$$

$$= 156 > 131$$

Therefore, the web is noncompact at the mid-length, but slender at the top of the unbraced length.

The values of the web plastification factor, R_{pc}, and the web buckling factor, R_{pg}, are required to calculate the nominal flexural strength. At mid-length, the web is noncompact ($\lambda_{pw} < h_c/t_w \le \lambda_{rw}$); therefore, from AISC *Specification* Section F4 and Section 5.4 of this Design Guide, and using values from Table 5-2,

$$R_{pc} = \left[\frac{M_p}{M_{yc}} - \left(\frac{M_p}{M_{yc}} - 1\right)\left(\frac{\lambda - \lambda_{pw}}{\lambda_{rw} - \lambda_{pw}}\right)\right] \le \frac{M_p}{M_{yc}} \qquad \text{(5.4-5, } \textit{Spec.} \text{ Eq. F4-9b)}$$

$$= \left[\frac{1{,}750\,\text{kip-in.}}{1{,}580\,\text{kip-in.}} - \left(\frac{1{,}750\,\text{kip-in.}}{1{,}580\,\text{kip-in.}} - 1\right)\left(\frac{126 - 86.3}{131 - 86.3}\right)\right] \le \frac{1{,}750\,\text{kip-in.}}{1{,}580\,\text{kip-in.}}$$

$$= 1.01 < 1.11; \text{ therefore use } R_{pc} = 1.01$$

$R_{pg} = 1.0$ because the web is noncompact at this location

At the top of the 90-in. unbraced length, the web is slender; therefore, according to Section 5.4.1 of this Design Guide,

$$R_{pc} = 1.0$$

$$a_w = \frac{h_c t_w}{b_{fc} t_{fc}} \qquad \text{(5.4-7, } \textit{Spec.} \text{ Eq. F4-11)}$$

$$= \frac{19.5\,\text{in.}\left(0.125\,\text{in.}\right)}{6.00\,\text{in.}\left(0.250\,\text{in.}\right)}$$

$$= 1.63 \le 10.0 \text{ therefore use } a_w = 1.63$$

$$R_{pg} = 1 - \frac{a_w}{1{,}200 + 300 a_w}\left(\frac{h_c}{t_w} - 5.7\sqrt{\frac{E}{F_y}}\right) \le 1.0 \qquad \text{(5.4-6, } \textit{Spec.} \text{ Eq. F5-6)}$$

$$= 1 - \frac{1.63}{1{,}200 + 300\left(1.63\right)}\left(\frac{19.5\,\text{in.}}{0.125\,\text{in.}} - 5.7\sqrt{\frac{29{,}000\,\text{ksi}}{55\,\text{ksi}}}\right)$$

$$= 0.976$$

Lateral-Torsional Buckling—Lower Unbraced Length

Using the provisions for single linear tapered members with no plate changes, determine the nominal flexural strength, M_n, for the limit state of lateral-torsional buckling in the lower unbraced segment.

First, using AISC *Specification* Section F4 and Section 5.4 of this Design Guide, determine the elastic lateral-torsional buckling stress, F_{eLTB}, with $C_b = 1$ for the location of maximum flexural stress using properties at the middle of the lower unbraced length. The elastic lateral-torsional buckling stress is,

$$F_{eLTB}\ _{C_b=1} = \frac{1.0\pi^2 E}{\left(\frac{L_b}{r_t}\right)^2}\sqrt{1 + 0.078\frac{J}{S_{xc} h_o}\left(\frac{L_b}{r_t}\right)^2} \qquad \text{(5.4-10, } \textit{Spec.} \text{ Eq. F4-5)}$$

where

$$h_o = 15.8\,\text{in.} + 2\left(¼\text{ in.}/2\right)$$

$$= 16.1\ \text{in.}$$

$$h_c = h$$

$$= 15.8\,\text{in.}$$

$$a_w = \frac{h_c t_w}{b_{fc} t_{fc}}$$

$$= \frac{15.8\,\text{in.}\left(0.125\ \text{in.}\right)}{6.00\,\text{in.}\ \left(¼\ \text{in.}\right)} \qquad \text{(5.4-7, } \textit{Spec.} \text{ Eq. F4-11)}$$

$$= 1.32$$

$$r_t = \frac{b_{fc}}{\sqrt{12\left(\frac{h_o}{d} + \frac{1}{6}a_w\frac{h^2}{h_o d}\right)}} \qquad \text{(5.4-11, } \textit{Spec.} \text{ Eq. F4-10)}$$

$$= \frac{6.00\ \text{in.}}{\sqrt{12\left[\frac{16.1\ \text{in.}}{16.3\ \text{in.}} + \frac{1}{6}\left(1.32\right)\frac{\left(15.8\ \text{in.}\right)^2}{16.1\ \text{in.}\left(16.3\ \text{in.}\right)}\right]}}$$

$$= 1.58\ \text{in.}$$

$S_{xc} = S_x = 28.7\ \text{in.}^3$ from Table 5-2

$J = 0$, because the web is slender over some portion of this unbraced length.

Therefore,

$$\left(F_{eLTB}\right)_{C_b=1}=\frac{1.0\pi^2 E}{\left(\frac{L_b}{r_t}\right)^2}\sqrt{1+0.078\frac{J}{S_{xc}h_o}\left(\frac{L_b}{r_t}\right)^2} \qquad \text{(5.4-10, } \textit{Spec.} \text{ Eq. F4-5)}$$

$$=\frac{1.0\pi^2(29{,}000\,\text{ksi})}{\left(\frac{90.0\text{ in.}}{1.58\text{ in.}}\right)^2}\sqrt{1+0.078\left[\frac{0\text{ in.}^4}{28.7\text{ in.}^3(16.1\text{ in.})}\right]\left(\frac{90.0\,\text{in.}}{1.58\,\text{in.}}\right)^2}$$

$$=\frac{1.0\pi^2(29{,}000\text{ ksi})}{\left(\frac{90.0\text{ in.}}{1.58\text{ in.}}\right)^2}$$

$$=88.2\text{ ksi}$$

Find the location of maximum flexural stress.

For the case of a linear web taper and a linear moment taper to zero at the small end (small *P*-δ effects), the maximum flexural stress will always occur at the deep end.

LRFD	ASD
$f_{rmax}=f_2$ $=30.3$ ksi	$f_{rmax}=f_2$ $=20.3$ ksi

Calculate the elastic buckling multiplier with $C_b=1$, $\left(\gamma_{eLTB}\right)_{C_b=1}$.

LRFD	ASD
$\left(\gamma_{eLTB}\right)_{C_b=1}=\frac{\left(F_{eLTB}\right)_{C_b=1}}{f_{rmax}}$ $=\frac{88.2\text{ ksi}}{30.3\text{ ksi}}$ $=2.91$	$\left(\gamma_{eLTB}\right)_{C_b=1}=\frac{\left(F_{eLTB}\right)_{C_b=1}}{f_{rmax}}$ $=\frac{88.2\text{ ksi}}{20.3\text{ ksi}}$ $=4.34$

Calculate the nominal flexural strength due to lateral-torsional buckling at the top of the lower unbraced length. Select the equation for calculation of the nominal flexural strength, M_n, based on the following ratio:

LRFD	ASD
$\frac{\left(\gamma_{eLTB}\right)_{C_b=1}f_r}{F_y}=\frac{2.91(30.3\,\text{ksi})}{55\,\text{ksi}}$ $=1.60$	$\frac{\left(\gamma_{eLTB}\right)_{C_b=1}f_r}{F_y}=\frac{4.34(20.3\,\text{ksi})}{55\,\text{ksi}}$ $=1.60$

When $S_{xt}/S_{xc}\geq 0.7$,

$$F_L=0.7F_y \qquad \text{(5.4-14, } \textit{Spec.} \text{ Eq. F4-6a)}$$

and therefore,

$$\frac{F_L}{F_y}=0.7$$

Because $8.2 > \dfrac{(\gamma_{eLTB})_{C_b=1} f_r}{F_y} > \dfrac{F_L}{F_y}$, use Equation 5.4-19 to calculate M_n:

$$M_n = C_b R_{pg} R_{pc} M_{yc} \left[1 - \left(1 - \frac{F_L}{R_{pc} F_y} \right) \left(\frac{\pi \sqrt{\dfrac{F_y}{(\gamma_{eLTB})_{C_b=1} f_r}} - 1.1}{\pi \sqrt{\dfrac{F_y}{F_L}} - 1.1} \right) \right] \le R_{pg} R_{pc} M_{yc} \qquad (5.4\text{-}19)$$

where C_b for the lower unbraced length is determined using Section 5.4.1, the moment diagram in Figure 5-6, and the properties in Table 5-2, as follows:

LRFD	ASD
$f_0 = 0\,\text{ksi}$	$f_0 = 0\,\text{ksi}$
$f_{mid} = \dfrac{M_r}{S_{xc}} = \dfrac{560\,\text{kip-in.}}{28.7\,\text{in.}^3} = 19.5\,\text{ksi}$	$f_{mid} = \dfrac{M_r}{S_{xc}} = \dfrac{375\,\text{kip-in.}}{28.7\,\text{in.}^3} = 13.1\,\text{ksi}$
$f_2 = \dfrac{M_r}{S_{xc}} = \dfrac{1{,}120\,\text{kip-in.}}{37.0\,\text{in.}^3} = 30.3\,\text{ksi}$	$f_2 = \dfrac{M_r}{S_{xc}} = \dfrac{750\,\text{kip-in.}}{37.0\,\text{in.}^3} = 20.3\,\text{ksi}$
Because $\lvert 19.5\,\text{ksi} \rvert > \left\lvert \dfrac{0\,\text{ksi} + 30.3\,\text{ksi}}{2} \right\rvert$	Because $\lvert 13.1\,\text{ksi} \rvert > \left\lvert \dfrac{0\,\text{ksi} + 20.3\,\text{ksi}}{2} \right\rvert$
$f_1 = 2f_{mid} - f_2 \ge f_0$ (5.4-2) $= 2(19.5\,\text{ksi}) - 30.3\,\text{ksi}$ $= 8.70\,\text{ksi}$	$f_1 = 2f_{mid} - f_2 \ge f_0$ (5.4-2) $= 2(13.1\,\text{ksi}) - 20.3\,\text{ksi}$ $= 5.90\,\text{ksi}$
$C_b = 1.75 - 1.05\dfrac{f_1}{f_2} + 0.3\left(\dfrac{f_1}{f_2}\right)^2 \le 2.3$ (5.4-1) $= 1.75 - 1.05\left(\dfrac{8.70\ \text{ksi}}{30.3\ \text{ksi}}\right) + 0.3\left(\dfrac{8.70\ \text{ksi}}{30.3\ \text{ksi}}\right)^2$ $= 1.47 < 2.3$	$C_b = 1.75 - 1.05\dfrac{f_1}{f_2} + 0.3\left(\dfrac{f_1}{f_2}\right)^2 \le 2.3$ (5.4-1) $= 1.75 - 1.05\left(\dfrac{5.90\ \text{ksi}}{20.3\ \text{ksi}}\right) + 0.3\left(\dfrac{5.90\ \text{ksi}}{20.3\ \text{ksi}}\right)^2$ $= 1.47 < 2.3$

Therefore,

$$M_n = C_b R_{pg} R_{pc} M_{yc} \left[1 - \left(1 - \frac{F_L}{R_{pc} F_y} \right) \left(\frac{\pi \sqrt{\dfrac{F_y}{(\gamma_{eLTB})_{C_b=1} f_r}} - 1.1}{\pi \sqrt{\dfrac{F_y}{F_L}} - 1.1} \right) \right] \le R_{pg} R_{pc} M_{yc} \qquad (5.4\text{-}19)$$

$$= 1.47(0.976)(1.0)(2{,}040\,\text{kip-in.}) \left[1 - \left(1 - \frac{0.7}{1.0} \right) \left(\frac{\pi \sqrt{\dfrac{1}{1.60}} - 1.1}{\pi \sqrt{\dfrac{1}{0.7}} - 1.1} \right) \right] \le 0.976(1.0)(2{,}040\,\text{kip-in.})$$

$= 2{,}470$ kip-in. $> 1{,}990$ kip-in.; therefore, use $M_n = 1{,}990$ kip-in.

Check strength ratio.

LRFD	ASD
$\frac{M_r}{M_c} = \frac{M_r}{\phi_b M_n}$	$\frac{M_r}{M_c} = \frac{\Omega_b M_r}{M_n}$
$= \frac{1{,}120 \text{ kip-in.}}{0.90(1{,}990 \text{ kip-in.})}$	$= \frac{1.67(750 \text{ kip-in.})}{1{,}990 \text{ kip-in.}}$
$= 0.625$	$= 0.629$

Check lateral-torsional buckling strength at the middle of the lower unbraced length. The flexural stress at this location is,

LRFD	ASD
$f_r = \frac{M_r}{S_{xc}}$	$f_r = \frac{M_r}{S_{xc}}$
$= \frac{560 \text{ kip-in.}}{28.7 \text{ in.}^3}$	$= \frac{375 \text{ kip-in.}}{28.7 \text{ in.}^3}$
$= 19.5$ ksi	$= 13.1$ ksi

Select equation for calculation of nominal moment, M_n, based on the following ratio:

LRFD	ASD
$\frac{(\gamma_{eLTB})_{C_b=1} f_r}{F_y} = \frac{2.91(19.5 \text{ ksi})}{55 \text{ ksi}}$	$\frac{(\gamma_{eLTB})_{C_b=1} f_r}{F_y} = \frac{4.34(13.1 \text{ ksi})}{55 \text{ ksi}}$
$= 1.03$	$= 1.03$

Because $8.2 > \frac{(\gamma_{eLTB})_{C_b=1} f_r}{F_y} > \frac{F_L}{F_y}$, use Equation 5.4-19.

$$M_n = C_b R_{pg} R_{pc} M_{yc} \left[1 - \left(1 - \frac{F_L}{R_{pc} F_y} \right) \left(\frac{\pi \sqrt{\frac{F_y}{(\gamma_{eLTB})_{C_b=1} f_r}} - 1.1}{\pi \sqrt{\frac{F_y}{F_L}} - 1.1} \right) \right] \le R_{pg} R_{pc} M_{yc} \tag{5.4-19}$$

$$= 1.47(1.0)(1.01)(1{,}580 \text{ kip-in.}) \left[1 - \left(1 - \frac{0.7}{1.01} \right) \left(\frac{\pi \sqrt{\frac{1}{1.03}} - 1.1}{\pi \sqrt{\frac{1}{0.7}} - 1.1} \right) \right] \le 1.0(1.01)(1{,}580 \text{ kip-in.})$$

$= 1{,}800$ kip-in. $\le 1{,}600$ kip-in.; therefore use $M_n = 1{,}600$ kip-in.

Check strength ratio.

LRFD	ASD
$\frac{M_r}{M_c} = \frac{M_r}{\phi_b M_n}$	$\frac{M_r}{M_c} = \frac{\Omega_b M_r}{M_n}$
$= \frac{560 \text{ kip-in}}{0.90(1{,}600 \text{ kip-in.})}$	$= \frac{1.67(375 \text{ kip-in.})}{1{,}600 \text{ kip-in.}}$
$= 0.389$	$= 0.391$

The top end (larger end) of the lower unbraced length controls the available flexural strength using the limit state of lateral-torsional buckling.

Compression Flange Local Buckling—Lower Unbraced Length

Determine the nominal flexural strength, M_n, for the limit state of compression flange local buckling at the top of the lower unbraced segment.

The equation used for M_n depends on the compactness of the flange. Compare the width-thickness ratio of the flange at the top of the lower unbraced length to the limiting width-thickness ratio from AISC *Specification* Table B4.1, for flexure in flanges of doubly symmetric I-shaped built-up sections:

$$\frac{b_f}{2t_f} = \frac{6.00 \text{ in.}}{2(¼ \text{ in.})}$$

$$= 12.0$$

$$\lambda_{pf} = 8.73 \text{ (calculated previously)}$$

$$\lambda_{rf} = 0.95\sqrt{\frac{k_c E}{F_L}}$$

where

$$k_c = \frac{4}{\sqrt{\frac{h}{t_w}}} \tag{5.4-24}$$

$$= \frac{4}{\sqrt{\frac{19.5 \text{ in.}}{0.125 \text{ in.}}}}$$

$$= 0.320 < 0.35; \text{ therefore use } 0.35$$

$$F_L = 0.7F_y \tag{5.4-14, \textit{Spec.} Eq. F4-6a}$$

$$= 0.7(55 \text{ ksi})$$

$$= 38.5 \text{ ksi}$$

Therefore,

$$\lambda_{rf} = 0.95\sqrt{\frac{k_c E}{F_L}}$$

$$= 0.95\sqrt{\frac{0.35(29{,}000 \text{ ksi})}{38.5 \text{ ksi}}}$$

$$= 15.4 \quad \text{slender flange limit}$$

Because $8.73 < 12.0 < 15.4$, the compression flange is noncompact; therefore, use Equation 5.4-22. The nominal flexural strength at the top of the lower unbraced length is,

$$M_n = R_{pg}\left[R_{pc}M_{yc} - \left(R_{pc}M_{yc} - F_L S_{xc}\right)\left(\frac{\frac{b_f}{2t_f} - 0.38\sqrt{\frac{E}{F_y}}}{0.95\sqrt{\frac{k_c E}{F_L}} - 0.38\sqrt{\frac{E}{F_y}}}\right)\right] \tag{5.4-22}$$

$$M_n = 0.976\left\{1.0(2{,}030 \text{ kip-in.}) - \left[1.0(2{,}030 \text{ kip-in.}) - 38.5 \text{ ksi}(37.0 \text{ in.}^3)\right]\left(\frac{12.0 - 8.73}{15.4 - 8.73}\right)\right\}$$

$$= 1{,}690 \text{ kip-in.}$$

Determine the nominal flexural strength, M_n, for the limit state of compression flange local buckling at the middle of the lower unbraced length. Compare the width-thickness ratio of the flange at the middle of the lower unbraced length to the limiting width-thickness ratio from AISC *Specification* Table B4.1, for flexure in flanges of doubly symmetric I-shaped built-up sections:

$$\frac{b_f}{2t_f} = 12.0 \text{ (calculated previously)}$$

$$\lambda_{pf} = 0.38\sqrt{\frac{E}{F_y}}$$

$$= 8.73 \text{ (calculated previously)}$$

$$\lambda_{rf} = 0.95\sqrt{\frac{k_c E}{F_L}}$$

$$= 15.6 \text{ (calculated previously)}$$

where

$$k_c = \frac{4}{\sqrt{\frac{h}{t_w}}}$$

$$= \frac{4}{\sqrt{\frac{15.8 \text{ in.}}{0.125 \text{ in.}}}} \tag{5.4-24}$$

$$= 0.356$$

Because $0.35 < k_c < 0.76$, use $k_c = 0.356$

$F_L = 38.5$ ksi (calculated previously)

Therefore,

$$\lambda_{rf} = 0.95\sqrt{\frac{k_c E}{F_L}}$$

$$= 0.95\sqrt{\frac{0.356(29{,}000 \text{ ksi})}{38.5 \text{ ksi}}}$$

$$= 15.6 \quad \text{slender flange limit}$$

Because $8.73 < 12.0 < 15.6$, the compression flange is noncompact; therefore, use Equation 5.4-22. The nominal flexural strength for the limit state of compression flange local buckling at the middle of the lower unbraced length is,

$$M_n = R_{pg}\left\{R_{pc}M_{yc} - \left[\left(R_{pc}M_{yc} - F_L S_{xc}\right)\left(\frac{\frac{b_f}{2t_f} - 0.38\sqrt{\frac{E}{F_y}}}{0.95\sqrt{\frac{k_c E}{F_L}} - 0.38\sqrt{\frac{E}{F_y}}}\right)\right]\right\} \tag{5.4-22}$$

$$M_n = 1.0\left\{1.01(1{,}580 \text{ kip-in.}) - \left[1.01(1{,}580 \text{ kip-in.}) - 38.5 \text{ ksi}\left(28.7 \text{ in.}^3\right)\right]\left(\frac{12.0 - 8.73}{15.6 - 8.73}\right)\right\}$$

$$= 1{,}360 \text{ kip-in.}$$

Tension Flange Rupture—Lower Unbraced Length

Determine the nominal flexural strength for the limit state of tensile rupture of the tension flange at the bolt holes at the top of the lower unbraced length. From AISC *Specification* Section F13.1, this limit state applies if $F_u A_{fn} < Y_t F_y A_{fg}$. Also from Section F13.1, $Y_t = 1.0$ when $F_y/F_u < 0.8$.

$$\frac{F_y}{F_u} = \frac{55 \text{ ksi}}{70 \text{ ksi}}$$

$$= 0.786 < 0.8; \text{ therefore } Y_t = 1.0$$

$$A_{fg} = 6.00 \text{ in.}(¼ \text{ in.})$$

$$= 1.50 \text{ in.}^2$$

$$A_{fn} = 1.50 \text{ in.} - \tfrac{1}{4}\text{in.}(2)(^{11}\!/_{16} \text{ in.} + \tfrac{1}{16} \text{ in.})$$
$$= 1.13 \text{ in.}^2$$
$$70\,\text{ksi}\left(1.13\,\text{in.}^2\right) < 1.0\left(55\,\text{ksi}\right)\left(1.50\,\text{in.}^2\right)$$

79.1 kips < 82.5 kips; therefore, the tension flange rupture limit state applies.

The nominal flexural strength for the limit state of tensile rupture at the bolt holes at the top of the lower unbraced length is,

$$M_n = \frac{F_u A_{fn}}{A_{fg}} S_{xt} \tag{5.4-30}$$
$$= \frac{70 \text{ ksi}\left(1.13 \text{ in.}^2\right)}{1.50 \text{ in.}^2} 37.0 \text{ in.}^3$$
$$= 1{,}950 \text{ kip-in.}$$

Following is a summary of flexural strength ratios to be used in combined strength checks in Example 5.4 for the lower unbraced length.

Summary of Flexural Strengths—Lower Unbraced Length	
Lateral-torsional buckling Value at top of unbraced length governs	
LRFD	ASD
$\frac{M_r}{M_c} = \frac{M_r}{\phi_b M_n}$ $= \frac{1{,}120\,\text{kip-in.}}{0.90\left(1{,}980\,\text{kip-in.}\right)}$ $= 0.629$	$\frac{M_r}{M_c} = \frac{\Omega_b M_r}{M_n}$ $= \frac{1.67\left(750\,\text{kip-in.}\right)}{1{,}980\,\text{kip-in.}}$ $= 0.633$
Compression flange local buckling at mid-length	
LRFD	ASD
$\frac{M_r}{M_c} = \frac{560\,\text{kip-in.}}{0.90\left(1{,}360\,\text{kip-in.}\right)}$ $= 0.458$	$\frac{M_r}{M_c} = \frac{1.67\left(375\,\text{kip-in.}\right)}{1{,}360\,\text{kip-in.}}$ $= 0.460$
Compression flange local buckling at top of unbraced length	
LRFD	ASD
$\frac{M_r}{M_c} = \frac{1{,}120\,\text{kip-in.}}{0.90\left(1{,}690\,\text{kip-in.}\right)}$ $= 0.736$	$\frac{M_r}{M_c} = \frac{1.67\left(750\,\text{kip-in.}\right)}{1{,}690\,\text{kip-in.}}$ $= 0.741$

Compression flange local buckling at the top of the lower unbraced length governs the available flexural strength.

Upper Unbraced Length, L_b = 54.0 in.

Check web slenderness at the bottom, middle and top of the upper unbraced length, where the limiting width-thickness ratio of the web, $\lambda_{rw} = 131$ (from previous calculation):

$$\left(\frac{h_c}{t_w}\right)_{\text{bottom}} = \frac{19.5\,\text{in.}}{0.125\,\text{in.}}$$
$$= 156 > 131$$
$$\left(\frac{h_c}{t_w}\right)_{\text{mid-length}} = \frac{21.8\,\text{in.}}{0.125\,\text{in.}}$$
$$= 174 > 131$$

$$\left(\frac{h_c}{t_w}\right)_{top} = \frac{24.0\,\text{in.}}{0.125\,\text{in.}}$$
$$= 192 > 131$$

Therefore, the web is slender at all locations within the upper unbraced length.

In order to determine the nominal flexural strength, values of the web plastification factor, R_{pc}, and the web buckling factor, R_{pg}, must be calculated. At the bottom of the upper unbraced length, from calculations at the top of the lower unbraced length:

$R_{pc} = 1.0$
$R_{pg} = 0.976$

At the middle of the upper unbraced length:

$R_{pc} = 1.0$

$$R_{pg} = 1 - \frac{a_w}{1{,}200 + 300a_w}\left(\frac{h_c}{t_w} - 5.7\sqrt{\frac{E}{F_y}}\right) \le 1.0 \qquad \text{(5.4-6, } \textit{Spec.} \text{ Eq. F5-6)}$$

where

$$a_w = \frac{h_c t_w}{b_{fc} t_{fc}} \qquad \text{(5.4-7, } \textit{Spec.} \text{ Eq. F4-11)}$$
$$= \frac{21.8\,\text{in.}(0.125\,\text{in.})}{6.00\,\text{in.}(0.250\,\text{in.})}$$
$$= 1.82 \le 10.0\text{; therefore use } a_w = 1.82$$
$$R_{pg} = 1 - \frac{a_w}{1{,}200 + 300a_w}\left(\frac{h_c}{t_w} - 5.7\sqrt{\frac{E}{F_y}}\right) \le 1.0 \qquad \text{(5.4-6, } \textit{Spec.} \text{ Eq. F5-6)}$$
$$= 1 - \frac{1.82}{1{,}200 + 300(1.82)}\left(\frac{21.8\,\text{in.}}{0.125\,\text{in.}} - 5.7\sqrt{\frac{29{,}000\,\text{ksi}}{55\,\text{ksi}}}\right)$$
$$= 0.955$$

At the top of the upper unbraced length:

$R_{pc} = 1.0$

$$R_{pg} = 1 - \frac{a_w}{1{,}200 + 300a_w}\left(\frac{h_c}{t_w} - 5.7\sqrt{\frac{E}{F_y}}\right) \le 1.0 \qquad \text{(5.4-6, } \textit{Spec.} \text{ Eq. F5-6)}$$

where

$$a_w = \frac{h_c t_w}{b_{fc} t_{fc}} \qquad \text{(5.4-7, } \textit{Spec.} \text{ Eq. F4-11)}$$
$$= \frac{24.0\,\text{in.}(0.125\,\text{in.})}{6.00\,\text{in.}(0.250\,\text{in.})}$$
$$= 2.00 \le 10.0$$

Therefore, use $a_w = 2.00$.

$$R_{pg} = 1 - \frac{a_w}{1{,}200 + 300a_w}\left(\frac{h_c}{t_w} - 5.7\sqrt{\frac{E}{F_y}}\right) \le 1.0 \qquad \text{(5.4-6, } \textit{Spec.} \text{ Eq. F5-6)}$$
$$= 1 - \frac{2.00}{1{,}200 + 300(2.00)}\left(\frac{24.0\,\text{in.}}{0.125\,\text{in.}} - 5.7\sqrt{\frac{29{,}000\,\text{ksi}}{55\,\text{ksi}}}\right)$$
$$= 0.932$$

Lateral-Torsional Buckling—Upper Unbraced Length

Using the provisions for single linear tapered members with no plate changes, determine the nominal flexural strength, M_n, for the limit state of lateral-torsional buckling in the upper unbraced segment.

First, using the AISC *Specification* Section F4 and Section 5.4 of this Design Guide, determine the elastic lateral-torsional buckling stress, F_{eLTB}, with $C_b = 1$ for the location of maximum flexural stress using properties at the middle of the upper unbraced length. The elastic lateral-torsional buckling stress is,

$$\left(F_{eLTB}\right)_{C_b=1} = \frac{1.0\pi^2 E}{\left(\frac{L_b}{r_t}\right)^2}\sqrt{1+0.078\frac{J}{S_{xc}h_o}\left(\frac{L_b}{r_t}\right)^2} \qquad \text{(5.4-10, } \textit{Spec.} \text{ Eq. F4-5)}$$

where

$$\begin{aligned} h_o &= 21.8\,\text{in.} + 2\left(\tfrac{1}{4}\,\text{in./}2\right) \\ &= 22.1\,\text{in.} \\ h_c &= h \\ &= 21.8\,\text{in.} \end{aligned}$$

$$a_w = \frac{h_c t_w}{b_{fc} t_{fc}} \qquad (5.4\text{-}7)$$

$$= \frac{21.8\,\text{in.}\left(0.125\,\text{in.}\right)}{6.00\,\text{in.}\left(\tfrac{1}{4}\,\text{in.}\right)}$$

$$= 1.82$$

$$r_t = \frac{b_{fc}}{\sqrt{12\left(\frac{h_o}{d}+\frac{1}{6}a_w\frac{h^2}{h_o d}\right)}} \qquad \text{(5.4-11, } \textit{Spec.} \text{ Eq. F4-10)}$$

$$= \frac{6.00\,\text{in.}}{\sqrt{12\left[\frac{22.1\,\text{in.}}{22.3\,\text{in.}}+\frac{1}{6}(1.82)\frac{(21.8\,\text{in.})^2}{22.1\,\text{in.}(22.3\,\text{in.})}\right]}}$$

$$= 1.53\,\text{in.}$$

$S_{xc} = S_x = 42.4\,\text{in.}^3$ from Table 5-2

$J = 0$ because the web is slender throughout this unbraced length.

Therefore,

$$\left(F_{eLTB}\right)_{C_b=1} = \frac{1.0\pi^2 E}{\left(\frac{L_b}{r_t}\right)^2}\sqrt{1+0.078\frac{J}{S_{xc}h_o}\left(\frac{L_b}{r_t}\right)^2} \qquad \text{(5.4-10, } \textit{Spec.} \text{ Eq. F4-5)}$$

$$= \frac{1.0\pi^2\,29{,}000\,\text{ksi}}{\left(\frac{54.0\,\text{in.}}{1.53\,\text{in.}}\right)^2}\sqrt{1+0.078\frac{0\,\text{in.}^4}{42.4\,\text{in.}^3\left(22.1\,\text{in.}\right)}\left(\frac{54.0\,\text{in.}}{1.53\,\text{in.}}\right)^2}$$

$$= \frac{1.0\pi^2\,29{,}000\,\text{ksi}}{\left(\frac{54.0\,\text{in.}}{1.53\,\text{in.}}\right)^2}$$

$$= 230\ \text{ksi}$$

Find the location of maximum flexural stress.

By calculating $f_r = M_r/S_x$ at various locations along the unbraced length, it can be shown that the maximum flexural compression stress, f_{rmax}, occurs at the top of this unbraced length.

LRFD	ASD
$f_{rmax} = \frac{M_r}{S_{xc}}$ $= \frac{1{,}800 \text{ kip-in.}}{47.8 \text{ in.}^3}$ $= 37.7 \text{ ksi}$	$f_{rmax} = \frac{M_r}{S_{xc}}$ $= \frac{1{,}200 \text{ kip-in.}}{47.8 \text{ in.}^3}$ $= 25.1 \text{ ksi}$

Calculate elastic buckling multiplier with $C_b = 1$, $(\gamma_{eLTB})_{C_b=1}$.

LRFD	ASD
$(\gamma_{eLTB})_{C_b=1} = \frac{(F_{eLTB})_{C_b=1}}{f_{rmax}}$ $= \frac{230 \text{ ksi}}{37.7 \text{ ksi}}$ $= 6.10$	$(\gamma_{eLTB})_{C_b=1} = \frac{(F_{eLTB})_{C_b=1}}{f_{rmax}}$ $= \frac{230 \text{ ksi}}{25.1 \text{ ksi}}$ $= 9.16$

Check the nominal flexural strength due to lateral-torsional buckling at the top of the upper unbraced length. Select the equation for calculation of nominal flexural strength, M_n, based on the following ratio:

LRFD	ASD
$\frac{(\gamma_{eLTB})_{C_b=1} f_r}{F_y} = \frac{6.10(37.7 \text{ ksi})}{55 \text{ ksi}}$ $= 4.18$	$\frac{(\gamma_{eLTB})_{C_b=1} f_r}{F_y} = \frac{9.16(25.1 \text{ ksi})}{55 \text{ ksi}}$ $= 4.18$

The selection of the equation for M_n is also dependent on the value of F_L/F_y.

When $S_{xt}/S_{xc} \geq 0.7$,

$$F_L = 0.7F_y \qquad \text{(5.4-14, } \textit{Spec.} \text{ Eq. F4-6a)}$$

And therefore,

$$\frac{F_L}{F_y} = 0.7$$

Because $8.2 > \frac{(\gamma_{eLTB})_{C_b=1} f_r}{F_y} > \frac{F_L}{F_y}$, use Equation 5.4-19 to calculate M_n. The nominal flexural strength due to lateral-torsional buckling at the top of the upper unbraced length is,

$$M_n = C_b R_{pg} R_{pc} M_{yc} \left[1 - \left(1 - \frac{F_L}{R_{pc} F_y} \right) \left(\frac{\pi \sqrt{\frac{F_y}{(\gamma_{eLTB})_{C_b=1} f_r}} - 1.1}{\pi \sqrt{\frac{F_y}{F_L}} - 1.1} \right) \right] \leq R_{pg} R_{pc} M_{yc} \qquad (5.4\text{-}19)$$

where C_b for the upper unbraced length is determined using the moment diagram in Figure 5-6 as follows:

LRFD	ASD
$f_0 = \frac{M_r}{S_{xc}} = \frac{1{,}120 \text{ kip-in.}}{37.0 \text{ in.}^3} = 30.3 \text{ ksi}$	$f_0 = \frac{M_r}{S_{xc}} = \frac{750 \text{ kip-in.}}{37.0 \text{ in.}^3} = 20.3 \text{ ksi}$
$f_{mid} = \frac{M_r}{S_{xc}} = \frac{1{,}460 \text{ kip-in.}}{42.4 \text{ in.}^3} = 34.4 \text{ ksi}$	$f_{mid} = \frac{M_r}{S_{xc}} = \frac{975 \text{ kip-in.}}{42.4 \text{ in.}^3} = 23.0 \text{ ksi}$
$f_2 = \frac{M_r}{S_{xc}} = \frac{1{,}800 \text{ kip-in.}}{47.8 \text{ in.}^3} = 37.7 \text{ ksi}$	$f_2 = \frac{M_r}{S_{xc}} = \frac{1{,}200 \text{ kip-in.}}{47.8 \text{ in.}^3} = 25.1 \text{ ksi}$
Because $\lvert 34.4 \text{ ksi} \rvert > \left\lvert \frac{30.3 \text{ ksi} + 37.7 \text{ ksi}}{2} \right\rvert$	Because $\lvert 23.0 \text{ ksi} \rvert > \left\lvert \frac{20.3 \text{ ksi} + 25.1 \text{ ksi}}{2} \right\rvert$
$f_1 = 2f_{mid} - f_2 = 2(34.4 \text{ ksi}) - 37.7 \text{ ksi} = 31.1 \text{ ksi}$ (5.4-2)	$f_1 = 2f_{mid} - f_2 = 2(23.0 \text{ ksi}) - 25.1 \text{ ksi} = 20.9 \text{ ksi}$ (5.4-2)
$C_b = 1.75 - 1.05\frac{f_1}{f_2} + 0.3\left(\frac{f_1}{f_2}\right)^2 \le 2.3$ (5.4-1)	$C_b = 1.75 - 1.05\frac{f_1}{f_2} + 0.3\left(\frac{f_1}{f_2}\right)^2 \le 2.3$ (5.4-1)
$= 1.75 - 1.05\left(\frac{31.1 \text{ ksi}}{37.7 \text{ ksi}}\right) + 0.3\left(\frac{31.1 \text{ ksi}}{37.7 \text{ ksi}}\right)^2$	$= 1.75 - 1.05\left(\frac{20.9 \text{ ksi}}{25.1 \text{ ksi}}\right) + 0.3\left(\frac{20.9 \text{ ksi}}{25.1 \text{ ksi}}\right)^2$
$= 1.09 < 2.3$	$= 1.08 < 2.3$

Note that the difference in C_b between LRFD and ASD is due to rounding of f_1 and f_2.

Use ASD value: $C_b = 1.08$.

Therefore, the nominal flexural strength for the limit state of lateral-torsional buckling at the top of the upper unbraced length is,

$$M_n = C_b R_{pg} R_{pc} M_{yc} \left[1 - \left(1 - \frac{F_L}{R_{pc} F_y} \right) \left(\frac{\pi \sqrt{\frac{F_y}{(\gamma_{eLTB})_{C_b=1} f_r}} - 1.1}{\pi \sqrt{\frac{F_y}{F_L}} - 1.1} \right) \right] \le R_{pg} R_{pc} M_{yc} \quad (5.4\text{-}19)$$

$$= 1.08(0.932)(1.0)(2{,}630 \text{ kip-in.}) \left[1 - \left(1 - \frac{0.7}{1.0} \right) \left(\frac{\pi \sqrt{\frac{1}{4.18}} - 1.1}{\pi \sqrt{\frac{1}{0.7}} - 1.1} \right) \right] \le 0.932(1.0)(2{,}630 \text{ kip-in.})$$

$= 2{,}520$ kip-in. $\le 2{,}450$ kip-in.; therefore use $M_n = 2{,}450$ kip-in.

Check the strength ratio at the top of the unbraced length.

LRFD	ASD
$\frac{M_r}{M_c} = \frac{M_r}{\phi_b M_n}$ $= \frac{1{,}800\,\text{kip-in.}}{0.90(2{,}450\,\text{kip-in.})}$ $= 0.816$	$\frac{M_r}{M_c} = \frac{\Omega_b M_r}{M_n}$ $= \frac{1.67(1{,}200\,\text{kip-in.})}{2{,}450\,\text{kip-in.}}$ $= 0.818$

Check lateral-torsional buckling strength at the middle of the upper unbraced length. The flexural stress at this location is,

LRFD	ASD
$f_r = \frac{M_r}{S_{xc}}$ $= \frac{1{,}460\ \text{kip-in.}}{42.4\ \text{in.}^3}$ $= 34.4\ \text{ksi}$	$f_r = \frac{M_r}{S_{xc}}$ $= \frac{975\ \text{kip-in.}}{42.4\ \text{in.}^3}$ $= 23.0\ \text{ksi}$

Select equation for calculation of nominal flexural strength, M_n, based on the following ratio:

LRFD	ASD
$\frac{(\gamma_{eLTB})_{C_b=1} f_r}{F_y} = \frac{6.10(34.4\,\text{ksi})}{55\,\text{ksi}}$ $= 3.82$	$\frac{(\gamma_{eLTB})_{C_b=1} f_r}{F_y} = \frac{9.16(23.0\,\text{ksi})}{55\,\text{ksi}}$ $= 3.83$

Note that the difference between LRFD and ASD is due to rounding. Use ASD value of 3.83.

Because $8.2 > \frac{(\gamma_{eLTB})_{C_b=1} f_r}{F_y} > \frac{F_L}{F_y}$, use Equation 5.4-19. The nominal flexural strength for the limit state of lateral-torsional buckling at the middle of the upper unbraced length is,

$$M_n = C_b R_{pg} R_{pc} M_{yc} \left[1 - \left(1 - \frac{F_L}{R_{pc} F_y} \right) \left(\frac{\pi \sqrt{\frac{F_y}{(\gamma_{eLTB})_{C_b=1} f_r}} - 1.1}{\pi \sqrt{\frac{F_y}{F_L}} - 1.1} \right) \right] \le R_{pg} R_{pc} M_{yc} \tag{5.4-19}$$

$$= 1.08(0.955)(1.0)(2{,}330\,\text{kip-in.}) \left[1 - \left(1 - \frac{0.7}{1.0} \right) \left(\frac{\pi \sqrt{\frac{1}{3.83}} - 1.1}{\pi \sqrt{\frac{1}{0.7}} - 1.1} \right) \right] \le 0.955(1.0)(2{,}330\,\text{kip-in.})$$

$= 2{,}270$ kip-in. $> 2{,}230$ kip-in.; therefore use $M_n = 2{,}230$ kip-in.

Check the strength ratio at the middle of the unbraced length.

LRFD	ASD
$\frac{M_r}{M_c} = \frac{M_r}{\phi_b M_n}$ $= \frac{1{,}460 \text{ kip-in.}}{0.90(2{,}230 \text{ kip-in.})}$ $= 0.727$	$\frac{M_r}{M_c} = \frac{\Omega_b M_r}{M_n}$ $= \frac{1.67(975 \text{ kip-in.})}{2{,}230 \text{ kip-in.}}$ $= 0.730$

Check lateral-torsional buckling at the bottom of the upper unbraced length. The flexural stress at this location is,

LRFD	ASD
$f_r = \frac{M_r}{S_{xc}}$ $= \frac{1{,}120 \text{ kip-in.}}{37.0 \text{ in.}^3}$ $= 30.3 \text{ ksi}$	$f_r = \frac{M_r}{S_{xc}}$ $= \frac{750 \text{ kip-in.}}{37.0 \text{ in.}^3}$ $= 20.3 \text{ ksi}$

Select the equation for calculation of the nominal flexural strength, M_n, based on the following ratio:

LRFD	ASD
$\frac{(\gamma_{eLTB})_{C_b=1} f_r}{F_y} = \frac{6.10(30.3 \text{ ksi})}{55 \text{ ksi}}$ $= 3.36$	$\frac{(\gamma_{eLTB})_{C_b=1} f_r}{F_y} = \frac{9.16(20.3 \text{ ksi})}{55 \text{ ksi}}$ $= 3.38$

Note that the difference between LRFD and ASD is due to rounding. Use ASD value of 3.38.

Because $8.2 > \frac{(\gamma_{eLTB})_{C_b=1} f_r}{F_y} > \frac{F_L}{F_y}$, use Equation 5.4-19. The nominal flexural strength due to lateral-torsional buckling at the bottom of the upper unbraced length is,

$$M_n = C_b R_{pg} R_{pc} M_{yc} \left[1 - \left(1 - \frac{F_L}{R_{pc} F_y} \right) \left(\frac{\pi \sqrt{\frac{F_y}{(\gamma_{eLTB})_{C_b=1} f_r}} - 1.1}{\pi \sqrt{\frac{F_y}{F_L}} - 1.1} \right) \right] \le R_{pg} R_{pc} M_{yc} \tag{5.4-19}$$

$$= 1.08(0.976)(1.0)(2{,}030 \text{ kip-in.}) \left[1 - \left(1 - \frac{0.7}{1.0} \right) \left(\frac{\pi \sqrt{\frac{1}{3.38}} - 1.1}{\pi \sqrt{\frac{1}{0.7}} - 1.1} \right) \right] \le 0.976(1.0)(2{,}030 \text{ kip-in.})$$

$= 1{,}990$ kip-in. $> 1{,}980$ kip-in.; therefore use $M_n = 1{,}980$ kip-in.

Check the strength ratio at the bottom of the unbraced length.

LRFD	ASD
$\frac{M_r}{M_c} = \frac{M_r}{\phi_b M_n}$ $= \frac{1{,}120 \text{ kip-in.}}{0.90(1{,}980 \text{ kip-in.})}$ $= 0.629$	$\frac{M_r}{M_c} = \frac{\Omega_b M_r}{M_n}$ $= \frac{1.67(750 \text{ kip-in.})}{1{,}980 \text{ kip-in.}}$ $= 0.633$

The top end (largest end) of the unbraced length controls the available flexural strength using the limit state of lateral-torsional buckling.

Compression Flange Local Buckling—Upper Unbraced Length

Determine the nominal flexural strength, M_n, at the bottom of the upper unbraced length using the limit state of compression flange local buckling. From previous calculations at the top of the lower unbraced length:

$$M_n = 1{,}690 \text{ kip-in.}$$

Determine the nominal flexural strength, M_n, for the limit state of compression flange local buckling at the middle of the upper unbraced length. The selection of the appropriate equation is dependent on the flange compactness.

$$\frac{b_f}{2t_f} = 12.0 \text{ (calculated previously)}$$

From Table B4.1 of the AISC *Specification* for flexure in flanges of doubly symmetric built-up shapes,

$$\lambda_{pf} = 0.38\sqrt{\frac{E}{F_y}} \quad \text{compact flange limit}$$

$$= 8.73 \quad \left(\text{calculated previously}\right)$$

$$\lambda_{rf} = 0.95\sqrt{\frac{k_c E}{F_L}} \quad \text{slender flange limit}$$

where

$$k_c = \frac{4}{\sqrt{\frac{h}{t_w}}}$$

$$= \frac{4}{\sqrt{\frac{21.8 \text{ in.}}{0.125 \text{ in.}}}} \tag{5.4-24}$$

$$= 0.303 \; < \; 0.35; \text{ therefore use } 0.35$$

$$F_L = 38.5 \text{ ksi (calculated previously)}$$

Therefore,

$$\lambda_{rf} = 0.95\sqrt{\frac{k_c E}{F_L}}$$

$$= 0.95\sqrt{\frac{0.35(29{,}000 \text{ ksi})}{38.5 \text{ ksi}}}$$

$$= 15.4$$

Because $8.73 < 12.0 < 15.4$, the compression flange is noncompact; therefore, use Equation 5.4-22. The nominal flexural strength for the limit state of compression flange local buckling at the middle of the upper unbraced length is,

$$M_n = R_{pg}\left\{R_{pc}M_{yc} - \left[\left(R_{pc}M_{yc} - F_L S_{xc}\right)\left(\frac{\frac{b_f}{2t_f} - 0.38\sqrt{\frac{E}{F_y}}}{0.95\sqrt{\frac{k_c E}{F_L}} - 0.38\sqrt{\frac{E}{F_y}}}\right)\right]\right\} \tag{5.4-22}$$

$$M_n = 0.955\left\{1.0\left(2{,}330 \text{ kip-in.}\right) - \left\{\left[1.0\left(2{,}330 \text{ kip-in.}\right) - 38.5 \text{ ksi}\left(42.4 \text{ in.}^3\right)\right]\left(\frac{12.0 - 8.73}{15.4 - 8.73}\right)\right\}\right\}$$

$$= 1{,}900 \text{ kip-in.}$$

Determine the nominal flexural strength, M_n, for the limit state of compression flange local buckling at the top of the upper unbraced length.

$\frac{b_f}{2t_f} = 12.0$ previously calculated

$\lambda_{pf} = 8.73$ compact flange limit previously calculated

$$k_c = \frac{4}{\sqrt{\frac{h}{t_w}}} \tag{5.4-24}$$

$$= \frac{4}{\sqrt{\frac{24.0\,\text{in.}}{0.125\,\text{in.}}}}$$

$= 0.289 < 0.35$; therefore use 0.35, which is the same value used for the middle of the upper unbraced length

Therefore,

$\lambda_{rf} = 15.4$ slender flange limit (calculated previously)

Because $8.73 < 12.0 < 15.4$, the compression flange is noncompact; therefore, use Equation 5.4-22. The nominal flexural strength for the limit state of compression flange local buckling at the top of the upper unbraced length is,

$$M_n = R_{pg}\left\{R_{pc}M_{yc} - \left[\left(R_{pc}M_{yc} - F_L S_{xc}\right)\left(\frac{\frac{b_f}{2t_f} - 0.38\sqrt{\frac{E}{F_y}}}{0.95\sqrt{\frac{k_c E}{F_L}} - 0.38\sqrt{\frac{E}{F_y}}}\right)\right]\right\} \tag{5.4-22}$$

$$= 0.932\left\{1.0\left(2{,}630\,\text{kip-in.}\right) - \left\{\left[1.0\left(2{,}630\,\text{kip-in.}\right) - 38.5\,\text{ksi}\left(47.8\,\text{in.}^3\right)\right]\left(\frac{12.0 - 8.73}{15.4 - 8.73}\right)\right\}\right\}$$

$= 2{,}090\,\text{kip-in.}$

Tension Flange Rupture—Upper Unbraced Length

Determine the nominal flexural strength at the bottom of the upper unbraced length using the limit state of tensile rupture of the tension flange at the bolt holes. From previous calculations at the top of the lower unbraced length, at the bolt holes:

$M_n = 1{,}950$ kip-in.

The limit state of compression flange local buckling governs over the limit state of tension flange rupture at the bottom of the upper unbraced length, where

$M_n = 1{,}690$ kip-in.

Following is a summary of maximum flexural strength ratios for the upper unbraced length to be used in combined strength checks in Example 5.4.

Summary of Flexural Strengths—Upper Unbraced Length	
Lateral-torsional buckling Value at top of unbraced length governs	
LRFD	ASD
$\frac{M_r}{M_c} = \frac{M_r}{\phi_b M_n}$ $= \frac{1{,}800\text{ kip-in.}}{0.90(2{,}450\text{ kip-in.})}$ $= 0.816$	$\frac{M_r}{M_c} = \frac{\Omega_b M_r}{M_n}$ $= \frac{1.67(1{,}200\text{ kip-in.})}{2{,}450\text{ kip-in.}}$ $= 0.818$
Compression flange local buckling at bottom	
LRFD	ASD
$\frac{M_r}{M_c} = \frac{1{,}120\text{ kip-in.}}{0.90(1{,}690\text{ kip-in.})}$ $= 0.736$	$\frac{M_r}{M_c} = \frac{1.67(750\text{ kip-in.})}{1{,}690\text{ kip-in.}}$ $= 0.741$
Compression flange local buckling at mid-length	
LRFD	ASD
$\frac{M_r}{M_c} = \frac{1{,}460\text{ kip-in.}}{0.90(1{,}900\text{ kip-in.})}$ $= 0.854$	$\frac{M_r}{M_c} = \frac{1.67(975\text{ kip-in.})}{1{,}900\text{ kip-in.}}$ $= 0.857$
Compression flange local buckling at top	
LRFD	ASD
$\frac{M_r}{M_c} = \frac{1{,}800\text{ kip-in.}}{0.90(2{,}090\text{ kip-in.})}$ $= 0.957$	$\frac{M_r}{M_c} = \frac{1.67(1{,}200\text{ kip-in.})}{2{,}090\text{ kip-in.}}$ $= 0.959$

Compression flange local buckling at top of upper unbraced length governs.

5.4.8 Commentary on Example 5.3

Some additional strength could have been calculated for this example if R_{pg} had been calculated using the refinement to Equation 5.4-6 noted in Section 5.4.1. This was not done in the example in the interest of simplicity.

5.5 COMBINED FLEXURE AND AXIAL FORCE

The equations for combined flexure and axial force in the AISC *Specification* are essentially the same as those from the 1999 LRFD *Specification* but are substantially different from those in the 1989 ASD *Specification*. The differences from the 1989 ASD *Specification* are: (1) a different form of the interaction equations and (2) the assumption that second-order elastic effects are included in the calculation of the required strength. As a result, the interaction equations are significantly simplified.

In the 1989 *Specification* and earlier ASD editions, P-δ and P-Δ second-order effects were included in the ASD "member stability" interaction Equation H1-1 via the terms $C_m / \left(1 - \frac{f_a}{F'_e}\right)$ (note that for members with $K \le 1$, these terms captured P-δ effects only, whereas for $K > 1$, these terms captured both P-δ and P-Δ effects). This amplifier gives a very coarse approximation of the second-order effects in moment frame members subjected to both sway and nonsway moments. Because this amplifier was embedded within Equation H1-1, the corresponding second-order analysis was in effect implicit within the resistance calculations, rather than in the required strength. The 1989 ASD

Specification also required a second "member cross-section strength" interaction equation check, Equation H1-2. In this check, the second-order effects were entirely ignored. In the AISC *Specification*, both *P*-δ and *P*-Δ effects must be included explicitly, whenever either or both effects are significant. These effects are now included explicitly where necessary in the calculation of required strengths from the structural analysis.

A basic set of interaction equations, written in terms of forces and moments, rather than stress, is provided in Sections H1.1 and H1.2. These provide the simplest approach to checking interaction. A more refined approach is also provided in Section H1.3 that permits separate consideration of in-plane and out-of-plane buckling. A third, stress-based equation is provided as an alternate to the force-based equations in Section H2. The alternative stress-based equation gives a conservative solution that is useful for handling some unusual situations. It can be used as a conservative check for all cases.

The interaction of flexural tension flange rupture (*Specification* Section F13.1) with axial limit states is not explicitly addressed in the AISC *Specification*. Recommended procedures for such interaction checks are also included below. These are intended to provide realistic assessments of the interaction effects without unnecessary conservatism. These checks should be conducted using required strengths and section properties at the locations of holes in the tension flange, in addition to the other general interaction checks.

5.5.1 Force-Based Combined Strength Equations

(a) The basic equations for cases with either axial tension or compression are:

For $\frac{P_r}{P_c} \geq 0.2$

$$\frac{P_r}{P_c} + \frac{8}{9}\left(\frac{M_{rx}}{M_{cx}} + \frac{M_{ry}}{M_{cy}}\right) \leq 1.0 \quad \text{(5.5-1a, } \textit{Spec.} \text{ Eq. H1-1a)}$$

For $\frac{P_r}{P_c} < 0.2$

$$\frac{P_r}{2P_c} + \left(\frac{M_{rx}}{M_{cx}} + \frac{M_{ry}}{M_{cy}}\right) \leq 1.0 \quad \text{(5.5-1b, } \textit{Spec.} \text{ Eq. H1-1b)}$$

where

P_r = required axial strength, kips
P_c = available axial strength, kips; = P_n/Ω_c (ASD) or $\phi_c P_n$ (LRFD)
M_{rx} = required flexural strength about *x*-axis, kip-in.
M_{ry} = required flexural strength about *y*-axis, kip-in.
M_{cx} = available flexural strength about *x*-axis, kip-in. = M_{nx}/Ω_b (ASD) or $\phi_b M_{nx}$ (LRFD)
M_{cy} = available flexural strength about *y*-axis, kip-in. = M_{ny}/Ω_b (ASD) or $\phi_b M_{ny}$ (LRFD)
Ω_c = 1.67
Ω_b = 1.67
ϕ_c = 0.90
ϕ_b = 0.90

The absolute values of all the forces and moments should be used in these equations. All applicable in-plane and out-of-plane limit states must be considered in determining the ratios of required strength to available strength. Note that the equations do not include the second-order *P*-δ amplifier,

$$\frac{C_m}{1 - \frac{f_a}{F_e'}}$$

because the second-order elastic effects are assumed to have been included in the calculation of M_r.

(b) At locations of bolt holes in flanges subject to axial and/or flexural tension, tension flange rupture should be checked as follows.

$$\frac{P_r}{P_c} + \frac{M_{rx}}{M_{cx}} \leq 1.0 \qquad (5.5\text{-}2)$$

where

P_r = required axial strength, positive in tension, negative in compression, kips
P_c = available axial strength, kips; = P_n/Ω_t (ASD) or $\phi_t P_n$ (LRFD) with P_n calculated per Section 5.2.2
M_{rx} = required flexural strength; positive for tension in the flange under consideration, negative for compression
M_{cx} = available flexural strength about *x*-axis, kip-in. = M_{nx}/Ω_b (ASD) or $\phi_b M_{nx}$ (LRFD) with $M_{nx} = M_n$ taken as:

If $F_u A_{fn} < Y_t F_y A_{fg}$,

$$M_n = \frac{F_u A_{fn}}{A_{fg}} S_{xt} \leq F_y Z_x \qquad (5.5\text{-}3)$$

otherwise,

$$M_n = F_y Z_x \qquad (5.5\text{-}4)$$

where

Y_t = 1.0 for $F_y/F_u \leq 0.8$, otherwise $Y_t = 1.1$
Z_x = plastic section modulus calculated with bolt holes not taken into consideration, in.^{3}

Each flange having axial and/or flexural tension should be checked separately. The AISC *Specification* (AISC, 2005) does not have an explicit interaction check for rupture forces.

5.5.2 Separate In-Plane and Out-of-Plane Combined Strength Equations

For doubly symmetric prismatic members with bending primarily about one axis, the limit states involving in-plane and out-of-plane buckling may be combined and checked

separately (see Section H1.3 of the AISC *Specification*). In cases where the governing limit state in axial compression is in-plane buckling and the governing limit state in flexure is out-of-plane buckling, this approach may result in a more economical member design. For members under biaxial bending, if $M_r/M_c > 0.05$ for both axes, this procedure is not applicable.

There is insufficient information at this time to justify the extension of this procedure to tapered members or members with noncompact or slender cross sections. Consequently, it is recommended that these provisions not be used for members other than prismatic doubly symmetric compact members.

5.5.3 Stress-Based Combined Strength Equations

The following stress-based interaction equation is equivalent to AISC *Specification* Equation H2-1 provided in Section H2 of the AISC *Specification* and may be used in lieu of those previously listed for any member. The symbols used are slightly different than those used in the AISC *Specification* to prevent any confusion with those used in the 1989 ASD *Specification* (AISC, 1989).

$$\left|\frac{f_{ra}}{F_{ca}}+\frac{f_{rbx}}{F_{cbx}}+\frac{f_{rby}}{F_{cby}}\right| \le 1.0 \quad \text{(5.5-5, from } \textit{Spec.} \text{ Eq. H2-1)}$$

where

F_{ca} = available axial stress, ksi; = F_{cr}/Ω_c (ASD) or $\phi_c F_{cr}$ (LRFD)
F_{cbx} = available flexural stress about x-axis, ksi
= $M_{nx}/\Omega_b S$ (ASD) or $\phi_b M_{nx}/S$ (LRFD)
F_{cby} = available flexural stress about y-axis, ksi
= $M_{ny}/\Omega_b S$ (ASD) or $\phi_b M_{ny}/S$ (LRFD)
f_{ra} = required axial stress, ksi
f_{rbx} = required flexural stress about x-axis, ksi
f_{rby} = required flexural stress about y-axis, ksi
Ω_c = 1.67
Ω_b = 1.67
ϕ_c = 0.90
ϕ_b = 0.90

Although the *Specification* presents this equation in terms of principal-axis stresses, it is presented here in terms of the familiar x- and y- axes, because its application is limited to singly and doubly symmetric sections in this document.

In applying these equations, the sign of the required stresses may be taken into account to permit flexural and axial compression stresses of opposite sign to offset. However, there is always a point on the cross section where the flexural and axial compression stresses will be additive. Therefore, the net effect of using Equation H2-1 is a more conservative assessment than obtained using Equations H1-1. As in the other combined strength methods discussed earlier, it is assumed that all required second-order effects are included in the required stress terms.

Tapered I-shaped members can be checked by using the stresses at the flange tips. All applicable limit states should be considered when calculating the available stresses on each flange. The available stress on each flange should be calculated using the governing limit state for the member and the section modulus at that point. The required stress should be calculated using the same section modulus used to calculate the available stress at the point under consideration.

At locations of bolt holes in flanges subject to axial and/or flexural tension, tension flange rupture should be checked using Section 5.5.1(b). Each flange having axial and/or flexural tension should be checked separately. Alternately, the following stress-based procedure may be used. The required and available stresses computed using the following equations are fictitious and should not be used for any purpose other than Equation 5.5-6, but result in strength checks identical to those generated by Section 5.5.1(b):

$$\frac{f_{ra}}{F_{ca}}+\frac{f_{rbx}}{F_{cbx}} \le 1.0 \qquad (5.5\text{-}6)$$

where

F_{ca} = available axial stress, ksi
= P_c/A_g with P_c as defined in Section 5.5.1(b)
F_{cbx} = available flexural stress about x-axis, ksi
= M_c/S_x with M_c as defined in Section 5.5.1(b)
S_x = gross elastic section modulus calculated to the flange under consideration, in.^{3}
f_{ra} = required axial stress, ksi
= P_r/A_g, positive in tension, negative in compression
f_{rbx} = required flexural stress, ksi
= M_r/S_x, positive in tension, negative in compression

Example 5.4—Combined Axial Compression and Flexure

Given:

Check the strength of the member used in Examples 5.2 and 5.3 for combined axial compression and flexure using the required and available strengths from those examples.

Evaluate using AISC *Specification* Section H1.1, H1.3 (if permitted), and H2.

Axial strength ratios from Example 5.2:

In-Plane Flexural Buckling	
LRFD	ASD
$\frac{P_r}{P_c} = \frac{P_r}{\phi_c P_n}$ $= \frac{11.3\,\text{kips}}{0.90(168\,\text{kips})}$ $= 0.0747$	$\frac{P_r}{P_c} = \frac{\Omega_c P_r}{P_n}$ $= \frac{1.67(7.50\,\text{kips})}{168\,\text{kips}}$ $= 0.0746$
Out-of-Plane Flexural Buckling—Lower Unbraced Length	
LRFD	ASD
$\frac{P_r}{P_c} = \frac{11.3\,\text{kips}}{0.90(139\,\text{kips})}$ $= 0.0903$	$\frac{P_r}{P_c} = \frac{1.67(7.50\,\text{kips})}{139\,\text{kips}}$ $= 0.0901$
Out-of-Plane Flexural Buckling—Upper Unbraced Length	
LRFD	ASD
$\frac{P_r}{P_c} = \frac{11.3\,\text{kips}}{0.90(158\,\text{kips})}$ $= 0.0795$	$\frac{P_r}{P_c} = \frac{1.67(7.50\,\text{kips})}{158\,\text{kips}}$ $= 0.0793$

Flexural strength ratios from Example 5.3—At the top of the lower unbraced length:

Lateral-Torsional Buckling Value at Top of Lower Unbraced Length Governs	
LRFD	ASD
$\frac{M_r}{M_c} = \frac{M_r}{\phi_b M_n}$ $= \frac{1{,}120\,\text{kip-in.}}{0.90(1{,}980\,\text{kip-in.})}$ $= 0.629$	$\frac{M_r}{M_c} = \frac{\Omega_b M_r}{M_n}$ $= \frac{1.67(750\,\text{kip-in.})}{1{,}980\,\text{kip-in.}}$ $= 0.633$
Compression Flange Local Buckling at Mid-Length	
LRFD	ASD
$\frac{M_r}{M_c} = \frac{560\,\text{kip-in.}}{0.90(1{,}360\,\text{kip-in.})}$ $= 0.458$	$\frac{M_r}{M_c} = \frac{1.67(375\,\text{kip-in.})}{1{,}360\,\text{kip-in.}}$ $= 0.460$
Compression Flange Local Buckling at Top of Unbraced Length	
LRFD	ASD
$\frac{M_r}{M_c} = \frac{1{,}120\,\text{kip-in.}}{0.90(1{,}690\,\text{kip-in.})}$ $= 0.736$	$\frac{M_r}{M_c} = \frac{1.67(750\,\text{kip-in.})}{1{,}690\,\text{kip-in.}}$ $= 0.741$

Flexural strength ratios from Example 5.3—At the top of the upper unbraced length:

Lateral-Torsional Buckling Value at Top of Upper Unbraced Length Governs	
LRFD	ASD
$\frac{M_r}{M_c} = \frac{M_r}{\phi_b M_n}$ $= \frac{1{,}800 \text{ kip-in.}}{0.90(2{,}450 \text{ kip-in.})}$ $= 0.816$	$\frac{M_r}{M_c} = \frac{\Omega_b M_r}{M_n}$ $= \frac{1.67(1{,}200 \text{ kip-in.})}{2{,}450 \text{ kip-in.}}$ $= 0.818$
Compression Flange Local Buckling at Bottom	
LRFD	ASD
$\frac{M_r}{M_c} = \frac{1{,}120 \text{ kip-in.}}{0.90(1{,}690 \text{ kip-in.})}$ $= 0.736$	$\frac{M_r}{M_c} = \frac{1.67(750 \text{ kip-in.})}{1{,}690 \text{ kip-in.}}$ $= 0.741$
Compression Flange Local Buckling at Mid-Length	
LRFD	ASD
$\frac{M_r}{M_c} = \frac{1{,}460 \text{ kip-in.}}{0.90(1{,}900 \text{ kip-in.})}$ $= 0.854$	$\frac{M_r}{M_c} = \frac{1.67(975 \text{ kip-in.})}{1{,}900 \text{ kip-in.}}$ $= 0.857$
Compression Flange Local Buckling at Top	
LRFD	ASD
$\frac{M_r}{M_c} = \frac{1{,}800 \text{ kip-in.}}{0.90(2{,}090 \text{ kip-in.})}$ $= 0.957$	$\frac{M_r}{M_c} = \frac{1.67(1{,}200 \text{ kip-in.})}{2{,}090 \text{ kip-in.}}$ $= 0.959$

Tension flange rupture from Example 5.3:

At bolt holes, $M_c = M_{nx} = 1{,}950$ kip-in.

Solution A:

Applying the provisions of AISC *Specification* Section H1.1, use the worst-case in-plane and out-of-plane ratios for axial and flexure when checking each unbraced segment.

Combined Axial Compression and Flexure—Lower Unbraced Length

From previous calculations in Example 5.2 and 5.3 and as summarized earlier in this example, it is demonstrated that out-of-plane buckling controls the axial strength of the lower unbraced length and compression flange local buckling at the top of the lower unbraced length controls flexural strength.

$\frac{P_r}{P_c} < 0.2$; therefore, use Equation 5.5-1b and AISC *Specification* Equation H1-1b:

$$\frac{P_r}{2P_c} + \left(\frac{M_{rx}}{M_{cx}} + \frac{M_{ry}}{M_{cy}}\right) \le 1.0 \qquad \text{(5.5-1b, } \textit{Spec.} \text{ Eq. H1-1b)}$$

Applying this interaction equation with the strength ratios summarized previously in this example:

LRFD	ASD
$\frac{P_r}{2P_c} + \left(\frac{M_{rx}}{M_{cx}} + \frac{M_{ry}}{M_{cy}}\right) \le 1.0$ $\frac{0.0903}{2} + (0.736 + 0) = 0.781$	$\frac{P_r}{2P_c} + \left(\frac{M_{rx}}{M_{cx}} + \frac{M_{ry}}{M_{cy}}\right) \le 1.0$ $\frac{0.0901}{2} + (0.741 + 0) = 0.786$

Combined Axial Compression and Flexure—Upper Unbraced Length

From previous calculations in Example 5.2 and 5.3 and as summarized earlier in this example, it is demonstrated that out-of-plane buckling controls the axial strength of the upper unbraced length and compression flange local buckling at the top of the upper unbraced length controls flexural strength.

$\frac{P_r}{P_c} = 0.0795 < 0.2$, therefore, use Equation 5.5-1b and AISC *Specification* Equation H1-1b:

$$\frac{P_r}{2P_c} + \left(\frac{M_{rx}}{M_{cx}} + \frac{M_{ry}}{M_{cy}} \right) \le 1.0 \qquad \text{(5.5-1b, } \textit{Spec.} \text{ Eq. H1-1b)}$$

Applying this interaction equation with the strength ratios summarized earlier in this example gives:

LRFD	ASD
$\frac{0.0795}{2} + (0.957 + 0) = 0.997$	$\frac{0.0793}{2} + (0.959 + 0) = 0.999$

Combined Axial Tension and Flexure

Determine the available tensile strength due to the limit state of tensile rupture in the net section of the flange at the bolt holes located at the top of the lower unbraced length. From AISC *Specification* Section D3.3, the effective net area is,

$$A_e = A_n U$$

where

$$\begin{aligned} A_g &= 2b_f t_f + ht_w \\ &= 2(6 \text{ in.})(¼ \text{ in.}) + 19.5 \text{ in.}(0.125 \text{ in.}) \\ &= 5.44 \text{ in.}^2 \end{aligned}$$

$U = 1.0$ from Table D3.1

Therefore,

$$\begin{aligned} A_e &= A_n U \qquad \text{(}\textit{Spec.}\text{ Eq. D3-1)} \\ &= \left[A_g - 4(d_h + 1/16) t_f \right] 1.0 \\ &= \left[5.44 \text{ in}^2 - 4(11/16 \text{ in.} + 1/16 \text{ in.})¼ \text{ in.} \right] 1.0 \\ &= 4.69 \text{ in.}^2 \end{aligned}$$

Using AISC *Specification* Section D2, the available tensile strength based on the limit state of tensile rupture, P_c, is,

LRFD	ASD
$\begin{aligned} P_c &= \phi_t F_u A_e \\ &= 0.75(70 \text{ ksi})(4.69 \text{ in.}^2) \\ &= 246 \text{ kips} \end{aligned}$	$\begin{aligned} P_c &= \frac{F_u A_e}{\Omega_t} \\ &= \frac{70 \text{ ksi}(4.69 \text{ in.}^2)}{2.0} \\ &= 164 \text{ kips} \end{aligned}$

$$\begin{aligned} M_n &= \frac{F_u A_{fn}}{A_{fg}} S_{xt} \qquad (5.5\text{-}3) \\ &= 1{,}950 \text{ kip-in.} \end{aligned}$$

From Example 5.3, $F_u A_{fn} < Y_t F_y A_g$; therefore, the available flexural strength due to the limit state of tensile rupture of the tension flange is determined in accordance with AISC *Specification* Section F13.1. From Example 5.3, the nominal flexural strength is,

$$M_n = \frac{F_u A_{fn}}{A_{fg}} S_{xt} \qquad \text{(5.5-3, from } \textit{Spec.} \text{ Eq. F13-1)}$$

$$= 1{,}950 \text{ kip-in.}$$

The available flexural strength is,

LRFD	ASD
$M_{cx} = \phi_b M_{nx}$ $= 0.90(1{,}950 \text{ kip-in.})$ $= 1{,}760 \text{ kip-in.}$	$M_{cx} = \frac{M_{nx}}{\Omega_b}$ $= \frac{1{,}950 \text{ kip-in.}}{1.67}$ $= 1{,}170 \text{ kip-in.}$

Check the interaction Equation 5.5-2 (a reduced version of AISC *Specification* Equation H1-1b) given in this Design Guide for combined axial and flexural strength:

LRFD	ASD
On the flange in flexural tension: $\frac{P_r}{P_c} + \frac{M_{rx}}{M_{cx}} \le 1.0$ (5.5-2) $\frac{-11.3 \text{ kips}}{246 \text{ kips}} + \frac{1{,}120 \text{ kip-in.}}{1{,}760 \text{ kip-in.}} = 0.590 \le 1.0$ **o.k.**	On the flange in flexural tension: $\frac{P_r}{P_c} + \frac{M_{rx}}{M_{cx}} \le 1.0$ (5.5-2) $\frac{-7.50 \text{ kips}}{164 \text{ kips}} + \frac{750 \text{ kip-in.}}{1{,}170 \text{ kip-in.}} = 0.595 \le 1.0$ **o.k.**

By inspection, tension flange rupture cannot occur on the flange in flexural compression.

Solution B:

As discussed in Section 5.5.2, it is not recommended that AISC *Specification* Section H1.3 be applied to members other than doubly symmetric compact sections.

Solution C:

Apply AISC *Specification* Section H2 to the upper and lower unbraced lengths at the bottom, middle and top locations, using the required and available stresses calculated from section properties at those locations.

Lower Unbraced Length

Check combined axial compression and flexural strength at the bottom of the lower unbraced length. As given in Example 5.2, $h = 12.0$ in. and $A_g = 4.50$ in.^{2} at this location.

Axial strength is governed by out-of-plane flexural buckling of the lower unbraced length as determined previously. The required axial strength, P_r, was given and the nominal axial strength, P_n, was determined previously. Using the stress-based interaction Equation 5.5-5 of this Design Guide (similar to AISC *Specification* Equation H2-1), check the interaction of combined axial and flexural strength.

LRFD	ASD
$f_{ra} = \frac{P_r}{A_g}$ $= \frac{11.3\,\text{kips}}{4.50\,\text{in.}^2}$ $= 2.51\,\text{ksi}$ $F_{ca} = \frac{\phi_c P_n}{A_g}$ $= \frac{0.90(139\,\text{kips})}{4.50\,\text{in.}^2}$ $= 27.8\,\text{ksi}$ $\left\lvert \frac{f_{ra}}{F_{ca}} + \frac{f_{rbx}}{F_{cbx}} + \frac{f_{rby}}{F_{cby}} \right\rvert \le 1.0$ (5.5-5) Because there is no flexural stress at the bottom $\left\lvert \frac{2.51\,\text{ksi}}{27.8\,\text{ksi}} + 0 + 0 \right\rvert = 0.0903$	$f_{ra} = \frac{P_r}{A_g}$ $= \frac{7.50\,\text{kips}}{4.50\,\text{in.}^2}$ $= 1.67\,\text{ksi}$ $F_{ca} = \frac{P_n}{\Omega_c A_g}$ $= \frac{139\,\text{kips}}{1.67(4.50\,\text{in.}^2)}$ $= 18.5\,\text{ksi}$ $\left\lvert \frac{f_{ra}}{F_{ca}} + \frac{f_{rbx}}{F_{cbx}} + \frac{f_{rby}}{F_{cby}} \right\rvert \le 1.0$ (5.5-5) Because there is no flexural stress at the bottom $\left\lvert \frac{1.67\,\text{ksi}}{18.5\,\text{ksi}} + 0 + 0 \right\rvert = 0.0903$

Check combined axial compression and flexural strength at the middle of the lower unbraced length. As given in Example 5.3, $h = 15.8$ in. and $S_x = 28.7$ in.^{3}, and $A_g = 15.8$ in. (0.125 in.) + 2(6 in.) (¼ in.) = 4.98 in.^{2}

Axial strength is governed by out-of-plane flexural buckling of the lower unbraced length and flexural strength is governed by compression flange local buckling, as determined previously. Using the stress-based interaction Equation 5.5-5 of this Design Guide (similar to AISC *Specification* Equation H2-1), check the interaction of combined axial and flexural strength.

LRFD	ASD
$f_{ra} = \frac{P_r}{A_g}$ $= \frac{11.3\,\text{kips}}{4.98\,\text{in.}^2}$ $= 2.27\,\text{ksi}$ $F_{ca} = \frac{\phi_c P_n}{A_g}$ $= \frac{0.90(139\,\text{kips})}{4.98\,\text{in.}^2}$ $= 25.1\,\text{ksi}$ $f_{rbx} = \frac{M_{rx}}{S_x}$ $= \frac{560\,\text{kip-in.}}{28.7\,\text{in.}^3}$ $= 19.5\,\text{ksi}$ $F_{cbx} = \frac{\phi_c M_{nx}}{S_x}$ $= \frac{0.90(1{,}360\,\text{kip-in.})}{28.7\,\text{in.}^3}$ $= 42.6\,\text{ksi}$ $\left\lvert \frac{2.27\,\text{ksi}}{25.1\,\text{ksi}} + \frac{19.5\,\text{ksi}}{42.6\,\text{ksi}} + 0 \right\rvert = 0.548 \le 1.0$ **o.k.**	$f_{ra} = \frac{P_r}{A_g}$ $= \frac{7.50\,\text{kips}}{4.98\,\text{in.}^2}$ $= 1.51\,\text{ksi}$ $F_{ca} = \frac{P_n}{\Omega_c A_g}$ $= \frac{139\,\text{kips}}{1.67(4.98\,\text{in.}^2)}$ $= 16.7\,\text{ksi}$ $f_{rbx} = \frac{M_{rx}}{S_x}$ $= \frac{375\,\text{kip-in.}}{28.7\,\text{in.}^3}$ $= 13.1\,\text{ksi}$ $F_{cbx} = \frac{M_{nx}}{\Omega_b S_x}$ $= \frac{1{,}360\,\text{kip-in.}}{1.67(28.7\,\text{in.}^3)}$ $= 28.4\,\text{ksi}$ $\left\lvert \frac{1.51\,\text{ksi}}{16.7\,\text{ksi}} + \frac{13.1\,\text{ksi}}{28.4\,\text{ksi}} + 0 \right\rvert = 0.552 \le 1.0$ **o.k.**

Check combined axial compression and flexural strength at the top of the lower unbraced length. As given in Example 5.3, $h = 19.5$ in. and $S_x = 37.0$ in.^{3} and $A_g = 19.5$ in. (0.125 in.) + 2(6 in.)(¼ in.) = 5.44 in.^{2}

Axial strength is governed by out-of-plane flexural buckling and flexural strength is governed by compression flange local buckling in the lower unbraced length, as determined previously. Using the stress-based interaction Equation 5.5-5 of this Design Guide (similar to AISC *Specification* Equation H2-1), check the interaction of combined axial and flexural strength at the top of the lower unbraced length.

LRFD	ASD
$f_{ra} = \dfrac{P_r}{A_g}$	$f_{ra} = \dfrac{P_r}{A_g}$
$= \dfrac{11.3\,\text{kips}}{5.44\,\text{in.}^2}$	$= \dfrac{7.50\,\text{kips}}{5.44\,\text{in.}^2}$
$= 2.08\,\text{ksi}$	$= 1.38\,\text{ksi}$
$F_{ca} = \dfrac{\phi_c P_n}{A_g}$	$F_{ca} = \dfrac{P_n}{\Omega_c A_g}$
$= \dfrac{0.90\left(139\,\text{kips}\right)}{5.44\,\text{in.}^2}$	$= \dfrac{139\,\text{kips}}{1.67\left(5.44\,\text{in.}^2\right)}$
$= 23.0\,\text{ksi}$	$= 15.3\,\text{ksi}$
$f_{rbx} = \dfrac{M_{rx}}{S_x}$	$f_{rbx} = \dfrac{M_{rx}}{S_x}$
$= \dfrac{1{,}120\,\text{kip-in.}}{37.0\,\text{in.}^3}$	$= \dfrac{750\,\text{kip-in.}}{37.0\,\text{in.}^3}$
$= 30.3\,\text{ksi}$	$= 20.3\,\text{ksi}$
$F_{cbx} = \dfrac{\phi_c M_{nx}}{S_x}$	$F_{cbx} = \dfrac{M_{nx}}{\Omega_b S_x}$
$= \dfrac{0.90\left(1{,}690\,\text{kip-in.}\right)}{37.0\,\text{in.}^3}$	$= \dfrac{1{,}690\,\text{kip-in.}}{1.67\left(37.0\,\text{in.}^3\right)}$
$= 41.1\,\text{ksi}$	$= 27.4\,\text{ksi}$
$\left\lvert \dfrac{2.08\,\text{ksi}}{23.0\,\text{ksi}} + \dfrac{30.3\,\text{ksi}}{41.1\,\text{ksi}} + 0 \right\rvert = 0.828 \le 1.0$ **o.k.**	$\left\lvert \dfrac{1.38\,\text{ksi}}{15.3\,\text{ksi}} + \dfrac{20.3\,\text{ksi}}{27.4\,\text{ksi}} + 0 \right\rvert = 0.831 \le 1.0$ **o.k.**

Upper unbraced length

Check combined axial compression and flexural strength at the bottom of the upper unbraced length. As determined at the top of the lower unbraced length, $h = 19.5$ in., $A_g = 5.44$ in.^{2} and $S_x = 37.0$ in.^{3}

Axial strength is governed by out-of-plane flexural buckling and flexural strength is governed by compression flange local buckling in the upper unbraced length, as determined previously. Using the stress-based interaction Equation 5.5-5 of this Design Guide, check the interaction equation for combined axial and flexural strength at the bottom of the upper unbraced length.

LRFD	ASD
$f_{ra} = \frac{P_r}{A_g}$ $= \frac{11.3\,\text{kips}}{5.44\,\text{in.}^2}$ $= 2.08\,\text{ksi}$	$f_{ra} = \frac{P_r}{A_g}$ $= \frac{7.50\,\text{kips}}{5.44\,\text{in.}^2}$ $= 1.38\,\text{ksi}$
$F_{ca} = \frac{\phi_c P_n}{A_g}$ $= \frac{0.90(158\,\text{kips})}{5.44\,\text{in.}^2}$ $= 26.1\,\text{ksi}$	$F_{ca} = \frac{P_n}{\Omega_c A_g}$ $= \frac{158\,\text{kips}}{1.67(5.44\,\text{in.}^2)}$ $= 17.4\,\text{ksi}$
$f_{rbx} = \frac{M_{rx}}{S_x}$ $= \frac{1{,}120\,\text{kip-in.}}{37.0\,\text{in.}^3}$ $= 30.3\,\text{ksi}$ $F_{cbx} = \frac{\phi_c M_{nx}}{S_x}$ $= \frac{0.90(1{,}690\,\text{kip-in.})}{37.0\,\text{in.}^3}$ $= 41.1\,\text{ksi}$	$f_{rbx} = \frac{M_{rx}}{S_x}$ $= \frac{750\,\text{kip-in.}}{37.0\,\text{in.}^3}$ $= 20.3\,\text{ksi}$ $F_{cbx} = \frac{M_{nx}}{\Omega_b S_x}$ $= \frac{1{,}690\,\text{kip-in.}}{1.67(37.0\,\text{in.}^3)}$ $= 27.4\,\text{ksi}$
$\left\lvert \frac{2.08\,\text{ksi}}{26.1\,\text{ksi}} + \frac{30.3\,\text{ksi}}{41.1\,\text{ksi}} + 0 \right\rvert = 0.817 \le 1.0$ **o.k.**	$\left\lvert \frac{1.38\,\text{ksi}}{17.4\,\text{ksi}} + \frac{20.3\,\text{ksi}}{27.4\,\text{ksi}} + 0 \right\rvert = 0.820 \le 1.0$ **o.k.**

Check combined axial compression and flexural strength at the middle of the upper unbraced length. From Example 5.3, $h = 21.8$ in. and $S_x = 42.4$ in.^{3}, and $A_g = 21.8$ in. (0.125 in.) + 2(6 in.)(¼ in.) = 5.73 in.^{2}

Axial strength is governed by out-of-plane flexural buckling and flexural strength is governed by compression flange local buckling in the upper unbraced length, as determined previously. Using the stress-based interaction Equation 5.5-5 of this Design Guide, check the combined axial and flexural strength at the middle of the upper unbraced length.

LRFD	ASD
$f_{ra} = \frac{P_r}{A_g}$ $= \frac{11.3\,\text{kips}}{5.73\,\text{in.}^2}$ $= 1.97\,\text{ksi}$	$f_{ra} = \frac{P_r}{A_g}$ $= \frac{7.50\,\text{kips}}{5.73\,\text{in.}^2}$ $= 1.31\,\text{ksi}$
$F_{ca} = \frac{\phi_c P_n}{A_g}$ $= \frac{0.90(158\,\text{kips})}{5.73\,\text{in.}^2}$ $= 24.8\,\text{ksi}$	$F_{ca} = \frac{P_n}{\Omega_c A_g}$ $= \frac{158\,\text{kips}}{1.67(5.73\,\text{in.}^2)}$ $= 16.5\,\text{ksi}$
$f_{rbx} = \frac{M_{rx}}{S_x}$ $= \frac{1,460\,\text{kip-in.}}{42.4\,\text{in.}^3}$ $= 34.4\,\text{ksi}$ $F_{cbx} = \frac{\phi_c M_{nx}}{S_x}$ $= \frac{0.90(1,900\,\text{kip-in.})}{42.4\,\text{in.}^3}$ $= 40.3\,\text{ksi}$	$f_{rbx} = \frac{M_{rx}}{S_x}$ $= \frac{975\,\text{kip-in.}}{42.4\,\text{in.}^3}$ $= 23.0\,\text{ksi}$ $F_{cbx} = \frac{M_{nx}}{\Omega_b S_x}$ $= \frac{1,900\,\text{kip-in.}}{1.67(42.4\,\text{in.}^3)}$ $= 26.8\,\text{ksi}$
$\left\lvert \frac{1.97\,\text{ksi}}{24.8\,\text{ksi}} + \frac{34.4\,\text{ksi}}{40.3\,\text{ksi}} + 0 \right\rvert = 0.933 \le 1.0$ **o.k.**	$\left\lvert \frac{1.31\,\text{ksi}}{16.5\,\text{ksi}} + \frac{23.0\,\text{ksi}}{26.8\,\text{ksi}} + 0 \right\rvert = 0.938 \le 1.0$ **o.k.**

Check combined axial compression and flexural strength at the top of the upper unbraced length. As given in Examples 5.2 and 5.3, at the top of the lower unbraced length, $h = 24.0$ in., $A_g = 6.00$ in.^{2} and $S_x = 47.8$ in.^{3}

Axial strength is governed by out-of-plane flexural buckling and flexural strength is governed by compression flange local buckling in the upper unbraced length, as determined previously. Using the stress-based interaction Equation 5.5-5 of this Design Guide, check combined axial and flexural strength at the top of the upper unbraced length.

LRFD	ASD
$f_{ra} = \dfrac{P_r}{A_g}$ $= \dfrac{11.3\,\text{kips}}{6.00\,\text{in.}^2}$ $= 1.88\,\text{ksi}$	$f_{ra} = \dfrac{P_r}{A_g}$ $= \dfrac{7.50\,\text{kips}}{6.00\,\text{in.}^2}$ $= 1.25\,\text{ksi}$
$F_{ca} = \dfrac{\phi_c P_n}{A_g}$ $= \dfrac{0.90\left(158\,\text{kips}\right)}{6.00\ \text{in.}^2}$ $= 23.7\,\text{ksi}$	$F_{ca} = \dfrac{P_n}{\Omega_c A_g}$ $= \dfrac{158\,\text{kips}}{1.67\left(6.00\ \text{in.}^2\right)}$ $= 15.8\,\text{ksi}$
$f_{rbx} = \dfrac{M_{rx}}{S_x}$ $= \dfrac{1{,}800\,\text{kip-in.}}{47.8\,\text{in.}^3}$ $= 37.7\,\text{ksi}$	$f_{rbx} = \dfrac{M_{rx}}{S_x}$ $= \dfrac{1{,}200\,\text{kip-in.}}{47.8\,\text{in.}^3}$ $= 25.1\,\text{ksi}$
$F_{cbx} = \dfrac{\phi_c M_{nx}}{S_x}$ $= \dfrac{0.90\left(2{,}090\,\text{kip-in.}\right)}{47.8\,\text{in.}^3}$ $= 39.4\,\text{ksi}$	$F_{cbx} = \dfrac{M_{nx}}{\Omega_b S_x}$ $= \dfrac{2{,}090\,\text{kip-in.}}{1.67\left(47.8\,\text{in.}^3\right)}$ $= 26.2\,\text{ksi}$
$\left\lvert \dfrac{1.88\,\text{ksi}}{23.7\,\text{ksi}} + \dfrac{37.7\,\text{ksi}}{39.4\,\text{ksi}} + 0 \right\rvert = 1.04 > 1.0$ **n.g.**	$\left\lvert \dfrac{1.25\,\text{ksi}}{15.8\,\text{ksi}} + \dfrac{25.1\,\text{ksi}}{26.2\,\text{ksi}} + 0 \right\rvert = 1.04 > 1.0$ **n.g.**

Tension flange rupture

Check the tension flange at the bolt holes using the alternate stress-based interaction Equation 5.5-6 given in this Design Guide for combined axial tension and flexural strength. As previously given, at this location, $h = 19.5$ in., $A_g = 5.44$ in.^{2} and $S_x = 37.0$ in.^{3}

LRFD	ASD
$f_{ra} = \dfrac{P_r}{A_g}$	$f_{ra} = \dfrac{P_r}{A_g}$
$= \dfrac{-11.3\text{ kips}}{5.44\text{ in.}^2}$	$= \dfrac{-7.50\text{ kips}}{5.44\text{ in.}^2}$
$= -2.08$ ksi	$= -1.38$ ksi
$P_c = 246$ kips (calculated previously)	$P_c = 164$ kips (calculated previously)
$F_{ca} = \dfrac{P_c}{A_g}$	$F_{ca} = \dfrac{P_c}{A_g}$
$= \dfrac{246\text{ kips}}{5.44\text{ in.}^2}$	$= \dfrac{164\text{ kips}}{5.44\text{ in.}^2}$
$= 45.2$ ksi	$= 30.1$ ksi
$f_{rbx} = \dfrac{M_{rx}}{S_x}$	$f_{rbx} = \dfrac{M_{rx}}{S_x}$
$= \dfrac{1{,}120\text{ kip-in.}}{37.0\text{ in.}^3}$	$= \dfrac{750\text{ kip-in.}}{37.0\text{ in.}^3}$
$= 30.3$ ksi	$= 20.3$ ksi
$M_{cx} = 1{,}760$ kip-in. (calculated previously)	$M_{cx} = 1{,}170$ kip-in. (calculated previously)
$F_{cbx} = \dfrac{M_{cx}}{S_x}$	$F_{cbx} = \dfrac{M_{cx}}{S_x}$
$= \dfrac{1{,}760\text{ kip-in.}}{37.0\text{ in.}^3}$	$= \dfrac{1{,}170\text{ kip-in.}}{37.0\text{ in.}^3}$
$= 47.6$ ksi	$= 31.6$ ksi
$\dfrac{f_{ra}}{F_{ca}} + \dfrac{f_{rbx}}{F_{cbx}} \le 1.0$ (5.5-6)	$\dfrac{f_{ra}}{F_{ca}} + \dfrac{f_{rbx}}{F_{cbx}} \le 1.0$ (5.5-6)
$\dfrac{-2.08\text{ ksi}}{45.2\text{ ksi}} + \dfrac{30.3\text{ ksi}}{47.6\text{ ksi}} = 0.591 \le 1.0$ **o.k.**	$\dfrac{-1.38\text{ ksi}}{30.1\text{ ksi}} + \dfrac{20.3\text{ ksi}}{31.6\text{ ksi}} = 0.597 \le 1.0$ **o.k.**

Therefore, tension flange rupture cannot occur in the flange in flexural compression.

5.5.4 Commentary on Example 5.4

The strength-based method from the AISC *Specification* Sections H1.1 and H1.2 is simpler to apply than the stress-based provisions of Section H2 and provides more liberal results for this example.

5.6 SHEAR

Beam shear in tapered members is handled using the provisions of Chapter G of the AISC *Specification* with several minor modifications based on Falby and Lee (1976). Like prismatic members, tapered members with sufficiently stocky webs are subject to the limit state of shear yielding and those with webs having higher slenderness are subject to the limit states of elastic or inelastic buckling. The shear strength of stiffened web panels may be calculated with or without consideration of tension field action. If tension field action is used, additional detailing requirements must be met.

The web area, A_w, the web height to thickness ratio, h/t_w, and stiffener spacing to web height ratio, a/h, are all a function of web height. As a result, the shear strength of a web-tapered member varies along its length. For unstiffened webs, the shear strength should be checked on a cross section basis at least at the ends and at locations of any steps in the shear diagram or steps in the thickness of the web. For stiffened webs, a single shear tension field and/or shear buckling strength is calculated for each panel based predominantly on the cross-section geometry at the mid-length of the panel.

Due to an increase in the safety factor from 1.5 to 1.67 for shear yielding for all built-up members in ASD (and the use of a comparable $\phi_v = 0.90$ versus 1.0 in LRFD), ASD shear strengths calculated using the AISC *Specification* are 10% lower for stocky webs than they were under the 1989 provisions. The calculated strength of webs subject to buckling is not significantly different from that in the 1989 edition; however, the resistance equations have been simplified and non-dimensionalized. The tension and shear interaction limits from the previous ASD and LRFD *Specifications* have been removed from the AISC *Specification*. For members having sufficient flange size, the interaction between the flexural and shear resistances is negligible (White et al., 2008). In an extension to the AISC *Specification*, for members with small flange sizes, a reduced tension field strength may be determined, neglecting any anchorage from the flanges. The interaction between the flexural and shear resistances also may be neglected for this calculation of the shear strength.

Blodgett (1966) proposed a method to calculate a "modified shear," adding or subtracting the vertical component of force in sloped flanges to the required shear strength of webs of tapered members. This has not been included here due to the lack of research to validate the procedure.

5.6.1 Shear Strength of Unstiffened Webs

Webs without stiffeners, or with stiffeners spaced at more than three times the minimum web height in the panel, h_{min}, are defined as unstiffened. The available shear strength of these types of webs should be calculated on a cross section by cross section basis along the member length. Use the AISC *Specification* provisions for unstiffened webs with the cross-section properties at each location of interest. The required shear strength at any location along the member should not exceed the available strength calculated at that location.

Calculate the available shear strength as:

$$V_n = 0.6F_yA_wC_v \quad \text{(5.6-1, } \textit{Spec.}\text{ Eq. G2-1)}$$

$$\phi_v = 0.90\,(\text{LRFD}) \qquad \Omega_v = 1.67\,(\text{ASD})$$

where

$A_w = dt_w$

For $\dfrac{h}{t_w} \le 1.10\sqrt{\dfrac{k_vE}{F_y}}$

$$C_v = 1.0 \quad \text{(5.6-2, } \textit{Spec.}\text{ Eq. G2-3)}$$

For $1.10\sqrt{\dfrac{k_vE}{F_y}} < \dfrac{h}{t_w} \le 1.37\sqrt{\dfrac{k_vE}{F_y}}$

$$C_v = \frac{1.10\sqrt{k_vE/F_y}}{h/t_w} \quad \text{(5.6-3, } \textit{Spec.}\text{ Eq. G2-4)}$$

For $\dfrac{h}{t_w} > 1.37\sqrt{\dfrac{k_vE}{F_y}}$

$$C_v = \frac{1.51Ek_v}{\left(h/t_w\right)^2F_y} \quad \text{(5.6-4, } \textit{Spec.}\text{ Eq. G2-5)}$$

where

$$k_v = 5 \quad \text{(5.6-5)}$$

AISC *Specification* Section F13.2 specifies $\left(h/t_w\right) \le 260$ for unstiffened members.

5.6.2 Shear Strength of Stiffened Webs Without Using Tension Field Action

Webs with stiffeners at a clear spacing of not more than three times the smallest web height in the panel, h_{min}, are defined as stiffened. To calculate the available shear strength of these types of webs based on the limit state of web shear buckling, use the procedure from Section 5.6.1 with the cross section at the middle of the panel. The shear strength is taken as a constant along the entire panel length, equal to the value determined at the middle of the panel, but need not be taken at any location as less than would be calculated at that location without stiffeners ($k_v = 5$).

Calculate k_v as:

$$k_v = 5 + \frac{5}{\left(a/h_{avg}\right)^2} \quad \text{(5.6-6)}$$

where

a = clear distance between stiffeners

h_{avg} = average web height within the panel, equal to the web height at the middle of a panel with a linear web taper; for panels with a "pinch point," use the web height at that point

For panels with a change of web thickness, use the thickness of the thinner web.

The AISC *Specification* does not credit shear stiffeners spaced wider than $a/h = [260/(h/t_w)]^2$ with contributing to web shear strength. This limitation is arbitrary and was selected to facilitate handling during fabrication and erection of conventional steel structures. The authors recommend that this restriction can be waived if there is a means to handle members with stiffener spacings that exceed the limit.

Stiffeners at the boundaries of panels must be detailed in accordance with AISC *Specification* Section G2.2 using the web height at the stiffener location for h.

5.6.3 Shear Strength of Stiffened Webs Using Tension Field Action

The use of tension field action is restricted to shear panels having webs supported on all four sides by flanges and stiffeners within the following limits:

1. The panel must not be an end panel; however, Murray and Shoemaker (2002) indicate that moment end-plate splices can be relied on to provide tension field anchorage in negative moment regions (compression on bottom or inside flange).
2. The spacing of stiffeners must be such that the ratio of the clear spacing to the smallest web height, a/h_{min}, does not exceed 3.0.

Section G3.1 of the AISC *Specification* also restricts a/h to a maximum of $[260/(h/t_w)]^2$ for the use of tension field action (but not for the calculation of web shear buckling resistances based on the unstiffened web equations). This restriction comes from a fabrication and handling limit recommended by Basler (1961). The authors recommend that this limit can be exceeded if the manufacturer, shipper and erector can handle members that violate this restriction. Experimental shear strengths, including tension field action, are predicted adequately by the following equations for prismatic members that violate Basler's fabrication and handling limit (White and Barker, 2008).

Calculate the available shear strength for each web panel as follows:

1. Compute C_v using the average web height within the panel, h_{avg}, in Equations 5.6-2 through 5.6-4 and using Equation 5.6-6 for k_v.
2. The appropriate resistance factor and safety factor are:

$$\phi_v = 0.90 \text{ (LRFD)} \qquad \Omega_v = 1.67 \text{ (ASD)}$$

3. For web panels in which both:
   a. $\dfrac{t_w h_{avg}}{0.5\left(t_{ft} b_{ft} + t_{fc} b_{fc}\right)} \le 2.5$ (using the smallest pair of flanges in the panel) and
   b. $\dfrac{h_{avg}}{b_f} \le 6.0$ (using the smallest flange width in the panel)

   For $\dfrac{h_{avg}}{t_w} \le 1.10\sqrt{\dfrac{k_v E}{F_y}}$

$$V_n = 0.6 F_y A_w \tag{5.6-7}$$

   For $\dfrac{h_{avg}}{t_w} > 1.10\sqrt{\dfrac{k_v E}{F_y}}$

$$V_n = 0.6 F_y A_w \left(C_v + \frac{1 - C_v}{1.15\sqrt{1 + \left(a/h_{min}\right)^2}} \right) \tag{5.6-8}$$

   where:

$$A_w = h_{avg} t_w, \text{ in.}^2 \tag{5.6-9}$$

   h_{min} = smallest web height in the panel, in.

4. For web panels in which the flanges violate either of the 3.a or 3.b limits:

   For $\dfrac{h_{avg}}{t_w} \le 1.10\sqrt{\dfrac{k_v E}{F_y}}$

$$V_n = 0.6 F_y A_w \tag{5.6-10}$$

   For $\dfrac{h_{avg}}{t_w} > 1.10\sqrt{\dfrac{k_v E}{F_y}}$

$$V_n = 0.6 F_y A_w \left(C_v + \frac{1 - C_v}{1.15\left(a/h_{min} + \sqrt{1 + \left(a/h_{min}\right)^2}\right)} \right) \tag{5.6-11}$$

Equations 5.6-7 and 5.6-8 provide a reasonable estimate of the shear resistances based on the Falby and Lee (1976) equations for members with sufficiently large flange sizes and for web taper angles up to the maximum of 15°. The web panel aspect ratio is taken as a/h_{min} because the smaller web height tends to govern the angle of inclination of the tension field in most cases. The use of Equations 5.6-7 through 5.6-9 also provides a good estimate of the resistances determined by the Falby and Lee (1976) equations for all the cases considered by these authors. Equations 5.6-10 and 5.6-11 are

an extension of the AISC *Specification* provisions. This extension is incorporated within the AASHTO (2004 & 2007) provisions and is based on the studies by White et al. (2008). Equation 5.6-11 is referred in the literature to as the "true Basler" shear strength (Galambos, 1998). Equation 5.6-8 is based on the assumed development of a full tension field (uniform tensile diagonal stress) throughout the web panel. The "true Basler" shear strength given by Equation 5.6-11 is based on the assumed development of a tension field only within an effective band width b_e assumed in Basler's calculation of the angle of inclination of the tension field. The use of a/h_{min} along with Equations 5.6-8 and 5.6-11 tends to penalize web panels with smaller flanges, larger spacing of the stiffeners and/or larger web taper angle. As noted previously, the shear strength V_n is taken as a constant along the entire panel length. The required shear resistance must be less than or equal to the corresponding available shear resistance at all locations along the length of the panel.

Stiffeners used to provide the boundaries of panels designed using tension field action must be detailed in accordance with Sections G2.2 and G3.3 in the AISC *Specification*. The web height at the stiffener location should be used for h in the application of these provisions. The stiffener area should be checked using the values of C_v and V_r/V_c in each of the stiffened web panels adjacent to the stiffener. Also, in the case of two adjacent stiffened panels, the larger value for the stiffener area governs. The C_v and V_r/V_c from adjacent unstiffened webs do not apply.

5.6.4 Web-to-Flange Weld

The minimum required strength of the weld between the web and flange, V_{rw}, is determined as it would be for a prismatic member. A weld larger than the minimum size may be appropriate in the vicinity of connections.

$$V_{rw} = \frac{V_r Q}{I_x} \qquad (5.6\text{-}12)$$

where

V_{rw} = required weld shear strength, kip/in.
V_r = required beam shear strength, kips
I_x = x-axis moment of inertia, in.^{4}
Q = static moment of area of the flange taken about the neutral axis, in.^{3}

Example 5.5—Shear Strength of a Tapered Member

Given:

Determine the available shear strength of the member shown in Figure 5-7 using each of the following methods:

1. No stiffeners provided.
2. Stiffeners provided neglecting tension field action.
3. Stiffeners provided including tension field action.

Material Properties:

F_y = 55 ksi
F_u = 70 ksi

Geometric Properties:

Top flange = PL ¼ × 6
Bottom flange = PL ¼ × 6
Web thickness = 0.125 in.
Left web height = 18.0 in.
Right web height = 24.0 in.
Member length = 54.0 in.
Depth at center $= (18.0 \text{ in.} + 24.0 \text{ in.})/2$
$= 21.0$ in.

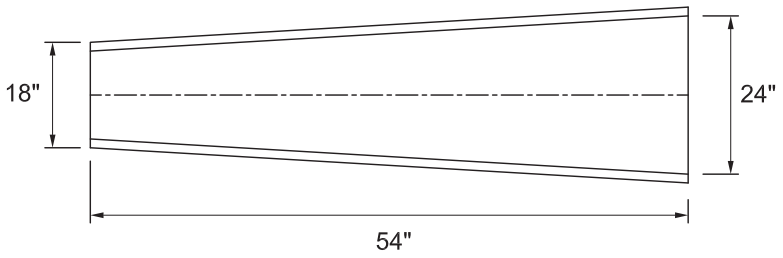

Fig. 5-7. Figure for Example 5-5.

Solution A: No stiffeners provided—compute strength at locations of interest using $k_v = 5$.

Determine the available shear strength at the ends of the member with no stiffeners.
At the left end of the member, check the *h/tw* limit for an unstiffened member:

$$\frac{h}{t_w} = \frac{18.0\,\text{in.}}{0.125\,\text{in.}}$$
$$= 144 < 260 \quad \textbf{o.k.}$$

From Section 5.6.1 of this Design Guide and AISC *Specification* Section G2:

$$V_n = 0.6F_yA_wC_v \qquad \text{(5.6-1, } \textit{Spec.}\text{ Eq. G2-1)}$$

where

$$A_w = dt_w$$
$$= \left[18.0\,\text{in.} + 2\left(\tfrac{1}{4}\,\text{in.}\right)\right]\left(0.125\,\text{in.}\right)$$
$$= 2.31\,\text{in.}^2$$

The equation for C_v is dependent on h/t_w. Because h/t_w exceeds the following value with $k_v = 5$ (no stiffeners), use AISC *Specification* Equation G2-5.

$$1.37\sqrt{\frac{k_vE}{F_y}} = 1.37\sqrt{\frac{5\left(29{,}000\,\text{ksi}\right)}{55\,\text{ksi}}}$$
$$= 70.3 < 144$$

$$C_v = \frac{1.51Ek_v}{\left(h/t_w\right)^2F_y} \qquad \text{(5.6-4, } \textit{Spec.}\text{ Eq. G2-5)}$$
$$= \frac{1.51\left(29{,}000\,\text{ksi}\right)\left(5\right)}{\left(144\right)^2\,55\,\text{ksi}}$$
$$= 0.192$$

Therefore,

$$V_n = 0.6F_yA_wC_v \qquad \text{(5.6-1, } \textit{Spec.}\text{ Eq. G2-1)}$$
$$= 0.6\left(55\,\text{ksi}\right)\left(2.31\,\text{in.}^2\right)\left(0.192\right)$$
$$= 14.6\,\text{kips}$$

The available shear strength is:

LRFD	ASD
$\phi V_n = 0.90\left(14.6\,\text{kips}\right)$ $= 13.1\,\text{kips}$	$\frac{V_n}{\Omega_v} = \frac{14.6\,\text{kips}}{1.67}$ $= 8.74\,\text{kips}$

At right end of segment, check the h/t_w limit for an unstiffened web:

$$\frac{h}{t_w} = \frac{24.0\,\text{in.}}{0.125\,\text{in.}}$$
$$= 192 < 260 \quad \textbf{o.k.}$$

From Section 5.6.1 of this Design Guide and AISC *Specification* Section G2:

$$V_n = 0.6F_yA_wC_v \qquad \text{(5.6-1, } \textit{Spec.} \text{ Eq. G2-1)}$$

where

$$\begin{aligned} A_w &= dt_w \\ &= \left[24.0\,\text{in.} + 2\left(\tfrac{1}{4}\,\text{in.}\right)\right]\left(0.125\,\text{in.}\right) \\ &= 3.06\ \text{in.}^2 \end{aligned}$$

The equation for C_v is dependent on h/t_w. Because h/t_w exceeds the following value with $k_v = 5$ (no stiffeners), use AISC *Specification* Equation G2-5.

$$\begin{aligned} 1.37\sqrt{\frac{k_vE}{F_y}} &= 1.37\sqrt{\frac{5\left(29{,}000\,\text{ksi}\right)}{55\,\text{ksi}}} \\ &= 70.3 < 192;\ \text{therefore,} \end{aligned}$$

$$C_v = \frac{1.51Ek_v}{\left(h/t_w\right)^2 F_y} \qquad \text{(5.6-4, } \textit{Spec.} \text{ Eq. G2-5)}$$

$$\begin{aligned} &= \frac{1.51\left(29{,}000\,\text{ksi}\right)\left(5\right)}{\left(192\right)^2 55\,\text{ksi}} \\ &= 0.108 \end{aligned}$$

Therefore,

$$V_n = 0.6F_yA_wC_v \qquad \text{(5.6-1, } \textit{Spec.} \text{ Eq. G2-1)}$$

$$\begin{aligned} &= 0.6\left(55\,\text{ksi}\right)\left(3.06\,\text{in.}^2\right)\left(0.108\right) \\ &= 10.9\,\text{kips} \end{aligned}$$

The available shear strength is:

LRFD	ASD
$\phi V_n = 0.90\left(10.9\,\text{kips}\right)$ $= 9.81\,\text{kips}$	$\dfrac{V_n}{\Omega_v} = \dfrac{10.9\,\text{kips}}{1.67}$ $= 6.53\,\text{kips}$

Solution B: Stiffeners provided—neglecting tension field action—compute strength at average depth.

Determine the available shear strength when stiffeners are provided, but neglect tension field action. Calculate the strength at the average depth. The authors recommend that the limit of $a/h = \left[260/\left(h/t_w\right)\right]^2$ can be ignored if the fabricator and erector agree to handle the members without this restriction.

From Section 5.6.1 of this Design Guide and AISC *Specification* Section G2:

$$V_n = 0.6F_yA_wC_v \qquad \text{(5.6-1, } \textit{Spec.} \text{ Eq. G2-1)}$$

where

$$\begin{aligned} A_w &= d_{avg}t_w \\ &= \left[21.0\ \text{in.} + 2\left(\tfrac{1}{4}\,\text{in.}\right)\right]\left(0.125\,\text{in.}\right) \\ &= 2.69\ \text{in.}^2 \end{aligned}$$

The equation for C_v is dependent on h/t_w and k_v.

$$\frac{h}{t_w} = \frac{21.0 \text{ in.}}{0.125 \text{ in.}}$$
$$= 168$$

For stiffened webs,

$$k_v = 5 + \frac{5}{(a/h)^2}$$

or

$$k_v = 5 \text{ when } a/h > 3.0 \text{ or } a/h > \left[\frac{260}{(h/t_w)}\right]^2$$

Assuming a clear distance of 54.0 in. between stiffeners, a/h_{avg} = 54 in./21 in. = 2.57 < 3.0, therefore,

$$k_v = 5 + \frac{5}{(2.57)^2}$$
$$= 5.76$$

Because h/t_w exceeds the following value with k_v = 5.76, use AISC *Specification* Equation G2-5 to calculate C_v.

$$1.37\sqrt{\frac{k_v E}{F_y}} = 1.37\sqrt{\frac{5.76(29{,}000 \text{ ksi})}{55 \text{ ksi}}}$$
$$= 75.5 < 168; \text{ therefore,}$$

$$C_v = \frac{1.51 E k_v}{(h/t_w)^2 F_y} \qquad \text{(5.6-4, } \textit{Spec.} \text{ Eq. G2-5)}$$

$$= \frac{1.51(29{,}000 \text{ ksi})(5.76)}{(168)^2 \, 55 \text{ ksi}}$$
$$= 0.162$$

Therefore,

$$V_n = 0.6 F_y A_w C_v \qquad \text{(5.6-1, } \textit{Spec.} \text{ Eq. G2-1)}$$
$$= 0.6(55 \text{ ksi})(2.69 \text{ in.}^2)(0.162)$$
$$= 14.4 \text{ kips}$$

The available shear strength is:

LRFD	ASD
$\phi V_n = 0.90(14.4 \text{ kips})$ $= 13.0 \text{ kips}$	$\frac{V_n}{\Omega_v} = \frac{14.4 \text{ kips}}{1.67}$ $= 8.62 \text{ kips}$

Note that the available strength is slightly less than the strength calculated without stiffeners at the far left end of the member above (8.74 kips ASD and 13.1 kips LRFD). The shear strength at the far left side may be taken as the larger value calculated without stiffeners at that location. Slightly to the right of the left end, the shear strength calculated without stiffeners decreases below the value calculated earlier with stiffeners, so this larger value is used for the remainder of the panel.

Solution C: Stiffeners provided—including tension field action—compute strength at average depth.

Determine the available shear strength when stiffeners are provided spaced at 54 in., including tension field action. Calculate the strength at the average depth.

Check tension field limits.

1. Not an end panel (assumed) **o.k.**
2. $a/h_{min} = 54.0$ in./18.0 in. = 3.0 **o.k.**
3. The authors recommend that the limit of $a/h = \left[260/\left(h/t_w\right)\right]^2$ can be ignored if the manufacturer and erector agree to handle the members without this restriction.

Therefore, tension field action may be considered.

Determine whether Equations 5.6-7 and 5.6-8 or 5.6-10 and 5.6-11 apply.

$$\frac{t_w h_{avg}}{0.5\left(t_{fl} b_{fl} + t_{fc} b_{fc}\right)} = \frac{0.125\,\text{in.}\left(21.0\,\text{in.}\right)}{0.5\left[2\left(6.00\,\text{in.}\right)\left(0.250\,\text{in.}\right)\right]}$$

$$= 1.75 \le 2.5 \quad \textbf{o.k.}$$

$$\frac{h_{avg}}{b_{f\,min}} = \frac{21.0\,\text{in.}}{6.00\,\text{in.}}$$

$$= 3.50 < 6.0 \quad \textbf{o.k.}$$

Therefore, use Equations 5.6-7 and 5.6-8.

$$\frac{a}{h_{avg}} = \frac{54.0\,\text{in.}}{21.0\,\text{in.}}$$

$$= 2.57$$

$$k_v = 5 + \frac{5}{\left(2.57\right)^2} \qquad (5.6\text{-}6)$$

$$= 5.76$$

$$1.37\sqrt{\frac{k_v E}{F_y}} = 1.37\sqrt{\frac{5.76\left(29{,}000\,\text{ksi}\right)}{55\,\text{ksi}}}$$

$$= 75.5 < \frac{h_{avg}}{t_w} = 168;\ \text{therefore,}$$

$$C_v = \frac{1.51 E k_v}{\left(h/t_w\right)^2 F_y} \qquad (5.6\text{-}4,\ \textit{Spec.}\ \text{Eq. G2-5})$$

$$= \frac{1.51\left(29{,}000\,\text{ksi}\right)\left(5.76\right)}{\left(168\right)^2 55\,\text{ksi}}$$

$$= 0.162$$

$$A_w = h_{avg} t_w$$

$$= 21.0\,\text{in.}\left(0.125\,\text{in.}\right) \qquad (5.6\text{-}9)$$

$$= 2.63\,\text{in.}^2$$

By inspection, $\frac{h_{avg}}{t_w} > 1.10\sqrt{\frac{k_v E}{F_y}}$; therefore,

$$V_n = 0.6F_yA_w\left(C_v + \frac{1-C_v}{1.15\sqrt{1+\left(a/h_{min}\right)^2}}\right) \tag{5.6-8}$$

$$= 0.6\left(55\,\text{ksi}\right)\left(2.63\,\text{in.}^2\right)\left(0.162 + \frac{1-0.162}{1.15\sqrt{1+\left(3.0\right)^2}}\right)$$

$$= 34.1\,\text{kips}$$

Shear strength at all locations within the panel.

LRFD	ASD
$\phi V_n = 0.90\left(34.1\,\text{kips}\right)$ $= 30.7\,\text{kips}$	$\frac{V_n}{\Omega_v} = \frac{34.1\,\text{kips}}{1.67}$ $= 20.4\,\text{kips}$

The weld between the flanges and web would be sized based on the required shear in the section using Equation 5.6-12.

5.7 FLANGES AND WEBS WITH CONCENTRATED FORCES

Tapered members are subject to the limit states given in the AISC *Specification* Section J10. With the exception of web sidesway buckling, these are localized limit states. As such, it is recommended that these limit states be checked using the member cross-section geometry at the location of interest.

At present there is no available test or theoretical studies for web sidesway buckling of tapered members. In the absence of such data it is recommended that the average depth along the unbraced length under consideration be used in AISC Equations J10-6 and J10-7.

For evaluating the panel zone at the intersection of tapered rafters and outside columns, the provisions of Chapter 5 of AISC Design Guide 16, *Flush and Extended Multiple Row Moment End-Plate Connections* (Murray and Shoemaker, 2002) are recommended.

5.8 ADDITIONAL EXAMPLES

The following examples repeat the geometry and loadings of Examples 1.2, 1.3 and 1.4 presented earlier, with the exception that the flanges are of different size, such that the cross section is singly symmetric, and the brace spacing is different on each flange. These examples illustrate the provisions for singly symmetric cross-section members and constrained-axis torsional column buckling.

Example 5.6—Tapered Column with Unequal Flanges and One-Sided Bracing

Given:

Evaluate the compressive strength of the member shown in Figure 5-8. The required concentric axial strength, including all second-order effects, is constant kips over the height of the column, neglecting the accumulating self-weight. From an in-plane structural analysis, $K_x = 1.0$. Assume K_y and $K_z = 1.0$.

Material Properties:

$F_y = 55$ ksi
$F_u = 70$ ksi

Geometric Properties:

Left (outside) flange = PL 7/32 in. × 6 in.
Although a 7/32-in.-thick flange plate is used in this example, the AISC *Steel Construction Manual* recommends that plate thicknesses up to and including 3/8 in. be specified in 1/16 in. increments.
Right (inside) flange = PL 5/16 in. × 6 in.
Web thickness = 0.125 in.
Outside flange bracing at 90.0 in. above the bottom
Girt depth = 8.00 in.
No bracing on inside flange

By inspection, the member must be checked for:

A. In-plane flexural buckling (one strength for the entire column)
B. Constrained-axis torsional buckling (one strength for the entire column)
C. Out-of-plane flexural buckling (check each unbraced length separately)

Torsional buckling need not be checked because the cross section is not doubly symmetric. Flexural-torsional buckling need not be checked because constrained-axis torsional buckling is being checked.

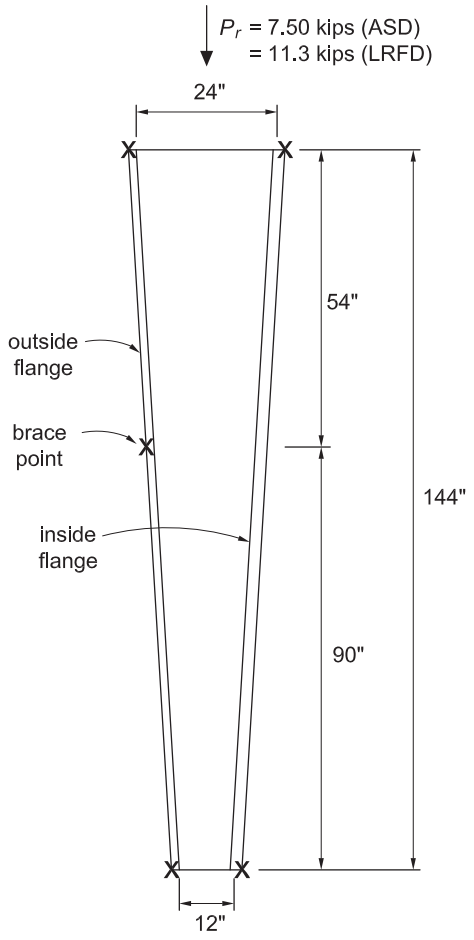

Fig. 5-8. Web-tapered column in Example 5.6.

Solution:

Table 5-3. Section Properties		
Top	h	24.0 in.
	h/t	192
	A_g	6.19 in.^{2}
	I_x	607 in.^{4}
at h/t = 131	h	16.4 in.
	h/t	131
	A_g	5.24 in.^{2}
Bottom	h	12.0 in.
	h/t	96.0
	A_g	4.69 in.^{2}
	I_x	136 in.^{4}

In-Plane Flexural Buckling Strength

Because the member has a single taper with no plate changes, use Equation 4.5-4 to determine P_{ex}.

$$P_{ex} = \frac{\pi^2 EI'_x}{L^2} \tag{4.5-4}$$

At bottom end, web height = 12.0 in., $I_{x,small} = 136$ in.^{4}
At top end, web height = 24.0 in., $I_{x,large} = 607$ in.^{4}

From Section 4.5.2, calculate I'_x at $x = 0.5L\left(\frac{I_{xSmall}}{I_{xLarge}}\right)^{0.0732}$ from the small end as follows:

$$x = 0.5L\left(\frac{I_{x,small}}{I_{x,large}}\right)^{0.0732}$$

$$= 0.5(144\text{ in.})\left(\frac{136\text{ in.}^4}{607\text{ in.}^4}\right)^{0.0732}$$

$$= 64.5\text{ in.}$$

Web height = 12.0 in. + (64.5 in./144 in.)(24.0 in. − 12.0 in.)
= 17.4 in.

I'_x = 299 in.^{4} (calculations not shown)

$$P_{ex} = \frac{\pi^2 EI'_x}{L^2} \tag{4.5-4}$$

$$= \frac{\pi^2(29{,}000\text{ ksi})(299\text{ in.}^4)}{(144\text{ in.})^2}$$

$$= 4{,}130\text{ kips}$$

Calculate F_{n1}, the nominal buckling stress without consideration of slender elements.

By inspection, under a constant axial force, the location with the largest ratio of f_r/F_y is the bottom end of the column.

From Table 5-3, $A_g = 4.69$ in.^{2}

$$F_e = \frac{P_{ex}}{A_g}$$
$$= \frac{4{,}130\,\text{kips}}{4.69\,\text{in.}^2}$$
$$= 881\,\text{ksi}$$
$$\frac{F_y}{F_e} = \frac{55\,\text{ksi}}{881\,\text{ksi}}$$
$$= 0.0624 \le 2.25;\ \text{therefore, use Equation 5.3-20b}$$
$$F_{n1} = \left[0.658^{\frac{F_y}{F_e}}\right] F_y \qquad (5.3\text{-}20b)$$
$$= \left[0.658^{0.0624}\right] 55\,\text{ksi}$$
$$= 53.6\,\text{ksi}$$

Calculate the nominal buckling strength multiplier, γ_{n1}, using the required stress, f_{rmax}, at the location where F_{n1} was computed (at the bottom end of the column):

LRFD	ASD
$f_{rmax} = \frac{P_r}{A_g}$	$f_{rmax} = \frac{P_r}{A_g}$
$= \frac{11.3\ \text{kips}}{4.69\ \text{in.}^2}$	$= \frac{7.50\,\text{kips}}{4.69\,\text{in.}^2}$
$= 2.41$ ksi	$= 1.60$ ksi
$\gamma_{n1} = \frac{F_{n1}}{f_{rmax}}$	$\gamma_{n1} = \frac{F_{n1}}{f_{rmax}}$
$= \frac{53.6\ \text{ksi}}{2.41\ \text{ksi}}$	$= \frac{53.6\ \text{ksi}}{1.60\ \text{ksi}}$
$= 22.2$	$= 33.5$

Locate critical section and calculate slenderness reduction factor, Q.

The critical section is where $\frac{f_r}{QF_y}$ is largest. Calculate this value at the bottom end of the column.

First, determine the slenderness reduction factor, Q, by checking the outside flange slenderness using AISC *Specification* Table B4.1. The flange width-thickness ratio is,

$$\lambda = \frac{b}{t}$$
$$= \frac{b_f}{2t_f}$$
$$= \frac{6.0\ \text{in.}}{2\left(\frac{7}{32}\ \text{in.}\right)}$$
$$= 13.7$$

From Table B4.1, for uniform compression in flanges of built-up I-shaped sections,

$$\lambda_r = 0.64\sqrt{\frac{k_c E}{F_y}}$$

where

$$k_c = \frac{4}{\sqrt{\frac{h}{t_w}}} \qquad (5.4\text{-}24)$$

$$= \frac{4}{\sqrt{\frac{12.0\,\text{in.}}{0.125\,\text{in.}}}}$$

$$= 0.408 \qquad 0.35 < k_c < 0.76$$

Therefore, use $k_c = 0.408$.

$$\lambda_r = 0.64\sqrt{\frac{k_c E}{F_y}} \qquad (\textit{Spec.}\ \text{Table B4.1})$$

$$= 0.64\sqrt{\frac{0.408\left(29{,}000\,\text{ksi}\right)}{55\,\text{ksi}}}$$

$$= 9.39 < 13.7;\ \text{therefore, outside flange is slender}$$

Determine the slenderness reduction factor, Q, using AISC *Specification* Section E7.1. For slender-element sections,

$$Q = Q_s Q_a$$

Determine the value of Q_s based on AISC *Specification* Section E7.1(b) for both flanges. The equation used for Q_s is dependent on the flange slenderness, λ, compared to the following value:

$$1.17\sqrt{\frac{k_c E}{F_y}} = 1.17\sqrt{\frac{0.408\left(29{,}000\,\text{ksi}\right)}{55\,\text{ksi}}}$$

$$= 17.2$$

$9.39 < 13.7 < 17.2$; therefore, apply AISC *Specification* Equation E7-8 to the outside flange,

$$Q_s = 1.415 - 0.65\left(\frac{b}{t}\right)\sqrt{\frac{F_y}{Ek_c}} \qquad (\textit{Spec.}\ \text{Eq. E7-8})$$

$$= 1.415 - 0.65\left(13.7\right)\sqrt{\frac{55\,\text{ksi}}{29{,}000\,\text{ksi}\left(0.408\right)}}$$

$$= 0.808$$

Determine Q_s for the inside flange slenderness where the width-thickness ratio is,

$$\lambda = \frac{b}{t}$$

$$= \frac{b_f}{2t_f}$$

$$= \frac{6.0\,\text{in.}}{2\left(5/16\,\text{in.}\right)}$$

$$= 9.60$$

and

$\lambda_r = 9.39$ from previous calculations for the inside flange

$\lambda_r = 9.39 < \lambda = 9.60$; therefore, the inside flange is slender.

$9.39 < 9.60 < 17.2$; therefore, apply AISC *Specification* Equation E7-8 to the inside flange,

$$Q_s = 1.415 - 0.65\left(\frac{b}{t}\right)\sqrt{\frac{F_y}{Ek_c}} \qquad \text{(Spec. Eq. E7-8)}$$

$$= 1.415 - 0.65(9.60)\sqrt{\frac{55\,\text{ksi}}{29{,}000\,\text{ksi}(0.408)}}$$

$$= 0.990$$

Check web slenderness at the bottom of the column:

$$\lambda = \frac{h}{t_w}$$

$$= \frac{12.0\,\text{in.}}{0.125\,\text{in.}}$$

$$= 96.0$$

Using AISC *Specification* Table B4.1, for uniform compression in webs of doubly symmetric I-shaped sections:

$$\lambda_r = 1.49\sqrt{\frac{E}{F_y}} \qquad \text{(Spec. Table B4.1)}$$

$$= 1.49\sqrt{\frac{29{,}000\,\text{ksi}}{55\,\text{ksi}}}$$

$= 34.2 < 96.0$; therefore, the web is slender

Calculate Q_a using AISC *Specification* Section E7.2:

$$Q_a = \frac{A_{eff}}{A_g} \qquad \text{(Spec. Eq. E7-16)}$$

where

$A = A_g$

$= 4.69\ \text{in.}^2$ from Table 5-3

$A_{eff} = b_f(t_{f,inside} + t_{f,outside}) + b_e t_w$

$$b_e = 1.92t\sqrt{\frac{E}{f}}\left[1 - \frac{0.34}{(b/t)}\sqrt{\frac{E}{f}}\right] \le b \qquad \text{(Spec. Eq. E7-17)}$$

With $f_r = f_{rmax}$ and γ_{n1} determined previously, the stress, f, at which the effective width is calculated is determined as follows:

LRFD	ASD
$f = \gamma_{n1} f_r$	$f = \gamma_{n1} f_r$
$= 22.2(2.41\,\text{ksi})$	$= 33.5(1.60\,\text{ksi})$
$= 53.5\,\text{ksi}$	$= 53.6\,\text{ksi}$

Note that the difference in f between LRFD and ASD is due to rounding. Use ASD value: $f = 53.6$ ksi and $b/t = h/t_w = 96.0$.

$$b_e = 1.92t\sqrt{\frac{E}{f}}\left[1-\frac{0.34}{(b/t)}\sqrt{\frac{E}{f}}\right] \le b \qquad \text{(Spec. Eq. E7-17)}$$

$$= 1.92(0.125\,\text{in.})\sqrt{\frac{29{,}000\ \text{ksi}}{53.6\,\text{ksi}}}\left[1-\frac{0.34}{96.0}\sqrt{\frac{29{,}000\ \text{ksi}}{53.6\,\text{ksi}}}\right]$$

$$= 5.12\,\text{in.} \le 12.0\,\text{in.}$$

$$A_{eff} = b_f(t_{f,inside} + t_{f,outside}) + b_e t_w$$

$$= 6.00\ \text{in.}\ (5/16\ \text{in.} + 7/32\ \text{in.}) + 5.12\ \text{in.}\ (0.125\ \text{in.})$$

$$= 3.83\ \text{in.}^2$$

Therefore,

$$Q_a = \frac{A_{eff}}{A_g} \qquad \text{(Spec. Eq. E7-16)}$$

$$= \frac{3.83\,\text{in.}^2}{4.69\,\text{in.}^2}$$

$$= 0.817$$

If both flanges are in compression under combined loading, Q_s is the lower of the two Q_s values calculated.

$Q_s = 0.808$ from outside flange

$$Q = Q_s Q_a$$
$$= 0.808(0.817)$$
$$= 0.660$$

If the outside flange is in tension under combined loading, Q_s is taken from the inside flange.

$Q_s = 0.990$ from inside flange

$$Q = Q_s Q_a$$
$$= 0.990(0.817)$$
$$= 0.809$$

For load cases where the inside flange is in compression, such as axial load with no moment, use $Q = 0.660$. However, calculations for this example will be carried out assuming the outside flange will be in tension under the combined loading in Example 5.8. It is conservative to use the smaller value of Q if the stress distribution is not known at the time of calculation.

LRFD	ASD
$\frac{f_r}{QF_y} = \frac{2.41\,\text{ksi}}{0.809(55\,\text{ksi})}$ $= 0.0542$	$\frac{f_r}{QF_y} = \frac{1.60\,\text{ksi}}{0.809(55\,\text{ksi})}$ $= 0.0360$

Calculate $\frac{f_r}{QF_y}$ at the top end of the column, although it is not likely to control.

From Table 5-3, $A_g = 6.19$ in.^{2}

Check the outside flange slenderness using AISC *Specification* Table B4.1:

$\lambda = 13.7$ from bottom of column determined earlier

From AISC *Specification* Table B4.1, for uniform compression in flanges of built-up I-shaped sections,

$$\lambda_r = 0.64\sqrt{\frac{k_c E}{F_y}}$$

where

$$k_c = \frac{4}{\sqrt{\frac{h}{t_w}}} \quad \text{(from AISC } \textit{Specification} \text{ Table B4.1 footnote a)} \tag{5.4-24}$$

$$= \frac{4}{\sqrt{\frac{24.0 \text{ in.}}{0.125 \text{ in.}}}}$$

$$= 0.289 < 0.35$$

$$\lambda_r = 0.64\sqrt{\frac{k_c E}{F_y}} \quad \text{(}\textit{Spec.}\text{ Table B4.1)}$$

$$= 0.64\sqrt{\frac{0.35(29{,}000\,\text{ksi})}{55\,\text{ksi}}}$$

$$= 8.69 < 13.7; \text{ therefore, outside flange is slender}$$

Determine the slenderness reduction factor, Q, using AISC *Specification* Section E7.1. For slender-element sections,

$$Q = Q_s Q_a$$

Determined the value of Q_s based on AISC *Specification* Section E7.1(b) for both flanges. The equation used for Q_s is dependent on the flange slenderness, λ, compared to the following value:

$$1.17\sqrt{\frac{k_c E}{F_y}} = 1.17\sqrt{\frac{0.35(29{,}000\,\text{ksi})}{55\,\text{ksi}}}$$

$$= 15.9$$

$8.69 < 13.7 < 15.9$; therefore, apply AISC *Specification* Equation E7-8 to the outside flange.

$$Q_s = 1.415 - 0.65\left(\frac{b}{t}\right)\sqrt{\frac{F_y}{Ek_c}} \quad \text{(}\textit{Spec.}\text{ Eq. E7-8)}$$

$$= 1.415 - 0.65(13.7)\sqrt{\frac{55\,\text{ksi}}{29{,}000\,\text{ksi}(0.35)}}$$

$$= 0.759$$

Determine Q_s for the inside flange slenderness.

$\lambda = b/t = 9.60$ from bottom of column determined previously
$k_c = 0.35$ from outside flange determined previously
$\lambda_r = 8.69 < 9.60 < 15.9$; therefore, AISC *Specification* Equation E7-8 applies

$$Q_s = 1.415 - 0.65\left(\frac{b}{t}\right)\sqrt{\frac{F_y}{Ek_c}} \quad \text{(}\textit{Spec.}\text{ Eq. E7-8)}$$

$$= 1.415 - 0.65(9.58)\sqrt{\frac{55\,\text{ksi}}{29{,}000\,\text{ksi}(0.35)}}$$

$$= 0.957$$

Check web slenderness:

$$\lambda = \frac{h}{t_w}$$
$$= \frac{24.0\,\text{in.}}{0.125\,\text{in.}}$$
$$= 192$$

As calculated previously,

$\lambda_r = 34.2 < 192$, therefore the web is slender.

As calculated previously,

$\lambda_r = 34.2 < 192$; therefore the web is slender.

Calculate Q_a using AISC *Specification* Section E7.2:

$$Q_a = \frac{A_{eff}}{A_g} \qquad \text{(Spec. Eq. E7-16)}$$

where

$A = A_g$
$= 6.19\ \text{in.}^2$ from Table 5-3

$A_{eff} = b_f\,(t_{f,\,inside} + t_{f,\,outside}) + b_e t_w$

$$b_e = 1.92t\sqrt{\frac{E}{f}}\left[1 - \frac{0.34}{(b/t)}\sqrt{\frac{E}{f}}\right] \le b \qquad \text{(Spec. Eq. E7-17)}$$

The stress, f, at which the effective width is calculated is determined as follows:

LRFD	ASD
$f_r = \frac{P_r}{A_g}$	$f_r = \frac{P_r}{A_g}$
$= \frac{11.3\,\text{kips}}{6.19\,\text{in.}^2}$	$= \frac{7.50\,\text{kips}}{6.19\,\text{in.}^2}$
$= 1.83\ \text{ksi}$	$= 1.21\ \text{ksi}$
$f = \gamma_{n1} f_r$	$f = \gamma_{n1} f_r$
$= 22.2(1.83\,\text{ksi})$	$= 33.5(1.21\,\text{ksi})$
$= 40.6\,\text{ksi}$	$= 40.5\,\text{ksi}$

Note that the difference in f between LRFD and ASD is due to rounding. Use ASD value: $f = 40.5$ ksi.

Therefore, with $b/t = 192$, the effective width is,

$$b_e = 1.92t\sqrt{\frac{E}{f}}\left[1 - \frac{0.34}{(b/t)}\sqrt{\frac{E}{f}}\right] \le b \qquad \text{(Spec. Eq. E7-17)}$$

$$= 1.92(0.125\,\text{in.})\sqrt{\frac{29{,}000\ \text{ksi}}{40.5\,\text{ksi}}}\left[1 - \frac{0.34}{192}\sqrt{\frac{29{,}000\ \text{ksi}}{40.5\,\text{ksi}}}\right]$$

$= 6.12\,\text{in.} \le 24.0\,\text{in.}$

$A_{eff} = b_f\,(t_{f,\,inside} + t_{f,\,outside}) + b_e t_w$
$= 6.00$ in. ($5/16$ in. + $7/32$ in.) + 6.12 in. (0.125 in.)
$= 3.95\ \text{in.}^2$

$$Q_a = \frac{A_{eff}}{A_g} \qquad \text{(Spec. Eq. E7-16)}$$

$$= \frac{3.96\,\text{in.}^2}{6.19\,\text{in.}^2}$$

$$= 0.640$$

If both flanges are in compression under combined loading, Q_s is the lower of the two Q_s values calculated.

$Q_s = 0.759$ from outside flange

$$Q = Q_s Q_a$$
$$= 0.759(0.640)$$
$$= 0.486$$

If the outside flange is in tension under combined loading, Q_s is taken from the inside flange.

$Q_s = 0.957$ from inside flange

$$Q = Q_s Q_a$$
$$= 0.957(0.640)$$
$$= 0.612$$

For load cases where the inside flange is in compression, such as axial load with no moment, use $Q = 0.486$. However, calculations for this example will be carried out assuming the outside flange will be in tension under the combined loading in Example 5.8. It is conservative to use the smaller value of Q if the stress distribution is not known at the time of calculation.

LRFD	ASD
$\frac{f_r}{QF_y} = \frac{1.83\,\text{ksi}}{0.612(55\,\text{ksi})}$	$\frac{f_r}{QF_y} = \frac{1.21\,\text{ksi}}{0.612(55\,\text{ksi})}$
$= 0.0544$	$= 0.0359$

Calculate $\frac{f_r}{QF_y}$ at $h/t_w = 131$ (location where k_c reaches lower limit of 0.35).

First, determine the slenderness reduction factor, Q. First, check the outside flange slenderness using AISC *Specification* Table B4.1. The flange width-thickness ratio is,

$$\lambda = b/t$$
$$= 13.7 \text{ as determined previously for the bottom end of the column}$$

From Table B4.1, for uniform compression in flanges of built-up I-shaped sections,

$$\lambda_r = 0.64\sqrt{\frac{k_c E}{F_y}}$$

where

$k_c = 0.35$ as given

Therefore,

$$\lambda_r = 0.64\sqrt{\frac{k_c E}{F_y}} \qquad \text{(Spec. Table B4.1)}$$

$$= 0.64\sqrt{\frac{0.35(29{,}000\,\text{ksi})}{55\,\text{ksi}}}$$

$$= 8.69 < 13.7; \text{ therefore, outside flange is slender}$$

Determine the slenderness reduction factor, Q, using AISC *Specification* Section E7.1. For slender-element sections,

$$Q = Q_s Q_a$$

Determine the value of Q_s based on AISC *Specification* Section E7.1(b) for both flanges. The equation for Q_s is dependent on the flange slenderness, λ, compared to the following value:

$$1.17\sqrt{\frac{k_c E}{F_y}} = 1.17\sqrt{\frac{0.35(29{,}000\,\text{ksi})}{55\,\text{ksi}}}$$
$$= 15.9$$

$8.69 < 13.7 < 15.9$; therefore, apply AISC *Specification* Equation E7-8 to the outside flange,

$$Q_s = 1.415 - 0.65\left(\frac{b}{t}\right)\sqrt{\frac{F_y}{Ek_c}} \qquad \text{(Spec. Eq. E7-8)}$$
$$= 1.415 - 0.65(13.7)\sqrt{\frac{55\,\text{ksi}}{29{,}000\,\text{ksi}(0.35)}}$$
$$= 0.759$$

Determine Q_s for the inside flange slenderness using the following values:

$\lambda = 9.58$ determined previously for the bottom of the column
$k_c = 0.35$ as given
$\lambda_r = 8.60$ as determined previously < 9.58; therefore, inside flange is slender

$$Q_s = 1.415 - 0.65\left(\frac{b}{t}\right)\sqrt{\frac{F_y}{Ek_c}} \qquad \text{(Spec. Eq. E7-8)}$$
$$= 1.415 - 0.65(9.58)\sqrt{\frac{55\,\text{ksi}}{29{,}000\,\text{ksi}(0.35)}}$$
$$= 0.957$$

Check web slenderness:

$$\lambda = \frac{h}{t_w}$$
$$= 131 \text{ as given}$$

$\lambda_r = 34.2 < 131$, therefore web is slender.

Calculate Q_a using AISC *Specification* Section E7.2:

$$Q_a = \frac{A_{eff}}{A_g} \qquad \text{(Spec. Eq. E7-16)}$$

where

$A = A_g$
$= 5.24$ in.^{2} from Table 5-3
$A_{eff} = b_f\,(t_{f,\,inside} + t_{f,\,outside}) + b_e t_w$

$$b_e = 1.92t\sqrt{\frac{E}{f}}\left[1 - \frac{0.34}{(b/t)}\sqrt{\frac{E}{f}}\right] \le b \qquad \text{(Spec. Eq. E7-17)}$$

The stress, f, at which the effective width is calculated is determined as follows:

LRFD	ASD
$f_r = \frac{P_r}{A_g}$ $= \frac{11.3\,\text{kips}}{5.24\ \text{in.}^2}$ $= 2.16\ \text{ksi}$ $f = \gamma_{n1} f_r$ $= 22.2(2.16\ \text{ksi})$ $= 48.0\ \text{ksi}$	$f_r = \frac{P_r}{A_g}$ $= \frac{7.50\,\text{kips}}{5.24\,\text{in.}^2}$ $= 1.43\ \text{ksi}$ $f = \gamma_{n1} f_r$ $= 33.5(1.43\ \text{ksi})$ $= 47.9\ \text{ksi}$

Note that the difference in f between LRFD and ASD is due to rounding. Use ASD value: $f = 47.9$ ksi.

Calculate the effective width with $b/t = h/t_w = 131$ and $b = h = 16.4$ in. from Table 5-3:

$$b_e = 1.92t\sqrt{\frac{E}{f}}\left[1 - \frac{0.34}{(b/t)}\sqrt{\frac{E}{f}}\right] \le b \qquad \text{(Spec. Eq. E7-17)}$$

$$= 1.92(0.125\,\text{in.})\sqrt{\frac{29{,}000\ \text{ksi}}{47.9\ \text{ksi}}}\left[1 - \frac{0.34}{131}\sqrt{\frac{29{,}000\ \text{ksi}}{47.9\ \text{ksi}}}\right]$$

$$= 5.53\,\text{in.} \le 16.4\,\text{in.}$$

$$A_{eff} = b_f\,(t_{f,\,inside} + t_{f,\,outside}) + b_e t_w$$

$$= 6.00\ \text{in.}\ (5/16\ \text{in.} + 7/32\ \text{in.}) + 5.53\ \text{in.}\ (0.125\ \text{in.})$$

$$= 3.88\,\text{in.}^2$$

Therefore,

$$Q_a = \frac{A_{eff}}{A_g} \qquad \text{(Spec. Eq. E7-16)}$$

$$= \frac{3.88\,\text{in.}^2}{5.24\,\text{in.}^2}$$

$$= 0.740$$

If both flanges are in compression under combined loading, Q_s is the lower of the two Q_s values calculated.

$Q_s = 0.759$ from outside flange

$$Q = Q_s Q_a$$
$$= 0.759(0.740)$$
$$= 0.562$$

If the outside flange is in tension under combined loading, Q_s is taken from the inside flange.

$Q_s = 0.956$ from inside flange

$$Q = Q_s Q_a$$
$$= 0.957(0.740)$$
$$= 0.708$$

For load cases where the inside flange is in compression, such as axial load with no moment, use $Q = 0.562$. However, calculations for this example will be carried out assuming the outside flange will be in tension under the combined loading in Example 5.8. It is conservative to use the smaller value of Q if the stress distribution is not known at the time of calculation.

LRFD	ASD
$\frac{f_r}{QF_y} = \frac{2.16\,\text{ksi}}{0.708(55\,\text{ksi})}$ $= 0.0555$	$\frac{f_r}{QF_y} = \frac{1.43\,\text{ksi}}{0.708(55\,\text{ksi})}$ $= 0.0367$

The location where $h/t_w = 131$ is the critical one, because $\frac{f_r}{QF_y}$ is the largest at that point.

Calculate the nominal buckling stress at the critical location with the highest ratio of f_r/QF_y.

As determined earlier, the critical location occurs where $h/t_w = 131$.

$Q = 0.708$ previously calculated

From a previous calculation, $P_{ex} = 4{,}130$ kips; therefore, the elastic critical buckling stress is,

$$F_e = \frac{P_{ex}}{A_g}$$

$$= \frac{4{,}130 \text{ kips}}{5.24 \text{ in.}^2}$$

$$= 788 \text{ ksi}$$

$$\frac{QF_y}{F_e} = \frac{0.708(55 \text{ ksi})}{788 \text{ ksi}}$$

$$= 0.0494 \le 2.25; \text{ therefore, use Equation 5.3-23b}$$

$$F_{cr} = \left[0.658^{\frac{QF_y}{F_e}}\right] QF_y \qquad \text{(5.3-23b)}$$

$$= \left[0.658^{0.0494}\right] 0.708(55 \text{ ksi})$$

$$= 38.1 \text{ ksi}$$

$$P_n = F_{cr} A_g \qquad \text{(5.3-6, } \textit{Spec.} \text{ Eq. E7-1)}$$

$$= 38.1 \text{ ksi}\left(5.24 \text{ in.}^2\right)$$

$$= 200 \text{ kips}$$

Calculate the in-plane strength ratio at the location of the highest ratio of f_r/QF_y.

LRFD	ASD
$\frac{P_r}{P_c} = \frac{P_r}{\phi_c P_n}$	$\frac{P_r}{P_c} = \frac{\Omega_c P_r}{P_n}$
$= \frac{11.3 \text{ kips}}{0.90(200 \text{ kips})}$	$= \frac{1.67(7.50 \text{ kips})}{200 \text{ kips}}$
$= 0.0628$	$= 0.0626$

Constrained-Axis Torsional Buckling

Determine the elastic constrained-axis torsional buckling load, P_{eCAT}, using Section 5.3.1 of this Design Guide and properties at the middle of the 144 in. inside unbraced length. The equation is,

$$P_{eCAT} = \left[\frac{\pi^2 E\left(C_w + I_y a_s^2\right)}{\left(K_z L_{b,inside}\right)^2} + GJ\right] \frac{1}{r_x^2 + r_y^2 + a_c^2} \qquad \text{(5.3-15)}$$

The section properties should be taken at the midpoint of the inside unbraced length as follows:

At bottom end, web height = 12.0 in.
At top end, web height = 24.0 in.
At mid-length, web height = 18.0 in.

$$A_g = 5.44 \text{ in.}^2$$
$$\bar{y} = 10.2 \text{ in. from outside}$$
$$I_x = 322 \text{ in.}^4$$
$$r_x = \sqrt{\frac{I_x}{A_g}}$$
$$= \sqrt{\frac{322 \text{ in.}^4}{5.44 \text{ in.}^2}}$$
$$= 7.69 \text{ in.}$$
$$I_y = 9.58 \text{ in.}^4$$
$$r_y = \sqrt{\frac{I_y}{A_g}}$$
$$= \sqrt{\frac{9.58 \text{ in.}^4}{5.44 \text{ in.}^2}}$$
$$= 1.33 \text{ in.}$$

The moment inertia about the *y*-axis for the outside flange is,

$$I_{y1} = \frac{7/32 \text{ in.} \left(6.00 \text{ in.}\right)^3}{12}$$
$$= 3.94 \text{ in.}^4$$

The moment inertia about the *y*-axis for the inside flange is,

$$I_{y2} = \frac{5/16 \text{ in.} \left(6.00 \text{ in.}\right)^3}{12}$$
$$= 5.63 \text{ in.}^4$$

The warping constant is calculated as,

$$C_w = \frac{h_o^2 I_{y1}}{\frac{I_{y1}}{I_{y2}} + 1} \qquad (5.3\text{-}16)$$

where

$$h_o = h + 0.5\left(t_{f1} + t_{f2}\right)$$
$$= 18.0 \text{ in.} + 0.5\left(5/16 \text{ in.} + 7/32 \text{ in.}\right)$$
$$= 18.3 \text{ in.}$$

Therefore,

$$C_w = \frac{h_o^2 I_{y1}}{\frac{I_{y1}}{I_{y2}} + 1} \qquad (5.3\text{-}16)$$
$$= \frac{\left(18.3 \text{ in.}\right)^2 3.94 \text{ in.}^4}{\frac{3.94 \text{ in.}^4}{5.63 \text{ in.}^4} + 1}$$
$$= 776 \text{ in.}^6$$

And the St. Venant's torsional constant is,

$$J = \frac{ht_w^3}{3} + \frac{b_{ft}t_{ft}^3}{3}\left(1-0.63\frac{t_{ft}}{b_{ft}}\right) + \frac{b_{fc}t_{fc}^3}{3}\left(1-0.63\frac{t_{fc}}{b_{fc}}\right) \tag{5.3-13}$$

$$= \frac{18.0\,\text{in.}\left(0.125\,\text{in.}\right)^3}{3} + \frac{6.00\text{ in.}\left(\frac{7}{32}\text{ in.}\right)^3}{3}\left(1-0.63\frac{\frac{7}{32}\text{ in.}}{6.00\text{ in.}}\right) + \frac{6.00\,\text{in.}\left(\frac{5}{16}\,\text{in.}\right)^3}{3}\left(1-0.63\frac{\frac{5}{16}\text{ in.}}{6.00\text{ in.}}\right)$$

$$= 0.0912\,\text{in.}^4$$

The distance from the center of the girt or purlin to the centroid of the column is,

$$a_c = \frac{\text{girt depth}}{2} + \bar{y}$$

$$= \frac{8.00\text{ in.}}{2} + 10.2\text{ in.}$$

$$= 14.2\text{ in.}$$

The distance from the center of the girt or purlin to the shear center of the column is,

$$a_s = a_c + y_o$$

where

$$y_o = \frac{t_{f1}}{2} + \frac{h_o I_{y2}}{I_y} - \bar{y} \tag{5.3-19}$$

$$= \frac{\frac{7}{32}\text{ in.}}{2} + \frac{18.3\,\text{in.}\left(5.63\,\text{in.}^4\right)}{9.58\,\text{in.}^4} - 10.2\,\text{in.}$$

$$= 0.664\,\text{in.}$$

Therefore,

$$a_s = a_c + y_o$$

$$= 14.2\,\text{in.} + 0.664\,\text{in.}$$

$$= 14.9\,\text{in.}$$

The elastic constrained-axis torsional buckling strength is,

$$P_{eCAT} = \left[\frac{\pi^2 E\left(C_w + I_y a_s^2\right)}{\left(K_z L_{b,\,inside}\right)^2} + GJ\right]\frac{1}{r_x^2 + r_y^2 + a_c^2} \tag{5.3-15}$$

$$= \left\{\frac{\pi^2\,29{,}000\,\text{ksi}\left[776\,\text{in.}^6 + 9.58\,\text{in.}^4\left(14.9\,\text{in.}\right)^2\right]}{\left[1.0\left(144\,\text{in.}\right)\right]^2} + 11{,}200\,\text{ksi}\left(0.0912\,\text{in.}^4\right)\right\}\frac{1}{\left(7.69\,\text{in.}\right)^2 + \left(1.33\,\text{in.}\right)^2 + \left(14.2\,\text{in.}\right)^2}$$

$$= 157\text{ kips}$$

Calculate F_{n1}, the nominal buckling stress without consideration of slender elements.

By inspection, under a constant axial force, the location with the largest ratio of f_r/F_y is the bottom end. From Section 5.3.2,

$$F_{n1} = \left[0.658^{\frac{F_y}{F_e}}\right]F_y \tag{5.3-20b}$$

where

$$F_e = \frac{P_{eCAT}}{A_g}$$

$A_g = 4.69\,\text{in.}^2$ previously calculated

Therefore,

$$F_e = \frac{157\,\text{kips}}{4.69\,\text{in.}^2}$$
$$= 33.5\,\text{ksi}$$

Calculate the following to verify that Equation 5.3-20b applies.

$$\frac{F_y}{F_e} = \frac{55\,\text{ksi}}{33.5\,\text{ksi}}$$
$$= 1.64 < 2.25;\ \text{therefore,}\ \text{use Equation 5.3-20b}$$

The nominal buckling stress, without consideration of slenderness effects is,

$$F_{n1} = \left[0.658^{\frac{F_y}{F_e}}\right] F_y \qquad (5.3\text{-}20b)$$
$$= \left[0.658^{1.64}\right] 55\,\text{ksi}$$
$$= 27.7\,\text{ksi}$$

Calculate the nominal buckling strength multiplier, γ_{n1}, using the required stress, f_{rmax}, at the bottom location where F_{n1} was computed:

LRFD	ASD
$f_{rmax} = \frac{P_r}{A_g}$	$f_{rmax} = \frac{P_r}{A_g}$
$= \frac{11.3\,\text{kips}}{4.69\,\text{in.}^2}$	$= \frac{7.50\,\text{kips}}{4.69\,\text{in.}^2}$
$= 2.41\ \text{ksi}$	$= 1.60\ \text{ksi}$
$\gamma_{n1} = \frac{F_{n1}}{f_{rmax}}$	$\gamma_{n1} = \frac{F_{n1}}{f_{rmax}}$
$= \frac{27.7\,\text{ksi}}{2.41\ \text{ksi}}$	$= \frac{27.7\,\text{ksi}}{1.60\ \text{ksi}}$
$= 11.5$	$= 17.3$

Locate critical section and calculate slenderness reduction factor, Q.

From calculations for in-plane buckling, it can be concluded that the critical location will be at the location where $h/t_w = 131$ (location where k_c reaches the lower limit of 0.35).

Determine the value of the slenderness reduction factor, Q, based on previous calculations.

For the outside flange:

$Q_s = 0.759$ from previous calculation

For the inside flange:

$Q_s = 0.957$ from previous calculation

For the web:

$$\lambda = \frac{h}{t_w}$$
$$= 131$$

$\lambda_r = 34.2 < 131$; as determined previously. Therefore, the web is slender.

Calculate Q_a using AISC *Specification* Section E7.2:

$$Q_a = \frac{A_{eff}}{A_g} \qquad \text{(Spec. Eq. E7-16)}$$

where

$A = A_g$

$= 5.24 \text{ in.}^2$ from Table 5-3

$A_{eff} = b_f\,(t_{f,\,inside} + t_{f,\,outside}) + b_e t_w$

$$b_e = 1.92t\sqrt{\frac{E}{f}}\left[1 - \frac{0.34}{(b/t)}\sqrt{\frac{E}{f}}\right] \le b \qquad \text{(Spec. Eq. E7-17)}$$

The stress, f, at which the effective width is calculated is determined as follows:

LRFD	ASD
$f_r = \dfrac{P_r}{A_g}$	$f_r = \dfrac{P_r}{A_g}$
$= \dfrac{11.3 \text{ kips}}{5.24 \text{ in.}^2}$	$= \dfrac{7.50 \text{ kips}}{5.24 \text{ in.}^2}$
$= 2.16 \text{ ksi}$	$= 1.43 \text{ ksi}$
$f = \gamma_{n1} f_r$	$f = \gamma_{n1} f_r$
$= 11.5(2.16 \text{ ksi})$	$= 17.3(1.43 \text{ ksi})$
$= 24.8 \text{ ksi}$	$= 24.7 \text{ ksi}$

Note that the difference in f between LRFD and ASD is due to rounding. Use ASD value: $f = 24.7$ ksi.

$$b_e = 1.92t\sqrt{\frac{E}{f}}\left[1 - \frac{0.34}{(b/t)}\sqrt{\frac{E}{f}}\right] \le b \qquad \text{(Spec. Eq. E7-17)}$$

$$= 1.92(0.125 \text{ in.})\sqrt{\frac{29{,}000 \text{ ksi}}{24.7 \text{ ksi}}}\left[1 - \frac{0.34}{131}\sqrt{\frac{29{,}000 \text{ ksi}}{24.7 \text{ ksi}}}\right]$$

$$= 7.49 \text{ in.} \le 16.4 \text{ in.}$$

$$A_{eff} = b_f\left(t_{f,\,inside} + t_{f,\,outside}\right) + b_e t_w$$

$$= 6.00 \text{ in.}(5/16 \text{ in.} + 7/32 \text{ in.}) + 7.49 \text{ in.}(0.125 \text{ in.})$$

$$= 4.12 \text{ in.}^2$$

$$Q_a = \frac{A_{eff}}{A_g} \qquad \text{(Spec. Eq. E7-16)}$$

$$= \frac{4.12 \text{ in.}^2}{5.24 \text{ in.}^2}$$

$$= 0.786$$

If both flanges are in compression under combined loading, Q_s is the lower of the two Q_s values calculated.

$Q_s = 0.759$ from outside flange

$Q = Q_s Q_a$

$= 0.759(0.786)$

$= 0.597$

If the outside flange is in tension under combined loading, Q_s is taken from the inside flange.

$Q_s = 0.957$ from inside flange

$$Q = Q_s Q_a$$
$$= 0.957(0.786)$$
$$= 0.752$$

For load cases where the inside flange is in compression, such as axial load with no moment, use $Q = 0.598$. However, calculations for this example will be carried out assuming the outside flange will be in tension under the combined loading in Example 5.8. It is conservative to use the smaller value of Q if the stress distribution is not known at the time of calculation.

LRFD	ASD
$\frac{f_r}{QF_y} = \frac{2.16\,\text{ksi}}{0.752(55\,\text{ksi})}$ $= 0.0522$	$\frac{f_r}{QF_y} = \frac{1.43\,\text{ksi}}{0.752(55\,\text{ksi})}$ $= 0.0346$

Calculate the nominal buckling strength at the critical location.

$Q = 0.752$ from the location where $h/t_w = 131$ as determined previously

$$F_e = \frac{P_{eCAT}}{A_g}$$
$$= \frac{157\,\text{kips}}{5.24\,\text{in.}^2}$$
$$= 30.0\,\text{ksi}$$
$$\frac{QF_y}{F_e} = \frac{0.752(55\,\text{ksi})}{30.0\,\text{ksi}}$$
$$= 1.38 < 2.25;\ \text{therefore, use Equation 5.3-23b or } \textit{Spec}.\ \text{Equation E7-2}$$
$$F_{cr} = \left[0.658^{\frac{QF_y}{F_e}}\right] QF_y \qquad (5.3\text{-}23b)$$
$$= \left[0.658^{1.38}\right] 0.752(55\,\text{ksi})$$
$$= 23.2\,\text{ksi}$$
$$P_n = F_{cr} A_g \qquad (5.3\text{-}6,\ \textit{Spec}.\ \text{Eq. E7-1})$$
$$= 23.2\,\text{ksi}\left(5.24\,\text{in.}^2\right)$$
$$= 122\,\text{kips}$$

Calculate the constrained-axis torsional buckling strength ratio.

LRFD	ASD
$\frac{P_r}{P_c} = \frac{P_r}{\phi_c P_n}$ $= \frac{11.3\,\text{kips}}{0.90(122\,\text{kips})}$ $= 0.103$	$\frac{P_r}{P_c} = \frac{\Omega_c P_r}{P_n}$ $= \frac{1.67(7.50\,\text{kips})}{122\,\text{kips}}$ $= 0.103$

Out-of-Plane Flexural Buckling Strength

By inspection and comparison with Example 5.2, it is apparent that out-of-plane flexural buckling will not control over constrained-axis torsional buckling. If this were not obvious, the checks would be identical to those in Example 5.2, except for the difference in section properties. Separate checks would be performed for the upper and lower unbraced lengths.

Column Strength

For the condition of pure axial compression, the column strength is the lowest strength calculated for the limit states of in-plane buckling of the whole column and constrained-axis torsional buckling of the whole column. Following is a summary of axial strengths due to in-plane flexural buckling.

Summary of Axial Strengths	
In-Plane Flexural Buckling	
LRFD	ASD
$\frac{P_r}{P_c} = \frac{P_r}{\phi_c P_n}$ $= \frac{11.3\,\text{kips}}{0.90\left(200\,\text{kips}\right)}$ $= 0.0628$	$\frac{P_r}{P_c} = \frac{\Omega_c P_r}{P_n}$ $= \frac{1.67\left(7.50\,\text{kips}\right)}{200\,\text{kips}}$ $= 0.0626$
Constrained-Axis Torsional Buckling	
LRFD	ASD
$\frac{P_r}{P_c} = \frac{11.3\,\text{kips}}{0.90\left(122\,\text{kips}\right)}$ $= 0.103$	$\frac{P_r}{P_c} = \frac{1.67\left(7.50\,\text{kips}\right)}{122\,\text{kips}}$ $= 0.103$

Constrained-axis torsional buckling governs the strength of the column.

The available strengths are calculated as:

LRFD	ASD
$\phi_c P_n = 0.90\left(122\,\text{kips}\right)$ $= 110\,\text{kips}$	$\frac{P_n}{\Omega_c} = \frac{122\ \text{kips}}{1.67}$ $= 73.1\,\text{kips}$

Example 5.7—Singly Symmetric Section Tapered Beam with One-Sided Bracing

Given:

Evaluate the flexural strength of the member from Example 5.6 with the required strength shown in Figure 5-9.

Material Properties:

$F_y = 55$ ksi
$F_u = 70$ ksi

Geometric Properties:

Left (outside) flange = PL 7⁄32 in. × 6 in.
Note: Although a 7⁄32-in.-thick flange plate is used in this example, the AISC *Steel Construction Manual* recommends that plate thicknesses up to and including 3⁄8 in. be specified in 1⁄16 in. increments.
Right (inside) flange = PL 5⁄16 in. × 6 in.
Web thickness = 0.125 in.
Outside flange bracing by a girt at 90.0 in. above bottom
No flange bracing on inside
Two 11⁄16-in.-diameter bolt holes in outside flange at brace points

Table 5-4. Section Properties and Strengths		
Top	h	24.0 in.
	S_{xc}	54.2 in.^{3}
	S_{xt}	45.5 in.^{3}
	Z_x	56.1 in.^{3}
	M_{yc}	2,980 kip-in.
	M_{yt}	2,500 kip-in.
	M_p	3,090 kip-in.
At girt	h	19.5 in.
	S_{xt}	35.0 in.^{3}
Mid-length	h	18.0 in.
	S_{xc}	38.6 in.^{3}
	S_{xt}	31.7 in.^{3}
	M_{yc}	2,120 kip-in.
	M_{yt}	1,740 kip-in.
	M_p	2,130 kip-in.
Bottom	h	12.0 in.
Note: S_{xc} refers to the inside flange and S_{xt} refers to the outside flange.		

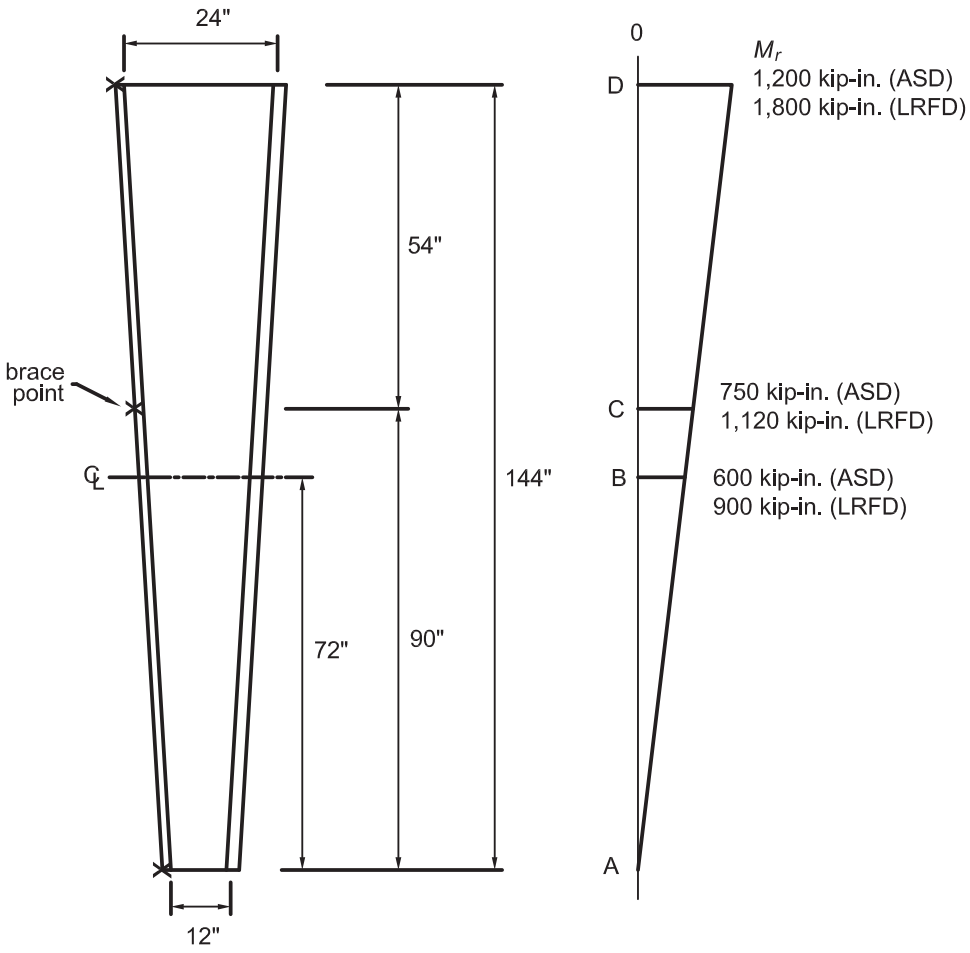

Fig. 5-9. Web-tapered flexural member in Example 5.7.

By inspection, the member must be checked for the following limit states:

a. Tension flange yielding
b. Lateral-torsional buckling
c. Compression flange local buckling
d. Tension flange rupture at the bolt holes

The compression flange yielding limit state need not be checked because the tension flange is smaller than the compression flange.

Inside unbraced length, L_b = 144 in.

Check web slenderness at the middle and top of unbraced length. Check not needed at bottom because $M_r = 0$.

At mid-length:

$\overline{y}_c = 8.35$ in. [distance from the extreme fiber of the compression (inside) flange to the centroid]

$$h_c = 2\left(\overline{y}_c - t_{fc}\right)$$
$$= 2\left(8.35 \text{ in.} - 5/16 \text{ in.}\right)$$
$$= 16.1 \text{ in.}$$
$$\left(\frac{h_c}{t_w}\right)_{\text{mid-length}} = \frac{16.1 \text{ in.}}{0.125 \text{ in.}}$$
$$= 129$$

$\overline{y}_p = 7.06$ in. [distance from the extreme fiber of the compression (inside) flange to the plastic neutral axis]

$$h_p = 2\left(\overline{y}_p - t_{fc}\right)$$
$$= 2\left(7.06 \text{ in.} - 5/16 \text{ in.}\right)$$
$$= 13.5 \text{ in.}$$

From Table 5-4:

M_{yt} = 1,740 kip-in.
M_{yc} = 2,120 kip-in.
M_p = 2,130 kip-in.

Using the AISC *Specification* Table B4.1, determine the limiting width-thickness ratios for compact and noncompact webs in flexure for singly symmetric I-shaped sections:

$$\lambda_{pw} = \frac{\frac{h_c}{h_p}\sqrt{\frac{E}{F_y}}}{\left(0.54\frac{M_p}{M_{y\,min}} - 0.09\right)^2} \le \lambda_{rw} \qquad \text{(}\textit{Spec.}\text{ Table B4.1)}$$

$$= \frac{\frac{16.1 \text{ in.}}{13.5 \text{ in.}}\sqrt{\frac{29{,}000 \text{ ksi}}{55 \text{ ksi}}}}{\left[0.54\left(\frac{2{,}130 \text{ kip-in.}}{1{,}740 \text{ kip-in.}}\right) - 0.09\right]^2}$$
$$= 84.0$$

$$\lambda_{rw} = 5.70\sqrt{E / F_y} \qquad \text{(}\textit{Spec.}\text{ Table B4.1)}$$
$$= 5.70\sqrt{29{,}000 \text{ ksi} / 55 \text{ ksi}}$$
$$= 131 > \lambda_{pw} = 84.0; \text{ therefore, use } \lambda_{pw} = 84.0$$

At the top:

$$\overline{y}_c = 11.2 \text{ in.}$$

$$h_c = 2\left(\overline{y}_c - t_{fc}\right)$$
$$= 2\left(11.2 \text{ in.} - 5/16 \text{ in.}\right)$$
$$= 21.8 \text{ in.}$$

$$\left(\frac{h_c}{t_w}\right)_{top} = \frac{21.8 \text{ in.}}{0.125 \text{ in.}}$$
$$= 174$$

$$\overline{y}_p = 10.1 \text{ in.}$$

$$h_p = 2\left(\overline{y}_p - t_{fc}\right)$$
$$= 2\left(10.1 \text{ in.} - 5/16 \text{ in.}\right)$$
$$= 19.6 \text{ in.}$$

From Table 5-4:

$M_{yt} = 2{,}500$ kip-in.
$M_{yc} = 2{,}980$ kip-in.
$M_p = 3{,}090$ kip-in.

Using the AISC *Specification* Table B4.1, determine the limiting width-thickness ratios for compact and noncompact webs in flexure for singly symmetric I-shaped sections:

$$\lambda_{pw} = \frac{\frac{21.8 \text{ in.}}{19.6 \text{ in.}}\sqrt{\frac{29{,}000 \text{ ksi}}{55 \text{ ksi}}}}{\left[0.54\left(\frac{3{,}090 \text{ kip-in.}}{2{,}500 \text{ kip-in.}}\right) - 0.09\right]^2} \qquad \text{(}\textit{Spec.}\text{ Table B4.1)}$$
$$= 76.6$$

$\lambda_{rw} = 131$ from previous calculation

Therefore, the web is noncompact at mid-length [$84.0 < (h_c/t_w = 129) < 131$] and slender at the top [$131 < (h_c/t_w = 174)$] of the unbraced length.

The values of the web plastification factor, R_{pc}, and the web buckling factor, R_{pg}, will be required to calculate the nominal flexural strength for the limit state of lateral-torsional buckling. At the mid-length, the web is noncompact; therefore, use from Section 5.4 of the this Design Guide and Section F4 of the AISC *Specification*:

$$R_{pc} = \left[\frac{M_p}{M_{yc}} - \left(\frac{M_p}{M_{yc}} - 1\right)\left(\frac{\lambda - \lambda_{pw}}{\lambda_{rw} - \lambda_{pw}}\right)\right] \le \frac{M_p}{M_{yc}} \qquad \text{(5.4-5, }\textit{Spec.}\text{ Eq. F4-9b)}$$
$$= \left[\frac{2{,}130 \text{ kip-in.}}{2{,}120 \text{ kip-in.}} - \left(\frac{2{,}130 \text{ kip-in.}}{2{,}120 \text{ kip-in.}} - 1\right)\left(\frac{129 - 84.0}{131 - 84.0}\right)\right] \le \frac{2{,}130 \text{ kip-in.}}{2{,}120 \text{ kip-in.}}$$
$= 1.00 \le 1.00$, therefore $R_{pc} = 1.00$

$R_{pg} = 1.0$ because the web is noncompact at this location.

At the top, the web is slender; therefore,

$$R_{pc} = 1.00 \le \frac{M_p}{M_{yc}}$$

$$1.00 \le \frac{3{,}090 \text{ kip-in.}}{2{,}980 \text{ kip-in.}} = 1.04, \text{ therefore } R_{pc} = 1.00$$

$$R_{pg} = 1 - \frac{a_w}{1{,}200 + 300a_w}\left(\frac{h_c}{t_w} - 5.7\sqrt{\frac{E}{F_y}}\right) \le 1.0 \qquad \text{(5.4-6, }\textit{Spec.}\text{ Eq. F5-6)}$$

where

$$a_w = \frac{h_c t_w}{b_{fc} t_{fc}} \le 10.0 \qquad (5.4\text{-}7)$$

$$= \frac{21.8\,\text{in.}(0.125\,\text{in.})}{6.00\,\text{in.}(5/16\,\text{in.})} = 1.45 \le 10.0, \text{ therefore use } a_w = 1.45$$

Therefore,

$$R_{pg} = 1 - \frac{a_w}{1{,}200 + 300a_w}\left(\frac{h_c}{t_w} - 5.7\sqrt{\frac{E}{F_y}}\right) \le 1.0 \qquad (5.4\text{-}6, \textit{Spec.}\ \text{Eq. F5-6})$$

$$= 1 - \frac{1.45}{1{,}200 + 300(1.45)}\left(\frac{21.8\,\text{in.}}{0.125\,\text{in.}} - 5.7\sqrt{\frac{29{,}000\,\text{ksi}}{55\,\text{ksi}}}\right)$$

$$= 0.961$$

Using the provisions of Section 5.4.3 for members with a single linear taper and no plate changes, determine the nominal flexural strength, M_n, of the member for the limit state of lateral-torsional buckling.

First, using AISC *Specification* Section F4, determine the elastic lateral-torsional buckling stress, F_{eLTB}, with $C_b = 1$ for the location of maximum flexural stress using properties at the middle of the unbraced length.

$$\left(F_{eLTB}\right)_{C_b=1} = \frac{1.0\pi^2 E}{\left(\frac{L_b}{r_t}\right)^2}\sqrt{1 + 0.078\frac{J}{S_{xc}h_o}\left(\frac{L_b}{r_t}\right)^2} \qquad (5.4\text{-}10, \textit{Spec.}\ \text{Eq. F4-5})$$

where

$h_o = 18.0\ \text{in.} + 0.5(5/16\ \text{in.} + 7/32\ \text{in.})$

$= 18.3\ \text{in.}$

$h_c = 16.1$ in. from previous calculation

$$a_w = \frac{h_c t_w}{b_{fc} t_{fc}} \qquad (5.4\text{-}7)$$

$$= \frac{16.1\,\text{in.}(0.125\,\text{in.})}{6.00\,\text{in.}(5/16\,\text{in.})}$$

$$= 1.07$$

$$r_t = \frac{b_{fc}}{\sqrt{12\left(\frac{h_o}{d} + \frac{1}{6}a_w\frac{h^2}{h_o d}\right)}} \qquad (5.4\text{-}11)$$

$$= \frac{6.00\,\text{in.}}{\sqrt{12\left(\frac{18.3\,\text{in.}}{18.5\,\text{in.}} + \frac{1}{6}(1.07)\frac{(18.0\,\text{in.})^2}{18.3\,\text{in.}(18.5\,\text{in.})}\right)}}$$

$$= 1.61\,\text{in.}$$

$S_{xc} = 38.6\,\text{in.}^3$ from Table 5-4

$J = 0$, because the web is slender over some portion of this unbraced length.

Therefore,

$$\left(F_{eLTB}\right)_{C_b=1} = \frac{1.0\pi^2 E}{\left(\frac{L_b}{r_t}\right)^2}\sqrt{1 + 0.078\frac{J}{S_{xc}h_o}\left(\frac{L_b}{r_t}\right)^2} \qquad (5.4\text{-}10, \textit{Spec.}\ \text{Eq. F4-5})$$

$$= \frac{1.0\pi^2(29{,}000\,\text{ksi})}{\left(\frac{144\,\text{in.}}{1.61\,\text{in.}}\right)^2}\sqrt{1+0.078\frac{0\,\text{in.}^4}{38.6\,\text{in.}^3\,(18.3\,\text{in.})}\left(\frac{144\,\text{in.}}{1.61\,\text{in.}}\right)^2}$$

$$= \frac{1.0\pi^2(29{,}000\,\text{ksi})}{\left(\frac{144\,\text{in.}}{1.61\,\text{in.}}\right)^2}$$

$$= 35.8\,\text{ksi}$$

Find location of maximum flexural compression stress.

For the case of a linear web taper and a linear moment taper to zero at the small end (small *P*-δ effects), the maximum flexural stress will always occur at the deep end (top).

LRFD	ASD
$f_{rmax} = \frac{M_r}{S_{xc}}$ $= \frac{1{,}800\,\text{kip-in.}}{54.2\,\text{in.}^3}$ $= 33.2\,\text{ksi}$	$f_{rmax} = \frac{M_r}{S_{xc}}$ $= \frac{1{,}200\,\text{kip-in.}}{54.2\,\text{in.}^3}$ $= 22.1\,\text{ksi}$

Calculate the elastic buckling multiplier, $(\gamma_{eLTB})_{C_b=1}$, with $C_b = 1$:

LRFD	ASD
$(\gamma_{eLTB})_{C_b=1} = \frac{(F_{eLTB})_{C_b=1}}{f_{rmax}}$ $= \frac{35.8\,\text{ksi}}{33.2\,\text{ksi}}$ $= 1.08$	$(\gamma_{eLTB})_{C_b=1} = \frac{(F_{eLTB})_{C_b=1}}{f_{rmax}}$ $= \frac{35.8\,\text{ksi}}{22.1\,\text{ksi}}$ $= 1.62$

Check LTB strength at top of unbraced length.

Calculate the nominal flexural strength due to the limit state of lateral-torsional buckling at the top of the unbraced length. Select the equation for calculation of the nominal flexural strength, M_n, based on the following ratio, where $f_r = f_{rmax}$:

LRFD	ASD
$\frac{(\gamma_{eLTB})_{C_b=1} f_r}{F_y} = \frac{1.08(33.2\,\text{ksi})}{55\,\text{ksi}}$ $= 0.652$	$\frac{(\gamma_{eLTB})_{C_b=1} f_r}{F_y} = \frac{1.62(22.1\,\text{ksi})}{55\,\text{ksi}}$ $= 0.651$

Note that the difference between LRFD and ASD is due to rounding. Use ASD value of 0.651.

When $S_{xt}/S_{xc} \geq 0.7$,

$$F_L = 0.7F_y \qquad \text{(5.4-14, } \textit{Spec.} \text{ Eq. F4-6a)}$$

and therefore,

$$\frac{F_L}{F_y} = 0.7$$

Because $\frac{(\gamma_{eLTB})_{C_b=1} f_r}{F_y} < \frac{F_L}{F_y}$ and the web is slender, use Equation 5.4-20.

$$M_n = C_b R_{pg} (\gamma_{eLTB})_{C_b=1} f_r S_{xc} \le R_{pg} M_{yc} \tag{5.4-20}$$

where C_b is determined using Section 5.4.1 and the moment diagram in Figure 5-9 is determined as follows:

LRFD	ASD
$f_0 = 0.0\,\text{ksi}$	$f_0 = 0.0\,\text{ksi}$
$f_{mid} = \frac{M_r}{S_{xc}} = \frac{900\text{ kip-in.}}{38.6\text{ in.}^3} = 23.3\text{ ksi}$	$f_{mid} = \frac{M_r}{S_{xc}} = \frac{600\text{ kip-in.}}{38.6\text{ in.}^3} = 15.5\text{ ksi}$
$f_2 = \frac{M_r}{S_{xc}} = \frac{1{,}800\,\text{kip-in.}}{54.2\text{ in.}^3} = 33.2\text{ ksi}$	$f_2 = \frac{M_r}{S_{xc}} = \frac{1{,}200\,\text{kip-in.}}{54.2\text{ in.}^3} = 22.1\text{ ksi}$
Because $\lvert 23.3\,\text{ksi}\rvert > \left\lvert \frac{0\text{ ksi} + 33.2\text{ ksi}}{2} \right\rvert$	Because $\lvert 15.5\,\text{ksi}\rvert > \left\lvert \frac{0\text{ ksi} + 22.1\text{ ksi}}{2} \right\rvert$
$f_1 = 2f_{mid} - f_2 = 2(23.3\,\text{ksi}) - 33.2\,\text{ksi} = 13.4\text{ ksi}$ (5.4-2)	$f_1 = 2f_{mid} - f_2 = 2(15.5\,\text{ksi}) - 22.1\,\text{ksi} = 8.90\text{ ksi}$ (5.4-2)
$C_b = 1.75 - 1.05\frac{f_1}{f_2} + 0.3\left(\frac{f_1}{f_2}\right)^2 \le 2.3$ (5.4-1)	$C_b = 1.75 - 1.05\frac{f_1}{f_2} + 0.3\left(\frac{f_1}{f_2}\right)^2 \le 2.3$ (5.4-1)
$= 1.75 - 1.05\left(\frac{13.4\,\text{ksi}}{33.2\,\text{ksi}}\right) + 0.3\left(\frac{13.4\,\text{ksi}}{33.2\,\text{ksi}}\right)^2$	$= 1.75 - 1.05\left(\frac{8.90\,\text{ksi}}{22.1\,\text{ksi}}\right) + 0.3\left(\frac{8.90\,\text{ksi}}{22.1\,\text{ksi}}\right)^2$
$= 1.38 < 2.3$	$= 1.38 < 2.3$

Therefore, the nominal flexural strength for the limit state of lateral-torsional buckling at the top of the member is,

LRFD	ASD
$M_n = C_b R_{pg} (\gamma_{eLTB})_{C_b=1} f_r S_{xc} \le R_{pg} M_{yc}$	$M_n = C_b R_{pg} (\gamma_{eLTB})_{C_b=1} f_r S_{xc} \le R_{pg} M_{yc}$
$= 1.38(0.961)(1.08)(33.2\,\text{ksi})(54.2\,\text{in.}^3)$	$= 1.38(0.961)(1.62)(22.1\,\text{ksi})(54.2\,\text{in.}^3)$
$\le 0.961(2{,}980\,\text{kip-in.})$	$\le 0.961(2{,}980\,\text{kip-in.})$
$= 2{,}580\,\text{kip-in.} \le 2{,}860\,\text{kip-in.}$	$= 2{,}570\,\text{kip-in.} \le 2{,}860\,\text{kip-in.}$
Use $M_n = 2{,}580\,\text{kip-in.}$	Use $M_n = 2{,}570\,\text{kip-in.}$

Check the strength ratio at the top of the member.

LRFD	ASD
$\frac{M_r}{M_c} = \frac{M_r}{\phi_b M_n}$ $= \frac{1{,}800\,\text{kip-in.}}{0.90\left(2{,}580\,\text{kip-in.}\right)}$ $= 0.775$	$\frac{M_r}{M_c} = \frac{\Omega_b M_r}{M_n}$ $= \frac{1.67\left(1{,}200\,\text{kip-in.}\right)}{2{,}570\,\text{kip-in.}}$ $= 0.780$

Check the lateral-torsional buckling strength at the middle of the unbraced length. The flexural stress at this location is,

LRFD	ASD
$f_r = \frac{M_r}{S_{xc}}$ $= \frac{900\,\text{kip-in.}}{38.6\,\text{in.}^3}$ $= 23.3\ \text{ksi}$	$f_r = \frac{M_r}{S_{xc}}$ $= \frac{600\,\text{kip-in.}}{38.6\,\text{in.}^3}$ $= 15.5\ \text{ksi}$

Select the equation for calculation of the nominal flexural strength, M_n, based on the following ratio:

LRFD	ASD
$\frac{\left(\gamma_{eLTB}\right)_{C_b=1} f_r}{F_y} = \frac{1.08\left(23.3\,\text{ksi}\right)}{55\,\text{ksi}}$ $= 0.458$	$\frac{\left(\gamma_{eLTB}\right)_{C_b=1} f_r}{F_y} = \frac{1.62\left(15.5\,\text{ksi}\right)}{55\,\text{ksi}}$ $= 0.457$

Note that the difference between LRFD and ASD is due to rounding. Use ASD value of 0.457.

Because $\frac{\left(\gamma_{eLTB}\right)_{C_b=1} f_r}{F_y} \le \frac{F_L}{F_y}$, and the member has a slender web, use Equation 5.4-21. The nominal flexural strength for the limit state of lateral-torsional buckling at the middle of the unbraced length is,

$$M_n = C_b \left(\gamma_{eLTB}\right)_{C_b=1} f_r S_{xc} \le R_{pc} M_{yc} \tag{5.4-21}$$

where

C_b = 1.38 (calculated previously)
$(\gamma_{eLTB})_{c_b=1}$ = 1.08 for LRFD; 1.62 for ASD (calculated previously)
f_r = 23.3 ksi for LRFD; 15.5 ksi for ASD (calculated previously)
S_{xc} = 38.6 in.^{3} from Table 5-4
R_{pc} = 1.0 (determined previously)
M_{yc} = 2,120 kip-in. from Table 5-4

Therefore:

LRFD	ASD
$M_n = C_b\left(\gamma_{eLTB}\right)_{C_b=1} f_r S_{xc} \le R_{pc} M_{yc}$ $= 1.38(1.08)(23.3 \text{ ksi})(38.6 \text{ in.}^3) \le 1.00(2{,}120 \text{ kip-in.})$ $= 1{,}340 \text{ kip-in.} \le 2{,}120 \text{ kip-in.}$ Use $M_n = 1{,}340$ kip-in.	$M_n = C_b\left(\gamma_{eLTB}\right)_{C_b=1} f_r S_{xc} \le R_{pc} M_{yc}$ $= 1.38(1.62)(15.5 \text{ ksi})(38.6 \text{ in.}^3) \le 1.00(2{,}120 \text{ kip-in.})$ $= 1{,}340 \text{ kip-in.} \le 2{,}120 \text{ kip-in.}$ Use $M_n = 1{,}340$ kip-in.

Check the strength ratio at the middle of the unbraced length.

LRFD	ASD
$\frac{M_r}{M_c} = \frac{M_r}{\phi_b M_n}$ $= \frac{900 \text{ kip-in.}}{0.90(1{,}340 \text{ kip-in.})}$ $= 0.746$	$\frac{M_r}{M_c} = \frac{\Omega_b M_r}{M_n}$ $= \frac{1.67(600 \text{ kip-in.})}{1{,}340 \text{ kip-in.}}$ $= 0.748$

The lateral-torsional buckling strength is controlled by the top of the unbraced length because the strength ratio is greater at the top.

Check the following local limit states at the middle and top of the unbraced length: tension flange yielding, compression flange local buckling, and tension flange rupture at the bolt holes.

Tension Flange Yielding

According to AISC *Specification* Section F4.4 and Section 5.4 of this Design Guide, when $S_{xt} < S_{xc}$, the nominal flexural strength for the limit state of tension flange yielding is determined as follows:

$$M_n = R_{pt} M_{yt} \qquad (\textit{Spec.}\text{ Eq. F4-14})$$

$$= R_{pt} F_y S_{xt} \qquad (5.4\text{-}25)$$

where

$S_{xt} = 31.7$ in.^{3} from Table 5-4

At the middle of the unbraced length, the web plastification factor, R_{pt}, is dependent on the following slenderness parameters:

$$\lambda = \frac{h_c}{t_w}$$

$$= 129$$

$$\lambda_{pw} = 84.0$$

$$\lambda_{rw} = 131$$

Because $\lambda_{pw} < \frac{h_c}{t_w} \le \lambda_{rw}$, use Equation 5.4-27.

$$R_{pt} = \left[\frac{M_p}{M_{yt}} - \left(\frac{M_p}{M_{yt}} - 1\right)\left(\frac{\lambda - \lambda_{pw}}{\lambda_{rw} - \lambda_{pw}}\right)\right] \le \frac{M_p}{M_{yt}} \qquad (5.4\text{-}27)$$

$$= \left[\frac{2{,}130 \text{ kip-in.}}{1{,}740 \text{ kip-in.}} - \left(\frac{2{,}130 \text{ kip-in.}}{1{,}740 \text{ kip-in.}} - 1\right)\left(\frac{129 - 84.0}{131 - 84.0}\right)\right] \le \frac{2{,}130 \text{ kip-in.}}{1{,}740 \text{ kip-in.}}$$

$= 1.01 \le 1.22$; therefore, use 1.01

Therefore,

$$M_n = R_{pt} F_y S_{xt} \quad (5.4\text{-}25)$$
$$= 1.01(55 \text{ ksi})(31.7 \text{ in.}^3)$$
$$= 1{,}760 \text{ kip-in.}$$

Determine the nominal flexural strength at the top of the unbraced length. The web plastification factor, R_{pt}, is dependent on the following slenderness parameters:

$$\frac{h_c}{t_w} = 174 \text{ (calculated previously)}$$
$$\lambda_{rw} = 131$$

From Section 5.4.5, for $\frac{h_c}{t_w} > \lambda_{rw}$,

$$R_{pt} = 1.0$$

and from Table 5-4, at the top,

$$S_{xt} = 45.5 \text{ in.}^3$$

Therefore,

$$M_n = R_{pt} F_y S_{xt} \quad (5.4\text{-}25)$$
$$= 1.0(55 \text{ ksi})(45.5 \text{ in.}^3)$$
$$= 2{,}500 \text{ kip-in.}$$

Compression Flange Local Buckling

Determine the nominal flexural strength, M_n, at the middle of the unbraced length using the limit state of compression flange local buckling. The selection of the appropriate equation is dependent on the flange compactness.

$$\frac{b_f}{2t_f} = \frac{6.00 \text{ in.}}{2(5/16 \text{ in.})}$$
$$= 9.60$$

From Table B4.1 of the AISC *Specification* for flexure in flanges of singly symmetric I-shaped sections,

$$\lambda_{pf} = 0.38\sqrt{\frac{E}{F_y}} \quad \text{compact flange limit}$$
$$= 0.38\sqrt{\frac{29{,}000 \text{ ksi}}{55 \text{ ksi}}}$$
$$= 8.73$$
$$\lambda_{rf} = 0.95\sqrt{\frac{k_c E}{F_L}} \quad \text{slender flange limit}$$

where

$$k_c = \frac{4}{\sqrt{\frac{h}{t_w}}} \quad (5.4\text{-}24)$$
$$= \frac{4}{\sqrt{\frac{18.0 \text{ in.}}{0.125 \text{ in.}}}}$$
$$= 0.333 < 0.35; \text{ therefore use } 0.35$$
$$F_L = 38.5 \text{ ksi (calculated previously)}$$

Therefore,

$$\lambda_{rf} = 0.95\sqrt{\frac{k_c E}{F_L}}$$
$$= 0.95\sqrt{\frac{0.35(29{,}000\ \text{ksi})}{38.5\,\text{ksi}}}$$
$$= 15.4$$

Because 8.73 < 9.58 < 15.4, the compression flange is noncompact; therefore, use Equation 5.4-22. The nominal flexural strength for the limit state of compression flange local buckling at the middle of the unbraced length is,

$$M_n = R_{pg}\left[R_{pc}M_{yc} - \left(R_{pc}M_{yc} - F_L S_{xc}\right)\left(\frac{\frac{b_f}{2t_f} - 0.38\sqrt{\frac{E}{F_y}}}{0.95\sqrt{\frac{k_c E}{F_L}} - 0.38\sqrt{\frac{E}{F_y}}}\right)\right] \quad (5.4\text{-}22)$$
$$= 1.0\left\{1.00\left(2{,}120\,\text{kip-in.}\right) - \left[1.00\left(2{,}120\,\text{kip-in.}\right) - 38.5\,\text{ksi}\left(38.6\,\text{in.}^3\right)\right]\left(\frac{9.60 - 8.73}{15.4 - 8.73}\right)\right\}$$
$$= 2{,}040\,\text{kip-in.}$$

Determine the nominal flexural strength for the limit state of compression flange local buckling at the top of the unbraced length. The selection of the appropriate equation is dependent on the compression flange compactness.

$$\frac{b_f}{2t_f} = \frac{6.00\,\text{in.}}{2\left(5/16\,\text{in.}\right)}$$
$$= 9.60$$
$$\lambda_{pf} = 8.73 \text{ compact flange limit (previously calculated)}$$
$$k_c = \frac{4}{\sqrt{\frac{h}{t_w}}}$$
$$= \frac{4}{\sqrt{\frac{24.0\,\text{in.}}{0.125\,\text{in.}}}} \quad (5.4\text{-}24)$$
$$= 0.289 < 0.35; \text{therefore, use } 0.35$$
$$\lambda_{rf} = 0.95\sqrt{\frac{k_c E}{F_L}} \text{ slender flange limit}$$
$$= 0.95\sqrt{\frac{0.35\left(29{,}000\,\text{ksi}\right)}{38.5\,\text{ksi}}}$$
$$= 15.4$$

Because 8.73 < 9.60 < 15.4, the compression flange is noncompact; therefore, use Equation 5.4-22. The nominal flexural strength for the limit state of compression flange local buckling at the top of the unbraced length is,

$$M_n = R_{pg}\left[R_{pc}M_{yc} - \left(R_{pc}M_{yc} - F_L S_{xc}\right)\left(\frac{\frac{b_f}{2t_f} - 0.38\sqrt{\frac{E}{F_y}}}{0.95\sqrt{\frac{k_c E}{F_L}} - 0.38\sqrt{\frac{E}{F_y}}}\right)\right] \quad (5.4\text{-}22)$$

where

F_L = 38.5 ksi
M_{yc} = 2,980 kip-in. from Table 5-4
R_{pg} = 0.961 (previously calculated)
R_{pc} = 1.0 (previously determined)
S_{xc} = 54.2 in.^{3} from Table 5-4

$$M_n = R_{pg}\left[R_{pc}M_{yc} - \left(R_{pc}M_{yc} - F_L S_{xc}\right)\left(\frac{\frac{b_f}{2t_f} - 0.38\sqrt{\frac{E}{F_y}}}{0.95\sqrt{\frac{k_c E}{F_L}} - 0.38\sqrt{\frac{E}{F_y}}}\right)\right] \tag{5.4-22}$$

$$= 0.961\left\{1.0\left(2{,}980\,\text{kip-in.}\right) - \left[1.0\left(2{,}980\,\text{kip-in.}\right) - 38.5\,\text{ksi}\left(54.2\,\text{in.}^3\right)\right]\left(\frac{9.60 - 8.73}{15.4 - 8.73}\right)\right\}$$

$$= 2{,}750\,\text{kip-in.}$$

Tension Flange Rupture

Determine the nominal flexural strength for the limit state of tensile rupture of the tension flange due to the bolt holes at the girt location.

From AISC *Specification* Section F13.1, if $F_u A_{fn} < Y_t F_y A_{fg}$, then the tension flange rupture limit state applies,

where

Y_t = 1.0 for $F_y/F_u \le 0.8$

$$\frac{F_y}{F_u} = \frac{55\,\text{ksi}}{70\,\text{ksi}}$$

$$= 0.786 < 0.8;\ \text{therefore}\ Y_t = 1.0$$

$$A_{fg} = 6.00\,\text{in.}\left(\tfrac{7}{32}\,\text{in.}\right)$$

$$= 1.31\ \text{in.}^2$$

$$A_{fn} = 1.31\ \text{in.} - \tfrac{7}{32}\,\text{in.}\left(2\right)\left(1\tfrac{1}{16}\,\text{in.} + \tfrac{1}{16}\,\text{in.}\right)$$

$$= 0.982\ \text{in.}^2$$

Thus,

$$70\ \text{ksi}\left(0.982\ \text{in.}^2\right) < 1.0\left(55\ \text{ksi}\right)\left(1.31\ \text{in.}^2\right)$$

68.7 kips < 72.1 kips; therefore, the tension flange rupture limit state applies

The nominal flexural strength, M_n, at the holes in the tension flange is,

$$M_n = \frac{F_u A_{fn}}{A_{fg}} S_x \tag{*Spec.* Eq. F13-1}$$

where

S_{xt} = 35.0 in.^{3} at the girt, from Table 5-3

Therefore,

$$M_n = \frac{70\,\text{ksi}\left(0.982\,\text{in.}^2\right)}{1.31\,\text{in.}^2}35.0\,\text{in.}^3$$

$$= 1{,}840\,\text{kip-in.}$$

Maximum flexural strength ratios

For a summary of strength ratios to be used in combined strength checks in Example 5.8, see below.

Summary of Flexural Strengths	
Lateral-Torsional Buckling Value at Top of Unbraced Length Governs	
LRFD	ASD
$\frac{M_r}{M_c} = \frac{M_r}{\phi_b M_n}$ $= \frac{1{,}800\,\text{kip-in.}}{0.90\left(2{,}580\,\text{kip-in.}\right)}$ $= 0.775$	$\frac{M_r}{M_c} = \frac{\Omega_b M_r}{M_n}$ $= \frac{1.67\left(1{,}200\,\text{kip-in.}\right)}{2{,}570\,\text{kip-in.}}$ $= 0.780$
Tension Flange Local Yielding at Top	
LRFD	ASD
$\frac{M_r}{M_c} = \frac{1{,}800\,\text{kip-in.}}{0.90\left(2{,}500\,\text{kip-in.}\right)}$ $= 0.800$	$\frac{M_r}{M_c} = \frac{1.67\left(1{,}200\,\text{kip-in.}\right)}{2{,}500\,\text{kip-in.}}$ $= 0.802$
Tension Flange Rupture at Girt	
LRFD	ASD
$\frac{M_r}{M_c} = \frac{1{,}120\,\text{kip-in.}}{0.90\left(1{,}840\,\text{kip-in.}\right)}$ $= 0.676$	$\frac{M_r}{M_c} = \frac{1.67\left(750\,\text{kip-in.}\right)}{1{,}840\,\text{kip-in.}}$ $= 0.681$
Lateral-Torsional Buckling at Mid-Length	
LRFD	ASD
$\frac{M_r}{M_c} = \frac{900\,\text{kip-in.}}{0.90\left(1{,}340\,\text{kip-in.}\right)}$ $= 0.746$	$\frac{M_r}{M_c} = \frac{1.67\left(600\,\text{kip-in.}\right)}{1{,}340\,\text{kip-in.}}$ $= 0.748$
Tension Flange Yielding at Mid-Length	
LRFD	ASD
$\frac{M_r}{M_c} = \frac{900\,\text{kip-in.}}{0.90\left(1{,}760\,\text{kip-in.}\right)}$ $= 0.568$	$\frac{M_r}{M_c} = \frac{1.67\left(600\,\text{kip-in.}\right)}{1{,}760\,\text{kip-in.}}$ $= 0.569$

Tension flange yielding governs.

Example 5.8—Combined Axial Compression and Flexure

Given:

Check the strength of the member used in Examples 5.6 and 5.7 for combined axial compression and flexure, using the required and available strengths from those examples.

Evaluate using AISC Specification Section H1.1, H1.3 (if permitted), and H2.

Axial strength ratios from Example 5.6:

In-Plane Flexural Buckling	
LRFD	ASD
$\frac{P_r}{P_c} = \frac{P_r}{\phi_c P_n}$ $= \frac{11.3\,\text{kips}}{0.90(200\,\text{kips})}$ $= 0.0628$	$\frac{P_r}{P_c} = \frac{\Omega_c P_r}{P_n}$ $= \frac{1.67(7.50\,\text{kips})}{200\,\text{kips}}$ $= 0.0626$
Out-of-Plane Constrained-Axis Torsional Buckling	
LRFD	ASD
$\frac{P_r}{P_c} = \frac{11.3\,\text{kips}}{0.90(122\,\text{kips})}$ $= 0.103$	$\frac{P_r}{P_c} = \frac{1.67(7.50\,\text{kips})}{122\,\text{kips}}$ $= 0.103$

Flexural strength ratios from Example 5.7:

Lateral-Torsional Buckling at Top	
LRFD	ASD
$\frac{M_r}{M_c} = \frac{M_r}{\phi_b M_n}$ $= \frac{1{,}800\,\text{kip-in.}}{0.90(2{,}580\,\text{kip-in.})}$ $= 0.775$	$\frac{M_r}{M_c} = \frac{\Omega_b M_r}{M_n}$ $= \frac{1.67(1{,}200\,\text{kip-in.})}{2{,}570\,\text{kip-in.}}$ $= 0.780$
Tension Flange Local Yielding at Top	
LRFD	ASD
$\frac{M_r}{M_c} = \frac{1{,}800\,\text{kip-in.}}{0.90(2{,}500\,\text{kip-in.})}$ $= 0.800$	$\frac{M_r}{M_c} = \frac{1.67(1{,}200\,\text{kip-in.})}{2{,}500\,\text{kip-in.}}$ $= 0.802$
Tension Flange Rupture at Girt	
LRFD	ASD
$\frac{M_r}{M_c} = \frac{1{,}120\,\text{kip-in.}}{0.90(1{,}840\,\text{kip-in.})}$ $= 0.676$	$\frac{M_r}{M_c} = \frac{1.67(750\,\text{kip-in.})}{1{,}840\,\text{kip-in.}}$ $= 0.681$
Lateral-Torsional Buckling at Mid-Length	
LRFD	ASD
$\frac{M_r}{M_c} = \frac{900\,\text{kip-in.}}{0.90(1{,}340\,\text{kip-in.})}$ $= 0.746$	$\frac{M_r}{M_c} = \frac{1.67(600\,\text{kip-in.})}{1{,}340\,\text{kip-in.}}$ $= 0.748$
Tension Flange Yielding at Mid-Length	
LRFD	ASD
$\frac{M_r}{M_c} = \frac{900\,\text{kip-in.}}{0.90(1{,}760\,\text{kip-in.})}$ $= 0.568$	$\frac{M_r}{M_c} = \frac{1.67(600\,\text{kip-in.})}{1{,}760\,\text{kip-in.}}$ $= 0.569$

Solution A:

Use AISC *Specification* Section H1.1, and the worst case in-plane and out-of-plane ratios for axial and flexure when checking the unbraced length.

Out-of-plane constrained-axis torsional buckling controls axial strength.

$\frac{P_r}{P_c} = 0.103 < 0.2$; therefore, use Equation 5.5-1b.

$$\frac{P_r}{2P_c} + \left(\frac{M_{rx}}{M_{cx}} + \frac{M_{ry}}{M_{cy}} \right) \le 1.0 \qquad \text{(5.5-1b, } \textit{Spec.} \text{ Eq. H1-1b)}$$

Tension flange yielding at the top of the unbraced length controls flexural strength.

LRFD	ASD
$\frac{0.103}{2} + (0.800 + 0) = 0.852$	$\frac{0.103}{2} + (0.802 + 0) = 0.854$

Tension Flange Rupture

From Example 5.7, $F_u A_{fn} < Y_t F_y A_g$; therefore, check tension flange rupture.

Check bolt holes at girt.
Calculate axial tensile strength.

$$\begin{aligned} A_g &= 6.00\,\text{in.}(0.313\,\text{in.} + 0.219\,\text{in.}) + 19.5\,\text{in.}(0.125\,\text{in.}) \\ &= 5.63\,\text{in.} \\ A_e &= A_n U \\ &= \left[A_g - 4(d_h + \tfrac{1}{16}) t_f \right] 1.0 \\ &= \left[5.63\,\text{in.}^2 - 2(1\tfrac{1}{16}\,\text{in.} + \tfrac{1}{16}\,\text{in.})\,0.219\,\text{in.} \right] 1.0 \\ &= 5.30\,\text{in.}^2 \end{aligned}$$

LRFD	ASD
$P_c = \phi_t F_u A_e$ $= 0.75(70\,\text{ksi})(5.30\,\text{in.}^2)$ $= 278$ kips	$P_c = \frac{F_u A_e}{\Omega_t}$ $= \frac{70\,\text{ksi}(5.30\,\text{in.}^2)}{2.00}$ $= 186$ kips

$$M_{nx} = \frac{F_u A_{fn}}{A_{fg}} S_{xt} \qquad \text{(5.5-3)}$$
$$= 1{,}840 \text{ kip-in.}$$

LRFD	ASD
$M_{cx} = \phi_b M_{nx}$ (5.5-3) $= 0.90(1{,}840 \text{ kip-in.})$ $= 1{,}660 \text{ kip-in.}$	$M_{cx} = \frac{M_{nx}}{\Omega_b}$ (5.5-3) $= \frac{1{,}840 \text{ kip-in.}}{1.67}$ $= 1{,}100 \text{ kip-in.}$
On the flange in flexural tension: $\frac{P_r}{P_c} + \frac{M_{rx}}{M_{cx}} \le 1.0$ (5.5-2) $\frac{-11.3 \text{ kips}}{278 \text{ kips}} + \frac{1{,}120 \text{ kip-in.}}{1{,}660 \text{ kip-in.}} = 0.634$	On the flange in flexural tension: $\frac{P_r}{P_c} + \frac{M_{rx}}{M_{cx}} \le 1.0$ (5.5-2) $\frac{-7.50 \text{ kips}}{186 \text{ kips}} + \frac{750 \text{ kip-in.}}{1{,}100 \text{ kip-in.}} = 0.641$

Solution B:

As discussed in Section 5.5.2, it is not recommended that AISC *Specification* Section H1.3 be applied to members other than doubly symmetric compact sections.

Solution C:

Using AISC Specification Section H2, select locations to check and use required and available stresses calculated from section properties at those locations.

Check at bottom of unbraced length.

$h = 12.0$ in., $A_g = 4.69$ in.^{2}
Axial strength is governed by out-of-plane constrained torsional buckling.

LRFD	ASD
$f_{ra} = \frac{P_r}{A_g}$ $= \frac{11.3 \text{ kips}}{4.69 \text{ in.}^2}$ $= 2.41 \text{ ksi}$ $F_{ca} = \frac{\phi_c P_n}{A_g}$ $= \frac{0.90(122 \text{ kips})}{4.69 \text{ in.}^2}$ $= 23.4 \text{ ksi}$ $\left\lvert \frac{f_{ra}}{F_{ca}} + \frac{f_{rbx}}{F_{cbx}} + \frac{f_{rby}}{F_{cby}} \right\rvert \le 1.0$ (5.5-5) Because there is no flexural stress at the bottom $\left\lvert \frac{2.41 \text{ ksi}}{23.4 \text{ ksi}} + 0 + 0 \right\rvert = 0.103$	$f_{ra} = \frac{P_r}{A_g}$ $= \frac{7.50 \text{ kips}}{4.69 \text{ in.}^2}$ $= 1.60 \text{ ksi}$ $F_{ca} = \frac{P_n}{\Omega_c A_g}$ $= \frac{122 \text{ kips}}{1.67(4.69 \text{ in.}^2)}$ $= 15.6 \text{ ksi}$ $\left\lvert \frac{f_{ra}}{F_{ca}} + \frac{f_{rbx}}{F_{cbx}} + \frac{f_{rby}}{F_{cby}} \right\rvert \le 1.0$ (5.5-5) Because there is no flexural stress at the bottom $\left\lvert \frac{1.60 \text{ ksi}}{15.6 \text{ ksi}} + 0 + 0 \right\rvert = 0.103$

Check at middle of unbraced length.
$h = 18.0$ in., $A_g = 5.44$ in.^{2}, $S_{xc} = 38.6$ in.^{3}, $S_{xt} = 31.7$ in.^{3}

Check flange in flexural compression.

Axial strength is governed by constrained torsional buckling. Flexural strength is governed by lateral-torsional buckling.

LRFD	ASD
$f_{ra} = \frac{P_r}{A_g}$ $= \frac{11.3\,\text{kips}}{5.44\,\text{in.}^2}$ $= 2.08\,\text{ksi}$ $F_{ca} = \frac{\phi_c P_n}{A_g}$ $= \frac{0.90(122\,\text{kips})}{5.44\,\text{in.}^2}$ $= 20.2\,\text{ksi}$ $f_{rbx} = \frac{M_{rx}}{S_x}$ $= \frac{900\,\text{kip-in.}}{38.6\,\text{in.}^3}$ $= 23.3\,\text{ksi}$ $F_{cbx} = \frac{\phi_c M_{nx}}{S_x}$ $= \frac{0.90(1{,}340\,\text{kip-in.})}{38.6\,\text{in.}^3}$ $= 31.2\,\text{ksi}$ $\left\lvert \frac{2.08\,\text{ksi}}{20.2\,\text{ksi}} + \frac{23.3\,\text{ksi}}{31.2\,\text{ksi}} + 0 \right\rvert = 0.850$	$f_{ra} = \frac{P_r}{A_g}$ $= \frac{7.50\,\text{kips}}{5.44\,\text{in.}^2}$ $= 1.38\,\text{ksi}$ $F_{ca} = \frac{P_n}{\Omega_c A_g}$ $= \frac{122\,\text{kips}}{1.67(5.44\,\text{in.}^2)}$ $= 13.4\,\text{ksi}$ $f_{rbx} = \frac{M_{rx}}{S_x}$ $= \frac{600\,\text{kip-in.}}{38.6\,\text{in.}^3}$ $= 15.5\,\text{ksi}$ $F_{cbx} = \frac{M_{nx}}{\Omega_b S_x}$ $= \frac{1{,}340\,\text{kip-in.}}{1.67(38.6\,\text{in.}^3)}$ $= 20.8\,\text{ksi}$ $\left\lvert \frac{1.38\,\text{ksi}}{13.4\,\text{ksi}} + \frac{15.5\,\text{ksi}}{20.8\,\text{ksi}} + 0 \right\rvert = 0.848$

Check flange in flexural tension.

Axial strength is governed by constrained torsional buckling (as earlier). Flexural strength is governed by tension flange yielding.

LRFD	ASD
$f_{rbx} = \frac{M_{rx}}{S_x}$ $= \frac{900\,\text{kip-in.}}{31.7\,\text{in.}^3}$ $= 28.4\,\text{ksi}$ $F_{cbx} = \frac{\phi_c M_{nx}}{S_x}$ $= \frac{0.90(1{,}760\,\text{kip-in.})}{31.7\,\text{in.}^3}$ $= 50.0\,\text{ksi}$ $\left\lvert \frac{2.08\,\text{ksi}}{20.2\,\text{ksi}} - \frac{28.4\,\text{ksi}}{50.0\,\text{ksi}} + 0 \right\rvert = 0.465$	$f_{rbx} = \frac{M_{rx}}{S_x}$ $= \frac{600\,\text{kip-in.}}{31.7\,\text{in.}^3}$ $= 18.9\,\text{ksi}$ $F_{cbx} = \frac{M_{nx}}{\Omega_b S_x}$ $= \frac{1{,}760\,\text{kip-in.}}{1.67(31.7\,\text{in.}^3)}$ $= 33.2\,\text{ksi}$ $\left\lvert \frac{1.38\,\text{ksi}}{13.4\,\text{ksi}} - \frac{18.9\,\text{ksi}}{33.2\,\text{ksi}} + 0 \right\rvert = 0.466$

Check at top of unbraced length.
$h = 24.0$ in., $A_g = 6.19$ in.^{2}, $S_{xc} = 54.2$ in.^{3}, $S_{xt} = 45.5$ in.^{3}

Check flange in flexural compression.

Axial strength is governed by constrained torsional buckling. Flexural strength is governed by lateral-torsional buckling.

LRFD	ASD
$f_{ra} = \frac{P_r}{A_g}$ $= \frac{11.3\,\text{kips}}{6.19\,\text{in.}^2}$ $= 1.83\,\text{ksi}$ $F_{ca} = \frac{\phi_c P_n}{A_g}$ $= \frac{0.90\left(122\,\text{kips}\right)}{6.19\,\text{in.}^2}$ $= 17.7\,\text{ksi}$ $f_{rbx} = \frac{M_{rx}}{S_x}$ $= \frac{1{,}800\,\text{kip-in.}}{54.2\,\text{in.}^3}$ $= 33.2\,\text{ksi}$ $F_{cbx} = \frac{\phi_c M_{nx}}{S_x}$ $= \frac{0.90\left(2{,}580\,\text{kip-in.}\right)}{54.2\,\text{in.}^3}$ $= 42.8\,\text{ksi}$ $\left\lvert \frac{1.83\,\text{ksi}}{17.7\,\text{ksi}} + \frac{33.2\,\text{ksi}}{42.8\,\text{ksi}} + 0 \right\rvert = 0.879$	$f_{ra} = \frac{P_r}{A_g}$ $= \frac{7.50\,\text{kips}}{6.19\,\text{in.}^2}$ $= 1.21\,\text{ksi}$ $F_{ca} = \frac{P_n}{\Omega_c A_g}$ $= \frac{122\,\text{kips}}{1.67\left(6.19\,\text{in.}^2\right)}$ $= 11.8\,\text{ksi}$ $f_{rbx} = \frac{M_{rx}}{S_x}$ $= \frac{1{,}200\,\text{kip-in.}}{54.2\,\text{in.}^3}$ $= 22.1\,\text{ksi}$ $F_{cbx} = \frac{M_{nx}}{\Omega_b S_x}$ $= \frac{2{,}570\,\text{kip-in.}}{1.67\left(54.2\,\text{in.}^3\right)}$ $= 28.4\,\text{ksi}$ $\left\lvert \frac{1.21\,\text{ksi}}{11.8\,\text{ksi}} + \frac{22.1\,\text{ksi}}{28.4\,\text{ksi}} + 0 \right\rvert = 0.881$

Check flange in flexural tension.

Axial strength is governed by constrained torsional buckling (as determined previously). Flexural strength is governed by tension flange yielding.

LRFD	ASD
$f_{rbx} = \frac{M_{rx}}{S_x}$ $= \frac{1{,}800\,\text{kip-in.}}{45.5\,\text{in.}^3}$ $= 39.6\,\text{ksi}$ $F_{cbx} = \frac{\phi_c M_{nx}}{S_x}$ $= \frac{0.90\left(2{,}500\,\text{kip-in.}\right)}{45.5\,\text{in.}^3}$ $= 49.5\,\text{ksi}$ $\left\lvert \frac{1.83\,\text{ksi}}{17.7\,\text{ksi}} - \frac{39.6\,\text{ksi}}{49.5\,\text{ksi}} + 0 \right\rvert = 0.697$	$f_{rbx} = \frac{M_{rx}}{S_x}$ $= \frac{1{,}200\,\text{kip-in.}}{45.5\,\text{in.}^3}$ $= 26.4\,\text{ksi}$ $F_{cbx} = \frac{M_{nx}}{\Omega_b S_x}$ $= \frac{2{,}500\,\text{kip-in.}}{1.67\left(45.5\,\text{in.}^3\right)}$ $= 32.9\,\text{ksi}$ $\left\lvert \frac{1.21\,\text{ksi}}{11.8\,\text{ksi}} - \frac{26.4\,\text{ksi}}{32.9\,\text{ksi}} + 0 \right\rvert = 0.700$

Tension flange rupture.

Check the tension flange at the bolt holes using Equation 5.5-6.

$h = 19.5$ in., $A_g = 5.63$ in.^{2}, $S_{xt} = 35.0$ in.^{3}

LRFD	ASD
$f_{ra} = \dfrac{P_r}{A_g}$	$f_{ra} = \dfrac{P_r}{A_g}$
$= \dfrac{-11.3\,\text{kips}}{5.63\,\text{in.}^2}$	$= \dfrac{-7.50\,\text{kips}}{5.63\,\text{in.}^2}$
$= -2.01\,\text{ksi}$	$= -1.33\,\text{ksi}$
from above, $P_c = 278$ kips	from above, $P_c = 186$ kips
$F_{ca} = \dfrac{P_c}{A_g}$	$F_{ca} = \dfrac{P_c}{A_g}$
$= \dfrac{278\,\text{kips}}{5.63\,\text{in.}^2}$	$= \dfrac{186\,\text{kips}}{5.63\,\text{in.}^2}$
$= 49.4\,\text{ksi}$	$= 33.0\,\text{ksi}$
$f_{rbx} = \dfrac{M_{rx}}{S_x}$	$f_{rbx} = \dfrac{M_{rx}}{S_x}$
$= \dfrac{1{,}120\,\text{kip-in.}}{35.0\,\text{in.}^3}$	$= \dfrac{750\,\text{kip-in.}}{35.0\,\text{in.}^3}$
$= 32.0\,\text{ksi}$	$= 21.4\,\text{ksi}$
from above, $M_{cx} = 1{,}660$ kip-in.	from above, $M_{cx} = 1{,}100$ kip-in.
$F_{cbx} = \dfrac{M_{cx}}{S_x}$	$F_{cbx} = \dfrac{M_{cx}}{S_x}$
$= \dfrac{1{,}660\,\text{kip-in.}}{35.0\,\text{in.}^3}$	$= \dfrac{1{,}100\,\text{kip-in.}}{35.0\,\text{in.}^3}$
$= 47.4\,\text{ksi}$	$= 31.4\,\text{ksi}$
$\dfrac{f_{ra}}{F_{ca}} + \dfrac{f_{rbx}}{F_{cbx}} \le 1.0$ (5.5-6)	$\dfrac{f_{ra}}{F_{ca}} + \dfrac{f_{rbx}}{F_{cbx}} \le 1.0$ (5.5-6)
$\dfrac{-2.01\,\text{ksi}}{49.4\,\text{ksi}} + \dfrac{32.0\,\text{ksi}}{47.4\,\text{ksi}} = 0.634$	$\dfrac{-1.33\,\text{ksi}}{33.0\,\text{ksi}} + \dfrac{21.4\,\text{ksi}}{31.4\,\text{ksi}} = 0.641$

Chapter 6
Frame Design

The following sections present topics relevant to the design of frames that are partially or entirely composed of tapered members. The emphasis is on configurations common in the metal building industry but this information remains applicable to fabricated members that are similar.

Considerable freedom is given to designers regarding the means of structural analysis, and it is beyond the scope of this Guide to fully explore all of the possibilities. The following sections discuss many of the issues that affect the accuracy of first- and second-order analysis, but they do not prescribe a detailed procedure to be followed. Regardless of the analysis approach selected, the accuracy of the analysis technique should be confirmed by comparison with the results of benchmark problems such as those provided in Appendix C.

6.1 FIRST-ORDER ANALYSIS OF FRAMES

As a practical matter, the vast majority of frames with tapered members are analyzed using computer software rather than by manual techniques. Although prismatic members are accurately modeled with ordinary beam elements in modern direct stiffness computer software, tapered members must either be modeled with specialized tapered beam elements or subdivided into a larger number of shorter prismatic elements to accurately represent the behavior of the tapered member.

In a design production environment, frames with tapered members are usually analyzed using specialized software that incorporates an element type specifically developed to model tapered members. These elements typically make use of numerical integration techniques to provide good but approximate results for member stiffness coefficients and fixed-end forces. The accuracy of these elements varies and depends on the element formulation and the fineness with which the element is internally subdivided in the numerical integration. Examples with accurately calculated stiffness coefficients are provided in Appendix C for reference.

Alternatively, a tapered member may be modeled in a planar matrix analysis using a series of short prismatic elements, as shown in Figure 6-1, with properties representing the average properties of the tapered member within the length of each short element. The accuracy of such modeling improves with a finer subdivision of the tapered member and eventually converges to the behavior of the tapered member with a sufficiently refined number of segments.

Several additional computer modeling issues arise from the properties of tapered members with unequal flange sizes. The centroidal axis of such a member is not located at the mid-depth. This axis shift should be accounted for in the computer model. Furthermore, a tapered I-shaped member with unequal flange areas does not have a straight centroidal axis. The axis curves toward the heavier flange.

Figure 6-2 illustrates a typical case. With a taper angle of 15°, the curvature of the axis shown is equivalent to an out-of-straightness of approximately $L/600$. When an axial compressive force, P, is present in the member, this curvature causes additional bending moments of P times the offset of the curved axis relative to a straight chord between the member ends. These additional moments cause additional transverse deflections toward the heavier flange, which increases the second-order P-δ moments along the member length. The use of numerous shorter segments to model the member will account for this curvature if the nodes at the end of each element are located at the element centroid, rather than along a straight line between the member ends.

At section transitions where tapered I-shaped members with different flange sizes meet in the model, there is usually an offset in the theoretical location of the centroidal axes, as shown in Figure 6-3. These offsets can be as much as several inches. This discontinuity can be handled by introducing a short link element between the centroids, or by shifting each axis slightly to join at a common location.

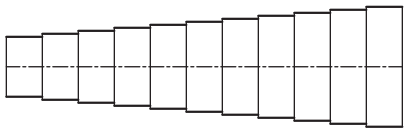

Fig. 6-1. Tapered member modeled as a series of prismatic segments.

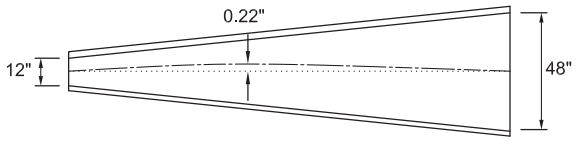

Top flange: PL ½ × 8
Bottom flange: PL ¼ × 8
Web: ¼ in.
Length: 134 in.
Taper angle: 15°

Fig. 6-2. Curved centroidal axis of singly symmetric tapered member.

Primary members in metal building frames are typically connected together using bolted end-plate connections. For analysis purposes, typical full-height end-plate connections are usually considered to be fully restrained (type FR) moment connections. Partial-height or thin end-plate connections are sometimes used as simple framing connections and are thus treated as pinned in the analysis model, even though they contribute some rotational stiffness to the system.

Beam shear stress levels are typically low in metal building frames due to the relatively deep sections used. Consequently, the effects of shear deformations are not generally included in the analysis. Designers should be aware of situations in which shear deformations could contribute substantially to deflections, such as in the case of short, heavily loaded beam spans, and account for them where significant.

A modeling assumption must be made regarding the stiffness of the region of moment connections where rafters and columns intersect. These shear panels are normally considered to be as stiff as or somewhat stiffer than the members framing into them, assuming the panels are not subject to shear buckling. Possible modeling techniques include continuing the member stiffness of the intersecting members to the work point or incorporating a more advanced approach using calculated panel stiffnesses. Given the large stiffness and short lengths of these regions, the effects of these choices on the frame deflections and the overall force distribution are usually minor. The assumption of a rigid panel zone may be somewhat unconservative.

Although the use of fixed-base columns can result in cost savings for tapered-member frames, for reasons of overall project economy, column base conditions are usually designed as simply supported. Partial restraint of column base plates can be included in the analysis model through the use of linear or nonlinear springs as appropriate, if the moment-rotation response can be quantified. Eroz et al. (2008) provide detailed suggestions for modeling simply supported column base details using an equivalent elastic-perfectly plastic rotational spring element.

In some cases, particularly frames with long spans and short columns, the distribution of forces and moments may be sensitive to lateral support movements caused by the thrust reactions at the outside column bases. During the design process, metal building designers are typically not aware of the details of the foundations that will be used to support the frames and thus generally assume the supports to be rigid in the vertical and lateral directions in the computer analysis. For this reason, it is advisable for designers of foundations to keep stresses low in elements that resist lateral movement of the footings (Newman, 2004).

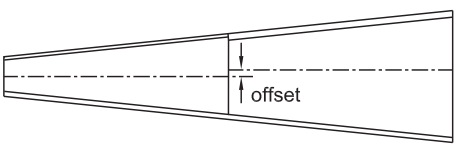

Fig. 6-3. Centroidal axis offset at plate change.

6.2 SECOND-ORDER ANALYSIS OF FRAMES

Although obtaining accurate first-order analysis results is not difficult with some attention to the details noted in Section 6.1, considerably more care in the choice of method, details of implementation, and structural modeling is required to obtain accurate second-order analysis results.

The first measure of success of a second-order analysis is the accuracy of the calculated nodal displacements and member end forces. All numerical methods of calculating second-order displacements and forces become increasingly inaccurate at higher levels of axial loading. For structures with relatively high levels of axial load relative to the sidesway buckling load of the structure or member, the influence of both P-Δ and P-δ effects is significant and must be included by some means to obtain accurate nodal displacements and member end forces. Depending on the type of second-order method being used, this can be done by either subdividing the beam and column elements into a sufficient number of smaller elements or by the direct inclusion of P-δ effects in the formulation of the structural stiffness matrix. It is recommended that accuracy checks be focused on nodal displacements, because the resulting member end forces and member unity checks tend to be as accurate as, or more accurate than, the displacements from which they are calculated.

Accurate P-δ results for the member forces between nodes must also be obtained, either directly from the analysis model or from the application of an appropriate amplifier. The familiar B_1 factor (see Equation 4.6-3a) is an example of such an amplifier. For prismatic members, "exact" closed-form P-δ formulations are readily available for several loading conditions with idealized pinned or fixed end supports. For web-tapered members, practical exact solutions are not available even for these idealized end conditions. Therefore, other approaches must be used.

When using the effective length method (ELM), subdivision of members such that $\alpha P_r/P_{e\ell}$ for each element is less than or equal to 0.02 will result in internal member forces sufficiently accurate that no B_1 amplifier or other calculation of the element internal P-δ moments is needed. Similarly, when using the direct analysis method (DM), the appropriate limit is $\alpha P_r/\overline{P}_{e\ell} \leq 0.02$, where $\overline{P}_{e\ell}$ is the element buckling load based on idealized simply supported end conditions and using the reduced elastic stiffnesses of the DM analysis model. Several suggested procedures are given in Sections 4.6.1 and 4.6.2 for cases where this level of subdivision is not desirable and the internal element P-δ moments are not otherwise accounted for in the element calculations.

Several solution methods for second-order analysis have been developed and are in use. Engineers must be aware of the limitations of the software they are using. Thorough benchmarking is essential to verify the number of elements per member necessary for worst-case member end conditions (see Appendix C), and then this number of elements per member can be employed with confidence for general analysis. Those programming second-order analysis features in software must also take into account issues of efficiency in implementation and computation. The following is a brief summary of the limitations and implementation issues for several widely used second-order analysis procedures.

6.2.1 *P*-Δ-Only Analysis

Many of the commonly used second-order analysis procedures, such as the fictitious lateral load method, the iterative gravity load method, and the negative stiffness method (Chen and Lui, 1991), include only the effects of *P*-Δ. Most of these specialized methods were developed to provide convenient solutions for rectangular framing systems and have not been proven to be accurate with the full range of geometries encountered in buildings. However, Eurocode 3 (CEN, 2005) permits the use of such methods for sloped rafter frames when the roof slope is not steeper than 26°, although it requires $\alpha P_r \le 0.09 P_{eL}$ in the rafters using their full on-slope length from column-to-column for the calculation of P_{eL}. When conducting an analysis with the DM, one should ensure $\alpha P_r \le 0.09 \overline{P}_{eL}$. For cases that violate the $0.09 P_{eL}$ or $0.09 \overline{P}_{eL}$ limit, the rafter stiffness may be calculated conservatively in the manner discussed in Section 6.2.5. *P*-Δ-only solutions using the iterative gravity load method or direct inclusion of the *P*-Δ geometric stiffness terms in the structural stiffness matrix are sufficiently general to handle metal building frame geometries without the roof slope limitation.

At higher levels of axial load relative to the member or frame buckling load encountered in some frames, *P*-Δ methods may not produce accurate nodal deflections or member end forces unless the beams and columns are subdivided into a sufficient number of shorter-length elements. In some cases, such subdivision will occur naturally as a result of accommodating locations where taper or plate changes occur. Otherwise, additional nodes and elements must be introduced to maintain a reasonable level of accuracy. The following recommendations ensure that an accuracy of 5% for the nodal deflections and 3% for the internal forces will be achieved at load levels up to 68% of the elastic buckling load in all sidesway cases and up to 66% of the elastic buckling load in all nonsway cases for the most demanding loadings and boundary conditions. These maximum limits correspond to sidesway displacement ratios ($\Delta_{2nd}/\Delta_{1st}$) larger than 3.0, and nonsway member transverse displacement ratios ($\delta_{2nd}/\delta_{1st}$) and end rotation ratios ($\theta_{2nd}/\theta_{1st}$) larger than 2.0, where Δ, δ and θ are calculated using nominal stiffness for ELM and reduced stiffness for DM. If a higher or lower limit for the axial load level is desired, these recommendations can be adjusted accordingly by studies similar to those conducted by Guney and White (2007). It is assumed that internal *P*-δ effects along the element lengths are handled using the procedures discussed in item 2 of Section 4.6.1 (ELM) or item 2 of Section 4.6.2 (DM).

Table 6-1. Member Subdivision for Sway Columns with Simply Supported Bases, *P*-Δ Analysis

Maximum $\alpha P_r/P_{eL}$ or $\alpha P_r/\overline{P}_{eL}$	Required Number of Elements	Maximum $\alpha P_r/P_{cr}$ or $\alpha P_r/\overline{P}_{cr}$
0.05	1	0.20
0.12	2	0.50
0.17	3	0.68

Table 6-2. Member Subdivision for Sway Columns with Top and Bottom Rotational Restraint, *P*-Δ Analysis

Maximum $\alpha P_r/P_{eL}$ or $\alpha P_r/\overline{P}_{eL}$	Required Number of Elements	Maximum $\alpha P_r/P_{cr}$ or $\alpha P_r/\overline{P}_{cr}$
0.12	1	0.24
0.23	2	0.24
0.31	3	0.38
0.47	4	0.51
0.58	5	0.62
0.68	6	0.68

Table 6-1 may be used as a guide to selecting subdivision intervals for *P*-Δ-only solutions in lateral-load resisting columns with nominally simply supported base conditions. Given a calculated value for $\alpha P_r/P_{eL}$ or $\alpha P_r/\overline{P}_{eL}$, or equivalently α/γ_{eL} or $\alpha/\overline{\gamma}_{eL}$, the required number of *P*-Δ elements per member is selected such that the maximum limit on $\alpha P_r/P_{eL} = \alpha/\gamma_{eL}$ or $\alpha P_r/\overline{P}_{eL} = \alpha/\overline{\gamma}_{eL}$ in the first column of the table is not exceeded. Although Table 6-1 indicates that three elements per member are required to obtain the desired analysis accuracy at $\alpha P_r = 0.15 P_{eL}$ when using the nominal elastic structural stiffness, the AISC *Specification* permits the use of a single element up to this level when using the reduced elastic stiffness with the DM. It is anticipated that future editions of the AISC *Specification* may require consideration of *P*-δ effects on the lateral displacements for $\alpha P_r > 0.05 \overline{P}_{eL}$ in stories with columns having simply supported base conditions when the DM is used.

Table 6-2 provides similar information to Table 6-1 for cases where the lateral-load resisting members have

Table 6-3. Member Subdivision for Rafters and Nonsway Columns, *P*-Δ Analysis		
Maximum $\alpha P_r/P_{eL}$ or $\alpha P_r/\overline{P}_{eL}$	Required Number of Elements	Maximum $\alpha P_r/P_{cr}$ or $\alpha P_r/\overline{P}_{cr}$
0.05	1	0.05
0.20	2	0.12
0.36	3	0.19
0.50	4	0.24
0.61	5	0.31
0.67	6	0.38
1.18	7	0.45
1.35	8	0.51
2.12	9	0.57
2.42	10	0.62
2.65	11	0.66

substantial rotational restraint at both ends, e.g., via fixed bases and/or FR moment connections to adjacent beams or rafters. Restraint conditions with an equivalent rotational stiffness of at least 1.5 EI'/L with the ELM, or 1.5 $(0.8EI'/L)$ with the DM, are assumed for a member end to be considered to have substantial rotational end restraint, where I' is defined with Equation 4.5-4.

Table 6-3 provides equivalent information for the subdivision of rafters and columns braced against translation at their top and bottom.

The third column in each of these tables gives the maximum value of $\alpha P_r/P_{cr}$ (or $\alpha P_r/\overline{P}_{cr}$) that can be achieved while maintaining 5% accuracy in the nodal displacements and 3% accuracy in the internal forces, where P_{cr} is the axial force at elastic system buckling using the ELM-based nominal elastic structure stiffness and $\overline{P}_{cr}$ is the corresponding axial force using the DM-based reduced elastic stiffness. The maximum $\alpha P_r/P_{cr}$ (or $\alpha P_r/\overline{P}_{cr}$) values do not necessarily correspond to the same critical loading and boundary conditions as the maximum $\alpha P_r/P_{eL}$ (or $\alpha P_r/\overline{P}_{eL}$) values. The required number of elements should be selected based on the member $\alpha P_r/P_{eL}$ (or $\alpha P_r/\overline{P}_{eL}$) values listed in the first column of the tables.

Sway columns that support substantial nonsway (gravity) moments should satisfy both Tables 6-2 and 6-3.

In some cases, the subdivision required to accommodate changes in flange and web plates and tapers will prove sufficient to satisfy the preceding requirements. If not, additional nodes and elements must be introduced into the model. More extensive discussions and background to the above tables can be found in Guney and White (2007).

Tables 6-1 through 6-3 are based predominantly on studies of prismatic frame members having a wide range of loadings and end conditions. They are applied to nonprismatic geometries assuming that the elastic stiffness of the nonprismatic members is represented with negligible error in the second-order analysis.

6.2.2 Analysis Using Elements that Include Both *P*-Δ and *P*-δ Effects in the Formulation

Accurate second-order analysis results can be achieved with fewer elements by accounting for *P*-Δ and *P*-δ effects directly in the element structural stiffness matrices. This can be accomplished by formulating the frame element stiffness equations accounting for the effects of both *P*-δ and *P*-Δ moments. In this case, additional element *geometric stiffness* terms are included with the element *P*-Δ stiffness terms at each step of the analysis. Using these types of elements, the structure stiffness depends in detail on the specific level of axial force in each element of the model. This can be contrasted with the *P*-Δ behavior of rectangular frames, where the sidesway stiffness depends only on the total vertical load in each story, rather than on the distribution of this load to the different columns. Nevertheless, because each term of the element stiffness matrix is proportional to the element axial load, the solution converges as soon as the axial loads in the members are stabilized. The element axial forces are sufficiently converged after the first-order solution for most practical metal building frames. An approach in which the iterations are halted after the second iteration is described as the "two cycles iterative method" by Chen and Lui (1991).

Using geometric stiffness terms based on cubic element displacements, all sway columns subjected primarily to end forces will generate deflection errors of no more than 5% and moment errors of no more than 3% at ratios of $\alpha P_r/P_{cr}$ or $\alpha P_r/\overline{P}_{cr}$ up to 0.83 without any subdivision. Nonsway members need not be subdivided into more than two elements to achieve $\alpha P_r/P_{cr}$ or $\alpha P_r/\overline{P}_{cr}$ up to 0.66, compared with as many as 11 elements for worst-case problems using *P*-Δ-only solutions having $\alpha P_r/P_{eL}$ or $\alpha P_r/\overline{P}_{eL} > 1.0$ (see Table 6-3). Use of a single element is sufficient for nonsway members in all cases when $\alpha P_r/P_{eL} \leq 0.17$ using the nominal elastic stiffness with the ELM or $\alpha P_r/\overline{P}_{eL} \leq 0.17$ using the reduced elastic stiffness with the DM.

Although the effects of *P*-δ on *P*-Δ are included in the previous types of analysis, it is still necessary to use a method such as that recommended in item 2 of Section 4.6.1 (with the ELM) or item 2 of Section 4.6.2 (with the DM) to determine accurate second-order moments between nodes, unless $\alpha P_r/P_{e\ell}$ or $\alpha P_r/\overline{P}_{e\ell}$ is less than or equal to 0.02 for each element. If Equations 4.6-2 or 4.6-5 are used to calculate the element internal moments between the nodes, $\alpha P_r/P_{e\ell}$ or $\alpha P_r/\overline{P}_{e\ell}$ must be less than or equal to 0.13 to ensure moment errors of no more than 3% in all cases.

In general, the results from second-order analysis software using the preceding types of frame elements can vary widely due to differences in implementation within global nonlinear frame analysis solution procedures. Therefore, it is essential that engineers thoroughly benchmark the specific software utilized in their design practice. Appendix C of this Guide provides a number of useful benchmark problems with an emphasis on second-order analysis of web-tapered frame members.

6.2.3 Alternative Amplified First-Order Analysis

White, Surovek and Kim (2007a) and White, Surovek and Chang (2007b) have demonstrated that second-order results can be obtained from a first-order analysis by using larger notional loads (or more specifically, by applying P-Δ shear forces corresponding to amplified story drifts). This approach provides a means of calculating credible second-order results without the need for software capable of second-order analysis. The procedure provides results with accuracy comparable to or better than other amplified first-order analysis techniques and is recommended as an alternative to first-order analysis with B_1/B_2 amplification. The first-order method (FOM) in AISC *Specification* Section C2.2b makes use of a streamlined form of this analysis procedure. However, the more general procedure outlined in White et al. (2007a, 2007b) gives better accuracy and may be used for either ELM or DM second-order analyses. Similar to first order analysis with B_1-B_2 amplification, this approach is based on a rectangular frame idealization. Therefore, its use must be subjected to limitations such as specified in Eurocode 3 (CEN, 2005) and discussed earlier in Section 6.2.1.

6.2.4 Required Accuracy of Second-Order Analysis

Historically, a 5% maximum unconservative error has been considered acceptable in the development and calibration of the AISC beam-column strength interaction equations relative to refined inelastic benchmark solutions (ASCE, 1997). In actuality, the ELM beam-column strength interaction equations used with an exact second-order elastic analysis can result in unconservative errors in the beam-column strength interaction unity checks as high as 8% relative to rigorous inelastic solutions for doubly symmetric I-shaped members subjected to major-axis bending (Maleck and White, 2003). Also, it is important to recognize that the errors in calculated internal moments are generally larger than the errors in the beam-column unity checks, and the errors in the calculated nodal displacements are usually larger than the errors in element internal nodal moments. Furthermore, it is useful to recognize that design standards typically permit implicit errors in some approximate second-order analysis solutions that are larger than 10% under practical loading conditions. For example, for a simply supported prismatic beam subjected to uniform primary bending moment, the AISC *Specification* B_1 equation gives a moment amplification of

$$B_1 = \frac{1}{1 - \alpha P_r / P_{e1}}$$

whereas the exact solution for the maximum second-order elastic moment amplification is (Chen and Lui, 1987)

$$A_F = \sec\left(\frac{\pi}{2}\sqrt{\frac{\alpha P_r}{P_{eL}}}\right)$$

At $\alpha P_r/P_{eL} = \alpha P_r/P_{e1} = \alpha/\gamma_{eL} = 0.67$, where the exact $A_F = 3.52$, B_1 is only equal to 3.0, an unconservative error of 14.8%. For use with the ELM, this level of accuracy is considered acceptable. However, the DM is generally more sensitive to analysis errors because the overall in-plane flexural buckling effects in sway frames are moved from the calculation of γ_e, P_e and/or KL in the determination of P_c in the ELM to the calculation of the amplified member internal moments in the DM. In fact, in cases where the DM design is based on $P_n = QP_y$, the in-plane flexural buckling effects are moved entirely from the determination of P_c to the calculation of the amplified member internal moments. Therefore, a smaller tolerance on the unconservative error in the internal second-order forces is needed for a DM second-order analysis. Also, it is important to emphasize that the DM second-order analysis results must be accurate compared with exact solutions using the reduced elastic stiffnesses. With these attributes in mind, the Commentary to Section 7.3 of the AISC *Specification* Appendix 7 suggests that estimated moment and deflection amplification values should both be accurate to within 3% of exact solutions at exact amplification levels of more than 2.5.

Given that the internal nodal moments generally are obtained from matrix analysis solutions with equal or better accuracy than the nodal displacements, and the internal beam-column unity checks are generally obtained with equal or better accuracy than the internal moments, the authors suggest that a 5% tolerance on nodal displacements is acceptable for practical second-order analysis solutions.

Although the AISC Commentary suggests that an accuracy of 3% is desired in an analysis for the DM, Section 7.3 of AISC *Specification* Appendix 7 permits second-order analysis without the consideration of P-δ effects on P-Δ at load levels as high as $\alpha P_r = 0.15\ P_{eL}$. The corresponding lateral displacement errors can be as high as 34% in the DM reduced stiffness model in extreme cases at this load level (e.g., a fixed-end cantilever or a simply supported sway column with complete rotational fixity at its top). However, the corresponding maximum unity check error in the beam-column strength interaction equations is limited to 8% in prismatic major-axis bending benchmarks. This maximum unity check error is consistent with the previously noted

maximum error implicitly tolerated by the ELM, when the unity checks based on an exact second-order analysis are compared with rigorous inelastic solutions. Nevertheless, the preceding upper-bound errors are slightly higher than might be considered acceptable. It is anticipated that future versions of the AISC *Specification* may require consideration of P-δ effects on the lateral displacements for $\alpha P_r > 0.05\overline{P}_{eL}$ in stories with columns having simply supported base conditions when the DM is used. Conversely, for columns having rotational restraint at both ends, Table 6-2 indicates that P-δ effects can be neglected in the calculation of the lateral displacements and member sidesway end moments when $\alpha P_r \leq 0.12\overline{P}_{eL}$.

6.2.5 Stiffness Reduction

As discussed in Section 4.6.2, when using the DM it is necessary to reduce the stiffness of members contributing to the lateral stability of the structure by at least 20% in the second-order analysis. It is the intent of the AISC *Specification* that this reduction be applied to all elements contributing to the stability of the structure, including moment connected beams, fixed column bases, etc. This reduction should not be applied when calculating first-order results, e.g., when checking service load deflections.

As a practical matter, it is recommended that the stiffness of all members be reduced by the same percentage for second-order analysis by adjusting the value of the modulus of elasticity, E. In addition to the simplicity of implementation, this has the advantage of avoiding unintended side-effects in the analysis that result from this stiffness reduction, such as differential column shortening.

For a DM or ELM second-order analysis by an amplified first-order analysis approach (e.g., B_1-B_2), or for the calculation of the in-plane γ_e for columns rigidly connected to rafters using story-stiffness-based equations, further reduction in the rafter stiffnesses is necessary in some situations (AISC, 2005a). Where the axial load in the rafters exceeds $0.05P_{eL}$ (i.e., $\alpha/\gamma_{eL} > 0.05$) using the nominal elastic stiffness, the overall stiffness of the rafters and the rotational restraint that the rafter provides at the top of a column is significantly reduced due to P-δ effects. If a second-order analysis is conducted using a frame element that incorporates both P-Δ and P-δ effects, or if a general P-Δ analysis is conducted using the element discretization recommended in Table 6-3, this stiffness reduction is properly captured and no other adjustment is necessary. However, when using an amplified first-order analysis or any P-Δ analysis based on a rectangular frame idealization for second-order load-displacement calculations with the ELM, or for calculation of γ_e values, and when using the FOM, the base equations do not consider the influence of axial force in the rafters on the rafter stiffnesses. Therefore, to account for these effects, it is recommended that the EI of the rafters within a given span be reduced as follows for the calculation of the sidesway deflections, sidesway stiffnesses, and sidesway amplification factors in these cases:

$$EI' = \left(1 - \frac{\alpha P_r}{P_{e(0.5L_{os})}}\right) EI \qquad (6.2\text{-}1a)$$

where $P_{e(0.5L_{os})}$ is calculated using $0.5L_{os}$, L_{os} is the full on-slope length of the rafters between the columns, and EI is the basic flexural rigidity used in the analysis. The use of $L = 0.5L_{os}$ in this calculation accounts for the fact that the rafters tend to be deformed in double-curvature bending in providing sidesway rotational restraint to the tops of the columns. Similarly, when using an amplified first-order analysis approach for the structural analysis with the DM, one should use

$$E\overline{I}' = \left(1 - \frac{\alpha P_r}{P_{e(0.5L_{os})}}\right) 0.8\tau_b EI \qquad (6.2\text{-}1b)$$

in the rafters when their axial force αP_r is greater than $0.05\overline{P}_{eL}$, or equivalently when $\alpha/\overline{\gamma}_{eL} > 0.05$.

As previously stated, the factor $0.8\tau_b$ in Equation 6.2-1b is easily accounted for in most software by reducing E. However, one should never use a reduced value of E in the member strength equations in the AISC *Specification* Chapters E through G. Component resistances should always be calculated using a nominal $E = 29{,}000$ ksi.

6.2.6 Load Levels for Second-Order Analysis

Second-order analysis is nonlinear by nature. Two important consequences arise:

1. Valid load combination results cannot be obtained by superimposing the results of second-order analyses conducted on individual load cases. A separate second-order analysis must be conducted for each load combination. However, if one uses an amplified first-order elastic analysis to determine the second-order internal forces, the results from the separate first-order analyses can be superposed to determine total first-order forces. Subsequently, the amplification factors for each load combination can be determined and applied to the total first-order internal displacements and/or forces.
2. Second-order analyses for use with either ELM or DM design must be conducted at ultimate load levels to obtain accurate second-order responses, even if the design is performed using ASD. Because ultimate load levels are not defined for ASD, the ASD loading combinations, including the notional loads, must be increased by a factor of 1.6 prior to conducting the analysis. The member forces from the second-order analysis are then divided by 1.6 to give required strengths for use with the ASD strength equations.

The factor of 1.6 is equivalent to the average load factor that would occur in LRFD combinations for structures with 100 percent live load, and is therefore somewhat conservative compared with realistic LRFD combinations. When an amplified first-order analysis is employed, the 1.6 factor can be included explicitly in the amplification factor expressions, and therefore one need not factor the forces up by 1.6 and then divide by 1.6 in this case.

LRFD load combinations are ultimate level loadings; therefore, the load combinations should not be factored up further prior to analysis. The results of the second-order LRFD analysis should be used directly in the member strength checks.

6.2.7 Notional Loads

Notional loads are fictitious lateral loads that account for a nominal out-of-plumbness of the frame. They are calculated as a percentage of the vertical load in the load combination being analyzed in the ELM and DM or as a function of the vertical load and first-order sidesway deflections in the FOM. The required magnitudes and conditions under which they must be added to other lateral loads are discussed in Section 4.6.

For simple rectangular tiered structures, the total notional load at each floor or roof level is calculated using the summation of the vertical load introduced at that level. One must not calculate the notional loads at each level from the accumulation of load at that level. The notional load is determined only from the load introduced at that level.

For more complicated situations, the application of notional loads can sometimes seem less straightforward. When in doubt about the application of notional loads, keep in mind that they are intended to simulate the effect of an initial uniform out-of-plumbness. Consideration of an out-of-plumb version of the frame will usually make clear the appropriate calculation of the notional loads.

All notional loads are applied in the same direction in any given load combination. For gravity-only load combinations that cause a net sidesway, the notional loads should be applied in the direction that increases the net sidesway. For structures with multiple stories or levels and in which the sidesway deformations are in different directions in different stories or levels, it is necessary to include a pair of load combinations, separately considering the notional loads associated with a uniform out-of-plumbness in each direction. For load combinations in which notional loads are combined with lateral loads, the notional loads should be applied in the same direction as the net applied lateral loads. For gravity-only combinations, if there is zero net first-order sidesway for a load combination, such as the case of a symmetrically loaded symmetrical structure, load combinations with notional loads in both directions should be considered separately, unless any symmetry in the design is enforced by other means.

For ASD designs using the ELM or DM, the notional loads must be calculated from the vertical loads including the 1.6 factor required for second-order analysis.

The total resultant horizontal force at any level due to the notional loads is actually a fictitious shear force that causes the same P-Δ_o moments as the physical vertical loads acting through the initial out-of-plumb displacements, Δ_o. Therefore, the net horizontal reactions due to the notional loads may be subtracted from the analysis results. However, as a practical matter, this may be more trouble than it is worth. Physical P-Δ_o shear forces do exist in columns and/or diagonal bracing members of many structures, although the sum of these shear forces across all the members of a story must be zero. The true distribution of these internal forces can be determined only by explicit modeling of the out-of-plumb geometry. For instance, in Figure 4-1, the lateral load resisting column has an additional shear force $P\Delta_o/L$ due to any initial out-of-plumbness Δ_o of the right-hand leaning column. This is balanced by the horizontal component of the axial force in the leaning column. In cases that may have significant physical internal P-Δ_o shear forces, the notional load approximation tends to give a reasonable estimate of the largest internal P-Δ_o shear forces. In lateral-load resisting frames, these P-Δ_o shear forces tend to be small (but not necessarily insignificant) compared with the other shear and axial force effects.

The following example illustrates the calculation of notional loads on a single-slope building shown in Figure 6-4, assuming an initial out-of-plumbness of $L/300$.

$$N_1 = N_4 = \frac{P\Delta_0}{L} = 10\,\text{kips}\left(\frac{1}{300}\right) = 0.0333\,\text{kips}$$

$$N_2 = N_3 = \frac{P\Delta_0}{L} = 25\,\text{kips}\left(\frac{1}{300}\right) = 0.0833\,\text{kips}$$

6.2.8 Explicit Out-of-Plumbness

In lieu of notional loads, the frame may be modeled using a uniform initial out-of-plumbness. For gravity-only load combinations, the out-of-plumbness should be in the direction of the first-order sway for the load combination under consideration. This can be determined by a preliminary first-order analysis using the plumb geometry. For structures with multiple stories or levels and in which the sidesway deformations are in different directions in different stories or levels, it is necessary to include a pair of load combinations, separately considering the influence of a uniform initial out-of-plumbness in each direction. If the structure has no sidesway for a particular gravity load combination—e.g., a symmetrical structure with symmetrical loading—separate load combinations with out-of-plumbness in both directions

should be considered unless any symmetry of the design is enforced by other means. For load combinations involving lateral loads, the out-of-plumbness should be in the direction of the lateral loads.

The magnitude of out-of-plumbness may be set using the guidelines in Section 4.4.3, with the height at each column top measured from its base. The following example illustrates the calculation of out-of-plumbness for a single-slope building shown in Figure 6-5, assuming an initial out-of-plumbness of $L/300$.

$$\Delta_1 = \frac{20\,\text{ft}\,(12\,\text{in./ft})}{300} = 0.800\,\text{in.}$$

$$\Delta_2 = \frac{23.3\,\text{ft}\,(12\,\text{in./ft})}{300} = 0.932\,\text{in.}$$

$$\Delta_3 = \frac{26.7\,\text{ft}\,(12\,\text{in./ft})}{300} = 1.07\,\text{in.}$$

$$\Delta_4 = \frac{40\,\text{ft}\,(12\,\text{in./ft})}{300} = 1.60\,\text{in.}$$

Applying the out-of-plumbness values to the column tops as shown will result in small changes in rafter analysis lengths between column tops. This can be avoided by moving all the nodes laterally by $0.0033H$, including the nodes at the column bases, where H is the height above the lowest elevation on the structure.

The AISC *Specification* explicitly permits the use of out-of-plumbness in lieu of notional loads with the DM, but does not explicitly state that this is allowed for the ELM. Because proper application of explicit out-of-plumbness will result in second-order deflections and forces equivalent to or more accurate than those obtained using notional loads, this approach can be used for the ELM also.

6.2.9 Lean-On Structures

Lean-on structures are elements of the structure that support gravity loads but that depend on the frame for lateral stability. Common examples in low-rise construction include portions of mezzanines, lean-tos, and concrete wall panels that are attached to the frame for lateral support, but whose gravity load is not carried by the frame. These elements increase the second-order deflections and forces and must be accounted for in the second-order analysis.

When using a general-purpose analysis package, lean-on structures can be accounted for by fully modeling them with the other portions of the frame. Alternatively, in many cases a complex lean-on structure may be simplified to a single dummy column that carries the gravity and is to the primary frame by a link.

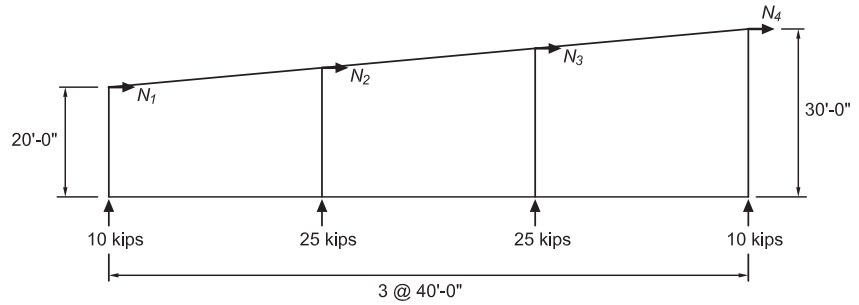

Fig. 6-4. Calculation of notional loads.

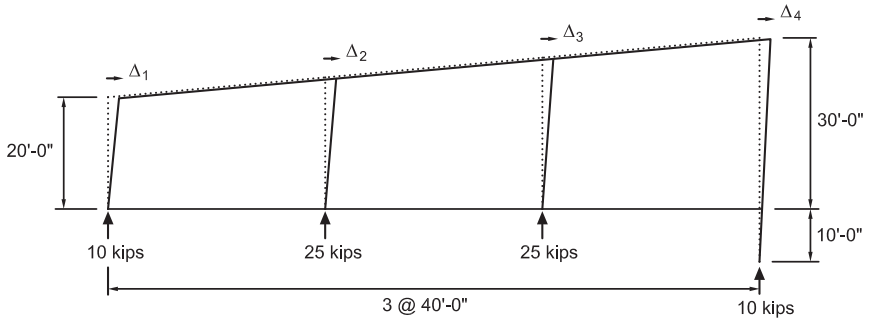

Fig. 6-5. Calculation of explicit out-of-plumbness.

The elements that must be properly modeled include:

1. The height of the lean-on structure column(s).
2. The magnitude of the vertical load that is laterally stabilized by the frame.
3. The notional loads contributed by the lean-on structure, or the out-of-plumbness if explicit out-of-plumbness is being modeled.

The following example illustrates the calculation of the dead load gravity and notional loads along with reasonable modeling simplifications for a gable frame laterally supporting a lean-to and concrete wall panels (see Figure 6-6). The frame tributary width is 25 ft, and the assumed out-of-plumbness is *L*/500. The vertical and notional loads shown are those in addition to the loads normally applied in a first-order analysis, contributed by the lean-to and tilt-up panels. Half the weight of the tilt-up panels is used because the centroid of the weight of the panels is at half the height of the outside columns rather than at the roof level. Y_2 only includes the right half of the lean-to roof dead load, because it is assumed that the left half and its notional load (N_3) would have already been included in the analysis at the location where the lean-to attaches to the gable frame. The vertical and notional loads from the lean-to and wall panels at the right side of the structure have been combined onto one fictitious column to simplify the model. From AISC *Specification* Appendix 7.3,

$$
\begin{aligned}
Y_1 &= \left[0.5(30\,\text{ft})(25\,\text{ft})(80\,\text{psf})\right]/1000 \\
&= 30.0\,\text{kips} \\
N_1 &= 0.002Y_i \\
&= 0.002(30.0\,\text{kips}) \\
&= 0.0600\,\text{kips} \\
Y_2 &= \left[0.5(15\,\text{ft})(25\,\text{ft})(80\,\text{pfs}) \right. \\
&\quad \left. +0.5(30\text{ ft})(25\text{ ft})(5\text{ psf})\right]/1000 \\
&= 16.9\,\text{kips} \\
N_2 &= 0.002Y_i \\
&= 0.002(16.9\,\text{kips}) \\
&= 0.0338\,\text{kips} \\
N_3 &= 0.002Y_i \\
&= \left[0.002(0.5)(30\text{ ft})(25\text{ ft})(5\text{ psf})\right]/1000 \\
&= 0.00375\,\text{kips}
\end{aligned}
$$

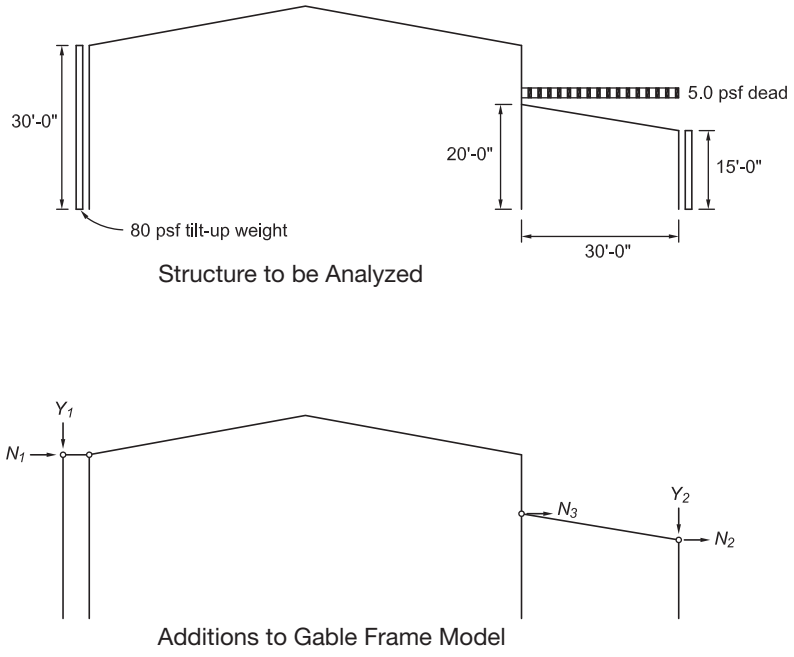

Fig. 6-6. Calculation of notional loads for lean-on structures.

6.3 ANALYSIS OF SINGLE-STORY CLEAR-SPAN FRAMES

Single-story clear-span frames, particularly those with unsupported gables, differ in a few important ways from the rectangular frames presumed in the majority of the AISC *Specification* analysis provisions.

6.3.1 Behavior of Single-Story Clear-Span Frames

The stability behavior of single-story clear-span frames is distinctly different from the stability behavior of multi-story building frames or multi-bay modular building frames because of the P-Δ and P-δ effects from the axial compression in the rafters. In single-story clear-span frames, gravity load restraining bending moments are developed at the knees of the frame by axial thrusts from the foundation. These axial thrusts are typically of a similar magnitude to the column axial forces. Conversely, in modular frames, the interior columns support a large portion of the gravity loads on the rafters and reduce the magnitude of the restraining bending moments in exterior columns. Also, in multi-story frames, the column shear forces induced by the bending of the columns under gravity loads act in opposite directions above and below each floor. These opposing shear forces tend to cancel with one another such that the axial force in the floor beams is relatively small. In addition, the span-to-depth ratio of floor beams tend to be smaller than that of rigid frame rafters. This is because floor loadings tend to be larger than ordinary roof loads; also, floor beams tend to be stiffer to satisfy floor deflection and floor vibration requirements. Due to the preceding attributes, the second-order effects in ordinary floor beams of multi-story frames and rafters of modular frames are usually small enough that they do not affect the stability behavior of the frame.

6.3.2 In-Plane Design Length of Rafters

The in-plane axial design length of beams or rafters in rectangular frames traditionally has been taken as the length between columns. In a span with an unsupported gable, a common industry practice has been to take the design length as the distance from column to ridge if there is a sufficient change in the pitch across the ridge. A sufficient change in the pitch is one that ensures that the gable cannot deflect downward enough to permit the rafter to buckle downward in a single half-wave between column supports. Industry practice has varied on this limit, down to as low as a roof pitch of ¼ on 12 on each side of the ridge. A small study conducted in conjunction with the development of this Guide showed that the reduction in rafter effective length for gable frames is primarily due to end rotation restraint from the columns rather than from the change in rafter pitch at the ridge. Consequently, when designing frames using the ELM, it is recommended that any reductions in the effective length below the full on-slope length between columns be based on a stability analysis of the rafter incorporating the restraint from the supporting columns. See Appendix B for a discussion of several rational approaches to calculating buckling parameters for rafters.

When using the DM, the recommendations discussed in items 4a through 4c of Section 4.6.2 should be followed. The DM is generally better suited for characterizing the true stability behavior of rafters, because it focuses directly on an appropriate second-order load-deflection analysis accounting for the reduced stiffness at ultimate load levels and overall geometric imperfection effects where they are important.

6.3.3 Sidesway Calculations for Gabled Frames

It is necessary to calculate the ratio of $\Delta_{2nd}/\Delta_{1st}$ to establish the applicability of the three AISC stability methods, to determine the applicability of the $K = 1$ provisions for the ELM, to determine whether notional loads are additive to lateral loads in the DM, and to implement the B_1-B_2 method, when it is used. For gable frames, some adjustment of this calculation is necessary to avoid underestimation of the second-order effects. The eaves of a frame with a gable where the ridge is not directly supported by a column will spread in opposite directions under gravity loading as the gable deflects vertically. Symmetrical deflections of this type do not contribute to a sidesway instability of the frame and should not be considered as frame sway when evaluating the magnitude of second-order effects. The average sway at the column tops weighted by the gravity load in each column is recommended for calculation of the overall net first- and second-order sidesway displacements as shown in the following example.

Calculate $\Delta_{2nd}/\Delta_{1st}$ referring to Figure 6-7.

$$\Delta_{1st} = \frac{-0.800\,\text{in.}\left(15\,\text{kips}\right)+1.20\,\text{in.}\left(20\,\text{kips}\right)}{15\,\text{kips}+20\,\text{kips}}$$
$$= 0.343\,\text{in.}$$
$$\Delta_{2nd} = \frac{-0.700\,\text{in.}\left(15\,\text{kips}\right)+1.30\,\text{in.}\left(20\,\text{kips}\right)}{15\,\text{kips}+20\,\text{kips}}$$
$$= 0.443\,\text{in.}$$
$$\frac{\Delta_{2nd}}{\Delta_{1st}} = \frac{0.443\,\text{in.}}{0.343\,\text{in.}} \quad \leftarrow\text{Correct (See following for incorrect solution)}$$
$$= 1.29$$

A calculation of $\Delta_{2nd}/\Delta_{1st}$ using the unaveraged maximum displacements would significantly underestimate the second-order effects as shown here.

$$\frac{\Delta_{2nd}}{\Delta_{1st}} = \frac{1.3\,\text{in.}}{1.2\,\text{in.}} \quad \leftarrow\text{Incorrect}$$
$$= 1.08$$

6.4 SERVICEABILITY CONSIDERATIONS

With the exception of seismic story drift, serviceability of low-rise structures has traditionally been evaluated using first-order elastic deflections. These are compared with empirical deflection standards that historically have provided for adequate serviceability when used as limits on first-order deflection. In most metal building frames, underestimation of the true second-order deflections under service loads does not cause problems because the preceding arbitrary limits are well within tolerances that would result in any significant structural or nonstructural damage. For this reason, it is recommended that first-order deflections continue to be used with these types of traditional serviceability limits.

One possible exception is the calculation of story drift where collision with an adjacent structure is a possibility. In this case, it would be prudent to use the second-order deflections for a more accurate assessment. Also, when there are specific structural or nonstructural elements that may be damaged at service load levels if specific deflection limits are exceeded, it is recommended that the second-order service-load deflections be calculated.

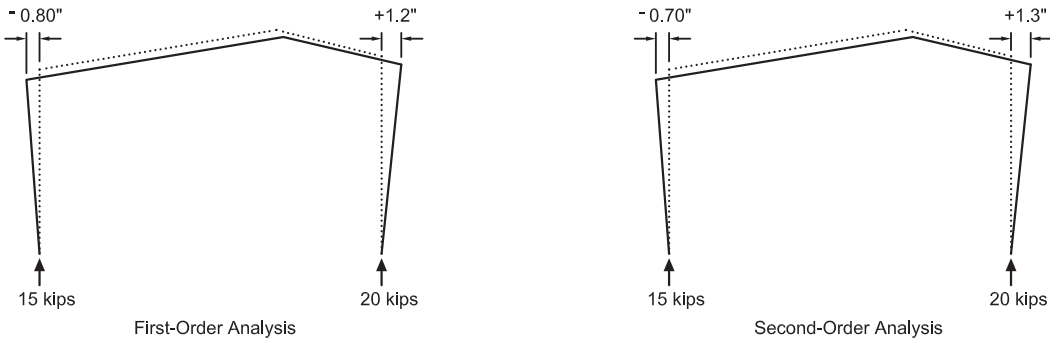

Fig. 6-7. Calculation of $\Delta_{2nd}/\Delta_{1st}$ for gabled frames.

Chapter 7
Annotated Bibliography

STABILITY DESIGN OF FRAMES COMPOSED OF TAPERED AND GENERAL NONPRISMATIC I-SHAPED MEMBERS

This bibliography summarizes the results of numerous research efforts aimed at the stability design of nonprismatic I-shaped members and the design of frames composed of nonprismatic I-shaped members. The research studies range primarily from the early 20th century up to the current time (October 2010). The references are arranged into the following categories and are discussed in chronological order in each of these categories:

- Column elastic flexural buckling
- Elastic flexural buckling of rectangular frames
- Elastic flexural buckling of gabled frames
- Elastic flexural buckling of crane buildings
- Column inelastic flexural buckling and design strength
- Planar first- and second-order elastic beam-column and/or frame analysis (planar analysis)
- Column constrained-axis torsional buckling
- Beam and beam-column elastic lateral-torsional buckling
- Beam and beam-column design resistances
- General behavior and design of frames composed of tapered I-shaped members

Column Elastic Flexural Buckling

Ostwald (1910). "Klassiker der exakten Wissenschaften" No. 175, Leipzig.

German translation of Euler's derivation of differential equation of the elastic deflection curve for columns with continuously varying cross section along their length. Euler discussed columns of various shapes, including a truncated cone and pyramid.

Lagrange (1770–1773). "Sur la figure des colonnes," *Misc. Taurinensia,* Vol. 5. (Reprinted in "Oeuvres de Lagrange," Vol. 2, Gauthier-Villars, Paris, 1868, pp. 125–170.)

Investigated the stability of elastic bars bounded by a surface of revolution of the second degree.

Vianello, L. (1898). "Graphische Untersuchung der Knickfestigkeit gerader Stäbe, *Zeitschrift des Vereines deutscher Ingenieure,* 42, p. 36.

Introduced the method of successive approximations into the field of engineering. Demonstrated a graphical procedure for the solution of column buckling problems.

Bairstow, L. and Stedman, E.W. (1914). "Critical Loads for Long Struts of Varying Sections," *Engineering,* 98, p. 403.

Calculated elastic flexural buckling loads assuming a variation of the moment of inertia according to a power of the distance along the bar.

Morley, A. (1914). *Engineering,* 97, p. 566 (and Vol. 104, p. 295, 1917).

Calculated elastic flexural buckling loads assuming a variation of the moment of inertia according to a power of the distance along the bar

Bleich, F. (1924). "Theorie und Berechnung der eisernen Bruchen," Springer, Berlin, p. 136.

Provided approximate solutions based on the energy method for some shapes of columns.

Dinnik, A.N. (1914). *I svest. Gornogo Inst*., Ekaterinoslav.

Dinnik, A.N. (1916). *Vestnik Ingenerov,* Moscow.

(The principal results of these papers were translated into English in the following papers:

Dinnik, A.N. (1929). "Design of columns of varying cross-section," *ASME Transactions,* AMP-51-11, Vol. 51, McGraw-Hill, New York, NY, pp. 165–171.

Dinnik, A.N. (1932). "Design of columns of varying cross-section," *ASME Transactions,* AMP-54-16, Vol. 54, McGraw-Hill, New York, NY, pp. 105–109.)

One of the first to analytically solve the differential equation of buckling for tapered members. Published formulas and coefficients of stability enabling elastic buckling load calculations without solving the governing differential equations. The solutions were based on assuming various parabolic laws for the stiffness in the end portions of the column.

Timoshenko, S.P. (1936). *Theory of Elastic Stability*, McGraw-Hill, New York, NY, 518 pp.

Provided the analytical solution for the elastic flexural buckling of a simply supported column subjected to an end load and a concentrated axial load at an intermediate location along its length as well as a step in the cross section at the location of the intermediate axial load. Provided analytical solutions for the elastic flexural buckling of a prismatic cantilever column subjected to distributed axial loads and combined end and distributed axial loads. Provided analytical solutions for the elastic flexural buckling of simply supported columns subjected to a constant axial compression with a stepped cross section composed of a prismatic center length having a larger moment of inertia than the end

prismatic lengths. Provided an analytical solution for the elastic flexural buckling of a cantilever column with a moment of inertia that varies according to a power of the distance along the member length, subjected to an internal axial force that also varies according to a power of the distance along the member length. Discussed energy method solutions for more general cases. Discussed the method of successive approximations for determination of column elastic flexural buckling loads and presented a graphical solution for the buckling of a simply supported stepped column subjected to constant axial compression using this method.

Newmark, N.M. (1943). "A Numerical Procedure for Computing Deflections, Moments and Buckling Loads," ASCE, *Transactions,* 108, 1161–1188.

Showed very effective practical solutions of column flexural buckling loads using the method of successive approximations along with finite difference expressions. The method is applicable to bars with any variation in cross section and with varying axial load. Showed example applications of this method to prismatic and stepped beams with various loading and support conditions. One of the examples shown is a propped cantilever, illustrating the application of the method to a statically indeterminate problem.

Salvadori, M.G. (1951). "Numerical Computation of Buckling Loads by Finite Differences," ASCE, *Transactions,* 116, 590–625.

Published numerical solutions of buckling problems taken from Timoshenko (1936) using the finite difference method as a method of successive approximations. Provided detailed discussions of numerical solution procedures based on the method of successive approximations for column flexural buckling problems. These developments were based largely on the research of Newmark (1943).

Bleich, F. (1952). *Buckling Strength of Metal Structures,* McGraw-Hill, New York, NY, 508 pp.

Provided solutions for elastic buckling of simply supported I-shaped columns with linear or parabolic taper, assuming an approximate variation of the moment of inertia as a power function along the length of the member. Provided an overview of the method of successive approximations in his Sections 27 and 28 (pp. 81–91), including a proof of its convergence. In addition, provided detailed discussions of numerical solution procedures utilized with the method of successive approximations for column flexural buckling problems. These developments were based largely on the research of Newmark (1943).

Timoshenko, S.P. and Gere, J.M. (1961). *Theory of Elastic Stability,* McGraw-Hill, New York, NY, 541 pp.

Provided the solution for constrained-axis lateral-torsional buckling of axially loaded members. Provided the various column buckling solutions from Timoshenko (1936) for nonprismatic columns and columns subjected to distributed loads. Expanded on the original discussion of the method of successive approximations provided by Timoshenko (1936) using the numerical procedures recommended by Newmark (1943).

Gere, J.M. and Carter, W.O. (1962). "Critical Buckling Loads for Tapered Columns," *Journal of the Structural Division,* ASCE, 88(ST1), 1–11.

Solved the differential equation of buckling for tapered columns using Bessel functions and numerical integration.

Butler, D.J. and Anderson, G.C. (1963). "The Elastic Buckling of Tapered Beam-Columns," *Welding Journal Research Supplement,* Vol. 42, No. 1.

and

Butler, D.J. (1966). "Elastic Buckling Tests on Laterally and Torsionally Braced Tapered I-Beams," *Welding Journal Research Supplement,* Vol. 45, No. 1.

Tested tapered I-shaped beams and channel sections tapered in both the web and flanges as cantilever beam-columns. The primary focus was on the elastic stability of the members and the bracing requirements.

Girijavallabhan, C.V. (1969). "Critical Buckling Loads for Tapered Columns," *ASCE Journal of the Structural Division,* 95(ST11), 2419–2431.

Provided finite difference procedures to obtain buckling solutions for simply supported general nonprismatic columns. Derived an equivalent flexural stiffness equation for efficient handling of a discontinuity in the moment of inertia within the unbraced length due to a step in the cross section.

Lee, G.C., Morrell, M.L. and Ketter, R.L. (1972). "Design of Tapered Members," *Welding Research Council Bulletin,* No. 173, 1–32.

Provided linearly tapered web member formulas that give the length of a prismatic column composed of the shallower end cross section that buckles elastically at the same level of axial load as a given member with a linearly tapered web depth. The formulas were developed by curve fitting to data obtained from solutions for five I-shapes representing a range of linearly tapered I-shaped member dimensions.

Iremonger, M.J. (1980). "Finite Difference Buckling Analysis of Non-uniform Columns," *Computers and Structures,* 12, 741–748.

Determined elastic buckling loads for tapered and stepped columns with various support conditions using the finite difference method and a matrix iteration technique. Solutions within 1% of the converged results were obtained with less than or equal to five segments for the example columns. Applied an effective moment of inertia at the step to analyze stepped columns.

Errnopoulos, J.C. (1986). "Buckling of Tapered Bars under Stepped Axial Loads," *Journal of Structural Engineering,* 112(6), 1346–1354.

Solved the differential equation of buckling exactly for tapered bars subjected to concentrated axial loads at various locations along their length. Considered three types of support conditions: fixed-free, hinged-hinged and fixed-hinged. Presented extensive charts and formulas for handling of a single intermediate axial load at any position along the member length in design. Concluded that for a given ratio of the axial loads and location of the intermediate load, (1) an optimized design of a tapered bar is possible such that the buckling load is maximized, and (2) there are cases where the buckling load of a tapered bar is smaller than that of a uniform bar having the moment of inertia at the mid-length. In these cases, the use of a tapered bar is not recommended.

Chen, W.F. and Lui, E.M. (1987). *Structural Stability, Theory and Implementation,* Elsevier, New York.

Discussed Newmark's (1943) numerical implementation of the method of successive approximations (in their Section 6.7). Provided an example solution for a prismatic cantilever column subjected to equal axial loads at its free end and mid-height.

Williams, F.W. and Aston, G. (1989). "Exact or Lower Bound Tapered Column Buckling Loads," *Journal of Structural Engineering,* 115(5), 1088–1100.

Developed tables that enable buckling loads to be determined for linearly tapered columns with uniformly distributed axial load applied along their length. Six combinations of end conditions were considered.

Bazant, Z.P. and Cedolin, L. (1991). *Stability of Structures—Elastic, Inelastic, Fracture and Damage Theories,* Oxford University Press, New York, 984 pp.

Discussed the mathematical basis for the method of successive approximations in their Section 5.8.

Wang, C.M., Wang, C.Y. and Reddy, J.N. (2005). *Exact Solutions for Buckling of Structural Members,* CRC Press, Boca Raton, FL, 207 pp.

Summarized a number of buckling solutions for columns with variable cross section, subjected to end compressive forces with and without distributed axial loads.

White, D.W. and Kim, Y.D. (2006). "A Prototype Application of the AISC (2005) Stability Analysis and Design Provisions to Metal Building Structural Systems," Report prepared for Metal Building Manufacturers Association, School of Civil and Environmental Engineering, Georgia Institute of Technology, January, 157 pp.

Summarized that the method of successive approximation (Timoshenko and Gere, 1961) can be set up using simple spreadsheet tools to provide highly accurate solutions for the elastic flexural buckling of general tapered and/or stepped nonprismatic I-shaped members with specified end conditions. Also, indicated that accurate approximations may be possible for linearly tapered web I-shaped members for simply supported end conditions by using a weighted average of the cross-section properties along the member length.

Kim, Y.D. and White, D.W. (2006d). "Elastic Torsional and Flexural-Torsional Buckling Estimates for I-shaped Members with Linearly-Tapered Webs," Structural Engineering Mechanics and Materials Report No. 53, School of Civil and Environmental Engineering, Georgia Institute of Technology, Atlanta, GA, 12 pp.,

Kim, Y.D. and White, D.W. (2007a). "Practical Buckling Solutions for Tapered Beam Members," *Proceedings*, Annual Technical Session, Structural Stability Research Council, University of Missouri, Rolla, MO, April, pp. 259–278.

and

Kim, Y.D. (2010). "Behavior and Design of Metal Building Frames with General Prismatic and Web-Tapered Steel I-Section Members," Doctoral Dissertation, School of Civil and Environmental Engineering, Georgia Institute of Technology, Atlanta, GA, 562 pp.

Showed that for a complete practical range of doubly symmetric tapered I-shaped members with both twisting and lateral displacement restrained at the brace points, the weak-axis flexural buckling resistance P_n based on the cross section at the middle of the unbraced length and the prismatic member Euler buckling equation is never more than 2% unconservative relative to the P_n obtained based on the rigorous consideration of potential flexural and torsional buckling modes for the tapered member.

Elastic Flexural Buckling of Rectangular Frames

Lee, G.C., Morrell, M.L. and Ketter, R.L. (1972). "Design of Tapered Members," *Welding Research Council Bulletin,* No. 173, 1–32.

Developed approximate member stability coefficients and slope-deflection equations for load-deflection or buckling analysis of frames composed of linearly tapered members. The coefficients are based on the assumption of the material being concentrated only in the flanges. Provided a design approach based on graphical charts for determination of effective length factors, K_γ, for sidesway buckling of rectangular clear-span frames with linearly tapered web columns and rotational restraint from prismatic beams. The influence of axial compression in the beams on the sidesway buckling load is not considered. Kim and White (2006a) compare these solutions to rigorous eigenvalue buckling calculations for two basic benchmark problems with ideal end rotational restraint (i.e., zero axial compression in the beams). The approximate solutions developed by Lee et al. (1972) are 9% conservative in the first of these benchmark problems and 19% conservative in the second benchmark problem.

Lee, G.C., Chen, Y.C. and Hsu, T.L. (1979). "Allowable Axial Stress of Restrained Multi-Segment, Tapered Roof Girders," *Welding Research Council Bulletin,* No. 248, May, 1-28.

Developed charts for calculation of equivalent effective length factors, K_γ, for doubly tapered I-shaped members. These charts were intended to facilitate the design of multi-segmented tapered roof girders. The corresponding effective length factor solutions were based on rectangular clear-span frame solutions in which the restraint from the adjacent members was expressed based on their elastic flexural properties, neglecting the influence of any axial compression in these members and neglecting any influence of frame sidesway on the rotational restraint provided by these members. The charts were applied to roof girders by taking the columns as the restraining members, thus neglecting the influence of axial compression and frame sidesway on the stiffnesses of these members in determining the rotational restraint at the ends of the girders. The resulting process results in a stability design in which the rafters are assumed to restrain the columns based on their first-order elastic stiffnesses (in the design of the columns), but then the columns are assumed to restrain the rafters based on their first-order elastic stiffnesses and no sidesway (in the design of the rafters). These are inconsistent assumptions that can lead to significant errors relative to rigorous sidesway buckling solutions for actual frames. The charts and procedures were not incorporated into the AISC ASD provisions but are summarized in Lee et al. (1981).

Lui, E.M. (1992). "A Novel Approach for K Factor Determination," *Engineering Journal,* AISC 29(4), 150–159.

Developed a story-stiffness-based method for calculation of column effective length factors in rectangular frameworks composed of prismatic members. Lui's equation utilizes the results from a first-order lateral load analysis for characterization of story sidesway stiffness, includes an approximate term that approximates the column *P*-small delta effects on sidesway buckling as a function of the ratio of the column sidesway end moments, and accounts for leaning column effects on the sidesway stability.

Cary, W.C. III and Murray, T.M. (1997). "Effective Lengths of Web-Tapered Columns in Rigid Metal Building Frames," Report No. CE/VPI-ST 97/06, May, 59 pp.

Extended Lui's (1992) story-stiffness-based approach for calculation of sidesway buckling effective lengths to rectangular frames with linearly tapered columns. The development simplifies Lui's calculation of the *P*-small delta effect by assuming reverse curvature bending and using the rigidity EI_o at the smallest cross section of the lateral-load resisting columns. The influence of axial compression in the beams or rafters on the sidesway buckling load is not considered.

Errnopoulos, J.C. (1997). "Equivalent Buckling Length of Non-uniform Member," *Journal of Constructional Steel Research,* 42(2), 141–158.

Derived nonlinear equilibrium equations for framed prismatic and nonprismatic compression members for nonsway and sway buckling on the basis of the slope deflection method. Results for the critical loads and the equivalent buckling lengths are presented in tabular and graphical form.

Jimenez, G.A. (2005). "Restrained Web-Tapered Columns, A Practical Design Approach," *Proceedings,* Annual Technical Session, Structural Stability Research Council, University of Missouri, Rolla, MO, pp. 225–240.

Discussed the second-order elastic analysis of rectangular frames using slope deflection equations with approximate coefficients from Lee et al. (1972). Investigated the use of the *K*-factor expression developed by Cary and Murray (1997) for rectangular frame geometries.

White, D.W. and Kim, Y.D. (2006). "A Prototype Application of the AISC (2005) Stability Analysis and Design Provisions to Metal Building Structural Systems," Report prepared for Metal Building Manufacturers Association, School of Civil and Environmental Engineering, Georgia Institute of Technology, January, 157 pp.

Presented a general story-stiffness-based equation for calculation of the elastic sidesway buckling load of general rectangular frames with equal or unequal height columns composed of tapered I-shaped members. The proposed equation is an extension of a story-stiffness-based buckling equation provided in the Commentary of AISC (2005) and gives similar results to the *K*-factor equation developed by Cary and Muray (1997). Results using the proposed equation were compared to rigorous matrix analysis eigenvalue buckling solutions. Discussed the importance of accounting for the reduced stiffness of beams and rafters in clear-span frames due to axial compression induced by the thrust from the foundation.

White, D.W., Surovek, A. and Chang, C.-J. (2007). "Direct Analysis and Design Using Amplified First-Order Analysis: Part 2—Moment Frames and General Framing Systems, *Engineering Journal,* AISC, Vol. 44, No. 4, 4th Quarter.

Presented a streamlined method for stability design of general framing systems based on the use of first-order elastic analysis to quantify the sidesway stiffness and the application of *P*-Δ shear forces calculated from amplified first-order elastic story drift values. Discussed the calculation of reduced beam stiffnesses in cases where the beams are subjected to large axial compression, e.g., due to large thrust from the foundation in some clear-span frames.

Elastic Flexural Buckling of Gabled Frames

Lu, L.W. (1965). "Effective Length of Columns in Gable Frames," *Engineering Journal,* AISC, January, 6–7.

Outlined a simple procedure for calculation of effective lengths for sidesway buckling of columns in gable frames, accounting for the influence of axial compression in the rafters.

Watwood, V.B. (1985). "Gable Frame Design Considerations," *Journal of Structural Engineering,* ASCE, 111(7), 1543–1558.

Discussed the calculation of the effective length for the rafters in an example gable frame, accounting for the rafter axial compression and the coupling with the sidesway stability of the overall structure. Suggested an approach to design of rafters subjected to significant axial compression that in essence takes the buckling load of the rafters as the axial force level in these members at incipient sidesway buckling of the full structure. This approach is equivalent to using an effective length factor for the rafters significantly larger than one for the example frame considered. White and Kim (2006) suggest that this approach to the design of the rafters is unnecessarily conservative.

Davies, J.M. (1990). "In-plane Stability in Portal Frames," *Structural Engineer,* 68(8).

Provided a simplified procedure for sidesway buckling analysis of symmetric clear-span gable frames composed of prismatic I-shaped members. The procedure accounts for the influence of axial compression in the rafters and the pitch of the rafters on the sidesway buckling resistance. The method focuses on the buckling analysis of a subassembly formed by one-half of the frame.

Davies, J.M. and Brown, B.A. (1996). *Plastic Design to BS 5950,* Steel Construction Institute, Blackwell Science, 326 pp.

Provided a comprehensive treatise on plastic design of steel frames using the BS 5950:1990. Gave extensive information on the design of pitched roof clear-span as well as multi-span frames by the British Standard using hot-rolled I-shaped members. Explained that rules in BS 5950 for checking when second-order effects may be ignored can be grossly unconservative for clear-span frames. This is because the BS 5950 procedures presuppose that clear-span frames buckle elastically in a sidesway mode solely due to the axial forces in the columns. In contrast, the authors show that the elastic buckling of clear-span frames is heavily influenced by the axial compressive force in the relatively long and more slender rafters. The authors recommended a simplified form of the transcendental equation developed by Davies (1990) for determining the elastic critical load of pinned base clear-span frames composed of prismatic members.

Silvestre, N. and Camotim, D. (1997). "Second-Order Effects in Pitched Roof Steel Frames," *Proceedings,* Annual Technical Session, Structural Stability Research Council, University of Missouri, Rolla, MO, pp. 85–98.

Proposed a method that allows for estimation of the second-order effects in one-bay pitched-roof symmetric clear-span frames accounting for both sidesway and column spreading modes of instability. The method requires the calculation of the first two buckling load values, the first buckling mode always being the sidesway (anti-symmetric) mode and the second being a column spreading (symmetric) mode. The authors identify three components of symmetric pitch-roof frame first-order moments:

1. Nonsway moments, obtained by artificially restraining the lateral deflections at the knees.
2. Symmetric sway moments, obtained by loading the knees with an equal and opposite part of the artificial reactions from step 1.
3. Anti-symmetric sway moments, obtained by loading the frame by the remainder of the previous artificial reactions.

The authors assume symmetrical loading on symmetrical frames; therefore, two equal loads are obtained for the loading in step 3. The authors found that both the symmetric and anti-symmetric bifurcation loads are influenced significantly by axial compression in the rafters. Also, they observed that the lowest eigenvalue buckling load is always associated with the anti-symmetric sidesway mode and that the ratio of the second buckling load to the first ranged from 1.04 to 2.43 in their fixed-base frames and 1.94 to 8.01 in their pinned-base frames. The frames had roof pitch angles varying from 6 to 18 degrees. The authors proposed a moment amplification equation that is similar to the AISC (2005) B_1-B_2 method but combines each of the three preceding moments with separate amplifiers based on the symmetric and anti-symmetric buckling modes for the symmetric sway and anti-symmetric sway first-order moments. Because the B_1-B_2 method is viewed as being too cumbersome by many practicing engineers, the proposed method is not likely to be of use for practical design. However, it does shed light on the underlying behavior.

Silvestre, N. and Camotim, D. (2002). "Post-Buckling Behavior, Imperfection Sensitivity and Mode Interaction in Pitched-Roof Steel Frames," *Proceedings,* Annual Technical Session, Structural Stability Research Council, University of Missouri, Rolla, MO, pp. 139–162.

Assessed the influence of the rafter compression and column base stiffness on anti-symmetric and symmetric post-buckling behavior and imperfection sensitivity in symmetric pitched roof clear-span frames. Studied frames subjected to

idealized loads causing one value of uniform axial compression in the columns and another value of uniform axial compression in the rafters. The frame members were prismatic in all cases. Identified the most detrimental frame imperfection configurations under anti-symmetric/symmetric mode coupling. Determined that second-order effects can be neglected in these types of frames when $1/\gamma_{AS} < 0.1 + 1/\gamma_S$ and $1/\gamma_S < 0.1$, where γ_S and γ_{AS} are the buckling load ratios in the symmetric and anti-symmetric modes. Observed that in addition to causing a reduction in the buckling loads, high rafter compression leads to imperfection sensitive behavior. Discovered that the most detrimental imperfection configuration corresponded to a pure symmetric mode shape. This indicates that anti-symmetric/symmetric mode interaction does not alter (increase) the frame imperfection sensitivity.

King, C. (2001a). *In-Plane Stability of Portal Frames to BS 5950-1:2000,* SCI Publication P292, Steel Construction Institute, Ascot, Berkshire, 213 pp.

Discussed the in-plane stability behavior of single-story frames (single bay and multiple bay) and explained three methods provided in the British Standard for design of these types of frames for in-plane stability: (1) the sway-check method, (2) the amplified moment method, and (3) the second-order analysis method. A large portion of the discussion addressed the application of plastic design methods for metal building frames fabricated from rolled I-shaped members with haunches at the knee joints. Plastic design with these types of members is commonly used to target the greatest economy in British practices versus the use of fabricated sections and thin webs in American practice. Discussed the separate second-order effects associated with "arching" or "snap-through" failure of rafters. Checks are instituted to guard against this mode of failure in multiple-bay frames with gables in each bay, moment continuity throughout the frame, and light interior columns. Discussed the importance of axial compression in the rafters of clear-span frames and contrasts this behavior with the behavior of beams in multiple-story rectangular frames. Suggested a simple reduction in the effective elastic stiffness of the rafters to account for the axial compression effects. This reduction may be expressed in the context of the AISC (2005) provisions and prismatic members as $(1 - \alpha P_r/P_{eL})$, where P_r is the required design axial force, $\alpha = 1.6$ in ASD and 1.0 in LRFD, $P_{eL} = \pi^2 EI/L^2$, and L is the total on-slope length of the rafters in the span under consideration for multiple-span frames or single-span frames sized by plastic design or on one-half of this length for single-span frames sized by elastic design.

King, C. (2001b). *Design of Single Span Steel Portal Frames to BS 5950-1:2000,* SCI Publication P252, Steel Construction Institute, Ascot, Berkshire.

Discussed best practices for design of single-story clear-span frames in the U.K. The guidance in this publication focused on the design of clear-span frames using hot rolled steel I-shapes. Two design examples were presented, one showing manual calculations and the other showing output from a standard computer program.

White, D.W., Surovek, A. and Chang, C.-J. (2007). "Direct Analysis and Design Using Amplified First-Order Analysis: Part 2—Moment Frames and General Framing Systems, *Engineering Journal,* AISC, Vol. 44, No. 4, 4th Quarter.

Summarized guidelines from Eurocode 3 (CEN 2005) indicating that rectangular frame idealizations presented in the paper may be applied as an acceptable approximation to gable and monoslope frames for roof slopes up to 1:2 (26°) and rafter axial compression $\alpha P_r \leq 0.09 P_{eL}$, where P_{eL} is the elastic flexural buckling load of an equivalent simply supported column having the rafter geometry and the full system length of the rafters. Suggested the calculation of P_{eL} for this check using the reduced flexural rigidity specified by the direct analysis method. Nonprismatic member geometry was not addressed; however, the concepts and procedures are readily extended to nonprismatic member geometry using the framework presented by White and Kim (2006).

Elastic Flexural Buckling of Crane Buildings

Lui, E.M. and Sun, M. (1995). "Effective Lengths of Uniform and Stepped Crane Columns," *Engineering Journal,* AISC, 3rd quarter, 98-106.

Gave a procedure for calculating the effective length factor for uniform prismatic and stepped prismatic crane columns with any values of relative shaft lengths, moments of inertia, and loading and boundary conditions. The procedure was based on the story-stiffness concept and took into account both member and frame stability effects. The procedures were based fundamentally on determining the axial force P_{Lcr} in the bottom portion of a crane column at incipient elastic sidesway buckling of a rectangular frame. The corresponding effective length factor for the bottom segment of the column was fundamentally related to P_{Lcr} by the equation $P_{Lcr} = \pi^2 EI_L/(K_L L_L)^2$, where L_L is the length of the lower segment and I_L is the moment of inertia of this segment. Similarly, the axial force P_{Ucr} in the top portion of the crane column at the incipient sidesway buckling of the structure was fundamentally related to the effective length factor of the top segment by $P_{Ucr} = \pi^2 EI_U/(K_U L_U)^2$. Consequently, $K_U = K_L\,(L_L/L_U)\,[(P_L/P_U)(I_U/I_L)]^{0.5}$. This approach generalized the effective length (or column elastic buckling load) calculations from a number of simplified procedures that have been used in practice for crane building design.

Galambos, T.V. (1988a). "Mill Building Columns," Chapter 12, *Guide to Stability Design Criteria for Metal Structures,* 4th Ed., T.V. Galambos (ed.), Wiley, New York, pp. 409–421.

Discussed traditional methods for stability design of crane columns.

White, D.W. and Kim, Y.D. (2006). "A Prototype Application of the AISC (2005) Stability Analysis and Design Provisions to Metal Building Structural Systems," Report prepared for Metal Building Manufacturers Association, School of Civil and Environmental Engineering, Georgia Institute of Technology, January, 157 pp.

Discussed generalized calculation of crane building flexural buckling loads using second-order matrix structural analysis. Explained how the direct analysis method can be applied to crane buildings, thus eliminating the need for calculation of crane column effective length factors.

Column Inelastic Flexural Buckling and Design Strength

Timoshenko, S.P. and Gere, J.M. (1961). *Theory of Elastic Stability,* McGraw-Hill, New York, 541 pp.

Discussed the calculation of inelastic buckling loads for nonprismatic bars using tangent modulus concepts. Observed, "We shall always be on the safe side if in such cases [variable cross-section members with a variation of the column tangent modulus along their length] we use formulas derived for elastic conditions and substitute them for E in the tangent modulus E_t calculated for the cross-section with the maximum compressive stress."

Kim, M.C., Lee, G.C. and Chang, K.C. (1995). "Inelastic Buckling of Tapered Members with Accumulated Strain," *Structural Engineering and Mechanics,* 3(6), 611–622.

Developed a beam finite element for analysis of tapered members considering three types of residual stress patterns and a stress-strain curve that is elastic-perfectly plastic-strain hardening. The investigation was concerned with the capacity of tapered members with accumulated strains resulting from previous loading history.

Jimenez Lopez, G.A. (1998). "Inelastic Stability of Tapered Structural Members," Doctoral Dissertation, University of Minnesota, Minneapolis-St. Paul, MN, 201 pp.

Conducted inelastic analyses using the beam-theory-based slope-deflection equations from Lee et al. (1972) and accounting for initial out-of-straightness, nominal Lehigh (Galambos and Ketter, 1959) residual stress effects, and end restraint effects. Constructed column curves for specific cases of linearly tapered I-shaped members, assuming compact cross-section behavior (i.e., no consideration of web or flange plate slenderness effects).

Jimenez, G. and Galambos, T.V. (2001). "Inelastic Stability of Pinned Tapered Columns," *Proceedings,* Annual Technical Session, Structural Stability Research Council, University of Missouri, Rolla, MO, pp. 143–158.

Presented inelastic buckling solutions for simply supported tapered columns and compared them with the nominal resistances calculated using the procedures in Appendix F of the AISC-LRFD *Specification* (1993). The design procedures in Appendix F of the AISC-LRFD *Specification* (1993) are based on Lee et al. (1972). Showed that the AISC-LRFD *Specification* (1993) produces conservative results for all the cases studied.

White, D.W. and Kim, Y.D. (2006). "A Prototype Application of the AISC (2005) Stability Analysis and Design Provisions to Metal Building Structural Systems," Report prepared for Metal Building Manufacturers Association, School of Civil and Environmental Engineering, Georgia Institute of Technology, Atlanta, GA, January, 157 pp.

and

Kim, Y.D. (2010). "Behavior and Design of Metal Building Frames with General Prismatic and Web-Tapered Steel I-Section Members," Doctoral Dissertation, School of Civil and Environmental Engineering, Georgia Institute of Technology, Atlanta, GA, 562 pp.

Developed a general procedure, based on AISC (2005), for calculation of column elastic or inelastic axial resistance for any type of prismatic or nonprismatic I-shaped member subjected to constant or variable axial compression along its length. The procedure considers all types of member cross-section geometries, including cross sections having slender plate elements under uniform axial compression. The procedure starts with (1) the calculation of a member elastic buckling load ratio $\gamma_e = F_e/f_r$, where F_e is the axial stress at the most highly stressed cross section along the length at incipient elastic buckling of the member and f_r is the corresponding design axial stress at this cross section, and (2) the calculation of the equivalent yield ratio f_r/QF_y at the most highly stressed cross section. The term γ_e can be applied to address not only flexural buckling, but also torsional, flexural-torsional, and constrained axis torsional buckling of columns as applicable. The calculation of inelastic column resistance parallels the approach taken by Lee et al. (1981), except that the calculation of the elastic buckling load is generalized within the γ_e parameter, and the design resistances are expressed in terms of γ_e rather than in terms of the length of an equivalent prismatic column composed of one of the column cross-sections. By using the term γ_e, the proposed procedure can be extended to provisions other than those in AISC (2005). In Kim (2010), an alternative approach using the AISI (2007) unified effective width equations is presented for calculating column axial resistance. The AISI (2007) approach provides more accurate solutions typically for box sections with slender elements and large KL/r.

First- and Second-Order Elastic Beam-Column and/or Frame Analysis (Planar Analysis)

Fogel, C.M. and Ketter, R.L. (1962). "Elastic Strength of Tapered Columns," *Journal of the Structural Division,* ASCE, 88(ST5), 67–105.

Focused on the interaction of axial thrust and bending moment with the first yield as the limit. Solved the governing differential equations using Bessel functions and numerical integration.

Karabolis, D.L. and Beskos, D.E. (1983). "Static, Dynamic and Stability Analysis of Structures Composed of Tapered Beams," *Computers and Structures,* 16(6), 731–748.

Developed a finite element for analysis of arbitrary cross-section members with a linearly varying depth. The element geometric stiffness matrix was constructed on the basis of shape functions corresponding to the exact static displacement function of a tapered member for the case of zero axial load. The approach shows good accuracy for stability analysis using four or five elements per member.

Aristizabal-Ochoa, J.D. (1987). "Tapered Beam and Column Elements in Unbraced Frame Structures," *Journal of Computing in Civil Engineering,* ASCE, 1(1), 35–49.

Derived closed form beam matrix equations for first-order planar analysis of frames with linearly tapered members.

Guo, C.Q. and Roddis, W.M.K. (1999). "The Significance of P-Δ Effects in Single-Story Metal Building Design," Structural Engineering and Engineering Materials SL Report 99-2, University of Kansas Center for Research, Lawrence, KS, 61 pp.

Studied second-order effects in representative clear-span and modular metal building frames. Determined that the P-Δ effects are small in clear-span frames but are significant in modular frames. All analyses were conducted at working load levels. Second-order effects were not considered at ultimate load levels.

Kim, Y.D. and White, D.W. (2006a). "Benchmark Problems for Second Order Analysis of Frames with Tapered-Web Members," Structural Engineering Mechanics and Materials Report No. 53, School of Civil and Environmental Engineering, Georgia Institute of Technology, Atlanta, GA, 10 pp.

Provided converged second-order elastic analysis solutions for two basic benchmark problems involving linearly tapered web members. Discussed the results using two representative second-order elastic analysis approaches, one in which the influence of the taper was accounted for directly within the element formulation and the other which used a larger number of standard prismatic beam elements. Also, compared to solutions based on the slope-deflection equations developed by Lee et al. (1972). Showed that the slope-deflection equations from Lee et al. can exhibit substantial error relative to the rigorous solutions even for relatively minor taper and small axial load.

Guney, E. and White, D.W. (2007). "Ensuring Sufficient Accuracy of Second-Order Frame Analysis Software," Structural Engineering Mechanics and Materials Report No. 55, School of Civil and Environmental Engineering, Georgia Institute of Technology, Atlanta, GA, May, 95 pp.

Studied the number of elements required to ensure less than 5% error in the nodal displacements and less than 3% error in the maximum internal moments for second-order elastic analysis of prismatic members with a wide range of loadings and end conditions. Also, addressed the number of elements required to ensure less than 2% error in eigenvalue buckling analysis solutions. Considered the requirements for P-Δ only analysis procedures as well as for standard element formulations based on a cubic transverse displacement approximation. Demonstrated that the cubic displacement-based formulation requires substantially fewer elements per member to achieve the desired levels of accuracy when the stability effects are significant. These recommendations may be applied for nonprismatic members based on the assumption that the elastic stiffness of these types of members is represented with negligible error.

Column Constrained-Axis Torsional Buckling

Kim, Y.D. and White, D.W. (2006d). "Elastic Torsional and Flexural-Torsional Buckling Estimates for I-shaped Members with Linearly-Tapered Webs," Structural Engineering Mechanics and Materials Report No. 53, School of Civil and Environmental Engineering, Georgia Institute of Technology, Atlanta, GA, 12 pp.,

Kim, Y.D. and White D.W. (2007a). "Practical Buckling Solutions for Tapered Beam Members," *Proceedings*, Annual Technical Session, Structural Stability Research Council, University of Missouri, Rolla, MO, April, pp. 259–278.

and

Kim, Y.D. (2010). "Behavior and Design of Metal Building Frames with General Prismatic and Web-Tapered Steel I-Section Members," Doctoral Dissertation, School of Civil and Environmental Engineering, Georgia Institute of Technology, Atlanta, GA, 562 pp.

Performed a finite element parametric study of the elastic constrained axis torsional buckling of I-shaped members with linearly tapered web depth and out-of-plane displacements constrained at the centroidal axis of purlins or girts attached to one flange. Used the three-dimensional beam finite element from Chang (2006). Showed that the constrained axis torsional buckling loads of tapered members can be estimated with good accuracy by using the analytical equations

for a prismatic member from Timoshenko and Gere (1961) or Bleich (1952), with the cross section geometry at the middle of the longer unbraced length of the inside flange.

Beam and Beam-Column Elastic Lateral-Torsional Buckling

Stussi, F. (1935). *Schweiz. Bauztg,* Vol 105, p. 123. (also *Publ. IABSE*, Vol. 3, p. 401).

Applied the method of successive approximations to investigate the lateral buckling of rectangular cross-section beams.

Bleich, F. (1952). *Buckling Strength of Metal Structures,* McGraw-Hill, New York, 508 pp.

Provided detailed discussions of numerical solution procedures based on the method of successive approximations for thin-walled open section beam lateral torsional buckling problems. These developments were based largely on the research of Salvadori (1951).

Lee, G.C. (1959). "On the Lateral Buckling of a Tapered Narrow Rectangular Beam," *Journal of Applied Mechanics,* 26, 457–458.

Established that for small tapering angles (15 degrees or less), Euler-Bernoulli theory for beams yields satisfactory results.

Culver, C.G. and Preg, S.M. (1968). "Elastic Stability of Tapered Beam-Columns," *Journal of the Structural Division,* ASCE, ST2, 455–470.

Derived the differential equations for elastic buckling of tapered I-shaped beam-columns. The differential equations were solved using the finite difference method. Solutions were presented in tables for design use.

Lee, G.C., Morrell, M.L. and Ketter, R.L. (1972). "Design of Tapered Members," *Welding Research Council Bulletin,* No. 173, 1–32.

Addressed the analysis of linearly tapered beam-columns of doubly symmetric I-shapes. Both in-plane and lateral-buckling strengths were determined using a Rayleigh-Ritz procedure. The authors developed tables enabling the designer to determine the length of an equivalent prismatic beam that buckles elastically at the same level of loading as applied to the web-tapered member.

Kitipornchai, S. and Trahair, N.S. (1972). "Elastic Stability of Tapered I-Beams," *Journal of the Structural Division,* ASCE, 98(ST3), 713–728.

Studied the elastic twisting and flexural-torsional buckling of tapered I-beams theoretically. Developed a general method of analysis and showed reasonable agreement with experiments conducted on beams with flange-width or web-depth taper. Showed that the elastic critical loads of depth-tapered beams do not vary greatly as the degree of taper increases. Indicated that this behavior is related to the insensitivity of the torsional stiffness to the degree of taper.

Morrell, M.L. and Lee, G.C. (1974). "Allowable Stresses for Web-Tapered Beams with Lateral Restraints," *Welding Research Council Bulletin,* No. 192, 1–12.

and

Lee, G.C. and Morrell, M.L. (1975). "Application of AISC design provisions for tapered members," *Engineering Journal,* AISC, 12(1), 1–13.

Developed factors that estimate the effects of restraint from adjacent unbraced segments and moment or flange stress gradients along the length on the elastic LTB resistance of linearly tapered web I-shaped members. These factors were incorporated as the parameter B in the AISC ASD provisions for linearly tapered members. The solutions built on the work by Lee et al. (1972) and focused on four idealizations:

1. Three equal unbraced segments with the largest moment M_2 located within the middle segment and a larger moment M_1 at one end of the three segments. The actual moment or stress distribution in the middle segment and whether M_1 occurs in the adjacent segment with the larger or the smaller end is not addressed in the resulting equation for B. The adjacent unbraced lengths were assumed to be torsionally simply supported at the ends of the three-segment assembly.
2. Two equal unbraced segments with the largest flexural stress occurring at the larger end and the smallest flexural stress occurring at the smaller end of the adjacent unbraced segments. The distribution of the flange flexural stresses along the unbraced length was not considered in the final equation for B. The adjacent unbraced lengths were assumed to be torsionally simply supported at the ends of the two-segment assembly.
3. Two equal unbraced segments with the largest flexural stress occurring at the smaller end and the smallest flexural stress occurring at the larger end of the adjacent unbraced segments. The distribution of the flange flexural stresses along the unbraced length was not considered in the final equation for B. The adjacent unbraced lengths were assumed to be torsionally simply supported at the ends of the two-segment assembly.
4. One unbraced length with a linear moment diagram having zero moment at the smaller end of the member and maximum moment at the larger end. Torsionally simply supported end conditions were assumed at the ends of the unbraced length.

The results from Kim and White (2006c, 2007a) indicate that the direct application of the Yura and Helwig (1996) C_b approach to determining the elastic LTB resistance gives an alternative highly accurate accounting for flange stress gradient effects. The procedure for handling end-restraint effects in prismatic members, recommended by Nethercot and Trahair (1976) and summarized in Galambos (1998), has good potential to be extended to linearly tapered members to

account for end restraint effects. This approach has been applied extensively for calculation of prismatic member LTB resistances (White and Jung, 2008; White and Kim, 2008).

Kitipornchai, S. and Trahair, N.S. (1975). "Elastic Behavior of Tapered Monosymmetric I-Beams," *Journal of the Structural Division,* ASCE, 101(ST8), 1661–1678.

Developed a general theory for the first-order bending and torsion of tapered monosymmetric I-beams. Explained additional terms that appear in the solutions due to the taper. Explained that the bending and torsion equations are interdependent in tapered monosymmetric I-beams such that the behavior cannot be separated into independent bending and torsion actions.

Hsu, T.L. and Lee, G.C. (1981). "Design of Beam Columns with Lateral-Torsional End Restraints," *Welding Research Council Bulletin,* No. 272, November, 1–23.

Developed charts of effective length factors *K* for estimation of the elastic LTB resistance of doubly symmetric prismatic beams for the two separate cases considered in the double-formula approach of the AISC ASD *Specification*: (1) only St. Venant torsional stiffness considered and (2) only warping torsional stiffness considered. Galambos (1988b) suggested that these equations may be applied for tapered beams with a small tapering ratio, but no limits were provided for this type of application. The charts are based on consideration of the ratio of the I_y/L of the unbraced length under consideration to the I_y/L of the adjacent unbraced length, which is assumed to provide restraint. The separate charts for the St. Venant and the warping torsion-based *K* values are approximately the same. The influence of the moments and moment gradients in the adjacent unbraced lengths were not considered. Only the relative first-order elastic properties of the unbraced lengths are considered. Nethercot and Trahair (1976) developed a design method for determining the elastic LTB resistances of doubly symmetric prismatic I-beams that provides a more correct accounting for the end restraint provided by adjacent segments. The Nethercot and Trahair approach is summarized in Galambos (1998). Concluded that beam-column design can be achieved best by considering two separate equations, one for in-plane and the other for out-of-plane failure modes.

Brown, T.G. (1981). "Lateral-Torsional Buckling of Tapered I-Beams," *Journal of the Structural Division,* ASCE, 107(ST4), 689–697.

Determined critical buckling loads for simply supported beams with a double linear web taper and tapered web cantilever beams using central finite differences. The effect of loads placed either above or below the centroid is included. Solutions by subsequent authors do not agree with Brown's solutions.

Wekezer, J.W. (1985). "Instability of Thin-Walled Bars," *Journal of Engineering Mechanics,* 111(7), 923–935.

and

Wekezer, J.W. (1985). "Nonlinear Torsion of Thin-Walled Bars of Variable Open Cross-Section," *International Journal of Mechanical Sciences,* 27(10), 631–641.

First research that studied the LTB of thin-walled tapered beams with arbitrary cross section and loading. Used a finite element formulation in which the walls were treated as membranes and both the in-plane cross-section deformations and the mid-surface shear strains were neglected. Andrade and Camotim (2005) indicate that the formulation is not fully consistent, mostly because the locus of shear centers is not properly handled.

Yang, Y.B. and Yau, J.-D. (1987). "Stability of Beams with Tapered I-Sections," *Journal of Engineering Mechanics,* ASCE, 113(9), 1337–1357.

Derived the differential equations of equilibrium for a doubly symmetric thin-walled open-section tapered I-beam and formulated a finite element based on these equations. Comparisons are made with other existing solutions. Andrade and Camotim (2005) indicate that the formulation adopts a number of simplifying assumptions and show slightly different solutions in benchmark problems.

Bradford, M.A. (1988). "Stability of Tapered I-Beams," *Journal of Constructional Steel Research,* 9(3), 19–216.

and

Bradford, M.A. and Cuk, P.L. (1988). "Elastic Buckling of Tapered Monosymmetric I-Beams," *Journal of Structural Engineering,* ASCE, 114(5), 977–996.

Developed a finite element formulation for I-beams having equal or unequal size flanges with uniform or variable width and with webs having constant or linearly tapered height. Andrade and Camotim (2005) indicate that the formulation adopts a number of simplifying assumptions and show slightly different solutions in benchmark problems. Proposed new design equations for use with the Australian Standard AS 1250 (SAA, 1987) and British Standard BS 5950 (BSI, 1985).

Braham, M. and Hanikenne, D. (1993). "Lateral Buckling of Web Tapered Beams: An Original Design Method Confronted with a Computer Simulation," *Journal of Constructional Steel Research,* 27, 23–36.

Analyzed linearly tapered web I-shaped members using a constant depth thin-walled open-section beam finite element, by discretizing the beams into 20 segments. Developed suggestions for design based on these results. Other authors have shown that the approach taken in this paper can lead to incorrect LTB solutions.

Rajasekaran, S. (1994a). "Equations for Tapered Thin-Walled Beams of Generic Open Section," *Journal of Engineering Mechanics,* ASCE, 120(8), 1607–1629.

and

Rajasekaran, S. (1994b). "Instability of Tapered Thin-Walled Beams of Generic Section, *Journal of Engineering Mechanics,* ASCE, 120(8), 1630–1640.

Derived nonlinear equilibrium equations valid for tapered beams with arbitrary cross sections, which were then solved by the finite element method. Andrade and Camotim (2005) indicate that Rajasekaran's derivation is inconsistent because it omits terms having the same order of magnitude as others which are retained.

Yura, J. and Helwig, T. (1996). "Bracing for Stability," Short Course Notes, Structural Stability Research Council.

Proposed a procedure for calculating the LTB strength of linearly tapered I-shaped beams based on the use of the AISC C_b equations, written in terms of the compression flange stresses, and the analytical elastic LTB equations for a prismatic member, using the tapered member cross section at the middle of the unbraced length.

Ronagh, H.R., Bradford, M.A. and Attard, M.M. (2000a). "Nonlinear Analysis of Thin-Walled Members of Variable Cross-section. Part I: Theory," *Computers and Structures,* 77, 285–299.

and

Ronagh, H.R., Bradford, M.A., and Attard, M.M. (2000b). "Nonlinear Analysis of Thin-Walled Members of Variable Cross-section. Part II: Application," *Computers and Structures,* 77, 301–313.

Formulated and applied a thin-walled open-section beam finite element for tapered cross-section members. Showed that their element agrees with the results from Kitipornchai and Trahair (1975) for the first-order analysis case. Applied their nonlinear element for elastic buckling analysis of doubly symmetric I-shaped members and compare to numerical solutions by a number of other authors.

Maquoi, R. (2004). "Recent European Advances in the Member Verification to Lateral Torsional Buckling," *Proceedings,* Annual Technical Session, Structural Stability Research Council, University of Missouri, Rolla, MO, pp. 265–284.

Described a MathCAD application named ELTBTB that addresses the elastic lateral-torsional buckling analysis of web-tapered beams. The program's scope includes simply supported single-span beam segments, doubly or singly symmetric I-shapes, web depth varying linearly between the segment ends with other cross-section dimensions remaining constant, and bending about the major-axis due to end moments only.

Andrade, A. and Camotim, D. (2003). "Lateral-Torsional Buckling of Singly symmetric Web-Tapered I-shaped Beams and Cantilevers," *Proceedings,* Annual Technical Session, Structural Stability Research Council, University of Missouri, Rolla, MO, pp. 233–254.

and

Andrade, A. and Camotim, D. (2005). "Lateral-Torsional Buckling of Singly symmetric Web-Tapered Beams: Theory and Application," *Journal of Engineering Mechanics,* ASCE, 131(6), 586–597.

Formulated the equations for elastic LTB of singly symmetric web-tapered I-shaped members. Evaluated the critical moments by the Rayleigh-Ritz method. Conducted a parametric study to assess the influence of web taper and section monosymmetry on elastic LTB predictions for cantilevers and simply supported beams. In the second paper, the authors demonstrated that replacing a tapered member by a piecewise prismatic one does not lead to the correct LTB solution. The authors also provided a list of various formulations in which there are known errors in the approach.

Andrade, A., Camotim, D. and e Costa, P.P. (2005). "Elastic Lateral Torsional Buckling Behavior of Doubly Symmetric Tapered Beam-Columns," *Proceedings,* Annual Technical Session, Structural Stability Research Council, University of Missouri, Rolla, MO, pp. 445–468.

Extended the previous work by Andrade and Camotim (2003) to include the influence of prebuckling displacements. The authors demonstrate that replacing a tapered member by a piecewise prismatic one does not lead to the correct LTB solution, regardless of the number of segments considered, since relevant behavior aspects due entirely to the cross-section variation are not captured.

Boissonnade, N. and Maquoi, R. (2005). "A Geometrically and Materially Non-linear 3-D Beam Finite Element for the Analysis of Tapered Steel Members," *Steel Structures,* 5, 413–419.

Developed a three-dimensional finite element based on application of thin-walled open-section beam theory. The authors demonstrated—analytically and numerically—that the use of prismatic beam finite elements for the analysis of tapered beams (by subdividing the member into small segments) can lead to significant errors when the behavior is influenced by torsion.

Chang, C.J. (2006). "Construction Simulation of Curved I-Girder Bridges," Ph.D. Dissertation, School of Civil and Environmental Engineering, Georgia Institute of Technology, Atlanta, GA, 340 pp.

Developed a beam finite element for three-dimensional analysis of tapered doubly and singly symmetric I-shaped members. Benchmark solutions indicated that the element gives predictions for elastic LTB similar to those presented by Yang and Yau (1987) and slightly more conservative than those presented by Andrade and Camotim (2005).

Kim, Y.D. and White, D.W. (2006c). "Elastic Lateral Torsional Buckling Estimates for I-shaped Members with Linearly-Tapered Webs," Structural Engineering Mechanics and Materials Report No. 54, School of Civil and Environmental Engineering, Georgia Institute of Technology, Atlanta, GA, 15 pp.

Kim, Y.D. and White, D.W. (2007a). "Practical Buckling Solutions for Tapered Beam Members," *Proceedings*, Annual Technical Session, Structural Stability Research Council, University of Missouri, Rolla, MO, April, pp. 259–278.

and

Kim, Y.D. (2010). "Behavior and Design of Metal Building Frames with General Prismatic and Web-Tapered Steel I-Section Members," Doctoral Dissertation, School of Civil and Environmental Engineering, Georgia Institute of Technology, Atlanta, GA, 562 pp.

Applied the beam element developed by Chang (2006) to study the accuracy of the LTB approximation suggested by Yura and Helwig (1996) for linearly tapered members subjected to various linear moment diagrams. Showed that the Yura and Helwig procedure gives an accurate estimate of the converged FEA solution. Improved results are obtained using the AASHTO (2004, 2007) C_b equation with the Yura and Helwig procedure.

Andrade, A., Camotim, D. and Dinis, P.B. (2007). "Lateral-Torsional Buckling of Singly Symmetric Web-Tapered Thin-Walled I-Beams: 1D Model vs. Shell FEA," *Computers and Structures*, Vol. 85, Issue 17–18, pp. 1343–1359.

Evaluated the one-dimensional model developed by Andrade and Camotim (2003) for capturing the correct elastic LTB loads and buckling modes for prismatic and web-tapered cantilevers and web-tapered simply supported beams. Compared elastic LTB solutions obtained using the one-dimensional beam model with the ones obtained by two-dimensional shell finite element analyses. Concluded that the one-dimensional predictions agree well with the shell finite element analysis results with or without consideration of the pre-buckling deflections. Noted large differences between the one-dimensional and shell finite element models for shorter beams, which are mainly due to either significant web and flange distortion or a localized web buckling in the vicinity of the loading points.

Andrade, A., Providencia, P. and Camotim, D. (2010). "Elastic Lateral-Torsional Buckling of Restrained Web-Tapered I-Beams," *Computers and Structures*, Vol. 88, Issue 21–22, pp. 1179–1196.

Demonstrated how to include the effects of linear elastic or rigid restraints in the one-dimensional model previously developed by Andrade and Camotim (2003) to capture the elastic buckling behavior of doubly symmetric thin-walled tapered beams. The considered restraints can be translational, torsional, minor-axis bending, and/or warping restraints. Illustrated that the use of prismatic elements, regardless of the number of elements considered, cannot provide the correct elastic LTB solutions for web-tapered I-section beams.

Beam and Beam-Column Design Resistances

Lee, G.C., Morrell, M.L. and Ketter, R.L. (1972). "Design of Tapered Members," *Welding Research Council Bulletin,* No. 173, 1–32.

Summarized an experimental and analytical investigation conducted to determine the behavior of tapered members. The results were used to develop design formulas. A discussion of special considerations required for analysis of frames including tapered members was included. Design aids for the determination of the effective length factor of a tapered column connected to a prismatic rafter were provided. The general design philosophy involved the application of modification factors adjusting the length to convert the tapered member to an equivalent prismatic member composed of the cross section at the shallower end for implicit calculation of the underlying elastic buckling strengths. Separate length modification factors were developed for St. Venant and warping torsion LTB resistances. The AISC ASD formulas for prismatic members were then applied to determine the web-tapered member strength.

Morrell, M.L. and Lee, G.C. (1974). "Allowable Stresses for Web-Tapered Beams with Lateral Restraints," *Welding Research Council Bulletin,* No. 192, 1–12.

and

Lee, G.C. and Morrell, M.L. (1975). "Application of AISC Design Provisions for Tapered Members," *Engineering Journal,* AISC, 12(1), 1–13.

Continued the work of Lee et al. (1972). Improved the flexural strength formulas from Lee et al. (1972) by incorporating the total resistance to lateral buckling and restraining effects of adjacent spans and accounting for moment or flexural stress gradients along the member lengths. Developed four modification equations that relate to common cases in practice: (1) maximum moment within the middle segment of three adjacent segments, (2) larger bending stress at the larger end of two adjacent segments, (3) larger bending stress at the smaller end of two adjacent segments, and (4) single segment with zero bending at shallower end of the tapered member.

Prawel, S.P., Morrell, M.L. and Lee, G.C. (1974). "Bending and Buckling Strength of Tapered Structural Members," *Welding Research Supplement,* Vol. 53, February, 75–84.

Performed experimental tests of 15 linearly tapered I-shaped members to investigate the inelastic buckling strength. The members were fabricated using a one-sided continuous weld of the flanges to the web, producing an unsymmetrical pattern of residual stresses with respect to the weak-axis of bending. Two sets of tapered members were tested: one fabricated from plates that were shear cut and the other fabricated from oxygen cut plates. Two of the tests were beam tests containing three unbraced segments and loaded by quarter point loads to produce uniform bending stress in the center segment. One was a beam test loaded at the quarter points to produce a flexural stress gradient in the center segment. The other 12 tests were beam-column tests with lateral support only at the ends of the members, cantilevered from one end support and loaded at various angles from the horizontal to produce both axial compression and bending.

Falby, W.E and Lee, G.C. (1976). "Tension-Field Design of Tapered Members," *Engineering Journal,* AISC, First Quarter 1976, 11–17.

Suggested four models for determining the shear tension-field strength of I-girder web panels bounded by vertical stiffeners, a horizontal top flange, and a sloping bottom flange: (1) for taper angles less than about 4 degrees, use of the average h/t_w and a/h with Basler's tension-field equations; (2) for taper angles less than about 7 degrees, two different adaptations of Basler's model in which the shear buckling contribution is calculated at the end of the panel at which the tension field diagonal intersects the top flange and in which the angle of inclination of the tension field is influenced by the depth at the opposite end of the panel; and (3) for taper angles greater than 7 degrees, a modified form of Basler's model that assumes only a partial tension field.

Lee, G.C., Chen, Y.C. and Hsu, T.L. (1979). "Allowable Axial Stress of Restrained Multi-Segment, Tapered Roof Girders," *Welding Research Council Bulletin,* No. 248, 1–28.

Presented graphical procedures for determination of the axial resistance for restrained multi-segment rafters. Design aids were presented for determination of the effective length factor K_γ for in-plane buckling of these types of members. This factor modified the length of a prismatic member having the same cross-section properties as the smallest section of the tapered member, such that the critical stress was the same as the tapered roof girder. The properties of the modified prismatic member could then be used to determine an effective length factor for the tapered column using the design aids developed by Lee et al. (1972). The developed procedures were not incorporated into the AISC ASD provisions but are summarized in Lee et al. (1981).

Salter, J.B., Anderson, D. and May, I.M. (1980). "Tests on Tapered Steel Columns," *The Structrual Engineer,* 58A(6), 189–193.

Performed eight experimental tests on one-half to one-third scale web-tapered welded I-shaped beam-columns. The ends of each member were pinned, with twisting and warping prevented. In three of the tests, lateral restraint was provided at the mid-length. The loading in all cases comprised axial load, together with a major-axis moment applied at one end. The five beam-columns without intermediate restraint failed by inelastic lateral-torsional buckling. Two of the beam-columns where an intermediate restraint was attached to the tension flange (in flexure) failed in a torsional mode. In one test, the compression flange (in flexure) had an intermediate lateral restraint. The failure of this test was by buckling of a plate forming part of the lateral restraint, but the loads were significantly higher, the deflections were markedly nonlinear, and the failure of the beam-column was judged to be imminent at this stage.

Lee, G.C. and Hsu, T.L. (1981). "Tapered Columns with Unequal Flanges," *Welding Research Council Bulletin,* No. 272, November, 15–23.

Presented design charts that address the strength of linearly tapered I-shaped members subjected to combined axial compression and major-axis bending and accounting for the different strength interaction curves associated with the flexural-torsional stability behavior of these types of members (relative to in-plane resistances). These charts were not incorporated into the AISC ASD provisions.

Shiomi, H., Nishikawa, S. and Kurata, M. (1983). "Tests on Tapered Steel Beam-Columns," *Transactions of JSCE,* 15, 99–101.

and

Shiomi, H. and Kurata, M. (1984). "Strength Formula for Tapered Beam-Columns," *Journal of Structural Engineering,* 110(7), 1630–1643.

Experimentally tested 24 beam-columns of full size welded I-shapes. Nineteen tests were made on laterally unsupported members (OT-series tests), and five tests were on laterally supported members (IT-series tests). The ends of each member were pinned, with twisting and warping prevented. The loading in all cases comprised axial load, together with a major-axis moment applied at one end.

Murray, T.M. (1986). "Stability of Gable Frame Panel Zone Plates," *Proceedings,* Annual Technical Session, Structural Stability Research Council, University of Missouri, Rolla, MO, pp. 317–325.

Experimentally tested ten L-shaped specimens representing the knee area of gable metal building frames with compression on the inside flanges at the knee. Evaluated the shear strength of the panel zone web plates in the knee area, where

the web plate is supported on two sides by the continuation of the outside column and rafter flanges. A full-depth moment connection end plate, approximately aligned with the inside column flange supported the third side. Either a full-depth or partial-depth column web stiffener approximately aligned with the inside rafter flange, supported the fourth side. The results showed that the AISC (2005) shear yield or shear buckling equations adequately predict the experimental strengths for the different cases where the equations apply. However, the results indicated that Basler's tension field equations as implemented in the AISC (2005) *Specification* accurately predict the panel zone strength only for specimens having full-depth column web stiffeners.

Sumner, E.A. III (1995). "Experimental and Analytical Investigation of the LRFD Strength of Tapered Members," M.S. Thesis, Charles Via Department of Civil Engineering, Virginia Polytechnic Institute and State University, Blacksburg, VA.

Studied the strength of the rigid knee portion of gable frames. Eight specimens consisting of a tapered column and a portion of a tapered rafter were tested under three types of loading that approximated gravity, lateral and cyclic load cases. Strengths calculated by AISC (1993) LRFD were compared with the experimentally determined capacities. The LRFD shear strength provisions were shown to be overly conservative. Procedures for application of the LRFD tension-field action model to account for the postbuckling strength of tapered webs were presented. The application of tension field action to end panels, panels with large aspect ratios and hybrid girders was also addressed.

Polyzois, D. and Raftoyiannis, I.G. (1998). "Lateral-Torsional Stability of Steel Web-Tapered I-Beams," *Journal of Structural Engineering,* ASCE, 124(10), 1208–1216.

Reexamined the modification factor equations from Morrell and Lee (1974) and Lee and Morrell (1975) and suggested changes that cover a wider range of geometry and loading cases. Questioned the use of one modification factor to account for both the moment or stress gradient and the restraint provided by adjacent segments. Developed separate modification factors for the stress gradient and the continuity effects for various load cases.

Jimenez Lopez, G.A. (1998). "Inelastic Stability of Tapered Structural Members," Doctoral Dissertation, University of Minnesota, Minneapolis-St. Paul, MN, 201 pp.

Conducted inelastic analyses using the beam-theory-based slope-deflection equations from Lee et al. (1972) (for analysis in the plane of bending) and accounting for initial out-of-straightness, nominal Lehigh (Galambos and Ketter, 1959) residual stress effects. Determined inelastic LTB resistances for compact-section beams and beam-columns based on thin-walled open-section beam theory equations and inelastic eigenvalue analysis. Compared inelastic analysis solutions to results from Salter et al. (1980), and Shiomi and Kurata (1984). Suggested a modified form of the equations from Lee et al. (1972) for design calculation of LTB resistances. Suggested a bilinear concave-up beam LTB strength curve for the inelastic transition region between $0.5M_p$ and M_p.

Miller, B.S. and Earls, C.J. (2003). "Behavior of Web-Tapered Built-Up I-Shaped Beams," Report CE/ST 28, Department of Civil and Environmental Engineering, University of Pittsburgh, 132 pp.

and

Miller, B.S. and Earls, C.J. (2003). "On Moment Capacity and Flexural Ductility in Doubly Symmetric Web-Tapered I-Girders," *Proceedings,* Annual Technical Session, Structural Stability Research Council, University of Missouri, Rolla, MO, pp. 267–280.

Studied the inelastic strength and ductility of web-tapered I-shaped beams using full, nonlinear finite element models created with ABAQUS. Considered a geometric imperfection dominated by web bend buckling and elastic out-of-plane bracing restraints. Did not consider residual stresses. Focused primarily on development of highly restrictive compactness criteria necessary to satisfy an idealized rotation capacity of three at the location of plastic hinges in web-tapered members.

Jimenez, G.A. (2006). "Further Studies on the Lateral-Torsional of Steel Web-Tapered Beam-Columns," *Proceedings,* Annual Technical Session, Structural Stability Research Council, University of Missouri, Rolla, MO, pp. 267–280.

Presented solutions for the elastic and inelastic lateral-torsional buckling of linearly tapered web depth compact I-shaped members. The beam-columns are subjected to axial force and to bending moments applied at both ends of the member. The Lehigh (Galambos and Ketter, 1959) residual stress pattern is assumed. Two types of solutions were considered: (1) finite difference solutions based on thin-walled open-section beam theory, and (2) an ANSYS three-dimensional Timoshenko beam finite element that includes cross section warping and accommodates linear web taper. The ANSYS solution gave slightly more conservative results. Comparisons were made with AISC (1999) *Specification* equations and with five test results from Salter et al. (1980). Suggested a modified form of the equations from Lee et al. (1972) for design calculation of LTB resistances. Suggested a bilinear concave-up beam LTB strength curve for the inelastic transition region between $0.5M_p$ and M_p.

White, D.W. and Kim, Y.D. (2006). "A Prototype Application of the AISC (2005) Stability Analysis and Design Provisions to Metal Building Structural Systems," Report prepared for Metal Building Manufacturers Association, School of Civil and Environmental Engineering, Georgia Institute of Technology, Atlanta, GA, January, 157 pp.

and

Kim, Y.D. (2010). "Behavior and Design of Metal Building Frames with General Prismatic and Web-Tapered Steel I-Section Members," Doctoral Dissertation, School of Civil and Environmental Engineering, Georgia Institute of Technology, Atlanta, GA, 562 pp.

Developed a general procedure, based on AISC (2005), for calculation of I-shaped member flexural resistances. For handling of the LTB limit state, the procedure parallels the method developed by the authors for generalized calculation of the column axial resistance. That is, the method is based on the independent calculation of the member elastic LTB resistance and the consideration of the compression flange stress at the most highly stressed cross section along the member length. Suggested a procedure from Yura and Helwig (1996) for calculation of the elastic LTB resistance of linearly tapered web depth members. This procedure is subsequently validated by Kim and White (2006c, 2007a), using elastic LTB solutions based on three-dimensional thin-walled open-section beam theory. The general procedures for calculating member flexural resistances developed in White and Kim (2006) and Kim (2010) are evaluated by Kim and White (2008, 2010) and Kim (2010).

Kim, Y.D. and White, D.W (2006b). "Full Nonlinear Finite Element Analysis Simulation of the LB-3 Test from Prawel et al. (1974)," Structural Engineering Mechanics and Materials Report No. 56, School of Civil and Environmental Engineering, Georgia Institute of Technology, Atlanta, GA, September, 15 pp.

Conducted full nonlinear finite element analysis using ABAQUS (HKS, 2006) for the beam test, LB-3 from Prawel et al. (1974). Four types of nominal residual stress patterns and three types of nominal geometric imperfections are tested. The finite element solutions and the experimental result provided by Prawel et al. (1974) are compared to the design strength calculated based on the procedures provided by White and Kim (2006). Suggested a nominal geometric imperfection involving flange sweep and three types of residual stress patterns for studying available experimental tests using finite element analysis. If specific geometric imperfections and residual stresses are provided, these initial conditions are suggested to be used in finite element simulations.

Kim, Y.D. and White, D.W. (2007b). "Assessment of Nominal Resistance Calculations for Web-Tapered I-shaped Members: Comparison to Experimental Tests and to Finite Element Simulations of Experimental Tests" Structural Engineering Mechanics and Materials Report No. 31, School of Civil and Environmental Engineering, Georgia Institute of Technology, Atlanta, GA, May, 59 pp.

Presented design strength calculations for all the tests from Prawel et al. (1974), Salter et al. (1980), and Shiomi and Kurata (1984) based on the internal forces at the maximum test resistance. Full, nonlinear finite element simulations are generated for selected tests. For all the tests, the experimental results show more capacity than the calculated nominal resistance except the LB-5 test from Prawel et al. (1974). Suggested to calculate the LTB resistance by scaling the LTB strength based on uniform flange stress with the stress gradient factor C_b. For all the tests governed by LTB in flexure, this approach predicts the flexural capacity that is close to the experimental test results. A residual stress pattern based on residual stress measurements by Prawel et al. (1974) is suggested by authors for further study of experimental tests unless a specific residual stress condition is defined otherwise.

Ozgur, C., Kim, Y.D. and White, D.W. (2007). "Consideration of End Restraint Effects in Web-Tapered Members," Structural Engineering Mechanics and Materials Report No. 32, School of Civil and Environmental Engineering, Georgia Institute of Technology, Atlanta, GA, June.

Adapted the design-based procedure developed by Nethercot and Trahair (1976) to the calculation of the elastic LTB resistance of web-tapered members accounting for end warping restraint from adjacent less critical unbraced lengths. Applied this procedure with the procedures presented in this Guide to obtain refined estimates of inelastic LTB resistances of a number of web-tapered members. Compared calculations to the maximum experimental resistances from one test conducted by Salter et al. (1980) and several tests conducted by Shiomi and Kurata (1984). Noted that the design of members using these types of procedures will in general increase the demands on the out-of-plane beam bracing system.

Kim, Y.D. and White, D.W. (2008). "Lateral Torsional Buckling Strength of Prismatic and Web-Tapered Beams," *Proceedings*, Annual Technical Session, Structural Stability Research Council, Missouri University of Science and Technology, Rolla, MO, April, pp.155–174.

Kim, Y.D. and White, D.W. (2010). " Lateral Torsional Buckling Strength of Prismatic and Web-Tapered Beams: Reliability Assessment," *Proceedings*, Annual Technical Session, Structural Stability Research, Council, Missouri University of Science and Technology, Rolla, MO, May, pp.725–744.

and

Kim, Y.D. (2010). "Behavior and Design of Metal Building Frames with General Prismatic and Web-Tapered Steel I-Section Members," Doctoral Dissertation, School of Civil and Environmental Engineering, Georgia Institute of Technology, Atlanta, GA, 562 pp.

Evaluated the general procedures developed in White and Kim (2006) and Kim (2010) for calculation of nominal flexural strength of general nonprismatic members by virtual test simulation using full-nonlinear finite element analysis. Demonstrated that flexural resistances of nonprismatic members are essentially the same as the ones of equivalent prismatic members with a given moment gradient factor and a given most highly stressed section within their unbraced lengths. Also demonstrated that virtual test simulation tends to provide smaller flexural resistances compared to experimental test results and the current AISC (2005, 2010) and AASHTO (2004, 2007) provisions. Concluded that these differences are largely due to the geometric imperfections and internal residual stresses being smaller on average in the physical tests compared to common deterministic values assumed in virtual simulation studies. Also demonstrated that, for deeper thin-walled sections, the calculation of M_n based on a elastic buckling ratio including C_b effect, γ_{eLTB} (a general procedure presented in Section 5.4.3 in this guide) provides better estimates compared to virtual test simulation results than the calculation of M_n by scaling up the uniform bending resistance (a procedure for single linear tapered members presented in Section 5.4.3). Proposed separate sets of recommendations for improved calculations of nominal LTB resistances based on the reliability assessments of experimental test data (White and Jung, 2008; White and Kim, 2008; Rightman, 2005) and virtual test simulation results (Kim and White, 2008; Kim and White, 2010; Kim, 2010).

General Behavior and Design of Frames Composed of Tapered I-shaped Members

Lee, G.C. (1959). "On the Lateral Buckling of a Tapered Narrow Rectangular Beam," *Journal of Applied Mechanics,* 26, 457–458.

Established that for small tapering angles (15° or less), Euler-Bernoulli theory for beams yields satisfactory results.

Boley, B.A. (1963). "On the Accuracy of the Bernoulli-Euler Theory for Beams of Variable Section," *Journal of Applied Mechanics,* 30, 373–378.

Found that normal stresses calculated using Euler-Bernoulli theory were accurate to within a few percent as long as the angle of taper was less than 15°.

Lee, G.C., Ketter, R.L. and Hsu, T.L. (1981). *The Design of Single Story Rigid Frames,* Metal Building Manufacturers Association, Cleveland, OH, 267 pp.

and

Galambos, T.V. (1988b). "Tapered Structural Members," *Guide to Stability Design Criteria for Metal Structures*, 4th Ed., Chapter 9, Wiley, New York, pp. 329–358.

Summarized the results from a multi-year research effort by the authors and numerous other investigators aimed at the design of steel single-story rigid frames. Presented methods that coordinated with and extended the AISC ASD approaches for design of prismatic members at the time of this work. The techniques discussed relied extensively on the use of charts and graphs. Six complete frame design examples were presented using AISC ASD provisions. The work summarized in this book formed the basis of the following AISC *Specifications*:

Appendix D (AISC 1978) 8th edition ASD manual
Appendix F4 (AISC 1986) 1st edition LRFD manual
Appendix F7 (AISC 1989) 9th edition ASD manual
Appendix F3 (AISC 1993) 2nd edition LRFD manual
Appendix F3 (AISC 1999) 3rd edition LRFD manual

These provisions were not widely accepted by the industry due to the limited range of member geometries considered as well as the required usage of design charts. They were no longer included within the AISC (2005) *Specification*.

Jerez, L. and Murray, T.M. (1980a). "Rigid Frame Studies, Full Scale Frame Tests SRL04 50 20/25 16/25," Progress Report to Star Manufacturing Company, Oklahoma City, OK, Fears Structural Engineering Laboratory, School of Civil Engineering and Environmental Science, University of Oklahoma, Norman, OK, July, 67 pp.

Jerez, L. and Murray, T.M. (1980b). "Rigid Frame Studies, Full Scale Frame Tests SRL04 60 40/25 20/20," Progress Report to Star Manufacturing Company, Oklahoma City, OK, Fears Structural Engineering Laboratory, School of Civil Engineering and Environmental Science, University of Oklahoma, Norman, OK, July, 119 pp.

Forest, R. and Murray, T.M. (1981a). "Rigid Frame Studies, Full Scale Frame Tests STR 60 12/15 10/25," Progress Report to Star Manufacturing Company, Oklahoma City, OK, Fears Structural Engineering Laboratory, School of Civil Engineering and Environmental Science, University of Oklahoma, Norman, OK, February, 83 pp.

Forest, R. and Murray, T.M. (1981b). "Rigid Frame Studies, Full Scale Frame Tests STR4 50 12/15 14/25," Progress Report to Star Manufacturing Company, Oklahoma City, OK, Fears Structural Engineering Laboratory, School of Civil Engineering and Environmental Science, University of Oklahoma, Norman, OK, July, 145 pp.

and

Forest, R. and Murray, T.M. (1982). "Rigid Frame Studies, Full Scale Frame Tests," Research Report No. FSEL/STAR 82-01, School of Civil Engineering and Environmental Science, University of Oklahoma, Norman, OK, 109 pp.

Tested four sets of two standard full-scale gable clear-span frames with 50- and 60-ft spans, a total of eight clear-span frames. One series had nonprismatic columns and rafters of shop-welded plates. The other series had prismatic columns and either prismatic or nonprismatic rafters. All the test setups consisted of two parallel frames spaced 24 ft apart. The tests were targeted at (1) verifying existing design procedures by Star Manufacturing Company to predict deflections and strength, (2) verifying design procedures published by Lee et al. (1981), and (3) determining bracing requirements for tapered steel members. Frame 1 failed due to an inadequate rafter compression flange brace near the knee. Frames 5 and 6 exhibited premature failures due to inadequate tightening of the end-plate moment connection bolts at the knees and at the ridge. Design predictions of vertical rafter deflections were accurate. Sidesway deflections were consistently smaller than predicted. This was due to the column base conditions, which were assumed perfectly pinned in the analysis. All the frames except 3 and 4 were tested under simulated full live load conditions. For the full live load tests to failure, all the frames reached more than 90% of the predicted failure load except frames 5 and 6. Frames 3 and 4 were tested using a combination of lateral load and unbalanced live load. These frames failed at 70% of the predicted lateral load failure level. In these tests, the stress gradient was small near the failure location and the stress was within 19% of the stress at failure under the vertical load alone. Hence, failure at this section translated into a significant reduction in the lateral load capacity. The test results were compared to the procedures suggested by Lee et al. (1981). A number of variations on the design assumptions were investigated. No consistent set of design rules adequately predicted the frame strengths for all the loading combinations.

Jenner, R.K., Densford, T.A., Astaneh-Asl, A. and Murray, T.M. (1985a). "Experimental Investigation of Rigid Frames Including Knee Connection Studies, Frame Assembly Tests," Report No. FSEL//MESCO 85-01, Fears Structural Engineering Laboratory, School of Civil Engineering and Environmental Science, University of Oklahoma, Norman, OK, June, 184 pp.

Jenner, R.K., Densford, T.A., Astaneh-Asl, A. and Murray, T.M. (1985b). "Experimental Investigation of Rigid Frames Including Knee Connection Studies, Frame FR1 Tests, Report No. FSEL//MESCO 85-02, Fears Structural Engineering Laboratory, School of Civil Engineering and Environmental Science, University of Oklahoma, Norman, OK, July, 210 pp.

and

Jenner, R.K., Densford, T.A., Astaneh-Asl, A. and Murray, T.M. (1985c). "Experimental Investigation of Rigid Frames Including Knee Connection Studies, Frame FR2 Tests, Report No. FSEL//MESCO 85-03, Fears Structural Engineering Laboratory, School of Civil Engineering and Environmental Science, University of Oklahoma, Norman, OK, August, 263 pp.

Tested eight knee assemblies connected by a moment end-plate connection and four clear-span frames with different types of columns and rafters. The knee assemblies were subjected to a single applied force such that the internal forces in the specimens were approximately actual design values for combined dead and live loads. The frame tests were conducted to study the accuracy of procedures for calculating frame strength and stiffness. Six load combinations were applied to the frames, including live load and wind load. All the knee area tests except one test failed due to panel zone plate yielding or buckling. One knee test failed due to yielding of the rafter web plate. The knee tests demonstrated that the 2005 AISC plate girder web yielding, plate buckling, and tension field action provisions may be used to design panel zone web plates if h is defined as the depth of the plate at the rafter. However, the investigators concluded that panel zone tension field action strengths should only be considered if a full-depth column web stiffener is used adjacent to the inside rafter flange, and that this stiffener must be welded to both column flanges and the column web. The frame tests failed at loads smaller than predicted failure loads using the measured cross section properties and coupon test results. The investigators concluded that the reason for the undercapacity of the experimental tests was the knee area flexibility, which caused an adverse redistribution of moments within the frames. This conclusion led to a suggestion for the use of thicker panel zone web plates.

Watwood, V.B. (1985). "Gable Frame Design Considerations," *Journal of Structural Engineering,* ASCE, 111(7), 1543–1558.

Discussed the sensitivity of an example clear-span gable frame to the assumed boundary conditions at the foundation level and to unbalanced gravity load. Discussed the calculation of the effective length for rafters, accounting for the rafter axial compression and the coupling with the sidesway stability of the overall structure. Suggested an approach to design of rafters subjected to significant axial compression that in essence takes the buckling load of the rafters as the axial force level in these members at incipient sidesway buckling of the full structure. This approach is equivalent to using an effective length factor for the rafters significantly larger than one for the example frame considered. White and Kim (2006) suggest that this approach to the design of the rafters is unnecessarily conservative.

Davis, B.D. (1996). "LRFD Evaluation of Full-Scale Metal Building Frame Tests," M.S. Thesis, Charles Via Department of Civil Engineering, Virginia Polytechnic Institute and State University, Blacksburg, VA, 255 pp.

Compared results from design strength calculations using AISC LRFD to experimental strengths measured from two full-scale tests of clear-span gable clear-span frames. Local buckling of the rafter flanges governed the design resistances as well as the experimental failure modes. The predictions of the experimental resistances were consistently conservative by a small margin.

White, D.W. and Kim, Y.D. (2006). "A Prototype Application of the AISC (2005) Stability Analysis and Design Provisions to Metal Building Structural Systems," Report prepared for Metal Building Manufacturers Association, School of Civil and Environmental Engineering, Georgia Institute of Technology, January, 157 pp.

Demonstrated how the AISC (2005) direct analysis method can be applied to general metal building structural systems. The direct analysis method is shown to provide the following distinct advantages:

- Its basis with respect to the handling of stability effects is more logical and straightforward.
- It provides an improved representation of the internal forces and moments throughout the structure at the strength limit of the most critical member or members.
- No *K* factor calculations are required.
- The design of all types of braced, moment and combined framing systems is handled in a unified and consistent fashion.

Provided detailed design calculations and comparisons to results using the AISC (2005) effective length method for a representative clear-span frame and a representative modular frame. Explained that the design behavior of metal building frames is typically dominated by flexure with the possible amplification of internal moments due to second-order effects. Showed that the effective length method places excessive emphasis on the stability behavior under a fictitious loading involving only concentric axial compression in the frame members.

Eroz, M., White, D.W. and DesRoches, R. (2008). "Direct Analysis of Gabled Frames with Partially Restrained Column Base Conditions," *Journal of Structural Engineering*, ASCE, 134(9), 1508–1517.

Developed a refined elastic-plastic component-based model of a representative nominally simple four-bolt base detail along with an intermediate to low value for the foundation stiffness from a spread footing. Studied the influence of the incidental restraint from these base conditions on the strength unity checks and the service deflections for a gable clear-span metal building frame. Used the procedures presented in this Guide for the strength limit states checks. Compared the results using the refined base model to results determined assuming ideally pinned base conditions and using nominal elastic springs equivalent to $G = 10$ in the AISC sidesway-uninhibited alignment chart. Observed a similar but marginal decrease in the member strength unity checks by using either the refined base model or the elastic $G = 10$ base model. The refined base model reduced the maximum service vertical and lateral deflections of the frame by nearly 10 and 20%, respectively, whereas the $G = 10$ base model reduced these deflections by approximately 2 and 9%, respectively.

Kim, Y.D. (2010). "Behavior and Design of Metal Building Frames with General Prismatic and Web-Tapered Steel I-Section Members," Doctoral Dissertation, School of Civil and Environmental Engineering, Georgia Institute of Technology, Atlanta, GA, 562 pp.

Provided detailed comparisons of 2D analysis results based on the AISC (2005) direct analysis and effective length methods as well as design calculations based on proposed design procedures. Conducted virtual test simulation of an entire frame system using a 3D full-nonlinear finite element analysis for two metal building framing systems. Discussed the results of virtual test simulation compared to the design check results of the two metal building frames.

APPENDIX A
Calculating γ_{eL} or P_{eL} for Tapered Members

P_{eL} is the nominal elastic flexural buckling strength of a member having ideal pinned-pinned end conditions. Because the internal axial force may vary along the member length, it is generally more convenient to work with the equivalent parameter, γ_{eL}. The nominal elastic buckling force in the column at any point for a particular load combination is γ_{eL} multiplied by the required strength in the column at that point, i.e., $P_{eL} = \gamma_{eL} P_r$. In terms of stresses, the nominal elastic buckling stress in the column at any point for a particular load combination is γ_{eL} multiplied by the required stress in the column at that point.

For a straight, geometrically perfect prismatic column with a constant axial force,

$$P_{eL} = \frac{\pi^2 EI}{L^2} \tag{A-1}$$

and

$$\gamma_{eL} = \frac{P_{eL}}{P_r} = \frac{\pi^2 EI}{P_r L^2} \tag{A-2}$$

For a tapered I-shaped member subjected to constant or varying internal axial force, there is no practical exact closed form solution for P_{eL} or γ_{eL}. The following procedures are recommended for calculating P_{eL} and/or γ_{eL} for tapered members.

A.1 EQUIVALENT MOMENT OF INERTIA

For tapered members subjected to constant internal axial loading, with a single taper angle and no change in the web or flange plates over the length, the following empirical equation gives results accurate to within several percent for the range of members considered in this document. This equation provides the flexural buckling strength of a prismatic member of the same length using an equivalent moment of inertia:

$$P_{eL} = \frac{\pi^2 EI'}{L^2} \tag{A-3}$$

$$\gamma_{eL} = \frac{P_{eL}}{P_r} \tag{A-4}$$

where:

I' = equivalent moment of inertia
= strong axis moment of inertia of the segment calculated using the depth at $0.5L$ $(I_{small}/I_{large})^{0.0732}$ from the small end
I_{small} = strong-axis moment of inertia at the small end
I_{large} = strong-axis moment of inertia at the large end
L = length of the tapered member

Example:

b_f = 8.00 in.
t_f = 0.500 in.
t_w = 0.188 in.
h_{left} = 18.0 in.
h_{right} = 36.0 in.
L = 360 in.
αP_r = 100 kips (α = 1.0 for LRFD and 1.6 for ASD)

Calculate moments of inertia at each end (not shown)

$I_{small} = 776 \text{ in.}^4$
$I_{large} = 3{,}400 \text{ in.}^4$

Calculate location of equivalent depth

$$x = 0.5L\left(\frac{776 \text{ in.}^4}{3{,}400 \text{ in.}^4}\right)^{0.0732}$$
$$= 0.449L$$

Calculate equivalent depth

$$h_{x=0.449L} = 18.0 \text{ in.} + \left[0.449\left(36.0 \text{ in.} - 18.0 \text{ in.}\right)\right]$$
$$= 26.1 \text{ in.}$$

Calculate equivalent moment of inertia

$$I' = I_{x=0.449L}$$
$$= 1{,}690 \text{ in.}^4$$

$$P_{eL} = \frac{\pi^2 EI'}{L^2}$$
$$= \frac{\pi^2 (29{,}000 \text{ ksi})\left(1{,}690 \text{ in.}^4\right)}{\left(360 \text{ in.}\right)^2} \tag{A-3}$$
$$= 3{,}730 \text{ kips}$$

With a required axial force of 100 kips

$$\gamma_{eL} = \frac{P_{eL}}{P_r}$$
$$= \frac{3{,}730 \text{ kips}}{100 \text{ kips}} \tag{A-4}$$
$$= 37.3$$

The equivalent moment of inertia, I', is intended for use only with Equation A-3.

Table A-1 shows a comparison of Equation A-3 with results from the method of successive approximations solution using 10 elements for a range of parameters. Note that the accuracy of the results is independent of member length.

Table A-1. Equivalent Moment of Inertia Accuracy											
Length, in.	b_f, in.	t_f, in.	t_w, in.	h_{small}, in.	h_{large}, in.	I_{small}, in.^{4}	I_{large}, in.^{4}	I', in.^{4}	P_{eL} (kips)		
									Equation A-3	Successive Approx.	% Err
120	5.0	0.188	0.188	8.0	10.0	39.54	64.46	50.67	1007	1008	-0.05
					20.0		316.9	119.3	2371	2380	-0.36
					30.0		851.3	209.5	4165	4177	-0.30
					40.0		1762	321.4	6387	6392	-0.08
	8.0	0.50	0.188	8.0	10.0	152.7	236.3	190.8	3792	3793	-0.02
					20.0		966.0	414.2	8233	8237	-0.04
					30.0		2284	691.6	13747	13724	0.17
					40.0		4283	1021	20289	20211	0.39
240	5.0	0.188	0.188	8.0	10.0	39.54	64.46	50.67	252	252	-0.05
					20.0		316.9	119.3	593	595	-0.36
					30.0		851.3	209.5	1041	1044	-0.30
					40.0		1762	321.4	1597	1598	-0.08
	8.0	0.50	0.188	8.0	10.0	152.7	236.3	190.8	948	948	-0.02
					20.0		966.0	414.2	2058	2059	-0.04
					30.0		2284	691.6	3437	3431	0.17
					40.0		4283	1021	5072	5053	0.39

For linearly tapered members subjected to nonuniform axial compression, γ_{eL} can be calculated conservatively as $P_{eI}/(P_r)_{max}$, where P_{eL} is calculated from Equation 4.5-4 and $(P_r)_{max}$ is the maximum internal axial compression along the member length.

Equation A-3 also may be applied to determine the value of P_{et} for linearly tapered member segments for use in determining the number of elements required per member for second-order analysis and for determining P-δ moments between element nodal locations.

A.2 METHOD OF SUCCESSIVE APPROXIMATIONS

P_{eL} and/or γ_{eL} can be determined by using the method of successive approximations (Timoshenko and Gere, 1961). This technique uses an iterative beam analysis to find the axial load, $\gamma_{eL}P_r$, at which the beam deflections resulting from applied P-δ moments are a uniform multiple, γ_{eL}, of the deflections assumed to calculate the P-δ moments. This method can handle multiple tapers, plate changes, and changes in axial loading along the length of the member.

The general procedure is as follows:

1. Assume an initial deflected shape of the member due to the P-δ moments. The method will converge for any reasonable initial assumption, but will converge with less iteration as the accuracy of the initial assumption increases.
2. Calculate the moments along the length of the member due to the required axial load at each point multiplied by the deflection at each point.
3. Perform a beam deflection analysis on the simple span beam using these moments to determine a new deflected shape.
4. If the deflections at the points along the member are a constant multiple of the assumed deflections, the analysis is complete and γ_{eL} is equal to this multiplier.
5. If the deflections at each point along the member are not a constant multiple of the assumed deflections, return to step 2 and proceed using the new deflected shape.
6. P_{eL} at any point is equal to $\gamma_{eL} \times P_r$, the axial load used at that point in the analysis.

Suggested implementation details based on Timoshenko and Gere (1961) and Newmark (1943) are:

1. Model the member by dividing it into a number of analysis elements with nodes at each end ["stations" in Timoshenko and Gere (1961)]. Nodes should be located at the ends of the member and changes in plates, taper or loading. Add additional nodes at a reasonable spacing between these. The accuracy of the method increases as the fineness of subdivision is

Table A-2. Equivalent Concentrated Loads

Equal Length Segments		Unequal Length Segments	
Multi-Linear *M/EI*			
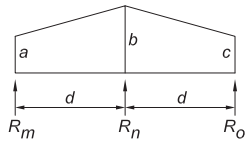	$R_m = \frac{d}{6}(2a+b)$ $R_n = \frac{d}{6}(a+4b+c)$ $R_o = \frac{d}{6}(b+2c)$	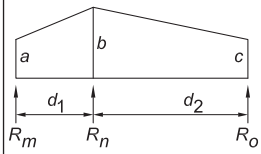	$R_m = \frac{d_1}{6}(2a+b)$ $R_n = \frac{d_1}{6}(a+2b)+\frac{d_2}{6}(2b+c)$ $R_o = \frac{d_2}{6}(b+2c)$
Parabolic *M/EI*			
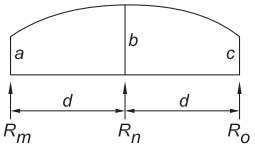	$R_m = \frac{d}{24}(7a+6b-c)$ $R_n = \frac{d}{12}(a+10b+c)$ $R_o = \frac{d}{24}(7c+6b-a)$	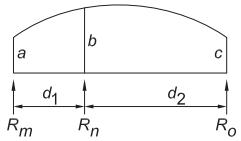	$R_m = \frac{d_1\left[d_2^2(4a+2b)+\ d_1d_2\,3(a+b)\ +d_1^2(b\ -\ c)\right]}{12d_2(d_1+d_2)}$ $R_n = \frac{d_1\left[d_2^2(2a+4b)+\ d_1d_2(a+5b)\ +d_1^2(b\ -\ c)\right]}{12d_2(d_1+d_2)}$ $+\frac{d_2\left[d_1^2(4b+2c)+\ d_1d_2(5b+c)\ +d_2^2(b\ -\ a)\right]}{12d_1(d_1+d_2)}$ $R_o = \frac{d_2\left[d_1^2(2b+4c)+\ d_1d_2\,3(b+c)\ +d_2^2(b\ -\ a)\right]}{12d_1(d_1+d_2)}$

increased. Do not include any angle changes or out-of-straightness in the model, even if they are present in the actual member.

2. To compute the deflection of the beam subject to the *P*-δ moment diagram, use the conjugate beam method. The applied loading for the analysis is the *M/EI* diagram from the assumed *P*-δ moments. Timoshenko and Gere give expressions for station point concentrated loads equivalent to the *M/EI* loading on the conjugate beam approximated by piecewise linear or parabolic segments. These equivalent concentrated load expressions approximate the continuously curved *M/EI* diagram, and simplify the calculations.

The concentrated load expressions provided by Timoshenko and Gere (1961) are listed in Table A-2 in the column labeled "Equal Length Segments." These expressions are based on the assumption that the member is divided into segments of equal length. Also included in Table A-2 are generalized versions of these functions that can be used at stations where segments of unequal length meet. This often occurs at a change of plates or taper. Note that for multi-linear *M/EI* cases, the calculation of the end reactions R_m and R_o requires equivalent concentrated loads only at the station corresponding to the reaction and at the adjacent station. The parabolic functions require three adjacent equivalent concentrated load values of *M/EI*; thus, any segment should be divided into a minimum of two parts if these expressions are used. The use of the parabolic expressions is recommended since they better approximate the shape of the *M/EI* diagram and result in greater accuracy for a given level of subdivision.

Any beam span analysis method capable of accurately analyzing an applied loading in the shape of the *P*-δ moment diagram divided by *EI* can be used in lieu of the conjugate beam method. The method will converge to an accurate solution given any reasonable initial deflection assumption, but will converge more quickly with a better starting guess. A first approximation using the deflected shape from a uniform transverse loading on the member produces good results.

Although a tapered member may have an internally curved centroidal axis due to unsymmetrical flanges or have kinks or offsets in the centroidal axis due to changes in geometry (such as at the ridge of rafters, pinch points in rafters or columns, or changes in cross section at any location within a frame), the *P*-δ moment calculations and beam span analysis should be conducted assuming a straight centroidal axis. Otherwise, the successive approximation method will not yield a unique buckling multiplier. Any bending moments arising from centroidal axis out-of-straightness are ultimately accounted for in the beam-column strength interaction equations.

It is recommended that engineers run the benchmark problems in Appendix C to establish the accuracy of their software and select a fineness of meshing appropriate for design. Appendix Section C.3 provides detailed calculations for γ_e and P_{eL} for two web-tapered columns using this method.

A.3 EIGENVALUE BUCKLING ANALYSIS

P_{eL} and/or γ_{eL} can be determined by an elastic eigenvalue buckling analysis. Many advanced finite element and/or frame analysis programs can calculate elastic buckling multipliers, γ_{eL}, for any assumed reference axial loading using numerical eigenvalue techniques. P_{eL} is then determined as the required axial compression strength, used as a reference load in the analysis, multiplied by γ_{eL}. The quality of such solutions depends on the accuracy of the tapered member modeling, element choice, and meshing. Computer programs that include only P-Δ effects will require finer subdivision than those that incorporate P-Δ and P-δ effects in their elements. The engineer should run the benchmark problems provided in Appendix C to establish the appropriateness of the computer program and modeling techniques prior to use in design.

Some care must be taken, possibly including review of the selected eigenvalue buckling mode shape by the engineer, to ensure that the lowest eigenvalue buckling mode has been determined. Although this technique has the advantage of handling essentially any imaginable geometry and loading, it may not be practical in a production environment unless the eigenvalue buckling solution is automated and integrated into the analysis-design software.

The preceding comments address only the calculation of member buckling loads, P_{eL}, or the buckling load ratios, γ_{eL}, based on the assumption of idealized pinned-pinned end conditions. The reader is referred to Section 6.3.2 and to Appendix B for discussion of methods for calculating the buckling load of members such as rafters in clear-span gable frames or fixed-base columns in braced frames accounting for the influence of end restraint from adjacent members and/or base conditions. These procedures may be used to address the in-plane stability effects in these types of members when designing by the ELM.

APPENDIX B
Calculating In-Plane γ_e Factors for the ELM

For frames with sufficiently low ratios of sidesway $\Delta_{2nd}/\Delta_{1st} \approx B_2$, the AISC *Specification* permits the use of an in-plane effective length factor, K, of 1.0 for each of the three design methods listed in the AISC *Specification* (DM, ELM, and FOM). For frames with $\Delta_{2nd}/\Delta_{1st}$ (or B_2) smaller than 1.1, the ELM may be used with $K = 1.0$. For frames with ratios of $\Delta_{2nd}/\Delta_{1st}$ (or B_2) above 1.5, the AISC *Specification* only permits the use of the DM, where $K = 1.0$. Consequently, there is no need to calculate buckling loads or γ_e factors other than those for simply supported conditions in either of these cases. For frames with $\Delta_{2nd}/\Delta_{1st}$ (or B_2) between 1.1 and 1.5, the engineer may choose to use the ELM. However, in this case, the effective length factors (or γ_e factors) must be calculated "from a sidesway buckling analysis of the structure" (AISC, 2005).

B.1 COLUMNS

The annotated bibliography in Chapter 7 reviews the past efforts at establishing procedures for the calculation of flexural buckling loads or effective length factors for tapered columns. The methods selected for inclusion in previous editions of the AISC *Specification* relied heavily on charts and graphs and had significant restrictions with regard to geometry and loading that limited their acceptance in the industry. The following methods do not require the use of charts or graphs and are adaptable to a wider range of structures.

B.1.1 Modified Story-Stiffness Method

The following modified story-stiffness method (White and Kim, 2006) is recommended for typical metal building frames that are rectangular or nearly rectangular in geometry.

Determine the story buckling multiplier, $\gamma_{e,\,story}$ as:

$$\gamma_{e,\,story} = \frac{\left(0.85 + 0.15R_L\right)\dfrac{H}{\Delta_H}}{\sum_{all}\dfrac{P_i}{L_i}} \qquad \text{(B-1)}$$

where

P_i = axial load in column i, kips
L_i = length of column i, in.
H = Total applied horizontal shear within the story, equal to the total applied horizontal load in single-story frames, kips.
Δ_H = average story drift due to the horizontal load, H, in.

$$R_L = \frac{\sum_{leaning}\dfrac{P_i}{L_i}}{\sum_{all}\dfrac{P_i}{L_i}} \qquad \text{(B-2)}$$

$\Sigma_{leaning}$ = summation over all leaning (pin-ended) columns
Σ_{all} = summation over all columns

γ_e is then taken as the $\gamma_{e.story}$ value for in-plane buckling of the sidesway resisting columns in the column strength design procedure given in Section 5.3, but not less than γ_{eL}. If $\Sigma_{all}P_i/L_i$ is zero, or if there is a net vertical tension in the story, take γ_e for any individual column in compression as γ_{eL}.

H and Δ_H may be calculated using a unit or arbitrary lateral loading at the rafter level in a first-order stiffness analysis. For frames with unequal height columns and/or gable frames, H should be subdivided and applied at the tops of the columns in proportion to the value of P_i/L_i for each column. This gives the most accurate representation of the sidesway stability effects and results in more uniform value of the story drift at the top of each of the columns. In most situations, the variation of $(P_i/L_i)/\Sigma_{all}\,(P_i/L_i)$ among different load combinations is small; therefore, it is usually acceptable to determine H/Δ_H from a single lateral load analysis based on any one of the design load combinations. If significant axial forces are present in the rafters in any load combination, the moment of inertia of the rafters should be reduced for that load combination in the preceding first-order analysis per Equation 6-1a. The largest rafter stiffness reduction for any combination can be conservatively used for all combinations.

The influence of incidental column base rotational restraint associated with the traditional $G = 10$ for nominally simple base conditions or $G = 1$ for nominally fixed base conditions is addressed in Equation B-1 by including the equivalent elastic rotational springs at the column bases in the model used to calculate Δ_H. Specific guidelines for these calculations are provided by Eroz, White and DesRoches (2008).

B.1.2 Eigenvalue Buckling Analysis

γ_e factors can be determined by an elastic eigenvalue buckling analysis. The eigenvalue analysis should be conducted using a second-order solution and an adequate number of elements must be employed. The elastic buckling multiplier for in-plane sidesway for the entire frame, $\gamma_{e.story}$, is determined from an eigenvalue analysis of the frame. The γ_e factor for each column is then taken as $\gamma_{e.story}$.

Table B-1. Maximum γ_e Error for Sway Columns with Simply Supported Bases, *P*-Δ Analysis	
Elements per Column	**Maximum Error for γ_e, %**
1	22
2	5
3	2

Table B-2. Maximum γ_e Error for Sway Columns with Top and Bottom Rotational Restraint, *P*-Δ Analysis	
Elements per Column	**Maximum Error for γ_e, %**
1	22
2	22
3	9
4	5
6	2

For single-story metal building frames, the lowest eigenvalue or first buckling mode from the eigenvalue analysis is usually the in-plane sidesway buckling mode. In rare cases such as gable frames with fixed-column bases combined with long rafter spans, the sidesway mode may be a higher eigenvalue mode.

B.1.2.1 Eigenvalue Buckling Solutions Using P-Δ-Only Analysis

Generally, a larger number of elements is required to obtain accurate eigenvalue sidesway buckling analysis solutions compared with the number specified for accurate load-deflection analysis in Sections 6.2.1 and 6.2.2. For sidesway-uninhibited columns with simply supported base conditions, the maximum potential errors of *P*-Δ-only buckling analyses are listed in Table B-1.

For sidesway-uninhibited columns with rotationally restrained base conditions, the maximum potential errors of *P*-Δ-only buckling analyses are listed in Table B-2. The percentage error is the same for one or two elements per column because, with equal rotational restraints at the column ends, the lateral displacement of a node at the column mid-length is the average of the member end lateral displacements. Therefore, the element chord rotation is the same in both of the column elements in a two-element solution.

B.1.2.2 Eigenvalue Buckling Solutions Using Elements That Include Both P-Δ and P-δ Effects

With the use of a more accurate element formulation that includes *P*-δ effects in the element stiffness matrices, a smaller number of elements is generally possible. For sidesway-uninhibited columns with simply supported or fixed-base conditions, the maximum potential error for elements derived based on a cubic transverse displacement assumption is approximately 1% using a single element per member.

All the preceding error limits are based on the assumption that the elastic stiffness of nonprismatic members is represented with negligible error in the matrix analysis solution.

B.2 RAFTERS

In general, buckling multipliers for rafters calculated using the preceding story buckling procedure will be excessively conservative, because the rafters are typically not participating directly in the frame in-plane buckling except to provide rotational stiffness to the tops of columns moment connected to the rafters. For this reason, the effective length factor of rafters moment-connected to columns have typically been taken as 1.0 by the industry with success.

An important question is that of the effective length of the rafter in a gable span with no vertical support at the gable ridge. A common industry practice has been to consider the effective length to be the distance from the column to the ridge if the roof slope is above some critical value. However, due to the spreading apart of the columns under gravity loads or under a buckling mode involving instability of the rafters in gable frames, the rafters generally tend to act more like a single member having a length equal to the overall on-slope length along the rafters L_{os}. Nevertheless, for clear-span gable frames with relatively short column heights from the base to the eaves, the columns tend to provide substantial rotational restraint to the ends of the rafters, such that the effective length factor, *K,* corresponding to L_{os} is close to 0.5. However, as column heights increase relative to the rafter span, the rafter effective length begins to increase significantly above the value of 0.5 often assumed. It is therefore recommended that rafter buckling multipliers be calculated using realistic end-restraint conditions. The influence of the axial compression in the columns on the restraint that they provide at the rafter ends should be considered.

B.2.1 Eigenvalue Buckling Analysis

Rafter γ_e factors can be determined by an elastic eigenvalue buckling analysis in a manner similar to that described for the columns in the previous section. The eigenvalue analysis

Table B-3. Maximum γ_e Error for Rafters and Nonsway Columns, *P*-Δ Analysis	
Elements per Rafter	**Maximum Error for γ_e, %**
1	NA
2	36
3	37
4	22
6	10
8	5
16	1

should be conducted using a second-order solution, and an adequate number of elements must be employed. The lowest elastic multiplier for in-plane buckling of the rafter, $\gamma_{e.rafter}$, is determined from an eigenvalue analysis of the frame.

In single-story clear-span gable frames, the lowest eigenvalue buckling mode of a rafter is seldom the lowest mode of the entire frame, except in rare cases such as frames with fixed column bases and short eave heights combined with long rafter spans. In most cases, $\gamma_{e.rafter}$ should be taken as the second lowest buckling eigenvalue. The engineer must in general inspect the buckling mode shapes to interpret whether the lowest or next lowest eigenvalue should be used for a given member. For modular frames and in floor girders of multi-story frames, the axial load level in the rafters at buckling is typically quite small. In these cases, use of anything other than γ_{eL} ($K = 1$) is hardly worthwhile for the rafters and/or floor girders.

B.2.1.1 Eigenvalue Buckling Solutions Using P-Δ-Only Analysis

For sidesway restrained columns and rafters with general end conditions, the maximum potential *P*-Δ-only buckling analysis errors are provided in Table B-3.

The maximum error for three elements is larger than for two elements because, for a prismatic member with both ends fully restrained, the use of three *P*-Δ elements actually increases the error in the calculation of the buckling load to 37% compared to an error of 22% using four elements. The two-element solutions exhibit the largest error in the buckling load (36%) when one end of the member is ideally pinned and the other end is ideally fixed.

If one compares these requirements to those listed in Table 6-3 of Section 6.2.1, it can be observed that the number of elements required to obtain accurate eigenvalue results is generally larger than that required to obtain accurate required second-order internal forces.

B.2.1.2 Eigenvalue Buckling Solutions Using Elements That Include Both P-Δ and P-δ Effects

With the use of a more accurate element formulation that includes *P*-δ effects in the element stiffness matrices, a significantly smaller number of elements is generally possible. For sidesway-inhibited columns and rafters with general end conditions, one should always have a node near the middle of the span. With the use of two approximately equal length elements of this type, the maximum potential error in the buckling analysis is approximately 3% (Guney and White, 2007).

All the preceding error limits are based on the assumption that the elastic stiffness of nonprismatic members is represented with negligible error in the second-order analysis solution.

B.2.2 Method of Successive Approximations

Rafter γ_e factors can be calculated using the method of successive approximations in a manner similar to that presented in Appendix A for calculating γ_{eL}. For the case of rafters with simple supports at both ends, the Appendix A method may be used exactly as shown. For the more common case, where the rafter ends are attached to columns and/or adjacent rafters with fully or partially restrained connections as defined by AISC (2005), the earlier method is still valid if the beam deflection analysis is conducted accounting for the rotational stiffness of the connections and/or the adjacent members at the rafter ends.

The rotational stiffness of each adjacent connected member can be determined using a stiffness model with a pinned support condition at the connection to the rafter, applying a unit end moment to that end and dividing the applied moment by the resulting end rotation. The end condition of the far end of the member should be representative of the actual conditions in the frame. If significant axial load is present in the adjacent member, the calculated rotational stiffness should be multiplied by $1-\frac{\alpha P_r}{P_{eL}}$, where P_{eL} is calculated using one of the methods in Appendix A.

The successive approximations procedure directly produces a γ_e for in-plane flexural column buckling, which can be used in the column strength evaluation in Section 5.3.

B.3 THE RELATIONSHIP BETWEEN *K* AND γ_e

Given a set of values for γ_e and γ_{eL} corresponding to in-plane flexural buckling, where γ_{eL} is based on idealized pinned-pinned end conditions and a given member length, *L*, the calculation of a member effective length factor is quite simple. The effective length factor can be determined as

$$K = \sqrt{\frac{\gamma_{eL}}{\gamma_e}} \tag{B-3}$$

That is, for any member geometry, the effective length factor is tied to the ratio of the buckling load accounting for the interaction of the member with adjacent components and/or with the overall structural system (γ_e) and the buckling load using idealized pinned-pinned end conditions. Equation B-3 is equivalent to K_γ in the discussions of prior developments in Section 2.1 and Chapter 7 of this Guide. Generally, $F_e = \gamma_e f_r$ is the important quantity for determination of the member axial compression resistance. For nonprismatic members, the preceding effective length factor is useful only as an indicator of the effect of adjacent components and/or the overall structural system on the member stability.

APPENDIX C
Benchmark Problems

This appendix provides a series of benchmark problems with closed formed and/or numerical solutions. These are intended to be used by the developers and users of software to establish the correctness and accuracy of their analysis procedures. Although the subject of this document is web-tapered members, solutions for prismatic members are also provided. These can be used to establish the correctness using prismatic members prior to adding the complexity of tapered members.

Three types of benchmark solutions are provided.

1. *Member stiffness coefficients:* Highly accurate first-order member stiffness coefficients for four different tapered member geometries. These can be used in evaluating the accuracy of the first-order part of the calculations. Developers can compare these coefficients with those generated within their programs. Software users can model these members with the corresponding end conditions and loadings for each of the columns in the stiffness matrices and compare the results with those provided (i.e., the stiffness coefficients K_{ij} correspond to the force at degree of freedom (dof) i due to a unit displacement at dof j; unit load can be applied at a single unrestrained dof for the member, then the corresponding displacement at this dof δ_i can be determined from the first-order analysis software and all the nodal forces may then be scaled by δ_j /1.0 for comparison to the values in column j of the stiffness matrix). Note that in all cases, all degrees of freedom are assumed to be fixed except the one released at the location of the applied load.
2. *Axial in-plane elastic buckling strengths:* These are used to verify the correctness of calculated values of P_{eL}, P_e, γ_{eL} and γ_e.
3. *Second-order member displacements and moments:* Solutions are provided for second-order displacements and bending moments under varying levels of axial load. It is recommended that software accuracy be established for prismatic members at axial load levels up to at least $\alpha P_r/P_{cr} = 0.67$, unless even higher levels are to be used. In general, the accuracy of second-order solutions will decline as the axial load level increases, so it is important to check accuracy at the highest percentage of the elastic buckling load that will be used. The axial load level of $\alpha P_r/P_{cr} = 0.67$ corresponds to a ratio of $\Delta_{2nd}/\Delta_{1st}$ in the vicinity of 3.0, which is within the range encountered in metal building construction.

C.1 PRISMATIC MEMBERS

Table C-1a defines five cases of loading and end conditions that cover a range of conditions encountered in metal buildings. Table C-1b gives accurate closed formed solutions for deflections, moments and P_{cr} for each case. It is suggested that the correctness of software be verified at levels up to at least $\alpha P_r/P_{cr} = 0.67$ using these prismatic cases before progressing to the verification of tapered members.

C.2 TAPERED MEMBERS

Presented here are several web-tapered benchmark problems. Because practical closed-form solutions are not available, the results are presented numerically. Additional discussion regarding the first two examples can be found in Kim and White (2006a).

The first-order analysis stiffness coefficients presented are derived with all degrees of freedom other than the one undergoing a unit displacement or rotation fully restrained. For the buckling strengths, sidesway deflections and sidesway moments, the values are derived using the "displacement boundary conditions" given for each example. The loads αP_r and H and the displacement boundary conditions are applied at the centroid of the member end cross sections. The loads αP_r and H are oriented parallel and perpendicular to a chord connecting these cross section centroids. For programs that require the outside flange of the column to be vertical and the applied loads to be vertical and horizontal, a coordinate transformation may be applied to the loads αP_r and H to obtain the appropriate vertical and horizontal loads. In each of the cases, the symbols A_m and I_m denote the area and moment of inertia with respect to the centroidal axis at the mid-span of the member. The ratios of the area and moment of inertia at the large end (A_L, I_L) and the small end (A_s, I_s) to A_m and I_m are also shown.

Table C-1a. Prismatic Benchmark Problems—Cases

Case	End Conditions and Loading
1	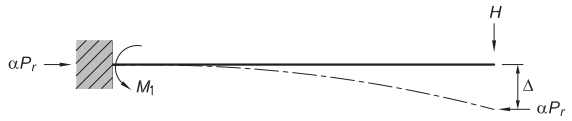
2	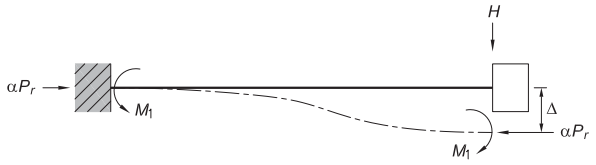
3	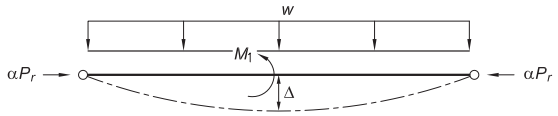
4	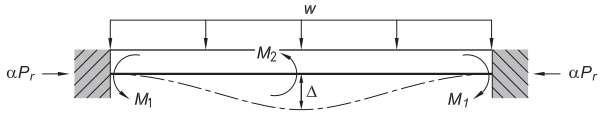
5	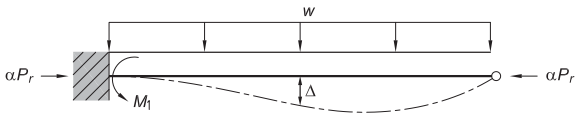

Table C-1b. Prismatic Benchmark Problems—Deflections, Moments and P_{cr}

Case	First-Order		Second-Order		
	Δ	M_1	P_{cr}	Δ	M_1
1	$\frac{HL^3}{3EI}$	HL	$\frac{P_{eL}}{4}$	$\frac{HL^3}{3EI}\left[\frac{3(\tan 2u - 2u)}{(2u)^3}\right]$	$HL\left[\frac{\tan 2u}{2u}\right]$
2	$\frac{HL^3}{12EI}$	$\frac{HL}{2}$	P_{eL}	$\frac{HL^3}{12EI}\left[\frac{3(\tan u - u)}{u^3}\right]$	$\frac{HL}{2}\left[\frac{\tan u}{u}\right]$
3	$\frac{5wL^4}{384EI}$	$\frac{wL^2}{8}$	P_{eL}	$\frac{5wL^4}{384EI}\left[\frac{12(2\sec u - u^2 - 2)}{5u^4}\right]$	$\frac{wL^2}{8}\left[\frac{2(\sec u - 1)}{u^2}\right]$
4	$\frac{wL^4}{384EI}$	$\frac{wL^2}{12}$	$4P_{eL}$	$\frac{wL^4}{384EI}\left[\frac{12(2 - 2\cos u - u\sin u)}{u^3 \sin u}\right]$	$\frac{wL^2}{12}\left[\frac{3(\tan u - u)}{u^2 \tan u}\right]$
5	$\frac{wL^4}{192EI}$	$\frac{wL^2}{8}$	$2.05P_{eL}$	$\frac{wL^4}{192EI}\left\{\frac{6}{u^4}\left[(2\sec u - {}^2u - 2) - \frac{(\tan u - u)(\sec u - 1)}{\left(\frac{1}{2u} - \frac{1}{\tan 2u}\right)}\right]\right\}$	$\frac{wL^2}{8}\left[\frac{2(\tan u - u)}{u^2\left(\frac{1}{2u} - \frac{1}{\tan 2u}\right)}\right]$

Notes: 1. For all cases: $P_{eL} = \frac{\pi^2 EI}{L^2}$, $u = \frac{\pi}{2}\sqrt{\frac{\alpha P_r}{P_{eL}}}$

2. For case 4: first-order: $M_2 = \frac{wL^2}{24}$, second-order: $M_2 = \frac{wL^2}{24}\left[\frac{6(u - \sin u)}{u^2 \sin u}\right]$

Table C-2.1. Sidesway Deflection and Moment				
$\frac{\alpha P_r}{P_{cr}}$	$\frac{\alpha P_r}{P_{eL}}$	$\frac{\alpha P_r}{P_{yo}}$	Δ, in.	M, kip-ft
0.00 (first-order)	0.000	0.000	0.223H	16.36H
0.10	0.037	0.282	0.246H	17.70H
0.20	0.074	0.564	0.277H	19.34H
0.30	0.111	0.847	0.316H	21.46H
0.40	0.148	1.129	0.367H	24.27H

Case 1: Moderately Tapered Doubly Symmetric Member Subject to Sidesway (see Figure C-1)

Geometric Properties:

Bottom web height = 9.5 in.
Top web height = 24.5 in.
Flanges = PL ¼ × 6
Web thickness = 0.125 in.
L = 16.36 ft (196.3 in.)
$H/\alpha P_r = 0.01$
$A_m = 5.125$ in.^{2}
$I_m = 274$ in.^{4}

Displacement boundary conditions: Simply supported base, rotation fully restrained at the top

First-Order Analysis Stiffness Coefficients

Units: kips, inches

$$k = \begin{bmatrix} 0.989\frac{EA_m}{L} & 0 & 0 & -0.989\frac{EA_m}{L} & 0 & 0 \\ 0 & 10.950\frac{EI_m}{L^3} & 3.685\frac{EI_m}{L^2} & 0 & -10.950\frac{EI_m}{L^3} & 7.264\frac{EI_m}{L^2} \\ 0 & 3.685\frac{EI_m}{L^2} & 2.029\frac{EI_m}{L} & 0 & -3.685\frac{EI_m}{L^2} & 1.656\frac{EI_m}{L} \\ -0.989\frac{EA_m}{L} & 0 & 0 & 0.989\frac{EA_m}{L} & 0 & 0 \\ 0 & -10.950\frac{EI_m}{L^3} & -3.685\frac{EI_m}{L^2} & 0 & 10.950\frac{EI_m}{L^3} & -7.264\frac{EI_m}{L^2} \\ 0 & 7.264\frac{EI_m}{L^2} & 1.656\frac{EI_m}{L} & 0 & -7.264\frac{EI_m}{L^2} & 5.607\frac{EI_m}{L} \end{bmatrix}$$

Large end: $A_L/A_m = 1.183$ and $I_L/I_m = 2.233$
Small end: $A_s/A_m = 0.817$ and $I_s/I_m = 0.292$

In-Plane Elastic Flexural Buckling Strength

P_{eL} = 1,757 kips
P_{cr} = 649 kips
P_{yo} = 230 kips

First-order and second-order deflections and bending moments at various axial load levels are shown in Table C-2.1.

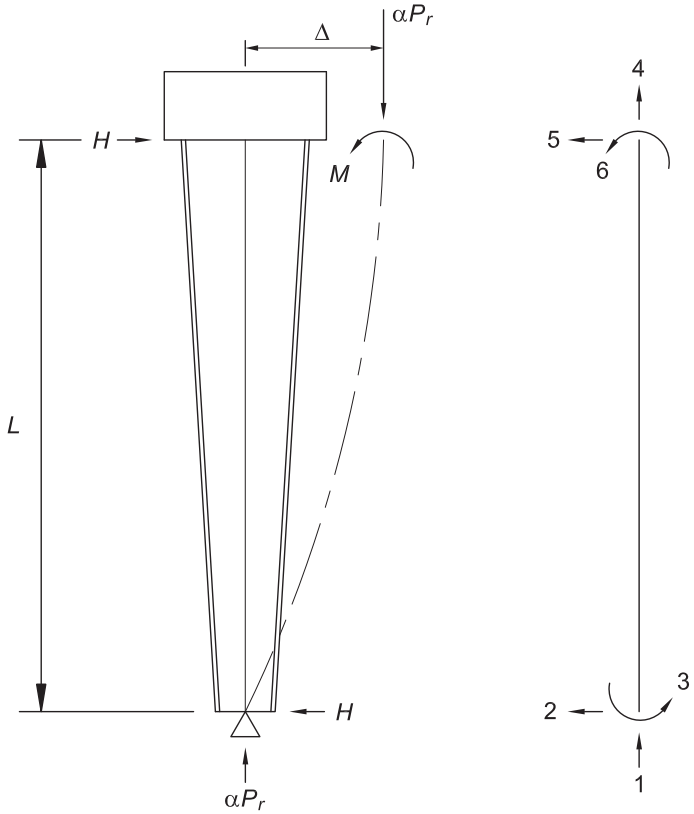

Fig. C-1. Moderately tapered doubly symmetric member subject to sidesway.

Table C-2.2. Sidesway Deflection and Moment				
$\frac{\alpha P_r}{P_{cr}}$	$\frac{\alpha P_r}{P_{eL}}$	$\frac{\alpha P_r}{P_{yo}}$	Δ, in.	M, kip-ft
0.00 (first-order)	0.000	0.000	0.0412H	15.10H
0.04	0.018	0.301	0.0395H	15.49H
0.08	0.036	0.601	0.0410H	15.91H
0.12	0.054	0.902	0.0428H	16.36H
0.16	0.072	1.203	0.0447H	16.86H

Table C-2.3. Sidesway Deflection and Moment				
$\frac{\alpha P_r}{P_{cr}}$	$\frac{\alpha P_r}{P_{eL}}$	$\frac{\alpha P_r}{P_{yo}}$	Δ, in.	M, kip-ft
0.00 (first-order)	0.000	0.000	0.0412H	15.10H
0.04	0.018	0.304	0.0428H	15.52H
0.08	0.036	0.607	0.0446H	15.98H
0.12	0.054	0.911	0.0465H	16.48H
0.16	0.072	1.214	0.0486H	17.03H

Case 2: Heavily Tapered Singly Symmetric Member Subject to Sidesway (see Figure C-2)

Case 2 is similar to Case 1 except that it has a relatively large taper angle and a singly symmetric cross section. The centroidal axis of this member is not straight due to the singly symmetric cross section.

In practice, it can be difficult to account for the minor effect of the curvature of the centroidal axis. Therefore, two solutions are provided:

1. An exact solution accounting for the curved centroidal axis
2. An approximate solution based on a straight reference axis with the moment of inertia varying along the length identically to that of the curved centroidal axis case

Geometric Properties:

Bottom web height = 9.125 in.
Top web height = 39.875 in.
Left flange = PL ½ × 6
Right flange = PL ⅜ × 6
Web thickness = 0.21875 in.
L = 15.1 ft (181.2 in.)
$H/\alpha P_r = 0.01$
A_m = 10.609 in.^{2}
I_m = 1,076 in.^{4}

Displacement boundary conditions: simply supported base, rotation fully restrained at the top

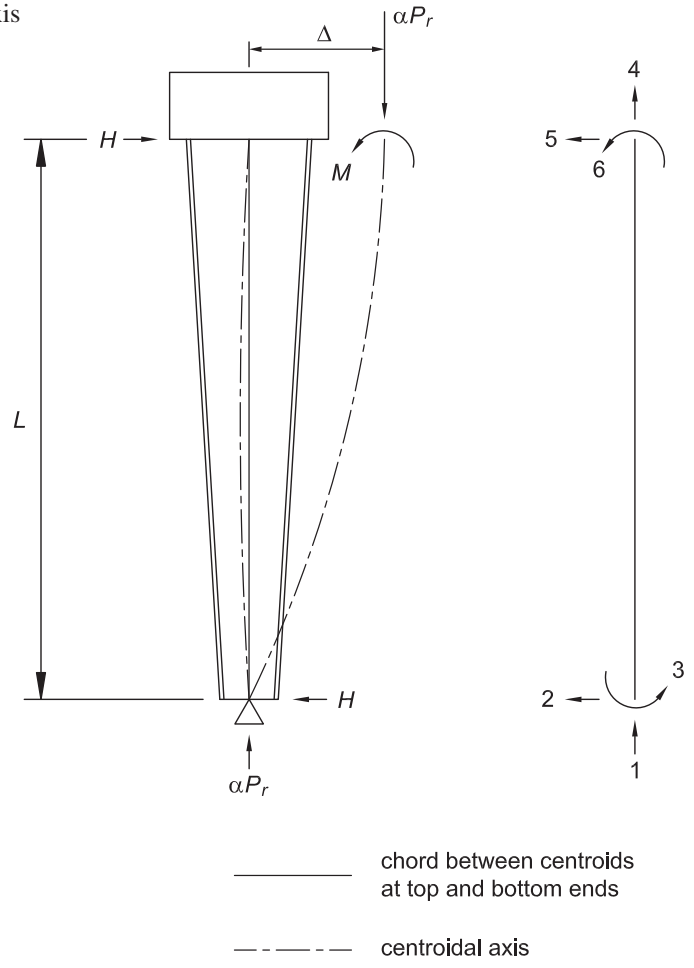

Fig. C-2. Heavily tapered singly symmetric member subject to sidesway.

1. Exact solution accounting for the curved centroidal axis
First-Order Analysis Stiffness Coefficients

Units: kips, inches

$$k = \begin{bmatrix} 0.966\frac{EA_m}{L} & (3.049e-4)\frac{EA_m}{L} & -0.0385\frac{EA_m}{L} & -0.966\frac{EA_m}{L} & -(3.049e-4)\frac{EA_m}{L} & 0.0938\frac{EA_m}{L} \\ (3.049e-4)\frac{EA_m}{L} & 9.801\frac{EI_m}{L^3} & 2.498\frac{EI_m}{L^2} & -(3.049e-4)\frac{EA_m}{L} & -9.801\frac{EI_m}{L^3} & 7.303\frac{EI_m}{L^2} \\ -0.0385\frac{EA_m}{L} & 2.498\frac{EI_m}{L^2} & 1.206\frac{EI_m}{L} & 0.0385\frac{EA_m}{L} & -2.498\frac{EI_m}{L^2} & 1.291\frac{EI_m}{L} \\ -0.966\frac{EA_m}{L} & -(3.049e-4)\frac{EA_m}{L} & 0.0385\frac{EA_m}{L} & 0.966\frac{EA_m}{L} & (3.049e-4)\frac{EA_m}{L} & -0.0938\frac{EA_m}{L} \\ -(3.049e-4)\frac{EA_m}{L} & -9.801\frac{EI_m}{L^3} & -2.498\frac{EI_m}{L^2} & (3.049e-4)\frac{EA_m}{L} & 9.801\frac{EI_m}{L^3} & -7.303\frac{EI_m}{L^2} \\ 0.0938\frac{EA_m}{L} & 7.303\frac{EI_m}{L^2} & 1.291\frac{EI_m}{L} & -0.0938\frac{EA_m}{L} & -7.303\frac{EI_m}{L^2} & 6.012\frac{EI_m}{L} \end{bmatrix}$$

Large end: $A_L/A_m = 1.317$ and $I_L/I_m = 3.041$
Small end: $A_s/A_m = 0.684$ and $I_s/I_m = 0.123$

In-Plane Elastic Flexural Buckling Strength

$P_{eL} = 6{,}683$ kips
$P_{cr} = 2{,}996$ kips
$P_{yo} = 399$ kips

First-order and second-order deflections and bending moments at various axial load levels are shown in Table C-2.2.

2. Approximate solution based on a straight reference axis

First-Order Analysis Stiffness Coefficients

Units: kips, inches

$$k = \begin{bmatrix} 0.966\frac{EA_m}{L} & 0 & 0 & -0.966\frac{EA_m}{L} & 0 & 0 \\ 0 & 9.793\frac{EI_m}{L^3} & 2.495\frac{EI_m}{L^2} & 0 & -9.793\frac{EI_m}{L^3} & 7.298\frac{EI_L}{L^2} \\ 0 & 2.495\frac{EI_m}{L^2} & 1.206\frac{EI_m}{L} & 0 & -2.495\frac{EI_m}{L^2} & 1.290\frac{EI_L}{L} \\ -0.966\frac{EA_m}{L} & 0 & 0 & 0.966\frac{EA_m}{L} & 0 & 0 \\ 0 & -9.793\frac{EI_m}{L^3} & -2.495\frac{EI_m}{L^2} & 0 & 9.793\frac{EI_m}{L^3} & -7.298\frac{EI_m}{L^2} \\ 0 & 7.298\frac{EI_m}{L^2} & 1.290\frac{EI_m}{L} & 0 & -7.298\frac{EI_m}{L^2} & 6.008\frac{EI_m}{L} \end{bmatrix}$$

Large end: $A_L/A_m = 1.317$ and $I_L/I_m = 3.038$
Small end: $A_s/A_m = 0.683$ and $I_s/I_m = 0.123$

In-Plane Elastic Flexural Buckling Strength

P_{eL} = 6,683 kips (equal to the value from case 1 to within four significant digits)
P_{cr} = 3,019 kips (1.008 of the value of P_{cr} for case 1)
P_{yo} = 398 kips (0.997 of the value of P_{yo} for case 1)

First-order and second-order deflections and bending moments at various axial load levels are shown in Table C-2.3.

The second-order displacements, Δ, and maximum moments at the top of the column, *M,* are slightly smaller in solution 1 than for the model with a straight reference axis in solution 2. This is due to the physical curvature of the centroidal axis modeled in solution 1 (the initial centroidal axis is curved to the left) and the influence of the axial force αP_r acting through the initial curvature of the physical centroidal axis. However, the solutions for the first-order stiffness are practically identical. There is some coupling between the axial and bending behavior in the first-order analysis solution of solution 1. This is indicated by nonzero stiffness coefficients in rows and columns 1 and 4 of the stiffness matrix in solution 1 where the stiffness coefficients are zero in the above solution. The solutions for P_{eL} are identical in both cases to within four significant digits and the solutions for P_{cr} are identical to within 0.8%.

Case 3: Tapered Doubly Symmetric Member Subject to Transverse Loading (see Figure C-3)

Case 3 is a propped cantilever subject to a uniformly distributed transverse load. The geometry of this case is similar to the geometry of the rafter of the Example 5.3 frame in Chapter 4 of Lee et al. (1981). The transverse load is applied normal to the centroidal axis of the member.

Geometric Properties:

Left end web height = 8.5 in.
Right end web height = 38.5 in.
Flanges = PL ¼ × 6
Web thickness = 0.1875 in.
L = 40.0 ft (480.0 in.)
$wL/\alpha P_r = 0.1$
$A_m = 7.406$ in.^{2}
$I_m = 625.8$ in.^{4}

Displacement boundary conditions: fully fixed at left end, simply supported at right end

First-Order Analysis Stiffness Coefficients

Units: kips, inches

$$k = \begin{bmatrix} 0.950\frac{EA_m}{L} & 0 & 0 & -0.950\frac{EA_m}{L} & 0 & 0 \\ 0 & 9.677\frac{EI_m}{L^3} & 7.328\frac{EI_m}{L^2} & 0 & -9.677\frac{EI_m}{L^3} & 2.349\frac{EI_m}{L^2} \\ 0 & 7.328\frac{EI_m}{L^2} & 6.085\frac{EI_m}{L} & 0 & -7.328\frac{EI_m}{L^2} & 1.243\frac{EI_m}{L} \\ -0.950\frac{EA_m}{L} & 0 & 0 & 0.950\frac{EA_m}{L} & 0 & 0 \\ 0 & -9.677\frac{EI_m}{L^3} & -7.327\frac{EI_m}{L^2} & 0 & 9.677\frac{EI_m}{L^3} & -2.349\frac{EI_m}{L^2} \\ 0 & 2.349\frac{EI_m}{L^2} & 1.243\frac{EI_m}{L} & 0 & -2.349\frac{EI_m}{L^2} & 1.106\frac{EI_m}{L} \end{bmatrix}$$

Large end: $A_L/A_m = 1.380$ and $I_L/I_m = 3.224$
Small end: $A_s/A_m = 0.620$ and $I_s/I_m = 0.107$

Table C-2.4. Sidesway Deflection and Moment							
$\frac{\alpha P_r}{P_{cr}}$	$\frac{\alpha P_r}{P_{eL}}$	$\frac{\alpha P_r}{P_{yo}}$	Δ_{mid}, in.	M_{neg}, kip-ft	f_{neg}, ksi	M_{pos}, kip-ft*	f_{pos}, ksi**
0.00 (first-order)	0.000	0.000	0.0273*wL*	7.501*wL*	0.870*wL*	1.950*wL*	0.726*wL*
0.10	0.197	0.427	0.0297*wL*	7.939*wL*	0.921*wL*	2.153*wL*	0.815*wL*
0.20	0.394	0.853	0.0327*wL*	8.475*wL*	0.983*wL*	2.407*wL*	0.928*wL*
0.30	0.591	1.280	0.0364*wL*	9.145*wL*	1.061*wL*	2.728*wL*	1.072*wL*

* The location of the maximum positive moment is 28 ft from the left-hand side (within two significant digits) in all cases.
** The location of the maximum flexural stress within the span is 32 ft from the left-hand side (within two significant digits) in all cases.

In-Plane Elastic Flexural Buckling Strength

$P_{eL} = 547$ kips
$P_{cr} = 1{,}078$ kips
$P_{yo} = 253$ kips

First-order and second-order deflections and bending moments at various axial load levels are shown in Table C-2.4.

Moment and Flange Stress Diagrams

1) $\alpha P_r / P_{cr} = 0.00$

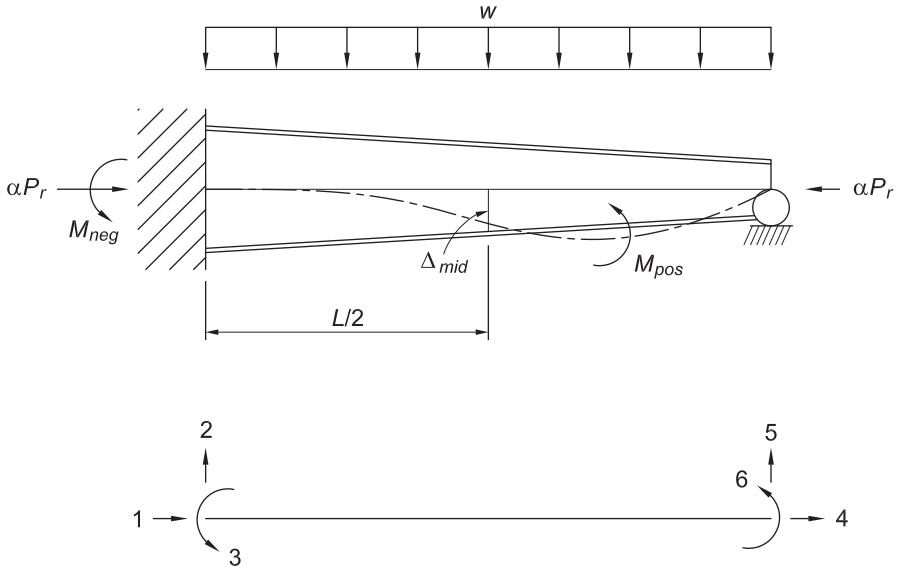

Fig. C-3. Propped cantilever.

C.3 METHOD OF SUCCESSIVE APPROXIMATIONS

C.3.1 γ_{eL} and P_{eL} of Simple Web-Tapered Column

The following spreadsheet-style calculations illustrate the steps in the solution for γ_{eL} and P_{eL} for the simple web-tapered column shown in Figure C-5 using the method of successive approximations. The first two cycles are shown along with the final iteration in Tables C-3a, b and c. The third through seventh iterations are not shown.

Geometric Properties:

Left flange = PL ¼ × 6
Right flange = PL ¼ × 6
Web thickness = 0.125 in.
Bottom web height = 12.0 in.
Top web height = 24.0 in.
Member length = 144 in.

Nodes are evenly distributed along the length of the member in columns 1 and 2 of Table C-3a. Nodes between the two end nodes each have two rows to allow a change in member properties and/or loading at each side of the node. In this example, there are no such changes. Depths and moments of inertias are calculated at each node in columns 3 and 4.

The assumed loading given in column 5 is a constant axial load of 7.50 kips at each node, a value taken from Example 5.2. The assumed deflection for the first iteration in column 6 is linearly tapered from zero at the ends to 10 in. at the center of the column. Although this is a poor estimate of the final deflected shape, it nonetheless results in convergence of the solution to four decimal places in eight iterations. A better initial estimate would reduce the number of iterations required to achieve the same accuracy.

The bending moment at each point is the axial load at that point, P, multiplied by the assumed deflection, δ. The curvature at that point is then $P\delta/EI$, tabulated in column 7. This curvature is then integrated twice using the conjugate beam method to calculate the deflections. In

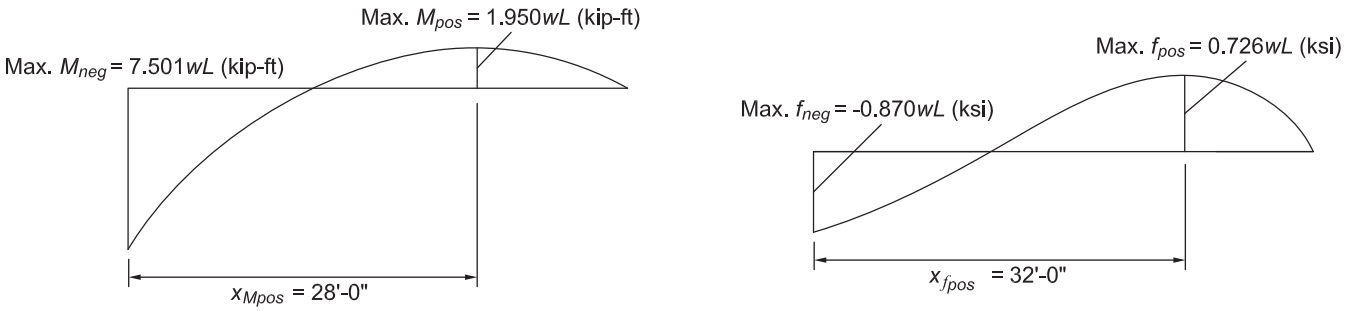

(a) $\alpha P_r/P_{cr} = 0$

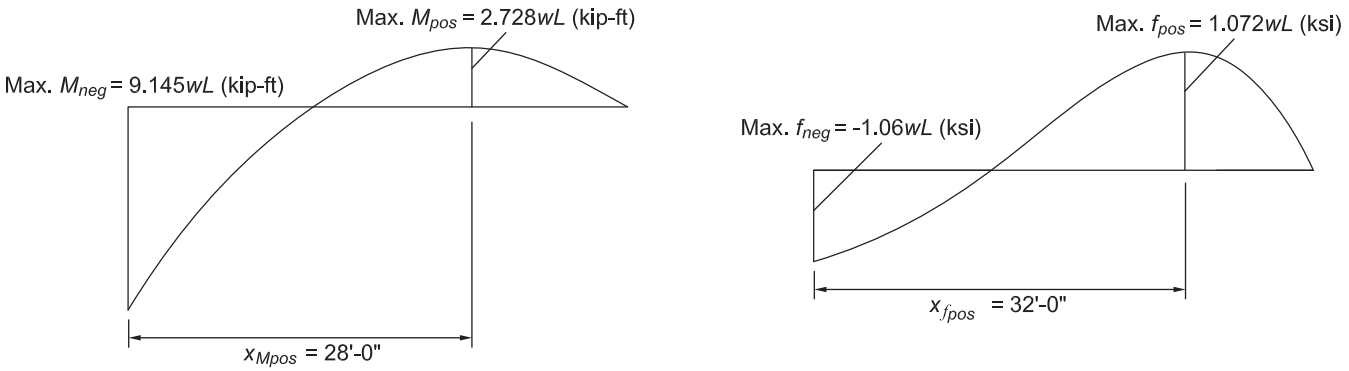

(b) $\alpha P_r/P_{cr} = 0.300$

Units: w (kips/ft), L (ft)

Fig. C-4. Moment diagrams for propped cantilever.

Table C-3a. Simple Tapered Column—First Iteration												
1	2	3	4	5	6	7	8	9	10	11	12	13
Node	*x* from top in.	Depth in.	Moment of Inertia in.^{4}	*P* kips	Assumed δ in.	*Pδ/EI* rad/in.	Conc. Curvature *M′/EI* rad	*(M′/EI)* ∗ *x* in.-rad	Average θ rad	δ in.	γ y_1/y_2	Next δ Estimate in.
0	0.0	24.50	585.1	7.50	0.000	0.00000000	–	–	0.000280	0.00000	–	0.000
1L	14.4	23.30	522.0	7.50	2.000	0.00000099	0.0000146	0.000210		0.00403	496.4	2.668
1R		23.30	522.0	7.50		0.00000099			0.000265			
2L	28.8	22.10	463.1	7.50	4.000	0.00000223	0.0000326	0.000938		0.00785	509.6	5.198
2R		22.10	463.1	7.50		0.00000223			0.000233			
3L	43.2	20.90	408.3	7.50	6.000	0.00000380	0.0000552	0.002386		0.01120	535.8	7.417
3R		20.90	408.3	7.50		0.00000380			0.000177			
4L	57.6	19.70	357.5	7.50	8.000	0.00000579	0.0000840	0.004839		0.01375	581.6	9.109
4R		19.70	357.5	7.50		0.00000579			0.000093			
5L	72.0	18.50	310.6	7.50	10.000	0.00000833	0.0001162	0.008363		0.01510	662.3	10.000
5R		18.50	310.6	7.50		0.00000833			-0.000023			
6L	86.4	17.30	267.4	7.50	8.000	0.00000774	0.0001110	0.009590		0.01477	541.5	9.783
6R		17.30	267.4	7.50		0.00000774			-0.000134			
7L	100.8	16.10	228.0	7.50	6.000	0.00000681	0.0000974	0.009820		0.01285	467.0	8.508
7R		16.10	228.0	7.50		0.00000681			-0.000231			
8L	115.2	14.90	192.1	7.50	4.000	0.00000539	0.0000767	0.008834		0.00952	420.2	6.304
8R		14.90	192.1	7.50		0.00000539			-0.000308			
9L	129.6	13.70	159.7	7.50	2.000	0.00000324	0.0000453	0.005876		0.00509	393.3	3.368
9R		13.70	159.7	7.50		0.00000324			-0.000353			
10	144.0	12.50	130.6	7.50	0.000	0.00000000	–	–		0.00000	–	0.000
						Σ	0.000633	0.05086	θ_{0-1} = 0.000633 – 0.05086/144 in. = 0.000280 rad			

this example, the *M/EI* curve in column 7 is reduced to a series of equivalent concentrated *M/EI* values in column 8 using the parabolic equations presented in Table A-2 of Section A.2 to simplify the subsequent beam span analysis. The reactions from the concentrated *M/EI* values in column 8 are then calculated using statics from the information in column 9. The top reaction is used as the average rotation between nodes 0 and 1 in column 10 and the rotations of each subsequent segment are taken as the previous rotation less the concentrated curvature value from column 8.

The average rotations in column 10 are then integrated to produce the deflections in column 11. The ratio of the assumed deflections to the calculated deflections, γ, is given in column 12. A new set of deflections estimates, normalized to a center deflection of 10.0 in. is then calculated in column 13 by multiplying each of the calculated deflections from column 11 by the value of γ at the center. This new set of deflection estimates then replaces those in column 6 for the next iteration. At convergence, the value of γ in column 12 will be essentially the same for all nodes, and the deflections estimated for the next cycle in column 13 will essentially equal those that were used in column 6.

If the assumed loading in column 5 is identical to P_r for the load combination under consideration, then γ_{eL} is equal to the final γ from column 12, otherwise

$\gamma_{eL} = \gamma_{\text{column 12}} \dfrac{P_{\text{column 5}}}{P_r}$. In either case, $P_{eL} = P_{\text{column5}}\,\gamma_{\text{column12}}$.

For this example, converged values of γ_{eL} = 531 and P_{eL} = 7.50 kips (531) = 3,980 kips are obtained after eight iterations.

From an eigenvalue buckling analysis using GT-Sabre (Chang, 2006), P_{eL} was calculated to be 3,878 kips, a difference of 2.6%.

Table C-3b. Simple Tapered Column—Second Iteration												
1	2	3	4	5	6	7	8	9	10	11	12	13
Node	*x* from top in.	Depth in.	Moment of Inertia in.^{4}	*P* kips	Assumed δ in.	*Pδ/EI* rad/in.	Conc. Curvature *M′/EI* rad	*(M′/EI) * x* in.-rad	Average θ rad	δ in.	γ y_1/y_2	Next δ Estimate in.
0	0.0	24.50	585.1	7.50	0.000	0.00000000	–	–	0.000342	0.00000	–	0.000
1L	14.4	23.30	522.0	7.50	2.668	0.00000132	0.0000193	0.000279		0.00492	542.3	2.681
1R		23.30	522.0	7.50		0.00000132			0.000322			
2L	28.8	22.10	463.1	7.50	5.198	0.00000290	0.0000421	0.001211		0.00956	543.5	5.209
2R		22.10	463.1	7.50		0.00000290			0.000280			
3L	43.2	20.90	408.3	7.50	7.417	0.00000470	0.0000678	0.002928		0.01360	545.4	7.408
3R		20.90	408.3	7.50		0.00000470			0.000213			
4L	57.6	19.70	357.5	7.50	9.109	0.00000659	0.0000947	0.005455		0.01666	546.7	9.076
4R		19.70	357.5	7.50		0.00000659			0.000118			
5L	72.0	18.50	310.6	7.50	10.000	0.00000833	0.0001192	0.008582		0.01836	544.7	10.000
5R		18.50	310.6	7.50		0.00000833			-0.000001			
6L	86.4	17.30	267.4	7.50	9.783	0.00000946	0.0001351	0.011673		0.01834	533.5	9.989
6R		17.30	267.4	7.50		0.00000946			-0.000136			
7L	100.8	16.10	228.0	7.50	8.508	0.00000965	0.0001374	0.013846		0.01637	519.6	8.919
7R		16.10	228.0	7.50		0.00000965			-0.000274			
8L	115.2	14.90	192.1	7.50	6.304	0.00000849	0.0001200	0.013821		0.01243	507.1	6.771
8R		14.90	192.1	7.50		0.00000849			-0.000394			
9L	129.6	13.70	159.7	7.50	3.368	0.00000546	0.0000757	0.009805		0.00676	498.2	3.682
9R		13.70	159.7	7.50		0.00000546			-0.000469			
10	144.0	12.50	130.6	7.50	0.000	0.00000000	–	–		0.00000	–	0.000
						Σ	0.000811	0.06760	θ_{0-1} = 0.000811 – 0.06760/144 in. = 0.000342 rad			

Table C-3c. Simple Tapered Column—Final Iteration												
1	2	3	4	5	6	7	8	9	10	11	12	13
Node	x from top in.	Depth in.	Moment of Inertia in.^{4}	P kips	Assumed δ in.	$P\delta/EI$ rad/in.	Conc. Curvature M'/EI rad	$(M'/EI) * x$ in.-rad	Average θ rad	δ in.	γ y_1/y_2	Next δ Estimate in.
0	0.0	24.50	585.1	7.50	0.000	0.00000000	–	–	0.000348	0.00000	–	0.000
1L	14.4	23.30	522.0	7.50	2.659	0.00000132	0.0000193	0.000278		0.00501	530.5	2.659
1R		23.30	522.0	7.50		0.00000132			0.000329			
2L	28.8	22.10	463.1	7.50	5.170	0.00000289	0.0000418	0.001205		0.00975	530.5	5.170
2R		22.10	463.1	7.50		0.00000289			0.000287			
3L	43.2	20.90	408.3	7.50	7.362	0.00000466	0.0000673	0.002906		0.01388	530.5	7.362
3R		20.90	408.3	7.50		0.00000466			0.000220			
4L	57.6	19.70	357.5	7.50	9.041	0.00000654	0.0000941	0.005419		0.01704	530.5	9.041
4R		19.70	357.5	7.50		0.00000654			0.000126			
5L	72.0	18.50	310.6	7.50	10.000	0.00000833	0.0001194	0.008600		0.01885	530.5	10.000
5R		18.50	310.6	7.50		0.00000833			0.000006			
6L	86.4	17.30	267.4	7.50	10.047	0.00000972	0.0001389	0.011999		0.01894	530.5	10.047
6R		17.30	267.4	7.50		0.00000972			-0.000133			
7L	100.8	16.10	228.0	7.50	9.033	0.00001025	0.0001458	0.014695		0.01703	530.5	9.033
7R		16.10	228.0	7.50		0.00001025			-0.000279			
8L	115.2	14.90	192.1	7.50	6.906	0.00000930	0.0001312	0.015115		0.01302	530.5	6.906
8R		14.90	192.1	7.50		0.00000930			-0.000410			
9L	129.6	13.70	159.7	7.50	3.776	0.00000612	0.0000846	0.010958		0.00712	530.5	3.776
9R		13.70	159.7	7.50		0.00000612			-0.000494			
10	144.0	12.50	130.6	7.50	0.000	0.00000000	–	–		0.00000	–	0.000
						Σ	0.000842	0.07118	θ_{0-1} = 0.000842 – 0.07118/144 in. = 0.000348 rad			

C.3.2 γ_{eL} of Stepped Web-Tapered Column

The following spreadsheet-style calculations illustrate the solution of P_{eL} for the fairly complex web tapered column, shown in Figure C-6, using the method of successive approximations. The initial two cycles are presented in Tables C-3d and C-3e, along with the final solution in Table C-3f. The third through eighth iterations are not shown. The procedure is identical to that just presented for the simple column, but the example illustrates the handling of abrupt changes in loading and geometry.

The upper shaft is divided into three elements of 32 in. and the lower shaft is divided into seven elements of 30 in. to create approximately equal length segments in the upper and lower shafts. Note that in the vicinity of node 3, where the step occurs, it is necessary to use the versions of the equations from Table A-2 for unequal element lengths. Also note that the eccentricities of the geometry and loading are ignored in the analysis.

The resulting γ in column 12 of Table C-3f for the final (ninth) iteration indicates that the in-plane elastic flexural buckling load for this column is 62.8 times the loads used in the analysis. This compares with a γ of 64.2 calculated from an elastic eigenvalue buckling analysis with concentric assumptions conducted using GT-Sabre (Chang, 2006), a difference of 2.2%.

Geometric Properties:

Top web height = 12.0 in.
Step web height = 33.0 in.
Bottom web height = 12.0 in.
Left flange = PL ½ × 8
Right flange below step = PL ¾ × 8
Right flange above step = PL ⅝ × 8
Web thickness above step = 0.188 in.
Web thickness below step = 0.250 in.

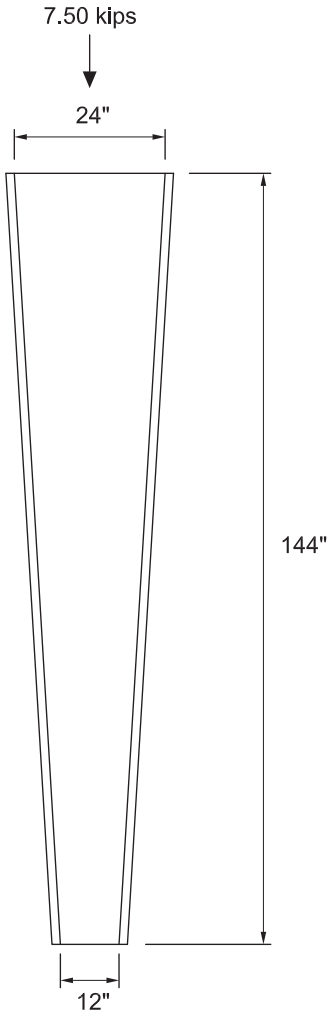

Fig. C-5. Example column.

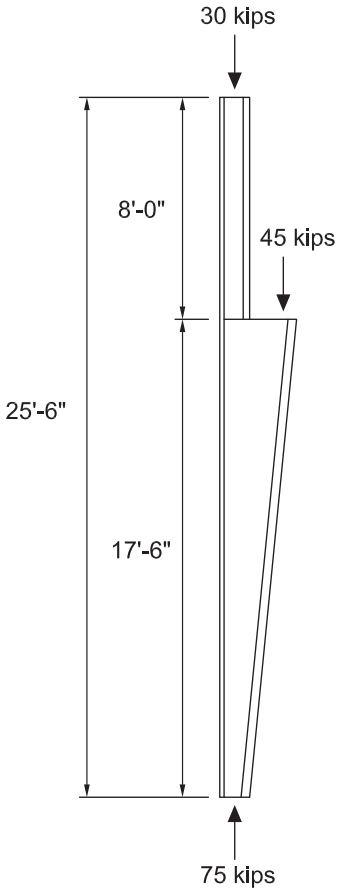

Fig. C-6. Stepped column.

Table C-3d. Complex Tapered Column—First Iteration												
1	2	3	4	5	6	7	8	9	10	11	12	13
Node	*x* from top in.	Depth in.	Moment of Inertia in.^{4}	*P* kips	Assumed δ in.	*Pδ/EI* rad/in.	Conc. Curvature *M′/EI* rad	*(M′/EI) * x* in.-rad	Average θ rad	δ in.	γ y_1/y_2	Next δ Estimate in.
0	0.0	13.13	379.0	30.00	0.000	0.00000000	–	–	0.001262	0.0000	–	0.000
1L	32.0	13.13	379.0	30.00	2.000	0.00000546	0.000175	0.0056		0.0404	49.520	3.429
1R		13.13	379.0	30.00		0.00000546			0.001087			
2L	64.0	13.13	379.0	30.00	4.000	0.00001092	0.000349	0.0224		0.0752	53.201	6.384
2R		13.13	379.0	30.00		0.00001092			0.000738			
3L	96.0	13.13	379.0	30.00	6.000	0.00001638	0.000312	0.0299		0.0988	60.726	8.390
3R		34.25	3515.6	75.00		0.00000441			0.000426			
4L	126.0	31.25	2855.7	75.00	8.000	0.00000725	0.000221	0.0278		0.1116	71.687	9.476
4R		31.25	2855.7	75.00		0.00000725			0.000206			
5L	156.0	28.25	2274.1	75.00	10.000	0.00001137	0.000332	0.0517		0.1178	84.911	10.000
5R		28.25	2274.1	75.00		0.00001137			-0.000126			
6L	186.0	25.25	1767.6	75.00	8.000	0.00001170	0.000350	0.0651		0.1140	70.179	9.679
6R		25.25	1767.6	75.00		0.00001170			-0.000476			
7L	216.0	22.25	1332.7	75.00	6.000	0.00001164	0.000347	0.0750		0.0997	60.173	8.467
7R		22.25	1332.7	75.00		0.00001164			-0.000823			
8L	246.0	19.25	965.9	75.00	4.000	0.00001071	0.000316	0.0778		0.0750	53.321	6.370
8R		19.25	965.9	75.00		0.00001071			-0.001140			
9L	276.0	16.25	663.8	75.00	2.000	0.00000779	0.000222	0.0612		0.0408	48.981	3.467
9R		16.25	663.8	75.00		0.00000779			-0.001361			
10	306.0	13.25	423.0	75.00	0.000	0.00000000	–	–		0.0000	–	0.000
						Σ	0.00262	0.4165	θ_{0-1} = 0.00262 – 0.4165/306 in. = 0.001262 rad			

Table C-3e. Complex Tapered Column—Second Iteration												
1	2	3	4	5	6	7	8	9	10	11	12	13
Node	*x* from top in.	Depth in.	Moment of Inertia in.^{4}	*P* kips	Assumed δ in.	*Pδ/EI* rad/in.	Conc. Curvature *M′/EI* rad	*(M′/EI)* ∗ *x* in.-rad	Average θ rad	δ in.	γ y_1/y_2	Next δ Estimate in.
0	0.0	13.13	379.0	30.00	0.000	0.00000000	–	–	0.001771	0.0000	–	0.000
1L	32.0	13.13	379.0	30.00	3.429	0.00000936	0.000296	0.0095		0.0567	60.528	3.670
1R		13.13	379.0	30.00		0.00000936			0.001474			
2L	64.0	13.13	379.0	30.00	6.384	0.00001743	0.000551	0.0352		0.1038	61.479	6.726
2R		13.13	379.0	30.00		0.00001743			0.000924			
3L	96.0	13.13	379.0	30.00	8.390	0.00002290	0.000445	0.0427		0.1334	62.889	8.641
3R		34.25	3515.6	75.00		0.00000617			0.000479			
4L	126.0	31.25	2855.7	75.00	9.476	0.00000858	0.000258	0.0326		0.1478	64.124	9.571
4R		31.25	2855.7	75.00		0.00000858			0.000221			
5L	156.0	28.25	2274.1	75.00	10.000	0.00001137	0.000341	0.0532		0.1544	64.771	10.000
5R		28.25	2274.1	75.00		0.00001137			-0.000121			
6L	186.0	25.25	1767.6	75.00	9.679	0.00001416	0.000424	0.0788		0.1508	64.198	9.766
6R		25.25	1767.6	75.00		0.00001416			-0.000544			
7L	216.0	22.25	1332.7	75.00	8.467	0.00001643	0.000489	0.1056		0.1344	62.974	8.708
7R		22.25	1332.7	75.00		0.00001643			-0.001033			
8L	246.0	19.25	965.9	75.00	6.370	0.00001706	0.000501	0.1233		0.1035	61.568	6.701
8R		19.25	965.9	75.00		0.00001706			-0.001534			
9L	276.0	16.25	663.8	75.00	3.467	0.00001351	0.000380	0.1050		0.0574	60.366	3.720
9R		16.25	663.8	75.00		0.00001351			-0.001915			
10	306.0	13.25	423.0	75.00	0.000	0.00000000	–	–		0.0000	–	0.000
						Σ	0.00369	0.5858	θ_{0-1} = 0.00369 – 0.5858/306 in. = 0.001776 rad			

Table C-3f. Complex Tapered Column—Final Iteration												
1	2	3	4	5	6	7	8	9	10	11	12	13
Node	*x* from top in.	Depth in.	Moment of Inertia in.^{4}	*P* kips	Assumed δ in.	*Pδ/EI* rad/in.	Conc. Curvature *M′/EI* rad	*(M′/EI)* ⋆ *x* in.-rad	Average θ rad	δ in.	γ y_1/y_2	Next δ Estimate in.
0	0.0	13.13	379.0	30.00	0.000	0.00000000	–	–	0.001847	0.0000	–	0.000
1L	32.0	13.13	379.0	30.00	3.712	0.00001013	0.000320	0.0102		0.0591	62.795	3.712
1R		13.13	379.0	30.00		0.00001013			0.001528			
2L	64.0	13.13	379.0	30.00	6.782	0.00001851	0.000584	0.0374		0.1080	62.795	6.782
2R		13.13	379.0	30.00		0.00001851			0.000944			
3L	96.0	13.13	379.0	30.00	8.678	0.00002369	0.000462	0.0444		0.1382	62.795	8.678
3R		34.25	3515.6	75.00		0.00000638			0.000481			
4L	126.0	31.25	2855.7	75.00	9.585	0.00000868	0.000261	0.0329		0.1526	62.795	9.585
4R		31.25	2855.7	75.00		0.00000868			0.000220			
5L	156.0	28.25	2274.1	75.00	10.000	0.00001137	0.000342	0.0533		0.1592	62.795	10.000
5R		28.25	2274.1	75.00		0.00001137			-0.000122			
6L	186.0	25.25	1767.6	75.00	9.771	0.00001430	0.000428	0.0796		0.1556	62.795	9.771
6R		25.25	1767.6	75.00		0.00001430			-0.000550			
7L	216.0	22.25	1332.7	75.00	8.735	0.00001695	0.000505	0.1090		0.1391	62.795	8.735
7R		22.25	1332.7	75.00		0.00001695			-0.001055			
8L	246.0	19.25	965.9	75.00	6.748	0.00001807	0.000531	0.1306		0.1075	62.795	6.748
8R		19.25	965.9	75.00		0.00001807			-0.001585			
9L	276.0	16.25	663.8	75.00	3.762	0.00001466	0.000412	0.1136		0.0599	62.795	3.762
9R		16.25	663.8	75.00		0.00001466			-0.001997			
10	306.0	13.25	423.0	75.00	0.000	0.00000000	–	–		0.0000	–	0.000
						Σ	0.00384	0.6110	θ_{0-1} = 0.00384 – 0.6110/306 in. = 0.001847 rad			

SYMBOLS

A Column cross-sectional area, in.^{2}

A_e Effective net area, in.^{2}

A_{eff} Summation of the effective areas of the cross section based on the reduced effective width, b_e, in.^{2}

A_{fg} Gross tension flange area, in.^{2}

A_{flange} Area of flange, in.^{2}

A_{fn} Net tension flange area, in.^{2}

A_g Gross area of member, in.^{2}

A_w Area of web, in.^{2}

B_1 Amplifier for nonsway moments

B_2 Amplifier for sway moments

C_b Lateral-torsional buckling modification factor for nonuniform member stress

C_d Seismic deflection amplification factor

C_m Coefficient to account for nonuniform moment in interaction equations

C_w Warping constant, in.^{6}

C_v Web shear coefficient

E Modulus of elasticity = 29,000 ksi

F_{ca} Available compressive stress, ksi

F_{cbx} Available flexural stress for bending about the x-axis, ksi

F_{cby} Available flexural stress for bending about the y-axis, ksi

F_{cr} Critical axial buckling stress, ksi

F_e Elastic critical buckling stress, ksi

F_e' Euler stress for a prismatic member divided by factor of safety, ksi

F_{eLTB} Elastic critical lateral-torsional buckling stress, ksi

F_{ey} Elastic flexural buckling stress about the minor axis, ksi

F_{ez} Elastic torsional buckling stress, ksi

F_L Assumed flexural extreme fiber stress at transition between elastic and inelastic regions, ksi

F_{n1} Nominal axial buckling stress, not including the effects of slender elements, ksi

F_r Generalized required axial stress, ksi

F_u Specified minimum tensile strength, ksi

F_y Specified minimum yield strength, ksi

F_{yf} Specified minimum yield strength of flange, ksi

F_{yw} Specified minimum yield strength of web, ksi

G Shear modulus of elasticity = 11,200 ksi

H Total lateral frame load

H Flexural constant

I Moment of inertia, in.^{4}

I' Moment of inertia of equivalent prismatic column of the same length, in.^{4}

I_{yc} Moment of inertia about y-axis referred to the compression flange, in.^{4}

I_{y1} Moment of inertia about y-axis of the smaller flange, in.^{4}

I_{y2} Moment of inertia about y-axis of the larger flange, in.^{4}

I_{xLarge} Moment of inertia about x-axis of the deeper end of the unbraced length, in.^{4}

I_{xSmall} Moment of inertia about x-axis of the shallower end of the unbraced length, in.^{4}

J St. Venant's torsional constant, in.^{4}

K Effective length factor

$K_\gamma g$ Effective length factor accounting for both end conditions and web taper

L Member length, in.

L_b Length between points that are braced against lateral displacement of compression flanges or braced against twist of the cross section, in.

L_{chord} Span length along the rafter chord between the cross-section centroids at the tops of the columns, in.

L_{os} On-slope length of rafter, in. = length of rafter between columns measured along the rafter top flange

L_z Torsional unbraced length, in.

M_{1st} Bending moment from first-order analysis, kip-in.

M_{2nd} Bending moment from second-order analysis, kip-in.

M_a ASD required flexural strength, kip-in.

$M_{e.LTB}$ Elastic lateral-torsional buckling strength, kip-in.

M_n Nominal flexural strength, kip-in.

M_{cx} Available flexural strength about x-axis (ASD or LRFD), kip-in.

M_{cy} Available flexural strength about y-axis (ASD or LRFD), kip-in.

M_p Plastic bending moment, kip-in.

M_r Required flexural strength (ASD or LRFD), kip-in.

M_{rx} Required flexural strength about x-axis (ASD or LRFD), kip-in.

M_{ry} Required flexural strength about y-axis (ASD or LRFD), kip-in.

M_u LRFD required flexural strength, kip-in.

M_{yc} Yield moment with respect to the compression flange, kip-in.

M_{yt} Yield moment with respect to the tension flange, kip-in.

P Vertical frame load, kips.

P-Δ Additional moment (couple) due to axial force acting through the relative transverse displacement of the member (or member segment) ends

P-δ Additional moment (couple) due to axial force acting through the transverse displacement of the cross-section centroid relative to a chord between the member (or member segment) ends

P_a ASD required axial strength, kips

P_c Available axial strength (ASD or LRFD), kips

P_{cr} Elastic flexural buckling load of a member segment of length ℓ based on actual end conditions

$\overline{P}_{cr}$ Elastic flexural buckling load of a member segment of length ℓ based on actual end conditions, calculated using the reduced stiffness specified by the direct analysis method (DM)

P_e Elastic buckling load, kips

P_{eCAT} Elastic constrained-axis torsional buckling load, kips

$P_{e\ell}$ Elastic flexural buckling load of a member segment of length ℓ based on idealized pinned-pinned end conditions, evaluated in the plane of bending, kips

$\overline{P}_{e\ell}$ Flexural buckling load in the plane of bending for a member segment of length ℓ, calculated using the reduced stiffness specified by the direct analysis method (DM) and using idealized pinned-pinned end conditions, kips

P_{eL} Elastic flexural buckling load of a member of length L based on idealized pinned-pinned end conditions, evaluated in the plane of bending, kips

$\overline{P}_{eL}$ Flexural buckling load in the plane of bending for a member of length L, calculated using the reduced stiffness specified by the direct analysis method (DM) and using idealized pinned-pinned end conditions, kips

P_{ey} Elastic out-of-plane flexural buckling load, kips

P_{ex} Elastic in-plane flexural buckling load, kips

P_{ez} Elastic torsional buckling load, kips

P_n Nominal axial strength, kips

P_{ni} Nominal axial in-plane compressive strength, kips

P_r Required axial strength (ASD or LRFD), kips

P_u LRFD required axial strength, kips

P_x Gravity load, kips

P_y Column yield strength, kips

P_{yo} Column yield strength at small end, kips

Q Static moment of area between extreme flange fiber and inside flange fiber, taken about the neutral axis

Q Full reduction factor for slender elements

Q_a Reduction factor for slender stiffened elements

Q_s Reduction factor for slender unstiffened elements

R_a ASD required strength (force or moment), kips or kip-in.

R_u LRFD required strength (force or moment), kips or kip-in.

R_r Generalized required strength (ASD or LRFD, force or moment), kips or kip-in.

R_n Nominal strength (force or moment), kips or kip-in.

R_{pc} Web plastification factor

R_{pg} Web buckling factor

S Section modulus, in.^{3}

S_{xc} Elastic section modulus referenced to compression flange, in.^{3}

S_{xt} Elastic section modulus referenced to tension flange, in.^{3}

V_a ASD required shear strength, kips

V_n Nominal shear strength, kips

V_r Required shear strength, kips

V_{rw} Required weld shear strength, kips

V_x Total lateral load at a story level, kips

V_u LRFD required design shear strength, kips

Y_i Vertical load introduced at level i, kips

Y_t Tension flange rupture factor

Z_x Plastic section modulus about the x-axis, in.^{3}

a Clear distance between transverse stiffeners, in.

a_c Distance from center of girt or purlin to centroid of column, in.

a_s Distance from center of girt or purlin to shear center of column, in.

a_w Ratio of two times the web area in compression due to strong axis flexure alone to the area of the compression flange

b_e Reduced effective width, in.

b_f Flange width, in.

b_{fc} Compression flange width, in.

d Full nominal depth of section, in.

d_h Bolt hole diameter, in.

h Web height, in.

h_c Twice the distance from the cross-section centroid to the inside face of the compression flange, in.

h_o Distance between flange centroids, in.

h_p Twice the distance from the plastic neutral axis to the inside face of the compression flange, in.

f Stress at which effective width of stiffened element is calculated, ksi

f_0 Flexural stress at opposite end of unbraced length from f_2, ksi

f_1 Stress computed from f_0 and f_2, ksi

f_2 Absolute value of largest compression stress at either end of an unbraced length, ksi

f_a Computed axial stress, ksi

f_{mid} Flexural stress at middle of unbraced length, ksi

f_r Generalized required stress, ksi

f_{ra} Required axial stress, ksi

f_{rbx} Required flexural stress for bending about the strong axis, ksi

f_{rby} Required flexural stress for bending about the weak axis, ksi

f_{rmax} Maximum required stress, ksi

k_c Coefficient for slender unstiffened elements

k_v Web plate buckling coefficient

l Length of member segment, in.

r Radius of gyration, in.

r_t Radius of gyration of the flange in flexural compression plus one third of the web area in compression due to the application of major axis bending moment alone, in.

t_f Flange thickness, in.

t_{fc} Compression flange thickness, in.

t_{ft} Tension flange thickness, in.

t_w Web thickness, in.

x Distance from small end of member where equivalent moment of inertia is calculated, in.

y_o Distance from shear center to centroid, in.

y_1 Assumed deflection, in.

y_2 Calculated deflection, in.

$\overline{y}$ Distance between extreme fiber and centroid, in.

α Factor used to convert the loads from the strength design load level to an ultimate strength load level (1.6 for ASD and 1.0 for LRFD)

γ Ratio of the assumed deflection to the calculated deflection

Δ Interstory frame drift due to lateral forces, in.

Δ_H Average first-order interstory frame drift due to lateral forces, in.

Δ_{1st} Story drift from first-order analysis, in.

Δ_{2nd} Story drift from second-order analysis, in.

δ Member transverse displacement between end points

δ_{1st} First order member transverse displacement between end points

δ_{2nd} Total second order member transverse displacement between end points, including first order displacement

γ_e Ratio of elastic axial buckling force (or stress) to required axial force (or stress)

γ_{eL} Ratio of elastic axial buckling force (or stress) to required axial force (or stress) of a member based on idealized pinned-pinned end conditions ($K = 1$), evaluated in the plane of bending

$\overline{\gamma}_{eL}$ Ratio of elastic axial buckling force (or stress) to required axial force (or stress) of a member based on idealized pinned-pinned end conditions ($K = 1$), evaluated in the plane of bending, calculated using the reduced stiffness specified by the direct analysis method (DM)

γ_{eLTB} Ratio of elastic lateral-torsional buckling moment (or stress) to required moment (or stress) of a member

γ_{n1} Ratio of axial buckling (or stress) to required axial force (or stress) of a member, without consideration of slender elements

$\gamma_{e.rafter}$ Elastic buckling multiplier for in-plane buckling of a rafter analyzed within the frame

$\gamma_{e.story}$ Elastic buckling multiplier for in-plane buckling of the entire frame story

λ Slenderness ratio

λ_r Limiting slenderness ratio between elastic and inelastic buckling

λ_p Limiting slenderness ratio between inelastic buckling and plastic yielding

ϕ Resistance factor (LRFD)

Ω Safety factor (ASD)

τ_b Stiffness reduction factor for use in direct analysis method (DM)

GLOSSARY

Allowable strength. Nominal strength divided by the safety factor, R_n/Ω.

Allowable stress design. Method of proportioning structural components such that the *allowable stresses* equal or exceed the *required stresses* of the component under the action of the *ASD* load combinations.

Amplified first-order elastic analysis. An approximate second-order analysis method, such as the "B_1-B_2" method, based on applying load or displacement amplification factors to the results from first-order elastic analysis.

ASD (allowable strength design). Method of proportioning structural components such that the *allowable strength* equals or exceeds the *required strength* of the component under the action of the *ASD* load combinations.

Available strength. Design strength or *allowable strength,* as appropriate.

Chord. Straight line between centroidal axis work points at each end of a member, segment or element.

Comprehensive second-order analysis. Second-order analysis that includes (1) P-Δ effects, (2) the effect of P-δ on P-Δ, and (3) P-δ amplification of internal moments between member ends.

Design strength. Resistance factor multiplied by *nominal strength*, ϕR_n.

DM. Direct analysis method.

Drift. Lateral deflection of structure.

Element. Portion of a member length between nodes in an analysis model.

ELM. Effective length analysis method.

FLB. Flange local buckling.

FOM. First-order analysis method.

In-plane. Relating to the plane of bending in a beam or beam-column.

Limit state. Condition in which a structure or component becomes unfit for service and is judged either to be no longer useful for its intended function (serviceability limit) or to have reached its ultimate load-carrying capacity (strength limit state).

LRFD (load and resistance factor design). Method of proportioning structural components such that the *design strength* equals or exceeds the *required strength* of the component under the action of the *LRFD* load combinations.

LTB. Lateral-torsional buckling.

Member. Column or beam with an analysis length from foundation to rafter (column) or on-slope dimension from column to column (beam), unless otherwise noted.

Modular frame. Multi-span rigid frame, usually having moment resisting exterior columns and interior columns carrying gravity only.

Node. Location at which rotations and/or displacements are calculated in an analysis model.

Nominal strength. Strength of a structure or component (without *resistance factor* or *safety factor* applied) to resist load effects.

Out-of-plane. Relating to the direction perpendicular to the plane of bending in a beam or beam-column.

Prismatic member. A member whose geometry and section properties are constant along its length.

Required strength. Forces, stresses and deformations acting on the structural component, determined by either structural analysis, for the LRFD or ASD load combinations, or as specified by the AISC *Specification*.

Required stress. Stresses and deformations acting on the structural component, determined by either structural analysis, for the LRFD or ASD load combinations, or as specified by the AISC *Specification*.

Resistance factor, ϕ. Factor that accounts for unavoidable deviations of the *nominal strength* from the actual strength and for the manner and consequences of failure.

Safety factor, Ω. Factor that accounts for deviations of the actual strength from the nominal strength, deviations of the actual load from the nominal load, uncertainties in the analysis that transforms the load into a load effect, and for the manner and consequences of failure.

Second-order analysis. Structural analysis in which the equilibrium conditions are formulated on the deformed structure; i.e., an analysis in which *second-order effects* (both P-δ and P-Δ, unless specified otherwise) are included.

Second-order effect. Effect of *loads* acting on the deformed configuration of a structure; includes P-δ effect and P-Δ effect.

Segment. Portion of a column or beam length considered for convenience in design, analysis or manufacturing.

Strength load combination. Load combination used to design the member or frame against structural limit states.

TFY. Tension flange yielding.

Web-tapered member. A member with flanges that are not parallel within some portion of its length due to tapering of the web.

REFERENCES

AASHTO (2004), *LRFD Bridge Design Specifications,* 3rd Ed., American Association of State Highway and Transportation Officials, Washington, DC.

AASHTO (2007), *LRFD Bridge Design Specifications*, 4th Ed., American Association of State Highway and Transportation Officials, Washington, DC.

AISC (1963), *Specification for the Design, Fabrication and Erection of Structural Steel for Buildings,* April 17, American Institute of Steel Construction, Chicago, IL.

AISC (1978), *Specification for the Design, Fabrication and Erection of Structural Steel for Buildings,* November 1, American Institute of Steel Construction, Chicago, IL.

AISC (1986), *Load and Resistance Factor Design Specification for Structural Steel Buildings,* September 1, American Institute of Steel Construction, Chicago, IL.

AISC (1989), *Specification for Structural Steel Buildings—Allowable Stress and Plastic Design,* June 1, American Institute of Steel Construction, Chicago, IL.

AISC (1993), *Load and Resistance Factor Design Specification for Structural Steel Buildings,* December 1, American Institute of Steel Construction, Chicago, IL.

AISC (1999), *Load and Resistance Factor Design Specification for Structural Steel Buildings,* December 27, American Institute of Steel Construction, Chicago, IL.

AISC (2005), *Specification for Structural Steel Buildings,* ANSI/AISC 360-05, March 9, American Institute of Steel Construction, Chicago, IL.

AISC (2005a), *Seismic Provisions for Structural Steel Buildings Including Supplement No. 1,* ANSI/AISC 341-05, March 9, ANSI/AISC 341s1-05, November 16, American Institute of Steel Construction, Chicago, IL.

AISC (2005b), *Basic Design Values,* American Institute of Steel Construction, Chicago, IL.

AISC (2010), *Specification for Structural Steel Buildings,* ANSI/AISC 360-10, June 22, American Institute of Steel Construction, Chicago, IL.

AISI (1996), *Specification for the Design of Cold-Formed Structural Steel Members,* American Iron and Steel Institute, Washington, DC.

AISI (2001), *North American Specification for the Design of Cold-Formed Structural Steel Members,* American Iron and Steel Institute, Washington, DC.

AISI (2007), *North American Specification for the Design of Cold-Formed Structural Steel Members,* American Iron and Steel Institute, Washington, DC.

Andrade, A., Camotim, D. and e Costa, P.P. (2005), "Elastic Lateral-Torsional Buckling Behavior of Doubly Symmetric Tapered Beam-Columns," *Proceedings,* Annual Technical Session, Structural Stability Research Council, University of Missouri, Rolla, MO, pp. 445–468.

Andrade, A., Camotim, D. and Dinis, P.B. (2007), "Lateral-Torsional Buckling of Singly Symmetric Web-Tapered Thin-Walled I-Beams: 1D Model vs. Shell FEA," *Computers and Structures*, Vol. 85, Issue 17-18, pp. 1343–1359.

ASCE (1997), *Effective Length and Notional Load Approaches for Assessing Frame Stability: Implications for American Steel Design*, American Society of Civil Engineers, Reston, VA.

ASCE (1998), *Minimum Design Loads for Buildings and Other Structures,* ASCE 7-98, American Society of Civil Engineers, Reston, VA.

ASCE (2005), *Minimum Design Loads for Buildings and Other Structures,* ASCE 7-05, American Society of Civil Engineers, Reston, VA.

Bachman, R.E., Drake, R.M., Johnson, M.W. and Murray, T.M. (2004), *Seismic Design Guide for Metal Building Systems,* International Code Council, Falls Church, VA.

Bairstow, L. and Stedman, E.W. (1914), "Critical Loads of Long Struts of Varying Sections," *Engineering,* Vol. 98, No. 403.

Basler, K. (1961), "Strength of Plate Girders in Shear," *Journal of the Structural Division,* ASCE, Vol. 104, No. 9, pp. 151–180.

Bazant, Z.P. and Cedolin, L. (1991), *Stability of Structures—Elastic, Inelastic, Fracture and Damage Theories,* Oxford University Press, New York, NY, 984 pp.

Bjorhovde, R., Colson, A. and Brozzetti, J. (1990), "Classification System for Beam-to-Columns Connections," *Journal of Structural Engineering,* ASCE, Vol. 116, No. 11, pp. 3059–3076.

Bleich, F. (1952), *Buckling Strength of Metal Structures*, McGraw-Hill, New York.

Blodgett, O.W. (1966), *Design of Welded Structures,* James F. Lincoln Arc Welding Foundation, Cleveland, OH, pp. 4.4-1–4.4-7.

Boissonnade, N. and Maquoi, R. (2005), "A Geometrically and Materially Non-linear 3-D Beam Finite Element for the Analysis of Tapered Steel Members," *Steel Structures,* Vol. 5, pp. 413-419.

BSI (1985), *BS 5950: Part 1: 1985, Structural Use of Steelwork in Buildings,* British Standards Institution, London.

Butler, D.J. (1966), "Elastic Buckling Tests on Laterally and Torsionally Braced Tapered I-Beams," *Welding Journal Research Supplement,* Vol. 45, No. 1.

Butler, D.J. and Anderson, G.C. (1963), "The Elastic Buckling of Tapered Beam-Columns," *Welding Journal Research Supplement,* Vol. 42, No. 1.

Cary, W.C. III and Murray, T.M. (1997), "Effective Lengths of Web-Tapered Columns in Rigid Metal Building Frames," Report No. CE/VPI-ST 97/06, May, 59 pp.

CEN (2005), Eurocode 3: *Design of Steel Structures, Part 1.1-General Rules and Rules for Buildings,* EN 1993-1-1:2005: E, Incorporating Corrigendum February 2006, European Committee for Standardization, Brussels, Belgium, 91 pp.

Chang, C.J. (2006), *GT-Sabre User Manual,* School of Civil and Environmental Engineering, Georgia Institute of Technology, Atlanta, GA.

Chen, W.F. and Lui, E.M.(1987), *Structural Stability, Theory and Implementation,* Elsevier, New York.

Chen, W.F. and Lui, E.M. (1991), *Stability Design of Steel Frames,* CRC Press, Boca Raton, FL.

Chen, Y., Shen, Z., Zheng, Q. and Chen, C. (2001), "Experimental Study on the Performance of Single Weld Joints in H-Shaped Steel Members," *Steel Structures 1,* Korean Society of Steel Construction, Seoul, South Korea, pp. 201–211.

Davies, J.M. (1990), "In-Plane Stability in Portal Frames," *Structural Engineer,* Vol. 68, No. 8.

Davies, J.M. and Brown, B.A. (1996), *Plastic Design to BS 5950,* Steel Construction Institute, Blackwell Science, 326 pp.

Davis, B.D. (1996), "LRFD Evaluation of Full-Scale Metal Building Frame Tests," M.S. Thesis, Charles Via Department of Civil Engineering, Virginia Polytechnic Institute and State University, Blacksburg, VA, 255 pp.

Deierlein, G. (2003), "Background and Illustrative Examples on Proposed Direct Analysis Method for Stability Design of Moment Frames," AISC Technical Committee 10 and AISC-SSRC Ad Hoc Committee on Frame Stability, Department of Civil and Environmental Engineering, Stanford University, 17 pp.

Deierlein, G. (2004), "Stable Improvements: Direct Analysis Method for Stability Design of Steel-Framed Buildings," *Structural Engineer,* November, pp. 24–28.

Dinnik, A.N. (1914), *I svest. Gornogo* Inst., Ekaterinoslav.

Dinnik, A.N. (1916), *Vestnik Ingenerov,* Moscow.

Dinnik, A.N. (1929), "Design of Columns of Varying Cross Sections," *ASME Transactions,* AMP-51-11, Vol. 51, McGraw-Hill, New York, pp. 165–171.

Dinnik, A.N. (1932), "Design of Columns of Varying Cross Sections," *ASME Transactions,* AMP-54-16, Vol. 54, McGraw-Hill, New York, pp.105–109.

Eroz, M., White, D.W. and DesRoches, R. (2008), "Direct Analysis and Design of Steel Frames Accounting for Partially Restrained Column Base Conditions," *Journal of Structural Engineering*, ASCE, Vol. 134, No. 9, pp. 1508–1517.

Falby, W.E and Lee, G.C. (1976), "Tension-Field Design of Tapered Members," *Engineering Journal,* AISC, First Quarter 1976, pp. 11–17.

Fisher, J.M. (2005), "Don't Stress Out," *Modern Steel Construction,* October 2005, American Institute of Steel Construction, Chicago, IL, pp. 41–42.

Forest, R. and Murray, T.M. (1982), "Rigid Frame Studies, Full Scale Frame Tests," Research Report No. FSEL/STAR 82-01, School of Civil Engineering and Environmental Science, University of Oklahoma, Norman, OK, 109 pp.

Galambos, T.V. (1998), *Guide to Stability Design Criteria for Metal Structures,* T.V. Galambos (ed.), Structural Stability Research Council, Wiley Interscience, New York, 911 pp.

Galambos, T.V. and Ketter, R.L. (1959), "Columns Under Combined Bending and Thrust," *Journal of the Engineering Mechanics Division,* ASCE, Vol. 85, No. 2, pp. 135–152.

Guney, E. and White, D.W. (2007), "Ensuring Sufficient Accuracy of Second-Order Frame Analysis Software," Structural Engineering Mechanics and Materials Report No. 55, School of Civil and Environmental Engineering, Georgia Institute of Technology, Atlanta, GA, May, 95 pp.

HKS (2006). ABAQUS Version 6.6/Standard User's Manual, HKS, Inc., Providence, RI.

IBC (2000), *International Building Code 2000,* International Code Council, Falls Church, VA.

Jenner, R.K., Densford, T.A., Astaneh-Asl, A. and Murray, T.M. (1985a), "Experimental Investigation of Rigid Frames Including Knee Connection Studies, Frame FR1 Tests, Report No. FSEL//MESCO 85-02, Fears Structural Engineering Laboratory, School of Civil Engineering and Environmental Science, University of Oklahoma, Norman, OK, July, 210 pp.

Jenner, R.K., Densford, T.A., Astaneh-Asl, A. and Murray, T.M. (1985b), "Experimental Investigation of Rigid Frames Including Knee Connection Studies, Frame FR2 Tests, Report No. FSEL//MESCO 85-03, Fears Structural Engineering Laboratory, School of Civil Engineering and Environmental Science, University of Oklahoma, Norman, OK, August, 263 pp.

Jimenez Lopez, G.A. (1998), "Inelastic Stability of Tapered Structural Members," Doctoral Dissertation, University of Minnesota, Minneapolis-St. Paul, MN, 201 pp.

Jimenez, G.A. (2005), "Restrained Web-Tapered Columns," A Practical Design Approach," *Proceedings,* Annual Technical Session, Structural Stability Research Council, University of Missouri, Rolla, MO, pp. 225–240.

Jimenez, G.A. (2006), "Further Studies on the Lateral-Torsional of Steel Web-Tapered Beam-Columns," *Proceedings,* Annual Technical Session, Structural Stability Research Council, University of Missouri, Rolla, MO, pp. 267–280.

Jimenez, G. and Galambos, T.V. (2001), "Inelastic Stability of Pinned Tapered Columns," *Proceedings,* Annual Technical Session, Structural Stability Research Council, University of Missouri, Rolla, MO, pp. 143–158.

Kim, Y.D. and White, D.W. (2006a), "Benchmark Problems for Second-Order Analysis of Frames with Tapered-Web Members," Structural Engineering Mechanics and Materials Report No. 53, School of Civil and Environmental Engineering, Georgia Institute of Technology, Atlanta, GA, April, 10 pp.

Kim, Y.D. and White, D.W (2006b), "Full Nonlinear Finite Element Analysis Simulation of the LB-3 Test from Prawel et al. (1974)," Structural Engineering Mechanics and Materials Report No. 56, School of Civil and Environmental Engineering, Georgia Institute of Technology, Atlanta, GA, September, 15 pp.

Kim, Y.D. and White, D.W (2007a), "Practical Buckling Solutions for Tapered Beam Members," *Proceedings*, Annual Technical Session, Structural Stability Research Council, University of Missouri, Rolla, MO, pp. 259–278.

Kim, Y.D. and White, D.W. (2007b), "Assessment of Nominal Resistance Calculations for Web-Tapered I-shaped Members: Comparison to Experimental Tests and to Finite Element Simulations of Experimental Tests," Structural Engineering Mechanics and Materials Report No. 31, School of Civil and Environmental Engineering, Georgia Institute of Technology, Atlanta, GA, May, 59 pp.

Kim, Y.D. (2010), "Behavior and Design of Metal Building Frames with General Prismtaic and Web-Tapered Steel I-Section Members," Doctoral Dissertation, School of Civil and Environmental Engineering, Georgia Institute of Technology, Atlanta, GA, 562 pp.

King, C. (2001a), *In-Plane Stability of Portal Frames to BS 5950-1:2000,* SCI Publication P292, Steel Construction Institute, Ascot, Berkshire, 213 pp.

King, C. (2001b), *Design of Single Span Steel Portal Frames to BS 5950-1:2000,* SCI Publication P252, Steel Construction Institute, Ascot, Berkshire.

Kuchenbecker, G.H., White, D.W. and Surovek-Maleck, A.E. (2004), "Simplified Design of Building Frames Using First-Order Analysis and K = 1.0," *Proceedings,* Annual Technical Session, Structural Stability Research Council, University of Missouri, Rolla, MO, pp. 119–138.

Lagrange (1770-1773), "Sur la figure des colonnes," *Misc. Taurinensia*, Vol. 5. (Reprinted in "Oeuvres de Lagrange," Vol. 2, Gauthier-Villars, Paris, 1868, pp. 125–170.)

Lee, G.C., Morrell, M.L. and Ketter, R.L. (1972), "Design of Tapered Members," *Welding Research Council Bulletin,* No. 173, pp. 1–32.

Lee, G.C. and Morrell, M.L. (1975), "Application of AISC Design Provisions for Tapered Members," *Engineering Journal,* AISC, Vol. 12, No. 1, pp. 1–13.

Lee, G.C., Chen, Y.C. and Hsu, T.L. (1979), "Allowable Axial Stress of Restrained Multi-Segment, Tapered Roof Girders," *Welding Research Council Bulletin,* No. 248, May, pp. 1–28.

Lee, G.C. and Hsu, T.L. (1981), "Tapered Columns with Unequal Flanges," *Welding Research Council Bulletin,* No. 272, November, pp. 15–23.

Lee, G.C., Ketter, R.L. and Hsu, T.L. (1981), *The Design of Single Story Rigid Frames,* Metal Building Manufacturers Association, Cleveland, OH, 267 pp.

Lu, L.W. (1965), "Effective Length of Columns in Gable Frames," *Engineering Journal,* AISC, January, pp. 6-7.

Lui, E.M. (1992), "A Novel Approach for K Factor Determination," *Engineering Journal,* AISC Vol. 29, No. 4, pp. 150–159.

Maleck, A.E. and White, D.W. (2003), "Direct Analysis Approach for the Assessment of Frame Stability: Verification Studies," *Proceedings,* Annual Technical Session, Structural Stability Research Council, University of Missouri, Rolla, MO, pp. 423–441.

Martinez-Garcia, J.M. and Ziemian, R.D. (2006), "Benchmark Studies to Compare Frame Stability Provisions," *Proceedings,* Annual Technical Session, Structural Stability Research Council, University of Missouri, Rolla, MO, pp. 425–442.

MBMA (2002), "Common Industry Practices—Section 6.8—Erection Tolerances," *Metal Building Systems Manual,* Metal Building Manufacturers Association, Cleveland, OH, pp. IV–19.

MBMA (2007), *Metal Building Systems Manual,* Metal Building Manufacturers Association, Cleveland, OH.

Morrell, M.L. and Lee, G.C. (1974), "Allowable Stresses for Web-Tapered Beams with Lateral Restraints," *Welding Research Council Bulletin,* No. 192, pp. 1–12.

Murray, T.M. and Shoemaker, W.L. (2002), *Flush and Extended Multiple-Row Moment End-Plate Connections,* Steel Design Guide 16. American Institute of Steel Construction, Chicago, IL.

Nair, R.S. (2005), "Stability and Analysis Provisions of the 2005 AISC *Specification* for Steel Buildings," *Proceedings* SEI/ASCE Structures Congress, ASCE, 3 pp.

Nethercot, D.A and Trahair, N.S. (1976), "Lateral Buckling Approximations for Elastic Beams," *The Structural Engineer,* Vol. 54, No. 6, pp. 197–204.

Newman, A. (2004), *Metal Building Systems: Design and Specification,* 2nd Ed., McGraw-Hill, New York.

Newmark, N.M. (1943), "A Numerical Procedure for Computing Deflections, Moments and Buckling Loads," *Transactions ASCE,* 108, pp. 1161–1188.

Ostwald (1910), "Klassiker der exakten Wissenschaften," No. 175, Leipzig, Germany.

Ozgur, C., Kim, Y.D. and White, D.W. (2007), "Consideration of End Restraint Effects in Web-Tapered Members," Structural Engineering Mechanics and Materials Report No. 32, School of Civil and Environmental Engineering, Georgia Institute of Technology, Atlanta, GA, June.

Polyzois, D. and Raftoyiannis, I.G. (1998), "Lateral-Torsional Stability of Steel Web-Tapered I-Beams," *Journal of Structural Engineering*, ASCE, Vol. 124, No. 10, pp. 1208–1216.

Prawel, S.P., Morrell, M.L. and Lee, G.C. (1974), "Bending and Buckling Strength of Tapered Structural Members," *Welding Research Supplement,* Vol. 53, February, pp. 75–84.

Righman, J.E. (2005), "Rotation Compatibility Approach to Moment Redistribution for Design and Rating of Steel I-Girders," Doctoral dissertation, West Virginia University, Morgantown WV, 363 pp.

SAA (1987), Draft Limit State Steel Structures Code AS 1250, Standards Association of Australia, Sydney.

Salter, J.B., Anderson, D. and May, I.M. (1980), "Tests on Tapered Steel Columns," *The Structural Engineer,* Vol. 58A, No. 6, pp. 189–193.

Salvadori, M.G. (1951), "Numerical Computation of Buckling Loads by Finite Differences," ASCE, *Transactions,* 116, pp. 590–625.

Shiomi, H., Nishikawa, S. and Kurata, M. (1983), "Tests on Tapered Steel Beam-Columns," *Transactions of JSCE,* 15, pp. 99–101.

Shiomi, H. and Kurata, M. (1984), "Strength Formula for Tapered Beam-Columns," *Journal of Structural Engineering,* Vol. 110, No. 7, pp. 1630–1643.

Silvestre, N. and Camotim, D. (2002), "Post-Buckling Behavior, Imperfection Sensitivity and Mode Interaction in Pitched-Roof Steel Frames," *Proceedings,* Annual Technical Session, Structural Stability Research Council, University of Missouri, Rolla, MO, pp. 139–162.

Surovek-Maleck, A.E. and White, D.W. (2004a), "Alternative Approaches for Elastic Analysis and Design of Steel Frames. I: Overview," *Journal of Structural Engineering,* ASCE, Vol. 130, No. 8, pp. 1186–1196.

Surovek-Maleck, A.E. and White, D.W. (2004b), "Alternative Approaches for Elastic Analysis and Design of Steel Frames. II: Verification Studies," *Journal of Structural Engineering,* ASCE, Vol. 130, No. 8, pp. 1197–1205.

Timoshenko, S.P. (1936), *Theory of Elastic Stability,* McGraw-Hill, New York, 518 pp.

Timoshenko, S.P. and Gere, J.M. (1961), *Theory of Elastic Stability,* McGraw-Hill, New York, 541 pp.

Watwood, V.B. (1985), "Gable Frame Design Considerations," *Journal of Structural Engineering,* ASCE, Vol. 111, No. 7, pp. 1543–1558.

White, D.W. (2010), "Structural Behavior of Steel," *Steel Bridge Design Handbook,* National Steel Bridge Alliance, Chapter 6.

White, D.W., Barker, M. and Azizinamini, A. (2008), "Shear Strength and Moment-Shear Interaction in Transversely-Stiffened Steel I-Girders," *Journal of Structural Engineering*, ASCE, Vol. 134, No. 9, pp. 1437–1449.

White, D.W. and Barker, M. (2008), "Shear Resistance of Transversely Stiffened Steel I-Girders," *Journal of Structural Engineering*, ASCE, Vol. 134, No. 9, pp. 1425–1436.

White, D.W. and Chang, C.J. (2007), "Improved Flexural Stability Design of I-shaped Members in AISC (2005)—A Case Study Comparison to AISC (1989) ASD," *Engineering Journal,* AISC, Vol. 44, No. 3, 3rd Quarter.

White, D.W. and Jung, S.-K. (2006), "Effect of Web Distortion on the Buckling Strength of Noncomposite Discretely-Braced I-Beams," *Engineering Structures,* doi:10.1016/j.engstruct.2006.09.020, 17 pp.

White, D.W. and Jung, S.-K. (2008), "Unified Flexural Resistance Equations for Stability Design of Steel I-shaped Members—Uniform Bending Tests," *Journal of Structural Engineering*, ASCE, Vol. 134, No. 9, pp. 1450–1470.

White, D.W. and Kim, Y.D. (2006), "A Prototype Application of the AISC (2005) Stability Analysis and Design Provisions to Metal Building Structural Systems," Report prepared for Metal Building Manufacturers Association, School of Civil and Environmental Engineering, Georgia Institute of Technology, January, 157 pp.

White, D.W. and Kim, Y.D. (2008), "Unified Flexural Resistance Equations for Stability Design of Steel I-shaped Members—Moment Gradient Tests," *Journal of Structural Engineering*, ASCE, Vol. 134, No. 9, pp. 1471–1486.

White, D.W., Surovek, A.E. and Kim, S.C. (2007a), "Direct Analysis and Design Using Amplified First-Order Analysis, Part 1—Combined Braced and Gravity Framing Systems," *Engineering Journal,* AISC, Vol. 44, No. 4, 4th Quarter.

White, D.W., Surovek, A.E. and Chang, C.J. (2007b), "Direct Analysis and Design Using Amplified First-Order Analysis, Part 2—Moment Frames and General Rectangular Framing Systems," *Engineering Journal,* Vol. 44, No. 4, 4th Quarter.

Yura, J. and Helwig, T. (1996), "Bracing for Stability," Short Course Notes, Structural Stability Research Council.